

Utah State University

DigitalCommons@USU

Reports

Utah Water Research Laboratory

January 1978

Unsaturated Transient Flow Through Heterogeneous Soils: Numerical Solutions and Analyses of Three-dimensional Axisymmetric Flows

Abdolhossien Nassehzadeh-Tabrizi

Roland W. Jeppson

Lyman S. Willardson

Follow this and additional works at: https://digitalcommons.usu.edu/water_rep



Part of the [Civil and Environmental Engineering Commons](#), and the [Water Resource Management Commons](#)

Recommended Citation

Nassehzadeh-Tabrizi, Abdolhossien; Jeppson, Roland W.; and Willardson, Lyman S., "Unsaturated Transient Flow Through Heterogeneous Soils: Numerical Solutions and Analyses of Three-dimensional Axisymmetric Flows" (1978). *Reports*. Paper 176.

https://digitalcommons.usu.edu/water_rep/176

This Report is brought to you for free and open access by the Utah Water Research Laboratory at DigitalCommons@USU. It has been accepted for inclusion in Reports by an authorized administrator of DigitalCommons@USU. For more information, please contact digitalcommons@usu.edu.



UNSATURATED TRANSIENT FLOW THROUGH HETEROGENEOUS
SOILS--Numerical Solutions and Analyses of
Three-dimensional Axisymmetric Flows

by

Abdolhossien Nassehzadeh-Tabrizi
Roland W. Jeppson
Lyman S. Willardson

Supported by

The National Science Foundation
Grant No. ENG 74-24314

Utah Water Research Laboratory
College of Engineering
Utah State University
Logan, Utah 84322

January 1978

TABLE OF CONTENTS

	Page
LIST OF TABLES	vi
LIST OF FIGURES	vii
LIST OF NOTATIONS	xvii
ABSTRACT	xxiii
INTRODUCTION	1
Objectives	4
REVIEW OF LITERATURE	7
Analytical Solutions	7
Empirical Equations	10
Solutions by Means of Numerical Techniques	11
Darcy's Law for Saturated and Unsaturated Systems	19
Darcy's Law for Saturated Soils	19
Darcy's Law for Unsaturated Media	21
Relations of Saturation and Hydraulic Conductivity to Capillary Pressure	22
Saturation-Capillary Pressure Relations	24
Saturation-Hydraulic Conductivity Relations	28
Hydraulic Conductivity-Capillary Pressure Relations	31
MODELING OF WATER MOVEMENT THROUGH POROUS MEDIA	35
Definition of the Physical Problem	35
The Mathematical Model	36
Assumptions in the Mathematical Formulation	37
DIFFERENTIAL EQUATIONS FOR DESCRIBING WATER MOVEMENT IN SOILS	39
Continuity Equation in Cylindrical Coordinates	39
The General Flow Equation	42

TABLE OF CONTENTS (Continued)

INITIAL AND BOUNDARY CONDITIONS	57
The Initial Conditions	57
The Boundary Conditions	58
Axis of Symmetry ① - ②	58
Surface of Water Application ② - ③	58
Surface Beyond Radius of Water Application ③ - ④	61
Outer Boundary Beyond the Radius of Influence ④ - ⑤	61
Bottom Boundary ⑤ - ①	62
FINITE DIFFERENCE SOLUTION	63
Finite Difference Operators for Interior Grid Points	64
Finite Difference Operators for Boundary Grid Points	68
Operator for Boundary ① - ②	68
Operator for Boundary ② - ③	68
Operator for Boundary ③ - ④	72
Operator for Boundary ④ - ⑤	73
Operator for Boundary ⑤ - ①	73
Method of Solution	75
Evaluating Derivatives of Jacobian D	79
(a) For the Soil Surface or First Row of Jacobian D	79
(b) For Flow Field or Interior Elements of Jacobian D	82
(c) For the Bottom Boundary or Bottom Row of Jacobian D	86
THE COMPUTER PROGRAM	89
Description and Structure of the Program	89
Main Program	89
Subroutine INITIA	94
Subroutine DERV	95
Subroutine TIMSTH	96
Function F1	96
Subroutine FJ	96
Function F3	97
Subroutine FIBNOK	97
Subroutine RITOUT	97

TABLE OF CONTENTS (Continued)

DATA AND SPECIFICATION REQUIRED TO OBTAIN A SOLUTION	101
Establishing Dimensions for the Problem	101
Defining Hydraulic Properties of the Soil	103
Residual Saturation	103
Pore-Size Distribution Exponent	104
Bubbling Pressure Head	104
Soil Porosity	104
Initialization of Hydraulic Head	104
Controlling the Flow of Computations	105
REPRESENTATIVE SOLUTIONS AND ANALYSIS OF RESULTS	107
Coaxial Graphs	192
Comparison of Results with the Results of a One-Dimensional Infiltration	198
Comparison of Numerical Solutions and Field Data	201
SUMMARY AND CONCLUSIONS	207
LITERATURE CITED	211
APPENDICES	223
Appendix I. Flow Chart	224
Appendix II. Fortran Program Listing Typical Input Data and Sample Solutions	227

LIST OF TABLES

Table	Page
1. Review of Some Available Numerical Solution of Flow Equation	13
2. Summary of Specification of Problems	110
3. Values of Hydraulic Properties of Soil Used in Matching	205
4. Summary of Results and Conclusions	209

LIST OF FIGURES

Figure	Page
1. Relationship Between Hydraulic Conductivity, K , and Moisture Content, θ , for Yolo Light Clay	23
2. Relation Between Effective Saturation and Capillary Pressure Head	25
3. Definitive Retention Curves Depicting the Relationships of the Parameters in the Theoretical Retention Function	27
4. Comparison of Hydraulic Conductivities Computed from Saturation-Pressure Data by a Modified Burdine Equation, with Those Measured in the Laboratory	29
5. Physical Conditions Representing Three-Dimensional Axisymmetric Transient Unsaturated Flow Through Heterogeneous Media From a Circular Application Area	36
6. Coordinate System. The Coordinates of Point G are: Cartesian: X, Y, Z and Cylindrical: Z, R, ϕ	39
7. Equation of Continuity in Cylindrical Coordinates	40
8. Formulation of the Boundary Value Problem for the Transient Unsaturated Three-Dimensional Axisymmetric Flow From a Circular Area Through Heterogeneous Porous Media	59
9. Effect of Variation of Bubbling Pressure, P_b , on Distribution of Dimensionless Capillary Pressure P_c Prior to Infiltration and at Dimensionless Time $\tau = 1.46$ from Maintaining the Surface Circle of Application at 90 Percent Saturation for Problems 1 through 3. The Values on the Curves Represent Capillary Pressure Head	111
10. Effect of Variation of Pore Size Distribution Exponent, λ , on Distribution of Dimensionless Capillary Pressure P_c Prior to Infiltration and at Dimensionless Time $\tau = 1.46$ From Maintaining the Surface Circle of Application at 80 Percent Saturation for Problems 1, 4, and 5. The Values of the Curves Represent Capillary Pressure Head	112

LIST OF FIGURES (Continued)

Figure	Page
11. Effect of Variation of Residual Saturation, S_r , on Distribution of Dimensionless Capillary Pressure P_c Prior to Infiltration and at Dimensionless Time $\tau = 1.46$ From Maintaining The Surface Circle of Application at 90 Percent Saturation for Problems 1, 6, and 7. The Values of the Curves Represent Capillary Pressure Head	113
12. Effect of Variation of Porosity, η , on Distribution of Dimensionless Capillary Pressure P_c Prior to Infiltration and at Dimensionless Time $\tau = 1.46$ from Maintaining the Surface Circle of Application at 90 Percent Saturation for Problems 1, 8, and 9. The Values of the Curves Represent Capillary Pressure Head	114
13. Effect of Variation of Saturated Hydraulic Conductivity, K_s , on Distribution of Dimensionless Capillary Pressure P_c^0 Prior to Infiltration and at Dimensionless Time $\tau = 1.46$ from Maintaining the Surface Circle of Application at 90 Percent Saturation for Problems 1, 10, and 11. The Values of the Curves Represent Capillary Pressure Head	115
14. Distribution of Saturation at Several Dimensionless Times Resulting from Maintaining the Surface Circle of Application at SSUR = 90 Percent Saturation for Homogeneous Soils (Problem No. 1)	117
15. Distribution of Saturation at Several Dimensionless Times Resulting from Maintaining Surface Circle of Application at SSUR = 90 Percent Saturation for Heterogeneous Soil, Problem No. 2	118
16. Distribution of Saturation at Several Dimensionless Times Resulting from Maintaining Surface Circle of Application at SSUR = 90 Percent Saturation for Heterogeneous Soil, Problem No. 3	119
17. Distribution of Saturation at Several Dimensionless Times Resulting from Maintaining Surface Circle of Application at SSUR = 90 Percent Saturation for Heterogeneous Soil, Problem No. 4	120
18. Distribution of Saturation at Several Dimensionless Times Resulting from Maintaining Surface Circle of Application at SSUR = 90 percent Saturation for Heterogeneous Soil, Problem No. 5	121

LIST OF FIGURES (Continued)

Figure	Page
19. Distribution of Saturation at Several Dimensionless Times Resulting from Maintaining Surface Circle of Application at SSUR = 90 Percent Saturation for Heterogeneous Soil, Problem No. 6	122
20. Distribution of Saturation at Several Dimensionless Times Resulting from Maintaining Surface Circle of Application at SSUR = 90 Percent Saturation for Heterogeneous Soil, Problem No. 7	123
21. Distribution of Saturation at Several Dimensionless Times Resulting from Maintaining Surface Circle of Application at SSUR = 90 Percent Saturation for Heterogeneous Soil, Problem No. 8	124
22. Distribution of Saturation at Several Dimensionless Times Resulting from Maintaining Surface Circle of Application at SSUR = 90 Percent Saturation for Heterogeneous Soil, Problem No. 9	125
23. Distribution of Saturation at Several Dimensionless Times Resulting from Maintaining Surface Circle of Application at SSUR = 90 Percent Saturation for Heterogeneous Soil, Problem No. 10	126
24. Distribution of Saturation at Several Dimensionless Times Resulting from Maintaining Surface Circle of Application at SSUR = 90 Percent Saturation for Heterogeneous Soil, Problem No. 11	127
25. Effect of Variation of Bubbling Pressure, P_b , on Position of Iso-saturation Lines Prior to Infiltration and at Dimensionless Time $\tau = 1.46$ from the Results of Solution of Problems 1 Through 3	128
26. Effect of Variation of Pore Size Distribution Exponent, λ , on Position of Iso-saturation Lines Prior to Infiltration and at Dimensionless Time $\tau = .50$ From the Results of Solution of Problems 1, 4, and 5	129
27. Effect of Variation Pore Size Distribution Exponent, λ , on Position of Iso-Saturation Lines Prior to Infiltration and at Dimensionless Times $\tau = 1.46$ From the Results of Solution of Problem 1, 4, and 5	130

LIST OF FIGURES (Continued)

Figure	Page
28. Effect of Variation of Residual Saturation, S_r , on Position of Iso-Saturation Lines Prior to Infiltration and at Dimensionless Time $\tau = .50$ from the Results of Solution of Problems 1, 6, and 7	131
29. Effect of Variation of Residual Saturation, S_r , on Position of Iso-Saturation Lines Prior to Infiltration and at Dimensionless Time $\tau = 1.46$ From the Results of Solution of Problems 1, 6, and 7	132
30. Effect of Variation of Porosity, η , on Position of Iso-Saturation Lines Prior to Infiltration and at Dimensionless Time $\tau = 1.46$ from the Results of Solution of Problems 1, 8, and 9	133
31. Effect of Variation Saturated Hydraulic Conductivity, K_0 , on Position of Iso-Saturation Lines Prior to Infiltration and at Dimensionless Time $\tau = 1.46$ From the Results of Solution of Problems 1, 10, and 11	134
32. Distribution of Saturations With Depth At Several Dimensionless Times At The Centerline And At A Radial Distance From The Centerline Equal to $r = r_a + 0.4 = 0.7$ Units For Problem No. 1 (Homogeneous Soil)	141
33. Distribution Of Saturations With Depth At Several Dimensionless Times At the Centerline And At A Radial Distance From the Centerline Equal to $r = r_a + 0.4 = 0.7$ Units For Problem No. 2 (Magnitude of Dimensionless Bubbling Pressure, P_b , Linearly Decreasing With Depth, 1.30 to 0.70).	141
34. Distribution of Saturations With Depth At Several Dimensionless Times At The Centerline And At A Radial Distance From The Centerline Equal to $r = r_a + 0.4 = 0.7$ Units For Problem No. 3 (Magnitude of Dimensionless Bubbling Pressure, P_b , Linearly Increasing With Depth, 0.70 to 1.30).	142
35. Distribution of Saturations With Depth At Several Dimensionless Times At the Centerline And At A Radial Distance From the Centerline Equal to $r = r_a + 0.4 = 0.7$ Units For Problem No. 4 (Magnitude of Pore Size Distribution Exponent, λ , Linearly Decreasing With Depth, 1.30 to 0.70)	142

LIST OF FIGURES (Continued)

Figure	Page
36. Distribution of Saturations With Depth At Several Dimensionless Times At the Centerline And At A Radial Distance From the Centerline Equal to $r = r_a + 0.4 = 0.7$ Units For Problem No. 5 (Magnitude of Pore Size Distribution Exponent, λ , Linearly Increasing With Depth, 0.70 to 1.30)	143
37. Distribution of Saturations With Depth At Several Dimensionless Times at the Centerline And At A Radial Distance From the Centerline Equal to $r = r_a + 0.4 = 0.7$ Units for Problem No. 6 (Magnitude of Residual Saturation, S_r , Linearly Decreasing with Depth, 0.25 to 0.05)	143
38. Distribution of Saturations With Depth At Several Dimensionless Times At the Centerline And At A Radial Distance From the Centerline Equal to $r = r_a + 0.4 = 0.7$ Units for Problem No. 7 (Magnitude of Residual Saturation, S_r , Linearly Increasing with Depth, 0.05 to 0.25)	144
39. Distribution of Saturations With Depth At Several Dimensionless Times At the Centerline And At A Radial Distance From the Centerline Equal to $r = r_a + 0.4 = 0.7$ Units for Problem No. 8 (Magnitude of Soil Porosity, η , Linearly Decreasing With Depth, 0.62 to 0.18)	144
40. Distribution of Saturations With Depth At Several Dimensionless Times at the Centerline And At a Radial Distance From the Centerline Equal to $r = r_a + 0.4 = 0.7$ Units for Problem No. 9 (Magnitude of Soil Porosity, η , Linearly Increasing With Depth, 0.18 to 0.62)	145
41. Distribution of Saturations With Depth At Several Dimensionless Times At the Centerline And At a Radial Distance From the Centerline Equal to $r = r_a + 0.4 = 0.7$ Units for Problem No. 10 (Magnitude of Saturated Hydraulic Conductivity, K_0 , Linearly Decreasing With Depth, 1.0 to 0.60)	145
42. Distribution of Saturations With Depth At Several Dimensionless Times At the Centerline And At a Radial Distance From the Centerline Equal to $r = r_a + 0.4 = 0.7$ Units for Problem No. 11 (Magnitude of Saturated Hydraulic Conductivity, K_0 , Linearly Increasing with Depth, 1.0 to 1.40)	146

LIST OF FIGURES (Continued)

Figure	Page
43. Effect of Variation of Dimensionless Bubbling Pressure, P_b , on Infiltration Capacity Curves Obtained From Solutions of Problems 1 through 3	149
44. Effects of Variation of Pore Size Distribution, λ , on Infiltration Capacity Curves Obtained From Solutions of Problem 1, 4, and 5	150
45. Effect of Variation of Residual Saturation, S_r , on Infiltration Capacity Curves Obtained From Solution of Problems 1, 6, and 7	151
46. Effect of Variation of Porosity, η , on Infiltration Capacity Curves Obtained From Solutions of Problems 1, 8, and 9	152
47. Effect of Variations of Saturated Hydraulic Conductivity, K_0 , on Infiltration Capacity Curves Obtained from Solutions of Problems 1, 10, and 11	153
48. Effect of Variation of Bubbling Pressure, P_b , on Volume of Water Absorbed With Time as Obtained from Solutions of Problems 1 through 3	155
49. Effect of Variation of Pore Size Distribution Exponent, λ , on Volume of Water Absorbed With Time as Obtained From Solutions of Problems 1, 4, and 5	156
50. Effect of Variation of Residual Saturation, S_r , on Volume of Water Absorbed With Time as Obtained From Solution of Problems 1, 6, and 7	157
51. Effect of Variation of Porosity, η , on Volume of Water Absorbed With Time as Obtained from Solutions of Problems 1, 8, and 9	158
52. Effect of Variation of Saturated Hydraulic Conductivity, K_0 , on Volume of Water Absorbed With Time as Obtained from Solutions of Problems 1, 10, and 11	159
53. Effect of Variation of Dimensionless Bubbling Pressure, P_b , on Vertical Depth of Penetration of Wetting Front with Time Obtained from Solutions of Problems 1 through 3	161

LIST OF FIGURES (Continued)

Figure	Page
54. Effect of Variation of Pore Size Distribution Exponent, λ , on Vertical Depth of Penetration of Wetting Front with Time Obtained from Solutions of Problems 1, 4, and 5	162
55. Effect of Variation of Residual Saturation, S_r , on Vertical Depth of Penetration of Wetting Front with Time Obtained From Solutions of Problems 1, 6, and 7	163
56. Effect of Variation of Porosity, η , on Vertical Depth of Penetration of Wetting Front With Time Obtained From Solutions of Problems 1, 8 and 9	164
57. Effect of Variation of Saturated Hydraulic Conductivity K_0 , on Vertical Depth of Penetration of Wetting Front with Time Obtained from Solutions of Problems 1, 10, and 11	165
58. Effect of Variation of Dimensionless Bubbling Pressure, P_b , on Lateral Movement of Wetting Front with Time for Problems 1 through 3	166
59. Effect of Variation of Pore Size Distribution Exponent, λ , on Lateral Movement of Wetting Front With Time for Problems 1, 4, and 5	167
60. Effect of Variation of Residual Saturation, S_r , on Lateral Movement of Wetting Front With Time for Problems 1, 6, and 7	168
61. Effect of Variation of Porosity, η , on Lateral Movement of Wetting Front with Time for Problems 1, 8, and 9	169
62. Effect of Variation of Saturated Hydraulic Conductivity, K_v , on Lateral Movement of Wetting Front with Time for Problems 1, 10, and 11	170
63. Effect of Different Values of Dimensionless Initial Hydraulic Head, h_0 , on Infiltration Capacity Curve Obtained From Solutions of Problems 1, 2, and 13	172
64. Effect of Different Values of Dimensionless Initial Hydraulic Head, h_0 , on Volume of Water Absorbed as Obtained from Solutions of Problems 1, 12, and 13	173

LIST OF FIGURES (Continued)

Figure	Page
65. Effect of Different Values of Dimensionless Initial Hydraulic Head, h_0 , on Vertical Depth of Penetration of Wetting Front with Time for Problems 1, 12, and 13	174
66. Effect of Different Values of Dimensionless Initial Hydraulic Head, h_0 , on Lateral Movement of Wetting Front with Time for Problems 1, 12, and 13	176
67. Changes in Saturation at the Centerline at a Dimensionless Depth of 0.4 Units as Obtained from Solutions to Problems 1, 12, and 13 in Different Values of Dimensionless Initial Hydraulic Head, h_0	177
68. Changes in Saturation on the Soil Surface at a Dimensionless Radial Distance from Centerline Equal to $r = r_a + 0.4$ Units as Obtained from Solutions to Problems 1, 12, and 13 with Different Values of Dimensionless Initial Hydraulic Head, h_0	178
69. Effect of Different Values of Dimensionless Application Rate, VK , on Vertical Depth of Penetration of Wetting Front with Time for Problems 14 through 18	179
70. Effect of Different Values of Dimensionless Application Rate, VK , on Lateral Movement of Wetting Front with Time for Problems 14 through 18	180
71. Changes in Vertical Depth of Penetration of Wetting Front with Dimensionless Application Rate, VK , for Different Dimensionless Time Parameter, τ , as Obtained From Solutions of Problems 14 through 18	181
72. Changes in Lateral Movement of Wetting Front Beyond the Radius of Circle of Application with Dimensionless Application Rate, VK , for Different Dimensionless Time Parameter, τ , as Obtained From Solutions of Problems 14 through 18	182
73. Changes in Saturation at Centerline on Soil Surface with Time for Different Values of Dimensionless Application Rate, VK , as Obtained from Solutions of Problems 14 through 18	184
74. Changes in Saturation on Soil Surface 0.4 Units Beyond the Circle of Application with Time, for Different Values of Dimensionless Application Rate, VK , as Obtained From Solutions of Problems 14 through 18	185

LIST OF FIGURES (Continued)

Figure	Page
75. Changes in Saturation at the Centerline at a Dimensionless Depth of 0.4 Units with Time for Different Values of Application Rate, VK , as Obtained from Solutions of Problems 14 through 18	186
76. Infiltration Capacity Curves per Total Area as Obtained From Solutions of Problems 1 and 19 through 21 in Which Dimensionless Radius of Application r_a , was Varied	188
77. Infiltration Capacity Curves Obtained From Solutions of Problems 1 and 19 through 21 in Which Dimensionless Radius of Application, r_a , Was Varied	189
78. Volume of Water Absorbed Curves Obtained From Solutions of Problems 1 and 19 through 21, in Which Dimensionless Radius of Application, r_a , was Varied	190
79. Changes in Saturation of 0.4 Units Depth on Centerline with Time for Different Radii of the Circle of Application as Obtained from Solutions of Problems 1 and 19 through 21	191
80. Graphical Solution Giving the Difference between the Instantaneous Infiltration Rate for Homogeneous and Heterogeneous Soil, ΔI . Based upon Linear Coefficients which Describe Heterogeneity as a Function of Depth	195
81. Graphical Solution Giving the Difference Between the Vertical Penetration of Wetting Front for Homogeneous and Heterogeneous Soil, ΔD . Based Upon Linear Coefficients Which Describe Heterogeneity as a Function of Depth	196
82. Graphical Solution Giving the Difference Between the Lateral Movement of Wetting Front for Homogeneous and Heterogeneous Soil, ΔR . Based Upon Linear Coefficients Which Describe Heterogeneity as a Function of Depth	197

LIST OF FIGURES (Continued)

Figure		Page
83.	Additional Infiltration Rate Due To Applying Water Over a Finite Circular Area	199
84.	Difference Between One-Dimensional and Three-Dimensional Axisymmetric Saturation at a Dimensionless Depth of 0.4 Units at (a) the Centerline and (b) Radial Distance, r_a	200
85.	Variation of Saturation with Time at 2 Inch Depth in The Soil at Lower Sheep Creek Beneath an Axisymmetric Infiltrometer	203
86.	Variation of Capillary Pressure with Time at 2-inch Depth in the Soil at Lower Sheep Creek Beneath an Axisymmetric Infiltrometer	204

LIST OF NOTATIONS

A	A soil parameter called sorptivity
AKV	A coefficient of K_v
AL	A coefficient of λ
APB	A coefficient of P_b
APOR	A coefficient of η
ASR	A coefficient of S_r
a	Soil parameter
a'	Coefficient of the equation for difference between 3-dimensional and 1-dimensional infiltration rate
B	Transmissivity soil parameter
BKV	B coefficient of K_v
BL	B coefficient of λ
BPB	B coefficient of P_b
BPOR	B coefficient of η
BSR	B coefficient of S_r
b	Soil parameter
b'	Exponent of the equation for difference between 3-dimensional and 1-dimensional infiltration rate
C	Cumulative infiltration
CKV	C coefficient of K_v
CL	C coefficient of λ
CPB	C coefficient of P_b
CPOR	C coefficient of η
CSR	C coefficient of S_r
D	Jacobian matrix

LIST OF NOTATIONS (Continued)

D	Dimensionless depth, or depth/L
d	Depth of water on soil
F	Function
g	Acceleration due to gravity
H	Soil water pressure head, $H = \frac{P}{\rho g}$
h	Hydraulic head or energy per unit weight of fluid being the sum of the elevation and pressure head
h_0	Dimensionless hydraulic head at which the soils exist initially under static equilibrium
h_s	Soil water suction head; $h_s = \frac{-P}{\rho g}$
h_t	Dimensionless hydraulic head, ($h_t = z - P_t$)
I	Dimensionless rate of infiltration
I'	Infiltration rate
I_0	Initial infiltration rate
I_∞	Final infiltration rate
I_{se}	Incomplete beta function ratio
i	Node index in r-direction
j	Node index in z-direction
K	Effective hydraulic conductivity
K	Index of discretized variable denoting time increment
K_a	A constant with units of velocity
K_f	Constant which governs the time required under given conditions for infiltration rate to change from its initial value I_0 to I_∞
K_v	A dimensionless quantity which is a function of depth
K_0	Saturated hydraulic conductivity
$K(\theta)$	Hydraulic conductivity, function of water content, θ

LIST OF NOTATIONS (Continued)

K_r	Relative hydraulic conductivity
k	The Intrinsic permeability
L	Characteristic length used for nondimensionalization
l	Length of the soil column
M	Empirical soil parameter represents I' at unit time
m	Iteration index (Newton-Raphson Method)
m'	Shape function of the retention curve
n	Is a constant between -1 and zero, that depends on the soil and its physical condition
N_r	Number of grid lines from the axis of symmetry to the outside radius of the problem
N_z	Number of grid lines from the surface to the bottom boundary
N_{2X}	Number of points in radial direction to outer edge of circle of application
P	Soil water pressure head
P_b	Dimensionless bubbling pressure head, function of depth z
P_b'	Bubbling pressure head, function of depth, z
P_c	Capillary pressure, $P_c = -P$
P_f	Capillary pressure at the fictitious inflection point
P_t	Dimensionless pressure head or pressure head/ L
P_o	Pressure head parameter
P_t'	Dummy variable of integration
P_1	Soil parameter having the same dimensions as P_c
R	Radial coordinate
R^2	Correlation coefficient

LIST OF NOTATIONS (Continued)

r	Dimensionless radial (horizontal) coordinate, or this coordinate/L
r_a	Dimensionless radius of circle of application, or this radius/L
r_f	Dimensionless radius of outer boundary of region of interest or this radius/L
S	Saturation, or volume of water divided by volume of voids
S_e	Effective saturation
S_r	Residual saturation as a function of depth, z
S_s	Saturation parameter denoting largest saturation obtained under imbibition
SSUR	Specified soil surface saturation
$S_{j,i}^{K+1}$	Saturation at any time step at each grid point
$S_{j,i}^0$	Initial saturation at each grid point
t	Time
V	Seepage velocity (flow rate per unit area)
\bar{V}	Seepage velocity vector
V_r	Seepage velocity component in the radial direction
V_ϕ	Seepage velocity component in the tangential direction
VK	Dimensionless application rate, $VK = \frac{W}{K_a}$
V_w^{K+1}	Volume of water in any time step at the region of wetting point
V_w^0	Initial volume of water in the soil at the region of wetting point
W	Seepage velocity component in the axial direction
X, Y, Z	Catesian coordinates
y	Depth of wet soil, measured from soil surface to wetting front

LIST OF NOTATIONS (Continued)

Z, R, ϕ	Cylindrical coordinates
z	Dimensionless axial (vertical) coordinate, or the coordinate/L
ξ	New dependent variable obtained from Kirchhoff transformation
ξ_0	Initial distribution of ξ
ψ	Dependent variable obtained from Kirchhoff transformation for homogeneous soils
ψ_a	A soil constant depending on the capillary forces acting on the moving boundary of the soil
η	Soil porosity
τ	Dimensionless time
λ	Pore size distribution exponent, function of depth, z
λ_0	Is the reference value of pore size distribution exponent at soil surface
ζ	Parameter
ρ	Density of water
μ	Dynamic viscosity of the water
θ	Volumetric water content
θ_0	Volumetric water content at saturation
$\Delta V_{j,i}$	Incremental volume of soil-air-water complex associated with any finite difference grid point
Δr	Mesh size in the r -direction
Δs	Dimensionless space increment, $\Delta s = \Delta Z = \Delta r$
ΔZ	Mesh size in the z -direction
$\Delta \tau$	Magnitude of the time step
Δ	Difference operator

LIST OF NOTATIONS (Continued)

- δ Central difference operator
- ∂ Partial differentiation operator

ABSTRACT

This study deals with unsaturated, unsteady water movement through heterogeneous porous media. The specific problem investigated is the transient three-dimensional axisymmetric flow resulting from water being applied on a horizontal circular area. The heterogeneity of the soil is described by allowing any or all of the five parameters in the Brooks-Corey equations to be any continuous function of depth.

Methodologies for obtaining numerical solutions to the resulting nonlinear partial differential equation and its associated initial-boundary value problem have been developed and implemented in a computer program. The numerical solution is based on the Crank-Nicolson method of finite differencing and the solution to the resulting system of nonlinear algebraic equations for each time step is by the Newton method combined with the line successive over-relaxation (LSOR) method.

The numerical solutions provide the following at each time step used: (1) the distribution of soil water saturation throughout the region, (2) the distribution of capillary pressure throughout the region, (3) the distribution of hydraulic head throughout the region, (4) the rate of infiltration if the area of application is specified at a given moisture level, (5) the extent and amount of lateral and vertical water movement, and (6) the rate of advance and position of the wetting front.

The solutions resulting from various variations of linearly specified heterogeneities have been studied and their influence of such quantities are infiltration rate or intake capacities and wetting front movements have been analyzed. To determine the effects of lateral water movement,

solution results from the axisymmetric solutions have been compared with solutions from a one-dimensional vertical flow model that permitted the same specification of heterogeneity.

A number of graphs are presented that illustrate influences of different soil heterogeneities. Coaxial graphs were developed to summarize the results of a number of solutions that relate the difference in infiltration in heterogeneous and homogeneous soils to the variations of the five parameters in the Brooks-Corey equations.

The numerical solutions are verified with reasonable agreement with field data at the Reynolds Creek experimental watershed obtained from experiments which duplicate the geometry of the mathematical model closely, if not the heterogeneity, also.

KEYWORDS: Soil Science, Water, Infiltration, Soils Pore-water Pressures, Irrigation, Heterogeneous, Axisymmetric, Unsaturated

INTRODUCTION

Water movement through porous media has been of great interest to mankind since early history. A scientific basis for the design of irrigation and drainage works was lacking until about a century ago, that is, until Henry Darcy, who, in 1856 found experimentally the famous basic linear law of flow of water through porous materials. Infiltration is defined as the process of the entry into the soil of water made available at the soil surface, together with the associated downward flow. Infiltration is an important factor in watershed management, ground water recharge, overland flow prediction and irrigation. Efficient water management requires accurate knowledge of the infiltration rate at which different soils will take water under different conditions. Most of the water falling on the ground surface moves through unsaturated soil during subsequent processes of drainage, evaporation and root extraction.

In more recent times, the flow equation has been solved analytically after making some simplifying assumptions and for simple boundary conditions. The majority of these solutions are for steady state isothermal flow through saturated isotropic homogeneous soils, an idealized case that does not exist in nature. The more complicated problems are unsteady flows through unsaturated heterogeneous media resulting in nonlinear partial differential equations for which no general exact solution is available.

During the past decade, knowledge of soil water flow under unsaturated conditions has advanced rapidly. High speed digital computers are used widely for solving initial-boundary-value problems numerically. Use of digital computers has allowed solution of more the realistic situation of flow of water in porous media. More detailed attention can now be devoted to unsaturated transient flow systems in heterogeneous porous media or soils. Steady state flow conditions do not exist for any appreciable time and heterogeneity of the soil is the rule rather than the exception in nature. At the present time, mathematical models for transient flow in heterogeneous porous media, with the exception by Watson and Whisler (109), assume that the soils consist of discrete layers of homogeneous soil. Basically this is little more than a modification of a numerical solution for homogeneous soils in which the hydraulic properties are changed between finite difference grid points while advancing the water through one layer to the next layer of soil. In the developed models, the hydraulic head and pressure head, but not the moisture content are assumed continuous across the interface of the two layers. The validity of this approach may be questioned because the soil water flow differential equation is developed under the assumption that all the dependent variables and their derivatives are continuous. The equation of flow describing water movement through soils is obtained by substituting Darcy's law into the differential form of the continuity equation. However, only the integral form of the continuity

equation is valid across an interface since in the derivative form the variables are discontinuous. In order for the differential form of the continuity equation to be valid, the seepage velocity and its derivative must be continuous. Furthermore, experimental results for steady downward flow through a sand into another sand having a slightly finer texture by Scott and Corey (91) demonstrates an abrupt (discontinuous) change in capillary pressure that can exist across the junction of two different sand layers. They assumed that pressure must be continuous regardless of abrupt change in texture and erroneously argue for a very rapid but continuous change in pressure which is unsupported by their data. If capillary pressure is not continuous, there would be an infinite pressure gradient at the interface of the layer. An alternative method is presented in this study that describes soil heterogeneity by specifying that the physical and hydraulic properties of the soil vary continuously as a function of depth. Jeppson and Nelson (47), Jeppson and Schreiber (48) and Watson and Whisler (109) used this approach to unsaturated flow problems in which they allowed only saturated hydraulic conductivity to vary with depth.

The problem which has been studied herein is one of three-dimensional axisymmetric unsaturated unsteady flow through homogeneous porous media resulting from water applied at the soil surface. In this problem heterogeneity is described by specifying that the hydraulic properties of the soil vary continuously with depth. The Brooks-Corey equations are used to describe the hydraulic properties (relative hydraulic conductivity and soil saturation) of the soil. The equations are relatively simple and also provide a reasonably good fit to capillary pressure-saturation and capillary pressure-hydraulic

conductivity data, and involve only three parameters, the residual saturation, S_r , pore size distribution exponent, λ , and bubbling pressure, P_b , whose magnitudes will depend upon the functions specified. Description of the soil heterogeneity by letting the saturated hydraulic conductivity, K_0 soil porosity n , as well as S_r , λ , and P_b be any continuous function of vertical coordinate allows for an infinite number of different problem specifications. Different solutions which were obtained for different problem specifications have been analyzed to determine influence of various distributions of heterogeneity and other factors on infiltration rate, amount and the distribution of soil moisture, accumulated infiltration, extent and amount of lateral moisture spreading and rate of advance and position of wetting front. The results obtained from the numerical solution are compared to field data from Lower Sheep Creek within the Reynolds Creek experimental watershed west of Boise, Idaho.

Objectives

1. To develop a computer program for numerically solving the initial-boundary-value problem which defines transient unsaturated isothermal flow (i.e., infiltration problems) in heterogeneous soils for three-dimensional, axisymmetric water movement.
2. To verify the numerical solution by comparing the results with field data of soil moisture and capillary pressure distribution.
3. To summarize and compile in the form of graphs, coaxial plots and/or equations, the results of a series of solutions in which different combinations of parameter values and problem specifications are varied to define how each of these effect such items of interest

as magnitude and characteristics of intake capacities, amount and distribution of moisture content increases, extent and amount of lateral moisture spreading, and rate of advance and position of wetting front.

It is expected that these relationships will provide considerable insight into what and how factors influence infiltration and prove valuable in classifying soils according to their infiltration properties.

REVIEW OF LITERATURE

Analytical Solutions

Green and Ampt (29) studied one-dimensional vertical infiltration under flooded conditions and presented the earliest infiltration equation based on Poiseuille's Law of capillary and on the analogy in which the soil is considered as "a bundle of capillary tubes." They assumed that the water content characteristic is a stepped curve and that the advancing water profile consists of two distinct zones, namely, a completely saturated upper part and a sharp and discontinuously separated lower zone that is at the original water content. It is also assumed that at the moving boundary of the wetting front, the suction is constant and equivalent to the air entry value.

The Equation (1) which was developed by Green and Ampt agrees well with laboratory experiment results but has disadvantages in that the rate of infiltration is expressed in terms of depth of penetration of wetting front. Green and Ampt equation is:

$$\frac{K_0}{\Delta\theta} t = y - (d + \psi_a) \ln \left(1 + \frac{y}{d + \psi_a} \right) \quad (1)$$

in which K_0 is the saturated hydraulic conductivity, L/T; $\Delta\theta$ is the difference between the original and saturated water content of soil, dimensionless; t is the time, T; y is the depth of wet soil, measured from soil surface to wetting front, L; d is the depth of water on soil

surface, L ; and ψ_a is a soil constant depending on the capillary forces acting on the moving boundary of the water, equivalent to air entry value, L .

Philip (72) analytically solved the one-dimensional flow equation and presented an equation to determine the infiltration rate. The equation is in the form of a series in terms of time and multipliers which depend on the water content. Equation (2) below shows the cumulative infiltration, C , in an expression in which only two terms of the solution series is included. The infiltration rate, I' , as a function of elapsed time (Equation 3) is derived by differentiation of Equation (2).

$$C = A \cdot t^{1/2} + B \cdot t \quad (2)$$

$$I' = 1/2 A t^{-1/2} + B \quad (3)$$

in which A is a soil parameter called sorptivity (capacity of a soil to release or absorb water) $L/T^{1/2}$; and B is a transmissivity soil parameter which results primarily from gravity forces (B becomes a progressively more important parameter in the equation with increasing time) L/T .

For large elapsed times, the term $A t^{-1/2}$ becomes insignificant, and parameter B in Equation (3) has to be equal to the saturated hydraulic conductivity.

Whisler and Bouwer (112) studied and compared the Green and Ampt equation, Equation (1), with the Philip equation, Equation (3). They concluded that the Green and Ampt equation, was not only simple to use, but also gave a better result.

Fok (22) compared the Green and Ampt and Philip infiltration equations. He showed that Philip's two term Equation can be derived from the Green and Ampt Equation, Equation (1).

Scott and Hanks (92) solved the one dimensional moisture flow equation by power series. They assumed that the diffusivity is an exponential function of moisture content, an approach which was used extensively by Gardner and Mayhugh (28) and is linear function of moisture content in another case. Also they assumed that diffusivity is a single-valued function of water content, and that a relation between soil moisture content and tension exists which is also a single valued function. They noted that if this analytical solution favorably compared with a numerical solution, there is reason to hope that the numerical solution may be successfully applied to more complicated problems.

Wooding (118) assumed that the hydraulic conductivity of an unsaturated soil is an exponential function of the pressure head. He used the method of linearization proposed by Philip (73, 74, 75) and reduced the nonlinear differential equation to a linear type and solved the problem of steady infiltration from a shallow, circular flooded area on a horizontal surface of a semi-infinite porous media, and showed the variation of soil moisture movement in a radial direction for different types of soils. Philip (75) assuming the hydraulic conductivity is an exponential function of moisture potential, applied Kirchhoff's transformation to linearize the nonlinear equation of steady flow, and obtained solutions for steady infiltration from a buried point source and spherical cavities. He stated for a small radius of spherical cavity the effect capillary dominates, but

gravitation force becomes more important when the radius increases. Philip (77) analyzed steady two and three dimensional infiltration in heterogeneous soils. He assumed that the hydraulic conductivity depends exponentially on both moisture content and depth, and applied Kirchhoff's transformation to linearize the nonlinear flow equation.

Raats (78) upon assuming that the hydraulic conductivity is an exponential function of pressure head, linearized the steady nonlinear axisymmetric flow equation by using matrix flux potential (Kirchhoff's Transformation). He analyzed steady infiltration from buried point sources and surface point sources, and obtained explicit equations for the pressure head, total head and matrix flux potential and the Stoke's stream function.

Empirical Equations

Kostiakov (55) suggested the following empirical equation for the infiltration rate, I' :

$$I' = Mt^n \quad (4)$$

in which I' is the quantity of water infiltrating a unit cross sectional area of soil per unit time; t is the elapsed time of infiltration; M is a constant that depends on the soil and its physical condition, and equals I' at unit time, t , (dimensionally inconsistent); and n is a constant between -1 and zero, that depends on the soil and its physical condition, and represents the arithmetic slope of the infiltration rate line with time on log-log paper, (dimensionless).

The Kostiakov equation, Equation (4), does not hold for large

values of time, because as the equation shows, the infiltration rate approaches zero instead of a constant value. However, because of its simplicity, and because it fits much infiltration data well over a short time interval, it is widely used in irrigation practices.

Horton (36) proposed the following equation for the infiltration rate, I' :

$$I' = I_{\infty} + (I_0 - I_{\infty}) \exp(-K_f t) \quad (5)$$

in which I_{∞} is the final infiltration rate, i.e., I' at $t = \infty$, L/T; I_0 is the initial infiltration rate, i.e., I' at $t = 0$, L/T; and K_f is a constant which governs the time required under given conditions for infiltration rate to change from its initial value I_0 to I_{∞} .

At large values of time, the infiltration rate, I' , decreases to nearly constant value I_{∞} .

Solutions by Means of Numerical Techniques

Unfortunately, the governing equation for unsaturated flow is nonlinear and boundary conditions are complicated. Exact analytical solutions of the partial differential equation governing the flow of water through the porous media are not available, except for oversimplified cases. Therefore, numerical approximations need to be employed to solve unsaturated flow problems. Freeze (24) reviewed the available literature of one-dimensional, vertical, unsaturated unsteady flow problems in soils studied by a number of researchers, and Remson, Hornberger and Molz (83) give an outline of published numerical solutions mostly applied to porous media flow. The numerical method most

widely used in the solution of the problems dealing with flow through porous media is the method of finite differences. Examples are: (1) Infiltration (32, 33, 11, 44, 38, 94), (2) flow towards wells (61, 102, 12, 18), (3) subsurface hydrology (34, 57, 58), (4) seepage through earth dams (25), (5) seepage from earth canals (15, 47), (6) trickle irrigation (6), (7) Drainage (60, 101, 50, 40, 104, 94, 89, 62, 83, 65).

Depending upon the nature of the problem, different forms of the flow equation have been used. Also auxiliary conditions differ to account for the geometry (one, two, or three dimensional), the medium characteristics (homogeneous or heterogeneous, and isotropic or anisotropic), the initial condition which must be specified for unsteady problems, and the boundary conditions. Table 1 summarizes various past problems studied by a number of researchers.

Gardner and Mayhugh (28) applied the Boltzman Transformation to concentration-dependent diffusivity equation which describes the movement of water in unsaturated soils, to reduce the partial differential equation to an ordinary differential equation. They assumed diffusivity to be an exponential function of water content, and observed that the distance to the wetting front during infiltration increased as the square root of time. There was a good agreement between measured distribution of water content and those predicted by their numerical solution.

Hanks and Bowers (32) in their pioneering work presented a method to solve the water flow equation for vertical infiltration in layered (heterogeneous) soils. They defined a variable time increment, Δt , as the time required for a constant amount of water to enter the soil

TABLE 1.--Review of Some Available Numerical Solution of Flow Equation.

Name (1)	Date and Reference (2)	Dimensions			Medium Characteristics			Flow Conditions		Saturation		
		1 (3)	2 (4)	3 (5)	Homo- geneous (6)	Layered (7)	Hetero- geneous (8)	Steady (9)	Un- steady (10)	Satura- ted (11)	Unsat- urated (12)	Com- posite (13)
Klute	1952 (51)	X			X				X		X	
Day and Luthin	1956 (20)	X			X				X		X	
Youngs	1957 (119)	X			X				X		X	
Philip	1957 (72)	X			X				X		X	
Isherwood	1959 (40)		X		X				X	X		
Hanks and Bower	1962 (32)	X				X			X		X	
Ashcroft, et al.	1962 (3)	X			X				X		X	
Nelson	1962 (68)			X			X	X				X
Reisenauer	1963 (79)			X			X	X				X
Reisenauer et al.	1963 (80)			X			X	X				X
Sewell and Van Schilfgaarde	1963 (95)		X		X			X			X	
Wang et al.	1964 (107)	X			X				X		X	
Whisler and Klute	1965 (113)	X			X				X		X	
Liakopoulos	1965 (56)	X			X				X		X	
Remson et al.	1965 (81)	X			X				X		X	

TABLE 1.--Continued.

Name (1)	Date and Reference (2)	Dimensions			Medium Characteristics			Flow Conditions		Saturation		
		1 (3)	2 (4)	3 (5)	Homo- geneous (6)	Layered (7)	Hetero- geneous (8)	Steady (9)	Un- steady (10)	Satura- ted (11)	Unsat- urated (12)	Com- posite (13)
Klute, Whisler and Scott	1965 (53)	X			X				X		X	
Staple	1966 (96)	X			X				X		X	
Rubin	1966 (87)	X			X				X		X	
Whisler and Klute	1966 (114)	X				X			X		X	
Kobayashi	1966 (54)	X			X				X		X	
Freeze and Witherspoon	1966 (26)		X				X	X		X		
Burejev and Burejeva	1966 (15)		X				X		X	X		
Rubin	1967 (88)	X			X				X		X	
Remson et al.	1967 (82)	X			X				X		X	
Whisler and Klute	1967 (115)	X			X				X			X
Ibrahim and Brutsaent	1968 (38)	X			X				X		X	
Rubin	1968 (89)		X		X				X			X
Freeze	1969 (24)	X			X				X		X	

TABLE 1.--Continued.

Name (1)	Date and Reference (2)	Dimensions			Medium Characteristics			Flow Conditions		Saturation		
		1 (3)	2 (4)	3 (5)	Homo- geneous (6)	Layered (7)	Hetero- geneous (8)	Steady (9)	Un- steady (10)	Satura- ted (11)	Unsat- urated (12)	Com- posite (13)
Whisler and Watson	1969 (116)	X			X				X		X	
Taylor and Luthin	1969 (102)		X		X				X	X		
Hounberger et al.	1969 (35)		X				X		X			X
Jeppson	1970 (42)			X	X				X		X	
Green et al.	1970 (30)		X				X		X		X	
Todsen	1971 (104)		X		X				X	X		
Brandt et al.	1971 (6)			X	X				X		X	
Burtsaert et al.	1971 (12)		X		X				X			X
Freeze	1971 (25)		X				X		X			X
Burtsaert	1971 (11)		X				X		X			X
Wei and Jeppson	1971 (110)			X	X			X			X	
Jeppson	1974 (44)			X	X				X		X	
van Der Ploeg et al.	1974 (106)			X	X				X		X	
Amerman	1976 (2)		X		X			X				X

profile. Since the infiltration rate of the soil decreases with time, the calculated time increment will be smaller at the beginning of infiltration computation relative to its value at later stages. They plotted the distribution of the pressure head and water content versus depth for layered soils (coarse soils overlaying a fine soil and vice versa). They noticed that for water content, there is a discontinuity at the boundary between the two layers, however, pressure distribution along the profile was continuous for all cases of heterogeneity. There was excellent agreement between the Hanks and Bowers numerical model and theoretical solution presented by Scott et al. (93) and Philip (71) for horizontal infiltration through a horizontal layer of soil at uniform initial water content.

Ashcroft et al., (3) developed a numerical solution for solving a one dimensional horizontal flow equation in a semi-infinite porous medium. They indicated that the results of their numerical method and the Boltzman transformation used by Gardner and Mayhugh (28) gave very similar solutions. Also they found that the experimental results are similar to the solutions obtained from both numerical solution and Boltzman transform techniques.

Jeppson (42) numerically solved the partial differential equation which describes three dimensional (axisymmetric) unsaturated flow in the soil below infiltrometers to determine the influence of soil properties, rate of application- and initial hydraulic head on the subsurface flow pattern (penetration and lateral movement of wetting front). He noticed that whenever a portion of flow field reaches to high values of relative saturation approximately 0.90, depending on the hydraulic properties of the soil, numerical difficulties occur in

the solution process unless the time increment, $\Delta\tau$, is decreased sufficiently. He suggested that the solution capability can be improved by transforming the dependent variable (hydraulic head) in general flow equation to a new variable ξ by means of the Kirchhoff Transformation. This latter technique has been widely used by many researchers (78, 118, 75, 89, 6, 103, 108).

The goal of this transformation is to linearize (under some conditions) and make the equation of flow more amenable to analytical solution methods.

Jeppson (43) reported that for problems in which a portion of flow region approaches unit saturation, the use of the Kirchhoff-Transformation in formulation of the mathematical problem of partially saturated transient flow from an infiltrometer improved the solution capabilities.

Brand, et al. (6) developed two mathematical models (a plane flow model and a cylindrical model) to analyze multi-dimensional, unsteady infiltration from a trickle source into homogeneous soils. In the case of the cylindrical model (axisymmetric) the emitters were placed far enough apart to prevent interaction between emitters. Upon applying the Kirchhoff Transformation, they introduced a new function of water content. They compared the numerical results with Wooding's solution for steady state infiltration from a circular pond for different values of time to show how the unsteady flow approaches steady state flow. For verification of this model, Bresler, et al., (7) conducted laboratory experiments. They compared the location of wetting front and water content distribution in both numerical solution and by experiment. They

concluded the agreement between theory and experiment was good and that application of the theory to the field is justified.

Wei and Jeppson (110) studied the problem of steady-state axisymmetric infiltration of water applied on a horizontal surface, to determine the influence of various soil properties on the flow pattern as well as on the magnitude of lateral movement of soil moisture (spreading effect). They used an inverse formulation for solution of the problem by finite difference method. They reported that the infiltration rate is closely related to various soil parameters and infiltration rate is higher at the edge of source circle than near center due to the spreading effect.

Watson and Whisler (109) studied the gravity drainage of a heterogeneous porous media. They defined the heterogeneity of porous media in terms of a linear variation of the saturated hydraulic conductivity with depth. They allowed the hydraulic conductivity to decrease with depth and obtained hydraulic head and water content profiles with depth. They reported that by applying one of the available experimental methods for determining saturated hydraulic conductivity in the field at different depths, it is possible to check the homogeneity of the profile.

Jeppson (44) studied different numerical techniques for solution of transient, three dimensional (axisymmetric), unsaturated moisture movement through homogeneous soil resulting from infiltration over a horizontal circular surface area. To minimize the difficulties due to the strong nonlinearities of the flow equation, he compared the three adaptations of Crank-Nicolson method and three variations of the alternating direction implicit (ADI) method. Since no constraints have

been seen in applying Crank-Nicolson method, he favored this method. In another effort Jeppson (45) used the previous model (Jeppson, 44) and compiled a series solution for different problem specification such as size of the circle of application and for different parameters describing the hydraulic properties of unsaturated soils. He stated that greater understanding of the infiltration process can result when one problem specification is incremented over a range of possible situations. Samadi (90) used Jeppson's (41) computer one-dimensional program to evaluate the effect of interaction between the soil parameters used to describe heterogeneity. He concluded that there is a minor to insignificant effect on infiltration due to interaction between the soil parameters. Based on the results of study, the additive law of effect can be applied in using the results.

Darcy's Law for Saturated and Unsaturated Systems

Darcy's Law for Saturated Soils.--In 1856 Henry Darcy (19) observed the characteristics of downward flow of water through saturated sand filters, and published his famous experimental law. Darcy's law states that the flow of water through a column of saturated soil is directly proportional to the head loss and inversely proportional to the length of path of flow. Darcy (19) used various potential gradients across columns of saturated, homogeneous granular materials and measured the flows. He found that

$$V = - K \frac{\Delta h}{l} \quad (6)$$

where V is the flux $L^3 T^{-1} / L^2$; l is the length of the column, L ; Δh is $\Delta(P/\rho g + Z)$, difference in hydraulic head, L ; K is hydraulic

conductivity, coefficient with units of velocity depending on the permeability of porous media. Hydraulic conductivity is related to intrinsic permeability, k , of the medium with units of L^2 , by the expression $K = k\rho g/\mu$ (intrinsic permeability depends only on the internal geometry of the medium); P is the pressure head, FL^{-2} ; Z is the elevation head, L ; ρ is the density of the fluid, FT^2L^{-4} ; g is the acceleration of gravity, LT^{-2} and μ is the dynamic viscosity of the fluid $FT L^{-2}$.

This basic linear law of soil water flow was originally found for vertical downward flow through saturated homogeneous sand column.

Muskat (67) found applicability of Darcy's law in any direction of flow in the earth's gravity field and generalized Darcy's law for saturated flow in three dimensional space as follows:

$$\bar{V} = - K \text{ grad. } h \quad (7)$$

in which \bar{V} is the velocity vector, LT^{-1} and h is the hydraulic head, L .

The negative sign indicates that flow occurs in the direction of decreasing hydraulic head. Since flow can occur only through the interconnected pores of saturated porous media, the velocity across any section must be thought of in a statistical sense. Muskat (67) noted that application of Navier-Stokes equations for porous media problems is particularly difficult regardless of making some logical simplification and neglecting the inertia forces due to very low velocities. This is because the use of Navier-Stokes equations that describe flow in a microscopic way requires knowledge of all different size of pores, which is practically impossible. Hall (31) and Hubbert (37) proved analytically that Darcy's law is a statistical macroscopic equivalent

of the Navier-Stokes equations of motion for the flow of water through porous media.

The limitations of Darcy's Law are:

1. The velocity of flow must be relatively low in order to neglect inertia forces.
2. There must be no interaction between the soil and fluid.
3. The fluid must be homogeneous and incompressible.

Olsen (69, 70) found good agreement between Darcy's equation and seepage flow in nonswelling soils. He also reported on soils containing swelling type clay (montmorillonite), in which there is interaction between fluid and soil for which Darcy's law is not applicable since the velocity becomes a nonlinear function of the head gradient.

Swartzendruber (97, 98, 99) suggests that this deviation from linearity is primarily due to non-Newtonian behavior of the fluid caused by soil-water-interaction.

Darcy's Law for Unsaturated Media.--Even though Darcy's equation was developed for saturated flow in homogeneous porous media, it has application to porous media problems that are partially saturated. Two important forces act on an element of volume of soil water, namely the gravitational force causing the element to fall down, and the capillary forces tending to transfer the element from zones of higher to zones of lower pressure. Buckingham (13) who studied the capillary flow of soil water, visualized that the flow of water through the soil is analogous to heat flow (Fourier's law) and to flow of electricity through a conductor (Ohm's law). He introduced the term capillary potential (analogous to electric potential) to describe the attraction of soil for water.

Richards (85) applied the heat flow equation to unsaturated flow and assumed that the flow of water in unsaturated media obeys Darcy's law. He developed a general equation of flow in unsaturated media in which the water content and capillary conductivity are independent functions of the capillary potential. The theory (85) was proven experimentally by Childs and Collis-George (17) and analytically by Hall (31). According to this theory, Darcy's law holds for flow of water in unsaturated media. In a modified form in which hydraulic conductivity, K , is a function of the volumetric water content, θ , Darcy's law for the flow of water through unsaturated porous media can be written as follows:

$$\bar{V} = - K(\theta) \text{ grad. } h \quad (8)$$

in which K is a variable even for homogeneous soil and rapidly becomes smaller as the water content θ decreases (see Fig. 1). Philip (76) noted the following reasons for $K(\theta)$:

1. As the water content decreases the actual cross-section for flow decreases.
2. The value of hydraulic conductivity is dependent to the square of pore radius, $K = k\rho g/\mu$ and larger pores are emptied first as saturation decreases.
3. As saturation decreases, continuity of water at interconnected pores fails and there can be no flow in the liquid phase.

Relations of Saturation and Hydraulic Conductivity to Capillary Pressure

Water content of soils has been determined gravimetrically in the laboratory for many years. Field as well as laboratory measurement of

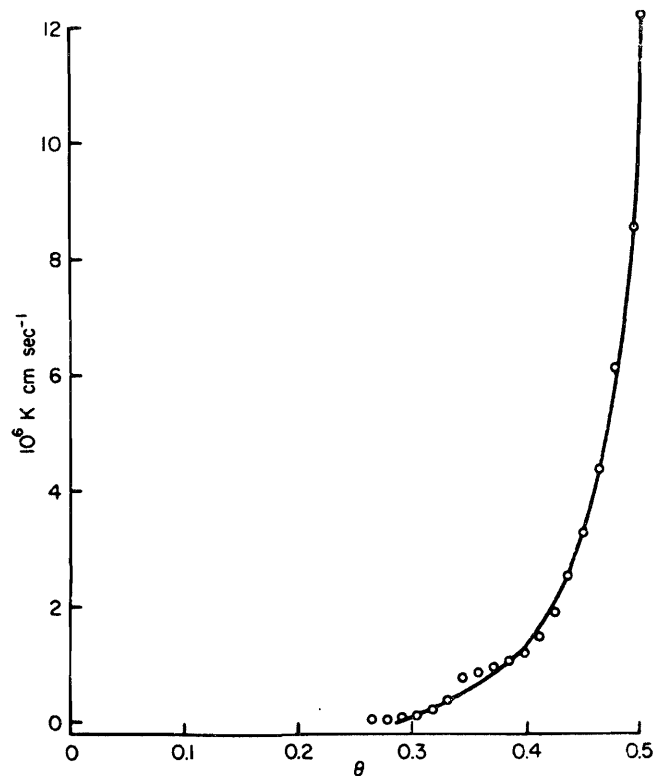


FIG. 1.--Relationship Between Hydraulic Conductivity, K , and Moisture Content, θ , for Yolo Light Clay (66).

water content can readily be obtained with devices such as the neutron meter or gamma probe. Tensiometers, pressure plates, and psychrometers are widely used to measure the capillary pressure (suction) in the partially saturated soils.

Buckingham (13), first suggested that water content and hydraulic conductivity of partially saturated soil are functions of capillary pressure. In order to obtain a solution to the flow equation, it is necessary to have functional relationships between saturation, capillary pressure and hydraulic conductivity. Klute (52) noted that less hysteresis is expected in the hydraulic conductivity-saturation relationship than in the hydraulic conductivity-capillary pressure relation. According to Child (16), Bear, Zaslavsky, and Irmay (39) and van Bavel (105), capillary pressure-saturation is hysteretic and

consequently the hydraulic conductivity-capillary pressure is hysteretic. Unfortunately, laboratory determinations of the capillary pressure-hydraulic conductivity relation are difficult and time consuming and in effect are impossible to obtain from field measurements.

The capillary pressure-hydraulic conductivity-saturation relationship is important in analyzing water movement through unsaturated soils. In order for the measured data to be useful in the numerical solution, they can be reduced in one of the following ways:

1. Tabular form of corresponding values of water content, hydraulic conductivity, and capillary pressure for their particular media (20, 32, 41, 115, 116, 33, 24, 30, 109).
2. Fitting the data with special functions (94, used exponential fits).
3. The functional forms of relationships in which some of these relationships are based on empirical fitting of data (27, 49). Some are based on conceptual idealized models of porous media "bundles of capillary tubes" coupled with empirical fitting (14).

The functional forms of these relationships in soil water flow modeling are highly desirable, especially when the relationship involves meaningful and measurable hydraulic and physical properties of the porous media. These relationships greatly reduce the computation time and computer storage space for the solution of flow problems and simplify the handling of input data and programming for solution of flow problems using the digital computer.

Saturation-Capillary Pressure Relations.--Taylor and Luthin (102) used the following equation:

$$\theta = \frac{\theta_0}{ah_s^3 + 1} \quad (9)$$

where, θ_0 , is the water content at saturation; h_s , suction head, and a is a soil parameter.

Brooks and Corey (8) carried out laboratory experiments on homogeneous and isotropic samples where air and water were nonwetting and wetting fluids, respectively. They found the experimental data of effective saturation S_e (defined in Equation 10 below) as a function of the ratio of capillary pressure to bubbling pressure plots close to a straight line on log-log graph paper for capillary pressure P_c greater than the bubbling pressure P_b (Fig. 2). Brooks and Corey suggested the empirical relationship of the following form:

$$S_e = \left(\frac{P_b}{P_c} \right)^\lambda, \text{ for } |P_c| \geq |P_b| \quad (10)$$

$$S_e = 1., \text{ for } |P_c| < |P_b| \quad (11)$$

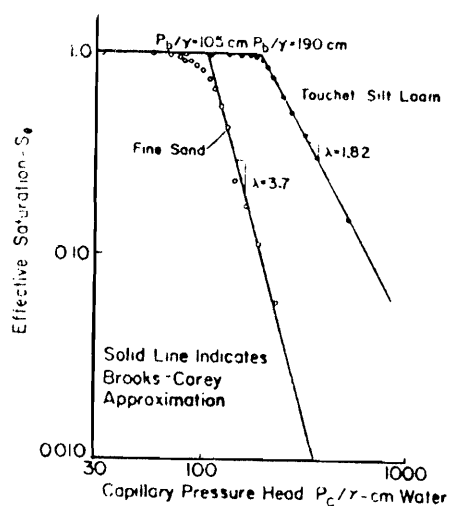


FIG. 2.--Relation Between Effective Saturation and Capillary Pressure Head (9).

in which λ is the negative of the slope of the plot on log-log graph paper and is defined as the pore-size distribution index. They found that for typical porous media λ is about 1.0, and ranges from 0.4 for aggregated clay soil to 5 or more for clean uniform sand. The λ is a dimensionless soil parameter and may depend on the liquid and capillary history of the system for some soils. Capillary pressure at $S_e = 1$ is equal to bubbling pressure ($P_c = P_b$) at which the air first begins to flow through the media.

The effective saturation is defined by

$$S_e = \frac{(S - S_r)}{(1 - S_r)} \quad (12)$$

in which saturation, S , is the ratio of volume of water to volume of voids and S_r , residual saturation (irreducible water). Fig. 2 shows capillary pressure-saturation curves and the Brooks-Corey approximations.

Brutsaert (10) proposed a more general relationship between capillary pressure and effective saturation S_e where

$$S_e = \frac{1}{\left(\frac{P_c}{P_b}\right)^b + a} \quad (13)$$

in which a and b are parameters whose magnitude depends on the soil type. In the case of $a = 0$, the Brooks-Corey equation will result.

Su and Brooks (100) used a Pearson Type VIII distribution function to develop a retention function which describes the retention of fluids in porous media as follows:

$$P_c = P_f \left(\frac{S - S_r}{a} \right)^{-m'} \left(\frac{1 - S}{b} \right)^{\frac{bm'}{a}} \quad (14)$$

where P_c is the capillary pressure, P_f is the capillary pressure at the fictitious inflection point, S is the saturation, m' the shape function of the retention curve, and therefore is a pore-size distribution parameter of the medium, and a and b are the domains of saturation separated by the fictitious inflection point (Fig. 3). The function was verified experimentally on the drainage and imbibition cycles. They assumed the Burdine integral is valid. Therefore, the relative hydraulic conductivity has been derived through the substitution of the retention function of the pressure, P , in the Burdine equation giving:

$$K_r = (S_e)^2 I_{S_e} \left(2m' + 1, \frac{-2bm'}{a} + 1 \right) \quad (15)$$

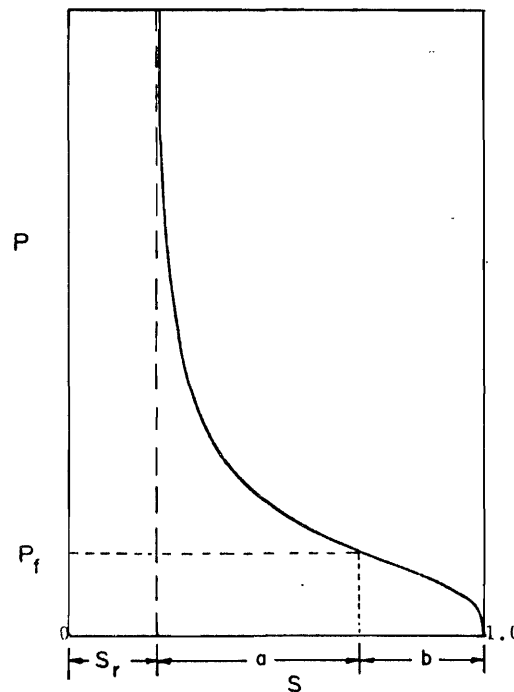


FIG. 3.--Definitive Retention Curves Depicting the Relationships of the Parameters in the Theoretical Retention Function (100).

where I_{S_e} is the incomplete beta function ratio with its arguments given in the parentheses.

Saturation-Hydraulic Conductivity Relations.--Irmay (39) used the following relation to relate saturation to hydraulic conductivity:

$$K_r = \frac{K}{K_0} = S_e^3 \quad (16)$$

in which K is the unsaturated hydraulic conductivity; K_0 is the saturated hydraulic conductivity and K_r is relative hydraulic conductivity.

The theory developed by Burdine (14) can be used with saturation-capillary pressure relations for determining saturation-hydraulic conductivity relationships. The use of Burdine theory are discussed by Brooks and Corey (8, 9). Fig. 4 shows that computed relative hydraulic conductivities from imbibition saturation pressure data, which were obtained from laboratory tests on distributed soil samples taken from the Reynolds Creek Experimental Watershed in southwestern Idaho, can produce satisfactory values when compared with observed values. Hydraulic conductivities computed by numerical integration of the modified Burdine Equation (17) are in good agreement with those obtained from equations developed by Millington and Quirk (63, 64), especially under desaturation conditions. To handle imbibition, a pressure head parameter P_0 is added to capillary pressure P to prevent division by zero as the soil becomes fully saturated, $P = 0$, and the saturation parameter, S_s , is replaced by 1.

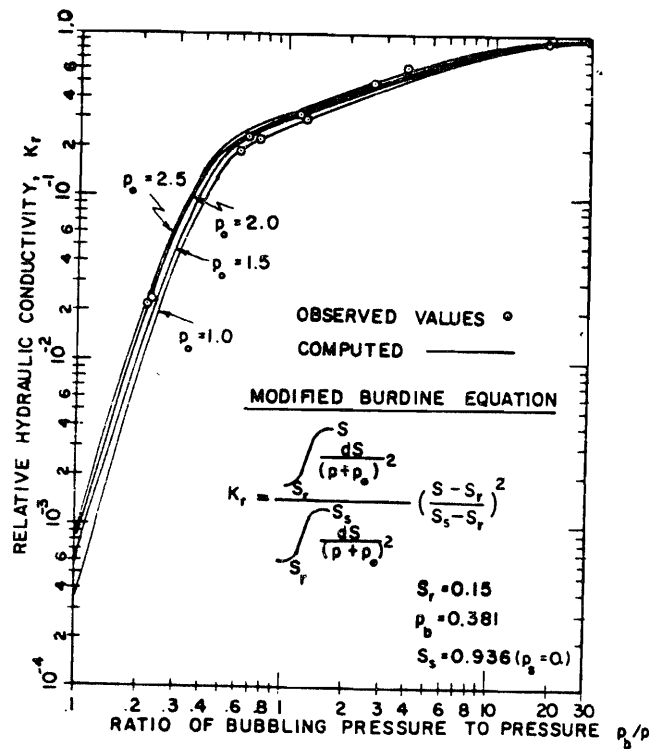


FIG. 4.--Comparison of Hydraulic Conductivities Computed from Saturation-Pressure Data by a Modified Burdine Equation, with Those Measured in the Laboratory (46).

$$K_r = \left[\frac{S - S_r}{S_s - S_r} \right]^2 \frac{\int_{S_r}^S \frac{ds}{(P + P_0)^2}}{\int_{S_r}^{S_s} \frac{ds}{(P + P_0)^2}} \quad (17)$$

in which P is the capillary pressure, L .

The modified Burdine equation (integral) for relative hydraulic conductivity in a simple form is given by Brooks and Corey (9) as:

$$K_r = \left[\frac{S - S_r}{1 - S_r} \right]^2 \frac{\int_0^S \frac{ds}{P_c^2}}{\int_0^1 \frac{ds}{P_c^2}} \quad (18)$$

Substituting Equation (10) into Equation (18) and changing S to S_e will result in

$$K_r = (S_e)^2 \frac{\int_0^{S_e} (S_e)^{2/\lambda} dS_e}{\int_0^1 (S_e)^{2/\lambda} dS_e} \quad (19)$$

upon integration of Equation (19), the relative hydraulic conductivity becomes:

$$K_r = (S_e)^{\frac{2 + 3\lambda}{\lambda}} \quad (20)$$

$$\epsilon = \frac{2 + 3\lambda}{\lambda} \quad (21)$$

When Equation (10) is substituted into Equation (20), the relative hydraulic conductivity as a function of capillary pressure is:

$$K_r = \frac{K}{K_0} = \left(\frac{P_b}{P_c} \right)^{2 + 3\lambda} \quad (22)$$

Application of the Brooks-Corey equations is limited to:

1. An isotropic porous media.
2. Relative hydraulic conductivities, $K_r = 1$ for $|P_c| < |P_b|$.
3. Conditions for which $S < S_r$, and even they are inaccurate at saturation slightly greater than S_r .

4. Stable porous media.

Hydraulic Conductivity-Capillary Pressure Relations.-- Richards (85) proposed a linear relation for hydraulic conductivity-capillary pressure which was used in some analytical solutions in the form

$$K_r = aH + b \quad (23)$$

in which a and b are constants; H is pressure head, $H = \frac{P_c}{\rho g}$

Gardner (27) made a survey of proposed equations and from studies of available data concluded that conductivity can be related to the capillary pressure by the following equation

$$K = \frac{a}{h_s^n + b} \quad (24)$$

where a, b, and n are constants depending on the soil, fluid and capillary pressure history of the system.

Taylor and Luthin (102) used the equation of the form

$$K = \frac{K_0}{ah_s^e + 1} \quad (25)$$

in which a is a constant.

Sewell and van Schilfgaarde (95) used the following equation

$$K_r = \frac{a}{P_c^b + a} \quad (26)$$

in which a and b are constants.

Wesseling and Wit (111) applied the relation in the form

$$k = ah_s^{-b} \quad (27)$$

where a and b are constants.

Raats (78) used the following equation

$$K = be^{aH} \quad (28)$$

in which a and b are constants. In this equation hydraulic conductivity is an exponential function of pressure head.

Brooks and Corey (8) used the Burdine (14) equation of relative hydraulic conductivity and their saturation-capillary pressure relation as presented earlier to derive the following equation

$$K_r = \left[\frac{P_b}{P_c} \right]^{2 + 3\lambda} \quad (29)$$

Experimental data from large number of soils show that equation (29) fits experimental data except for values of capillary pressure very close to the bubbling pressure.

King (49) found that the equation proposed by Gardner (27) is dimensionally inconsistent. He modified Gardner's equation and suggested the following dimensionless equation:

$$K_r = \frac{1}{\left(\frac{P_c}{P_1} \right)^a + b} \quad (30)$$

where a and b are positive dimensionless parameters. The parameter P_1 is positive having the same dimensions as P_c . King (49) found that the modified Gardner's equation gave a good fit to imbibition as well as

to drainage data. The Brooks-Corey equation and Gardner's approximation which was modified by King (49) are well known and widely used in solving unsaturated flow problems.

MODELING OF WATER MOVEMENT THROUGH POROUS MEDIA

Modeling is a process whereby physical conditions are simulated by using suitable mathematical equations (mathematical model). The steps involved in development of such models are:

1. Definition of physical problem
2. Mathematical model.

Definition of the Physical Problem

The particular problem which is described herein is that of unsteady unsaturated three-dimensional axisymmetric infiltration through heterogeneous soil from a circular horizontal area. The circular area over which the water enters the soil is very small compared with the total soil surface. Therefore, three-dimensional axisymmetric unsteady-unsaturated infiltration of water occurs. The water region of seepage below the water entry zone are symmetric about the vertical centerline. Therefore, the boundary value problem can be formulated for one half of any vertical plane containing the centerline of axis of symmetry. Fig. 5 shows the physical problem and typical assumed boundaries of the flow field. The soil is treated as a heterogeneous medium by letting the saturated hydraulic conductivity, K_0 , the soil porosity, n , residual saturation, S_r , pore size distribution exponent, λ , and bubbling pressure, P_b , be any continuous functions of the vertical coordinate. The soil is assumed to be isotropic. Since only the wetting cycle occurs in the solution, hysteresis is not considered in the soil characteristic

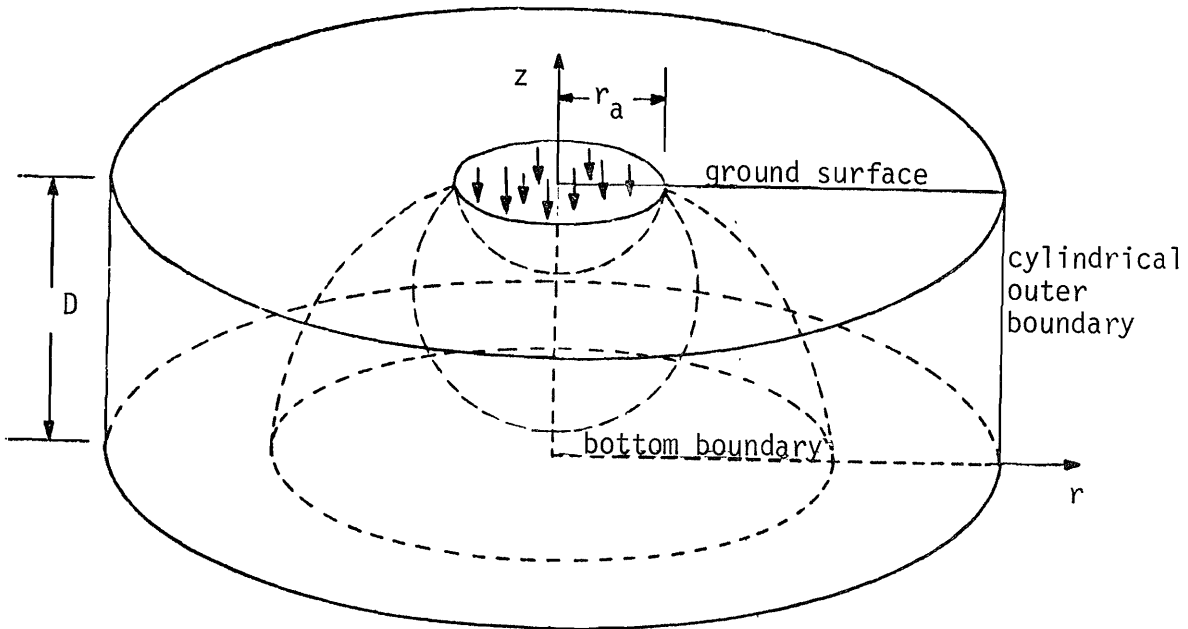


FIG. 5.--Physical Conditions Representing Three-Dimensional Axisymmetric Transient Unsaturated Flow Through Heterogeneous Media From a Circular Application Area.

relationships. The effect of evaporation from the soil surface is neglected.

The Mathematical Model

The mathematical model consists of the partial differential equations of flow through porous media which provide the basis for specification of the functioning system, together with the boundary and initial conditions. Assumptions are also made in the mathematical formulation and in analyzing the problem.

Assumptions in the Mathematical Formulation.--The following assumptions are included in the definition of the flow equation:

1. Darcy's law is valid in both saturated and unsaturated portions of the flow region. Inertia effects are neglected.
2. The water is incompressible ($\rho = \text{constant}$).
3. The porous medium is stable (exhibits no swelling, shrinkage or consolidation, $\eta = \text{constant}$ at any depth with time, but may be variable with depth).
4. Only the liquid phase of water is considered. Water vapor flow is neglected (vapor flow is small compared with the liquid flow).
5. No osmotic potentials affect the flow.
6. The flow is assumed to be isothermal.
7. The condition of flow is not affected by the biological process (uptake by plant, or biological action that may change the conductivity with time, etc.).
8. There is no interaction between soil and water.
9. The functions which describe the flow and their derivatives are assumed to be continuous, so that the differential form of the continuity equation is to be valid.
10. Air in the unsaturated parts of the system is assumed to be at atmospheric pressure, and there is no entrapped air in the system.
11. Since only the imbibition cycle is considered, it is assumed that the capillary pressure and hydraulic conductivity of the porous medium are single-valued, unique and continuous with soil water content (no hysteresis).

DIFFERENTIAL EQUATIONS FOR DESCRIBING WATER MOVEMENT IN SOILS

Continuity Equation in Cylindrical Coordinates

In axisymmetric flow problems, it is convenient to work with cylindrical coordinates. Since the pattern of axisymmetric flow is the same in all planes containing the axis of symmetry, (the Z-axis), it is independent of ϕ in cylindrical coordinate (Z, R, ϕ) with the exception of spiral type flow. Axisymmetric flow has no ϕ -component of velocity. The interrelationship of the coordinates for point G is shown in Fig. 6.

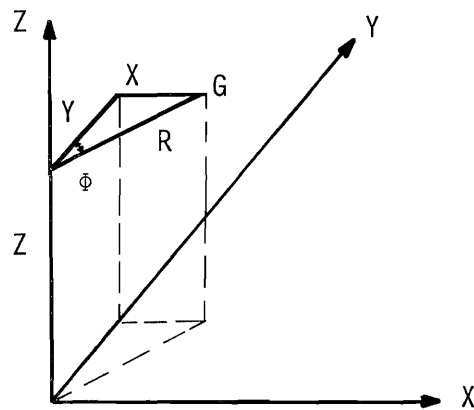


FIG. 6.--Coordinate System. The Coordinates of Point G are: Cartesian: X, Y, Z and Cylindrical: Z, R, ϕ .

Now, consider an elemental portion of a cylinder of dimensions δZ , δR , $\delta \phi$, through which fluid is flowing (Fig. 7). Assume the velocity at the center of the element, whose axis is parallel to the Z-axis, is V , and its axial, radial and tangential components are W , V_r and V_ϕ , respectively. The net gain in mass per unit time within a cylindrical element of three pairs of faces are:

$$\text{a. Axial} \quad - \frac{\partial}{\partial Z} (\rho W \cdot R \delta \phi \cdot \delta R) \delta Z \quad (31)$$

$$\text{b. radial} \quad - \frac{\partial}{\partial R} (\rho V_r \cdot R \delta \phi \cdot \delta Z) \delta R \quad (32)$$

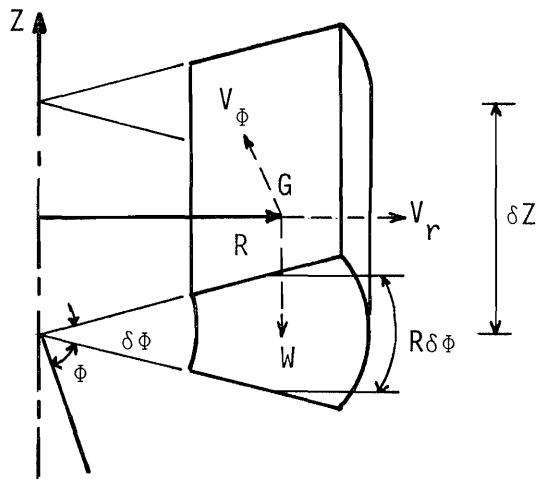


FIG 7.--Equation of Continuity in Cylindrical Coordinates.

$$c. \text{ Tangential} \quad - \frac{1}{R\delta\phi} (\rho V_{\phi} \cdot \delta R \cdot \partial Z) R\delta\phi \quad (33)$$

The total gain in mass per unit time of all faces is:

$$- \left[\frac{\partial}{\partial Z} (\rho W \cdot R\delta\phi \cdot \delta R) \delta Z + \frac{\partial}{\partial R} (\rho V_r \cdot R\delta\phi \cdot \delta Z) \delta R + \frac{1}{R\delta\phi} (\rho V_{\phi} \cdot \delta R \cdot \delta Z) R\delta\phi \right] \quad (34)$$

which should equal the time rate of increase in mass within the element

$$\frac{\partial}{\partial t} (\rho \cdot R\delta\phi \cdot \delta R \cdot \delta Z \cdot \theta) = \frac{\partial(\rho \cdot \theta)}{\partial t} (R\delta\phi \cdot \delta R \cdot \delta Z) \quad (35)$$

in which ρ is the density of water; and θ is soil water content on volume basis, thus

$$\begin{aligned} - \left[\frac{\partial}{\partial Z} (\rho W \cdot R\delta\phi \cdot \delta R) \delta Z + \frac{\partial}{\partial R} (\rho V_r \cdot R\delta\phi \cdot \delta Z) \delta R + \frac{1}{R\delta\phi} (\rho V_{\phi} \cdot \delta R \cdot \delta Z) R\delta\phi \right] \\ = \frac{\partial(\rho \cdot \theta)}{\partial t} (R\delta\phi \cdot \delta R \cdot \delta Z) \end{aligned} \quad (36)$$

Dividing the above equation by the volume element $(R\delta\phi \cdot \delta R \cdot \delta Z)$ yields the equation of continuity in cylindrical coordinate.

$$\frac{\partial(\rho W)}{\delta Z} + \frac{1}{R} \frac{\partial}{\partial R} (\rho V_r \cdot R) + \frac{1}{R\delta\phi} (\rho V_{\phi}) = - \frac{\partial(\rho \cdot \theta)}{\partial t} \quad (37)$$

for an incompressible fluid, ρ is constant, therefore

$$\frac{\partial W}{\delta Z} + \frac{1}{R} \frac{\partial}{\partial R} (V_r \cdot R) + \frac{1}{R} \frac{\partial V_{\phi}}{\partial \phi} = - \frac{\partial(\theta)}{\partial t} \quad (38)$$

In axisymmetric flow the transverse of tangential velocity $V_{\phi} = 0$ and equation of continuity becomes as:

$$\frac{\partial W}{\partial Z} + \frac{1}{R} \frac{\partial}{\partial R} (V_r \cdot R) = - \frac{\partial \theta}{\partial t} \quad (39)$$

$$\frac{\partial W}{\partial Z} + \frac{V_r}{R} + \frac{\partial(V_r)}{\partial R} = - \frac{\partial \theta}{\partial t} \quad (40)$$

Let,

$$\theta = \eta S \quad (41)$$

where η is the soil porosity; S is the soil saturation, which is the ratio of volume of water to volume of voids in a soil elemental volume. Equation (40) becomes

$$\frac{\partial W}{\partial Z} + \frac{V_r}{R} + \frac{\partial V_r}{\partial R} = - \eta \frac{\partial S}{\partial t} \quad (42)$$

The General Flow Equation

For homogeneous porous media, the Brooks and Corey's equations can be written as:

$$S_e = \frac{S - S_r}{1 - S_r} \quad (43)$$

$$S_e = \left(\frac{P_b}{P_t} \right)^\lambda \quad (44)$$

$$K_r = \left(\frac{P_b}{P_t} \right)^{2+3\lambda} \quad (45)$$

Therefore in case of heterogeneous porous media the saturation

and relative hydraulic conductivity can be obtained by the following equations, respectively:

$$S = S_r(z) + [1 - S_r(z)] \left[\frac{P_b(z)}{P_t(r,z)} \right]^{\lambda(z)} \quad (46)$$

and

$$K_r = \left[\frac{P_b(z)}{P_t(r,z)} \right]^{2+3\lambda(z)} \quad (47)$$

in which S is the saturation and varies as a function of depth and radial position; S_r is the residual saturation and is a given function of depth; P_b equals $P'_b/\gamma L$, is the dimensionless bubbling pressure, and is a given function of depth; P_t equals $P_c/\gamma L$, and is the dimensionless pressure head, and varies as a function of r and t ; r equals R/L and is the dimensionless radial coordinate; z equals Z/L and is the dimensionless axial coordinate; λ equals pore size distribution exponent and is a given function of depth; L equals a scaling length used to non-dimensionalize the radial and axial coordinates and pressure heads; K_r equals K/K_0 and is the relative hydraulic conductivity at each position in which K is the effective hydraulic conductivity and K_0 is the saturated hydraulic conductivity, which is constant for homogeneous soil.

The saturated hydraulic conductivity, K_0 , is defined as the product of a constant K_a , with units of velocity, and a dimensionless quantity which is a given function of the depth K_v , or

$$K_0(z) = K_a K_v(z) \quad (48)$$

where for the soil surface, the value of constant K_a will be taken equal to the saturated hydraulic conductivity on the surface; therefore $K_V(z) = 1.0$ on the soil surface. The effective hydraulic conductivity with velocity dimensions is defined as the saturated hydraulic conductivity, K_0 , multiplied by the relative hydraulic conductivity K_r .

$$K = K_0(z) K_r \quad (49)$$

$$K = K_a K_V(z) K_r (P_b, \lambda, P_t) \quad (50)$$

For three dimensional axisymmetric seepage flow through a porous medium, Darcy's law gives the velocity component in the radial, r , and axial, z , coordinate directions, respectively by:

$$h = Z + P_c \quad (51)$$

$$h_t = \frac{h}{\gamma L} \quad (52)$$

$$z = \frac{Z}{L} \quad (53)$$

$$r = \frac{R}{L} \quad (54)$$

$$P_t = \frac{-P_c}{\gamma L} \quad (55)$$

$$h_t = z - P_t \quad (56)$$

$$V_r = -K \frac{\partial h_t}{\partial r} = -K \left(\frac{\partial(z - P_t)}{\partial r} \right) = K \frac{\partial P_t}{\partial r} \quad (57)$$

$$W = -K \frac{\partial h_t}{\partial z} = -K \frac{\partial(z - P_t)}{\partial z} = K \left(\frac{\partial P_t}{\partial z} - 1 \right) \quad (58)$$

in which $K(r,z,p)$ is the hydraulic conductivity of the soil with a dimension of velocity, and h is the potential energy per unit weight of water with dimension of length as the sum of elevation head Z and pressure head P_c .

The pressure head is given by

$$P_c = \frac{P}{\rho g} = \frac{P}{\gamma} \quad (59)$$

in which P is the pressure of water and is positive for saturated zones and negative for partially saturated zones, g is the acceleration of gravity and ρ is the fluid density.

The partial differential equation which describes water movement through the heterogeneous soils can be derived by substituting Darcy's law into the differential form of the continuity of mass equation for three dimensional axisymmetric flow.

From Brook-Corey's Equation (46) we have

$$\begin{aligned} \frac{\partial S}{\partial t} &= \frac{S_r}{t} + \frac{\partial \left[(1-S_r) \left(\frac{P_b}{P_t} \right)^\lambda \right]}{\partial t} \\ &= (1 - S_r) \cdot \lambda \cdot \left(\frac{P_b}{P_t} \right)^{\lambda-1} \frac{\partial}{\partial t} \left(\frac{P_b}{P_t} \right) \\ &= (1 - S_r) \lambda \left(\frac{P_b}{P_t} \right)^{\lambda-1} \cdot \frac{P_t \frac{\partial P_b}{\partial t} - P_b \frac{\partial P_t}{\partial t}}{P_t^2} \\ &= - \lambda (1 - S_r) \frac{P_b^\lambda}{P_t^{\lambda+1}} \frac{\partial P_t}{\partial t} \end{aligned} \quad (60)$$

substituting seepage velocity components, Equations (57) and (58) and

term $\frac{\partial S}{\partial t}$ in the equation of continuity in cylindrical coordinates, Equation (42) we have

$$\frac{\partial(K \frac{\partial P_t}{\partial r})}{\partial R} + \frac{\partial[K(\frac{\partial P_t}{\partial z} - 1)]}{\partial Z} + \frac{K}{R} \frac{\partial P_t}{\partial r} = \frac{\eta\lambda(1-S_r)}{P_t} \left(\frac{P_b}{P_t}\right)^\lambda \frac{\partial P_t}{\partial t} \quad (61)$$

Hydraulic conductivity is defined as Equation (50) and let dimensionless time

$$\tau = \frac{K_a}{L} t \quad (62)$$

$$t = \frac{\tau L}{K_a} \quad (63)$$

$$dt = d\left(\frac{\tau L}{K_a}\right) = \left(\frac{L}{K_a}\right) d\tau \quad (64)$$

Substituting Equations (50) and (64) in Equation (61) and letting $R = rL$ and $Z = zL$, we have

$$\frac{K_a K_v \partial(K_r \frac{\partial P_t}{\partial r})}{L \partial r} + \frac{K_a \partial[K_v K_r (\frac{\partial P_t}{\partial z} - 1)]}{L \partial z} + \frac{K_a K_v K_r}{L r} \frac{\partial P_t}{\partial r} = \frac{\eta\lambda(1-S_r)}{P_t} \left(\frac{P_b}{P_t}\right)^\lambda \frac{K_a \partial P_t}{L \partial \tau} \quad (65)$$

Dividing Equation (65) by K_a and multiplying by L , the equation of flow in dimensionless form after using Brooks and Corey's Equation (60) is used to evaluate $\frac{\partial S}{\partial t}$ is

$$\frac{K_v \partial(K_r \frac{\partial P_t}{\partial r})}{\partial r} + \frac{\partial[K_v K_r (\frac{\partial P_t}{\partial z} - 1)]}{\partial z} + \frac{K_v K_r}{r} \frac{\partial P_t}{\partial r} = \frac{\eta\lambda(1-S_r)}{P_t} \left(\frac{P_b}{P_t}\right)^\lambda \frac{\partial P_t}{\partial \tau} \quad (66)$$

Rewriting Brooks-Corey's equation for heterogeneous media:

$$K_r = \left[\frac{P_b(z)}{P_t(r,z)} \right]^{2+3\lambda(z)} \quad (67)$$

$$\ln K_r = (2+3\lambda) \ln \left(\frac{P_b}{P_t} \right) \quad (68)$$

$$K_r = e^{(2+3\lambda) \ln \left(\frac{P_b}{P_t} \right)} \quad (69)$$

$$\frac{\partial K_r}{\partial z} = \frac{\partial K_r}{\partial P_b} \cdot \frac{\partial P_b}{\partial z} + \frac{\partial K_r}{\partial \lambda} \cdot \frac{\partial \lambda}{\partial z} + \frac{\partial K_r}{\partial P_t} \cdot \frac{\partial P_t}{\partial z} \quad (70)$$

$$\begin{aligned} \frac{\partial K_r}{\partial P_b} &= (2+3\lambda) \frac{P_b^{(1+3\lambda)}}{P_t^{(2+3\lambda)}} \\ &= (2+3\lambda) \frac{K_r}{P_b} \end{aligned} \quad (71)$$

$$\frac{\partial K_r}{\partial \lambda} = e^{(2+3\lambda) \ln \left(\frac{P_b}{P_t} \right)} \cdot \left[3 \ln \left(\frac{P_b}{P_t} \right) \right] \quad (72)$$

since

$$K_r = e^{(2+3\lambda) \ln \left(\frac{P_b}{P_t} \right)} \quad (73)$$

$$\frac{\partial K_r}{\partial \lambda} = 3 K_r \ln \left(\frac{P_b}{P_t} \right) \quad (74)$$

$$\begin{aligned} \frac{\partial K_r}{\partial P_t} &= \frac{- (2+3\lambda) P_t^{(1+3\lambda)} \cdot P_b^{(2+3\lambda)}}{P_t^{2(2+3\lambda)}} \cdot \frac{P_t}{P_t} \\ &= - (2+3\lambda) \frac{K_r}{P_t} \end{aligned} \quad (75)$$

Therefore

$$\frac{\partial K_r}{\partial z} = K_r \left[\frac{(2+3\lambda)}{P_b} \cdot \frac{\partial P_b}{\partial z} + 3 \ln \left(\frac{P_b}{P_t} \right) \frac{\partial \lambda}{\partial z} - \frac{(2+3\lambda)}{P_t} \frac{\partial P_t}{\partial z} \right] \quad (76)$$

$$\begin{aligned} \frac{\partial K_r}{\partial r} &= \frac{\partial K_r}{\partial P_t} \cdot \frac{\partial P_t}{\partial r} \\ &= - (2+3\lambda) \frac{K_r}{P_t} \cdot \frac{\partial P_t}{\partial r} \end{aligned} \quad (77)$$

Substituting Equation (76) and (77) in the Equation (66) we have

$$K_v \frac{\partial (K_r \frac{\partial P_t}{\partial r})}{\partial r} + \frac{\partial [K_v K_r (\frac{\partial P_t}{\partial z} - 1)]}{\partial z} + \frac{K_v K_r}{r} \frac{\partial P_t}{\partial r} - \frac{\eta \lambda (1-S_r)}{P_t} \left(\frac{P_b}{P_t} \right)^\lambda \frac{\partial P_t}{\partial \tau} = 0 \quad (78)$$

$$[K_v K_r \frac{\partial (\frac{\partial P_t}{\partial r})}{\partial r} + K_v (\frac{\partial P_t}{\partial r}) (\frac{\partial K_r}{\partial r})] + [K_v (K_r \frac{\partial (\frac{\partial P_t}{\partial z} - 1)}{\partial z} + (\frac{\partial P_t}{\partial z} - 1) \frac{\partial K_r}{\partial z})] \quad (79)$$

$$+ K_r (\frac{\partial P_t}{\partial z} - 1) \frac{\partial K_r}{\partial z}] + [\frac{K_v K_r}{P_t} \frac{\partial P_t}{\partial r}] - \frac{\eta \lambda (1-S_r)}{P_t} \left(\frac{P_b}{P_t} \right)^\lambda \frac{\partial P_t}{\partial \tau} = 0$$

$$[K_v K_r \frac{\partial^2 P_t}{\partial r^2} + K_v (\frac{\partial P_t}{\partial r}) (-\frac{2+3\lambda}{P_t} K_r \frac{\partial P_t}{\partial r})] + [K_v K_r \frac{\partial^2 P_t}{\partial z^2} + K_v (\frac{\partial P_t}{\partial z} - 1) \cdot \quad (80)$$

$$\begin{aligned} &K_r \left(\frac{2+3\lambda}{P_b} \cdot \frac{\partial P_b}{\partial z} + 3 \ln \left(\frac{P_b}{P_t} \right) \cdot \frac{\partial \lambda}{\partial z} - \frac{2+3\lambda}{P_t} \cdot \frac{\partial P_t}{\partial z} \right) + K_r \left(\frac{\partial P_t}{\partial z} - 1 \right) \frac{\partial K_v}{\partial z}] \\ &+ [\frac{K_v K_r}{r} \frac{\partial P_t}{\partial r}] - \frac{\eta \lambda (1-S_r)}{P_t} \left(\frac{P_b}{P_t} \right)^\lambda \frac{\partial P_t}{\partial \tau} = 0 \end{aligned}$$

dividing Equation (80) by K_r

$$\begin{aligned}
 & K_v \frac{\partial^2 P_t}{\partial r^2} - \frac{2+3\lambda}{P_t} K_v \left(\frac{\partial P_t}{\partial r} \right)^2 + K_v \frac{\partial^2 P_t}{\partial z^2} + \left(\frac{\partial P_t}{\partial z} - 1 \right) \left[K_v \left(\frac{2+3\lambda}{P_b} \frac{\partial P_b}{\partial z} \right. \right. \\
 & \left. \left. + 3 \ln \left(\frac{P_b}{P_t} \right) \frac{\partial \lambda}{\partial z} - \frac{2+3\lambda}{P_t} \frac{\partial P_t}{\partial z} \right) + \frac{\partial K_v}{\partial z} \right] + \frac{K_v}{r} \frac{\partial P_t}{\partial r} - \frac{n\lambda(1-S_r)}{P_t K_r} \\
 & \left(\frac{P_b}{P_t} \right)^\lambda \frac{\partial P_t}{\partial \tau} = 0 \tag{81}
 \end{aligned}$$

Equation (81) is a nonlinear parabolic partial differential equation, since the right hand side does not vanish. For the initially unsaturated soils the flow equation will remain parabolic at all times, since saturation occurs at most only at the surface of water application.

To obtain the required finite difference solutions to the initial-boundary value problem, a number of computer programs were written. Whenever there is an abrupt wetting front, the solution is less accurate than desirable even though a solution might be obtained. Across the wetting front, the change is too rapid for the second degree polynomial used in the finite differences equations to duplicate. Therefore, the continuous variables P_t or h_t are not defined adequately, a condition which is aggravated by the strongly nonlinear nature of the partial differential equation. Jeppson (43) indicated that a more straight forward approach is to introduce a new dependent variable by means of a Kirchhoff-Transformation (Ames, 1), that changes by a relative small amount at higher capillary pressure in comparison to its magnitude changes at low capillary pressure. This modification is necessary since across the wetting front the capillary pressure varies

rapidly from a large positive to a moderately negative magnitude. The introduced dependent variable obtained by applying the Kirchhoff-Transformation varies more smoothly across the wetting front than capillary pressure head, P_t , or the hydraulic head, h_t .

The Kirchhoff-Transformation is:

$$\psi = \int_1^{P_t} K_r d P_t' \quad (82)$$

in which P_t' is a dimensionless dummy variable of integration.

In the case of heterogeneous soils where the S_r , P_b , and λ are variable parameters in the Brooks-Corey's equations, using the Kirchhoff-Transformation will not produce a relationship between the new dependent variable and pressure head as it does for homogeneous soils. The integration of the Equation (82) is not possible for heterogeneous soils, because λ is a function of depth. For the integration it is necessary to define a specific variation of λ for a given problem. The Brooks-Corey Equation can be written as:

$$K_r = \left(\frac{P_b}{P_t} \right)^{2+3\lambda} \quad (83)$$

and define P_e as

$$P_e = \left(\frac{P_b}{L} \right)^{2+3\lambda} \quad (84)$$

$$K_r = P_e P_t^{-(2+3\lambda)} \quad (85)$$

and integration of Equation (82) in the case of homogeneous soil produces

$$\psi = \frac{1 - p_t^{-(1+3\lambda)}}{(1+3\lambda)} \quad (86)$$

For the integration of Equation (82) it is not desirable to have it be restricted to a functional variation of $\lambda(z)$, that allows it to be integrated. An alternative which introduces a new dependent variable ξ is defined by the equation

$$\xi = \frac{1 - p_t^{-(1+3\lambda_0)}}{1 + 3\lambda_0} \quad (87)$$

$$\zeta = [1 - (1+3\lambda_0)\xi] \quad (88)$$

$$p_t = [1 - (1+3\lambda_0)\xi]^{-\frac{1}{(1+3\lambda_0)}} = \zeta^{-\frac{1}{(1+3\lambda_0)}} \quad (89)$$

where λ_0 is a reference value of $\lambda(z)$ (values of λ at soil surface $z = D$) Equation (86) is the same as Equation (87) only the λ and ψ replaced with λ_0 and ξ .

The new variable ξ has the desirable characteristics that it changes much less abruptly across the wetting front.

Now it is possible to express

$$\frac{\partial p_t}{\partial z}, \frac{\partial p_t}{\partial r}, \frac{\partial p_t}{\partial \tau}, \frac{\partial^2 p_t}{\partial z^2}, \text{ and } \frac{\partial^2 p_t}{\partial r^2}$$

in terms of the new dependent variable ξ and its derivatives:

$$\frac{\partial \zeta}{\partial \xi} = -(1+3\lambda_0) \quad (90)$$

$$\frac{\partial p_t}{\partial z} = \frac{\partial p_t}{\partial \xi} \frac{\partial \xi}{\partial z} \quad (91)$$

$$\begin{aligned}
\frac{\partial P_t}{\partial \xi} &= - \frac{1}{(1+3\lambda_0)} [- (1+3\lambda_0)] [1 - (1+3\lambda_0)\xi]^{-\frac{1}{1+3\lambda_0}} [1 - (1+3\lambda_0)\xi]^{-1} \\
&= + \left[\frac{(1 - (1+3\lambda_0)\xi)^{-\frac{1}{1+3\lambda_0}}}{[1 - (1+3\lambda_0)\xi]} \right] = + \frac{P_t}{[1 - (1+3\lambda_0)\xi]} \\
&= \frac{P_t}{\zeta}
\end{aligned} \tag{92}$$

Therefore

$$\frac{\partial P_t}{\partial z} = \frac{P_t}{\zeta} \frac{\partial \xi}{\partial z} \tag{93}$$

Also, we can write

$$\frac{\partial P_t}{\partial r} = \frac{\partial P_t}{\partial \xi} \frac{\partial \xi}{\partial r} \tag{94}$$

and

$$\frac{\partial P_t}{\partial \tau} = \frac{\partial P_t}{\partial \zeta} \frac{\partial \zeta}{\partial \tau} \tag{95}$$

Therefore, from Equation (92) we have

$$\frac{\partial P_t}{\partial r} = \frac{P_t}{\zeta} \frac{\partial \xi}{\partial r} \tag{96}$$

and

$$\frac{\partial P_t}{\partial \tau} = \frac{P_t}{\zeta} \frac{\partial \xi}{\partial \tau} \tag{97}$$

Now for the second derivatives we can write:

$$\frac{\partial^2 P_t}{\partial z^2} = \frac{\partial \left(\frac{P_t}{\zeta} \right)}{\partial z} = \frac{\partial \left(\frac{P_t}{\zeta} \frac{\partial \xi}{\partial z} \right)}{\partial z} = \frac{P_t}{\zeta} \frac{\partial^2 \xi}{\partial z^2} + \frac{\partial \xi}{\partial z} \frac{\partial (P_t/\zeta)}{\partial z} \tag{98}$$

$$\begin{aligned}
\frac{\partial(P_t/\zeta)}{\partial z} &= \left[\frac{\partial(P_t/\zeta)}{\partial \xi} \frac{\partial \xi}{\partial z} \right] = \frac{\partial \xi}{\partial z} \left[\frac{1}{\zeta} \frac{\partial P_t}{\partial \xi} + \frac{P_t}{\zeta} \frac{\partial(1/\zeta)}{\partial \xi} \right] \\
&= \frac{\partial \xi}{\partial z} \left[\frac{1}{\zeta} \frac{P_t}{\zeta} + P_t \frac{\partial(1/\zeta)}{\partial \xi} \right] \\
&= \frac{\partial \xi}{\partial z} \left[\frac{P_t}{\zeta^2} + \frac{-(-(1+3\lambda_0))}{[1-(1+3\lambda_0)\xi]^2} \right] = \left[\frac{P_t}{\zeta^2} + \frac{P_t(1+3\lambda_0)}{\zeta^2} \right] \frac{\partial \xi}{\partial z} \quad (99)
\end{aligned}$$

Therefore

$$\begin{aligned}
\frac{\partial^2 P_t}{\partial z^2} &= \frac{P_t}{\zeta} \frac{\partial^2 \xi}{\partial z^2} + \left(\frac{\partial \xi}{\partial z} \right)^2 \left[\frac{P_t}{\zeta^2} + \frac{P_t(1+3\lambda_0)}{\zeta^2} \right] \\
&= \frac{P_t}{\zeta} \left[\frac{\partial^2 \xi}{\partial z^2} + \frac{2+3\lambda_0}{\zeta} \left(\frac{\partial \xi}{\partial z} \right)^2 \right] \quad (100)
\end{aligned}$$

and

$$\frac{\partial^2 P_t}{\partial r^2} = \frac{\partial \left(\frac{\partial P_t}{\partial r} \right)}{\partial r} = \frac{\partial \left(\frac{P_t}{\zeta} \frac{\partial \xi}{\partial r} \right)}{\partial r} = \frac{P_t}{\zeta} \frac{\partial^2 \xi}{\partial r^2} + \frac{\partial \xi}{\partial r} \frac{\partial(P_t/\zeta)}{\partial r} \quad (101)$$

$$\begin{aligned}
\frac{\partial(P_t/\zeta)}{\partial r} &= \left[\frac{1}{\zeta} \frac{\partial P_t}{\partial r} + P_t \frac{\partial(1/\zeta)}{\partial r} \right] \\
&= \left[\frac{1}{\zeta} \frac{P_t}{\zeta} \frac{\partial \xi}{\partial r} + P_t \frac{\partial(1/\zeta)}{\partial \xi} \frac{\partial \xi}{\partial r} \right] \\
&= \left[\frac{P_t}{\zeta^2} \frac{\partial \xi}{\partial r} + P_t \frac{(1+3\lambda_0)}{[1-(1+3\lambda_0)\xi]^2} \frac{\partial \xi}{\partial r} \right] \\
&= \left[\frac{P_t}{\zeta^2} + \frac{P_t(1+3\lambda_0)}{\zeta^2} \right] \frac{\partial \xi}{\partial r} \quad (102)
\end{aligned}$$

Therefore

$$\frac{\partial^2 P_t}{\partial r^2} = \frac{P_t}{\zeta} \frac{\partial^2 \xi}{\partial r^2} + \left(\frac{\partial \xi}{\partial r} \right)^2 \left[\frac{P_t}{\zeta^2} + \frac{P_t(1+3\lambda_0)}{\zeta^2} \right]$$

$$= \frac{P_t}{\zeta} \left[\frac{\partial^2 \xi}{\partial r^2} + \frac{2+3\lambda_0}{\zeta} \left(\frac{\partial \xi}{\partial r} \right)^2 \right] \quad (103)$$

The Equations (93), (96), (100), and (103) are the first and second derivatives of dimensionless hydraulic head P_t with respect to dimensionless depth, z , and dimensionless radius, r , and Equation (97) is the first derivative of P_t with respect to dimensionless time, τ , in the Equation (81). The values of $\frac{\partial \lambda}{\partial z}$ and $\frac{\partial K_v}{\partial z}$, $\frac{\partial P_b}{\partial z}$, η , S_r , and λ_0 in the general flow equation are known from the specified variation of hydraulic properties of the soil.

Substituting appropriate values of derivatives in the Equation (81) the more general equation of three dimensional transient flow of water through unsaturated, heterogeneous media will result in Equation (105).

$$\begin{aligned} F = & K_v \left[\frac{P_t}{\zeta} \left(\frac{\partial^2 \xi}{\partial r^2} + \frac{(2+3\lambda_0)}{\zeta} \left(\frac{\partial \xi}{\partial r} \right)^2 \right) \right] - K_v \left[\frac{2+3\lambda}{P_t} \left(\frac{P_t}{\zeta} \frac{\partial \xi}{\partial r} \right)^2 \right] \\ & + K_v \left[\frac{P_t}{\zeta} \left(\frac{\partial^2 \xi}{\partial z^2} + \frac{2+3\lambda_0}{\zeta} \left(\frac{\partial \xi}{\partial z} \right)^2 \right) \right] + \left(\frac{P_t}{\zeta} \frac{\partial \xi}{\partial z} - 1 \right) \left[K_v \left(\frac{2+3\lambda_0}{P_b} \frac{\partial P_b}{\partial z} \right) \right. \\ & \left. + 3 \ln \left(\frac{P_b}{P_t} \right) \frac{\partial \lambda}{\partial z} - \frac{2+3\lambda}{\zeta} \frac{\partial \xi}{\partial z} \right] + \left[\frac{K_v}{r} \frac{P_t}{\zeta} \frac{\partial \xi}{\partial r} \right] \\ & - \left[\frac{\eta \lambda (1-S_r)}{P_t K_r} \left(\frac{P_b}{P_t} \right)^\lambda \frac{P_t}{\zeta} \frac{\partial \xi}{\partial \tau} \right] = 0 \end{aligned} \quad (104)$$

Simplifying the above equation and using $K_r = \left(\frac{P_b}{P_t} \right)^{2+3\lambda}$, the above equation becomes:

$$\begin{aligned}
F = K_V \{ & \frac{P_t}{\zeta} \left[\frac{\partial^2 \xi}{\partial r^2} + \frac{\partial^2 \xi}{\partial z^2} + \frac{2+3\lambda_0}{\zeta} \left(\left(\frac{\partial \xi}{\partial r} \right)^2 + \left(\frac{\partial \xi}{\partial z} \right)^2 \right) \right] - \frac{(2+3\lambda) P_t}{\zeta^2} \left(\frac{\partial \xi}{\partial r} \right)^2 \\
& + \left(\frac{P_t}{\zeta} \frac{\partial \xi}{\partial z} - 1 \right) \left[\frac{(2+3\lambda)}{P_b} \frac{\partial P_b}{\partial z} + 3 \ln \left(\frac{P_b}{P_t} \right) \left(\frac{\partial \lambda}{\partial z} \right) - \frac{(2+3\lambda)}{\zeta} \frac{\partial \xi}{\partial z} \right] \\
& + \frac{P_t}{r\zeta} \frac{\partial \xi}{\partial r} \} + \left(\frac{P_t}{\zeta} \frac{\partial \xi}{\partial z} - 1 \right) \frac{\partial K_V}{\partial z} - \frac{\eta\lambda(1 - S_r)}{P_b(2+2\lambda)} \cdot \frac{P_t^{2+2\lambda}}{\zeta} \cdot \frac{\partial \xi}{\partial \tau} = 0
\end{aligned}
\tag{105}$$

INITIAL AND BOUNDARY CONDITIONS

The equation of flow is a nonlinear parabolic type, consequently, initial conditions and boundary conditions for the geometry of the flow field are necessary.

The Initial Conditions

Initial conditions must be specified for transient problems, including the distribution of the hydraulic head and moisture content throughout the region of flow prior to infiltration. The results from any time step solution serve as an initial condition to the new time step. This will enable the user to terminate the solution after any time step and store the results on tape in which those computed values can be picked up again as the initial condition to continue the computation. To start the solution it is assumed that prior to infiltration the movement of water is negligible everywhere in the soil and that static equilibrium exists which causes the hydraulic head to be constant throughout the flow field, or the capillary pressure (pressure head) varies linearly with depth of the soil profile. The water content of the soil profile increases (capillary pressure becomes less in absolute magnitude) with depth below the soil surface.

$$P_t = z - h_t \quad (106)$$

$$\xi = \frac{1 - (z-h_t)^{-(1+3\lambda_0)}}{(1 + 3 \lambda_0)} \quad (107)$$

The Boundary Conditions

The boundary conditions for any system geometry must be defined for the problem. The rectangular area in Fig. 8 shows the flow field and different segments of the boundaries having different boundary conditions.

Axis of Symmetry ① - ②.--The flow region below the circular water entry zone ② - ③ is symmetric about this boundary. For the homogeneous soils boundary ① - ② is a streamline and all constant head lines (equipotential) are perpendicular to the axis of symmetry. The boundary condition along the center line is

$$0 \leq z \leq D \quad (108)$$

$$r = 0 \quad (109)$$

Surface of Water Application ② - ③.--The surface over which the water is applied or water entry zone is assumed to be horizontal at a finite height above the drained layer. Only two conditions are given for boundary ② - ③.

a. The flux rate is specified. This conditions applies when the intake capacity of the soil is assumed to be greater than the water application rate. Consequently no portion of the seepage zone will be fully saturated.

The specified rate of flux can be a function of time (rain hystogram). All streamlines leave the surface of water application vertically. The boundary conditions for the water entry zone are:

$z = D$

$0 \leq r \leq r_a$

if flux specified

$$\frac{\partial \xi}{\partial r} = 0$$

$$\frac{\partial \xi}{\partial z} = \frac{1 - (1 + 3\lambda_0)\xi}{P_t} \left(\frac{W}{K} + 1 \right)$$

if saturation specified

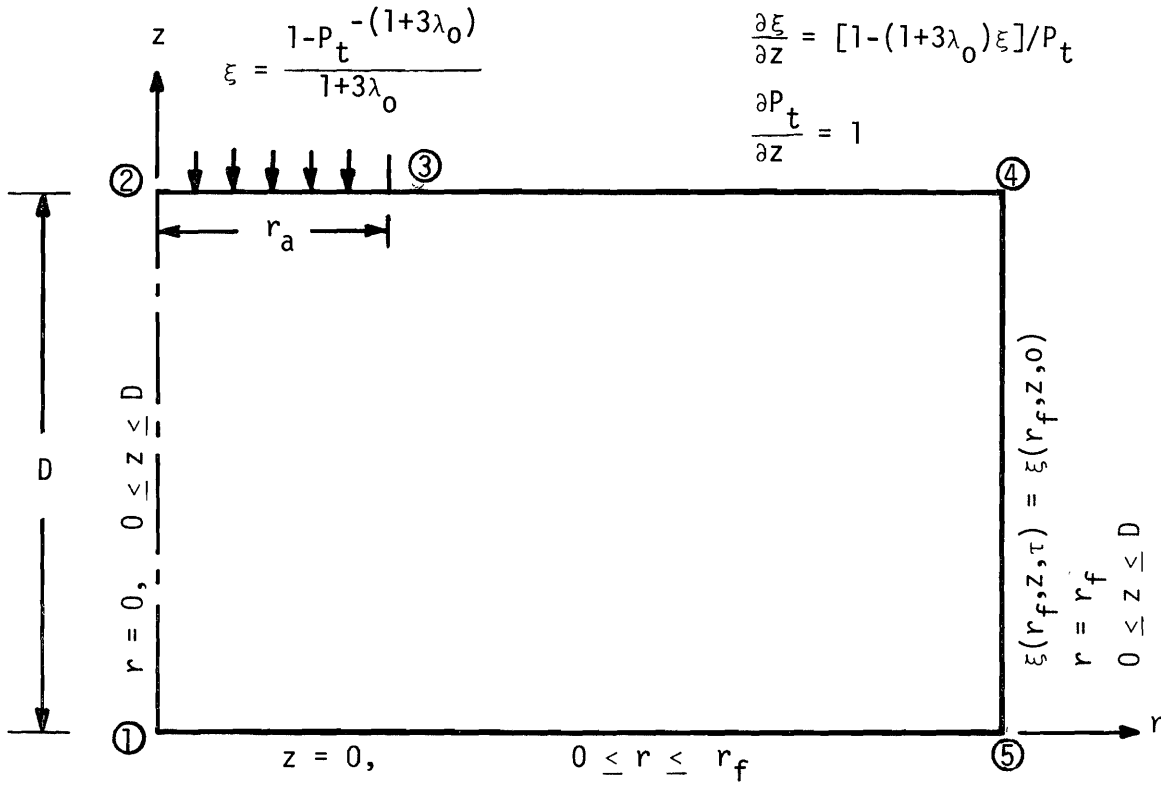
$$P_t = \frac{P_b}{\left(\frac{S - S_r}{1 - S_r} \right)^{1/\lambda}}$$

$z = D$

$r_f \geq r > r_a$

$$\frac{\partial \xi}{\partial z} = [1 - (1 + 3\lambda_0)\xi] / P_t$$

$$\frac{\partial P_t}{\partial z} = 1$$



if partially saturated:

$$\frac{\partial P_t}{\partial z} = 1$$

$$\frac{\partial \xi}{\partial z} = \frac{1 - (1 + 3\lambda_0)\xi}{P_t}$$

if saturated:

$$P_t = P_b \cdot \frac{1 - (1 + 3\lambda_0)\xi}{1 - (P_b)}$$

$$\xi = \frac{1 - (P_b)}{1 + 3\lambda_0}$$

FIG. 8.--Formulation of the Boundary Value Problem for the Transient Unsaturated Three-Dimensional Axisymmetric Flow From a Circular Area Through Heterogeneous Porous Media.

$$\frac{\partial \xi}{\partial r} = 0 \quad (110)$$

$$z = D \quad (111)$$

$$0 \leq r \leq r_a \quad (112)$$

$$\frac{\partial \xi}{\partial z} = \frac{[1 - (1+3\lambda_0)\xi]}{P_t} \left[\frac{W}{K} + 1 \right] \quad (113)$$

in which

$$K = K_a K_v(z) K_r(P_b, \lambda, P_t) \quad (114)$$

b. Surface saturation specified (Dirichlet boundary condition).
If the saturation at the circular water entry zone is specified, the values of pressure head or hydraulic head will be determined directly for this boundary. When the soil is completely saturated, the capillary pressure is equal to the bubbling pressure ($P_t = P_b$), and the rate of water application is equal to the intake capacity of the saturated soil. The specified saturation can be a function of time and boundary conditions as:

$$P_t = \frac{P_b}{\left(\frac{S-S_r}{1-S_r} \right)^{\frac{1}{\lambda}}} \quad (115)$$

$$\xi = \frac{1 - P_t^{-(1+3\lambda_0)}}{1 + 3\lambda_0} \quad (116)$$

Surface Beyond Radius of Water Application ③ - ④.--This surface is at a constant height, D , above drained layer, is horizontal and no evaporation occurs across it. The boundary condition is the same as the boundary ② - ③ except that there is not vertical flux rate $W = 0$. The boundary conditions are as

$$r_a < r \leq r_f \quad (117)$$

$$z = D \quad (118)$$

$$\frac{\partial \xi}{\partial z} = \frac{[1 - (1+3\lambda_0)\xi]}{P_t} \quad (119)$$

$$\frac{\partial P_t}{\partial z} = 1 \quad (120)$$

Outer Boundary Beyond the Radius of Influence ④ - ⑤.--The outer boundary is assumed far enough removed from the water source that no moisture movement will occur across this boundary and at all times it is in a static equilibrium condition. It is a Dirichlet type boundary and boundary value need not be evaluated in the solution of the problem. The condition is:

$$r = r_f \quad (121)$$

$$0 \leq z \leq D \quad (122)$$

$$h_0 = h \quad (123)$$

$$\xi(r_f, z, \tau) = \xi(r_f, z, 0) \quad (124)$$

in which r_f is the radius of influence and h_0 is the initial hydraulic head.

Bottom Boundary ⑤ - ①--A horizontal lower boundary at depth $z = 0$ is assumed to exist. Water will pass into this lower boundary after the soil profile becomes approximately saturated.

It is assumed that the surface of the bottom boundary is at a constant pressure. When the unit or maximum saturation is attained at this boundary, water will begin to pass through the boundary. The boundary conditions are

$$z = 0 \quad (125)$$

$$0 \leq r \leq r_f \quad (126)$$

when the soil profile is not fully saturated

$$\frac{\partial P_t}{\partial z} = 1 \quad (127)$$

$$\frac{\partial \xi}{\partial z} = \frac{1 - (1 + 3 \lambda_0) \xi}{P_t} \quad (128)$$

when unit saturation first occurs

$$P_t = P_b \quad (129)$$

$$\xi = \frac{1 - (P_b)^{-(1 + 3 \lambda_0)}}{1 + 3 \lambda_0} \quad (130)$$

FINITE DIFFERENCE SOLUTION

For this study the Crank-Nicolson method of differencing was chosen. In the Crank-Nicolson method, difference approximation of the derivatives with respect to the space coordinates z and r are weighted at the current and advanced time step equally as the derivative with respect to time, τ , is approximated by a second order central difference evaluated midway between these two time steps.

Generally, the finite difference equations will converge faster, when the truncation error involved is small. At the forward and backward difference approximation, the truncation error is of first order, $O(\Delta t)$. The central difference approximation has the advantage that the truncation error reduces from first order $O(\Delta t)$ to second order $O(\Delta t)^2$. Consequently, the Crank-Nicolson method provides a second order approximation in space and time with a truncation error of $O[(\Delta t)^2 + (\Delta z)^2 + (\Delta r)^2]$. Also the system of equations produced by the Crank-Nicolson method for boundary-value problems retains the computationally advantageous tridiagonal form. It is unconditionally stable for all values of ratio $\frac{\Delta t}{(\Delta x)^2}$.

In application of the Crank-Nicolson method for nonlinear problems, different schemes have been used by different researchers. One method which multiplies the average of the nonlinear coefficients evaluated at (K) and $(K+1)$ time levels, by the average of differences at (K) and $(K+1)$ time line is used by Forsythe and Wason (23), Douglas

(21); Remson, Hornberger and Molz, (83). In another method which takes the average of the two products of the nonlinear coefficient evaluated at (K) time level multiplied by the difference at (k) time level and nonlinear coefficient evaluated (k+1) time level multiplied by differences at the (K+1) time level was used by Richtmyer (86) and Jeppson (44).

This study utilizes the Crank-Nicolson method, and the second approach (44) was selected as it is easier in computation.

Finite Difference Operators for Interior Grid Points

The finite difference operator for Equation (105) can be obtained by replacing the derivatives by the first and second order central differences. If the δ 's and δ^2 's denote first and second central difference operators, we have:

$$2\Delta z \frac{\partial \xi}{\partial z} \approx \delta_z \xi = \xi_{j-1,i} - \xi_{j+1,i} \quad (131)$$

$$2\Delta r \frac{\partial \xi}{\partial r} \approx \delta_r \xi = \xi_{i,i+1} - \xi_{j,i-1} \quad (132)$$

$$\Delta z^2 \frac{\partial^2 \xi}{\partial z^2} \approx \delta_z^2 \xi = \xi_{j+1,i} + \xi_{j-1,i} - 2\xi_{j,i} \quad (133)$$

$$\Delta r^2 \frac{\partial^2 \xi}{\partial r^2} \approx \delta_r^2 \xi = \xi_{j,i+1} + \xi_{j,i-1} - 2\xi_{j,i} \quad (134)$$

and therefore,

$$\frac{\partial p_t}{\partial z} \approx \frac{P_t}{\zeta} \frac{\delta_z \xi}{2\Delta z} = \frac{P_t}{\zeta} \frac{(\xi_{j-1,i} - \xi_{j+1,i})}{2\Delta z} \quad (135)$$

$$\frac{\partial P_t}{\partial r} \approx \frac{P_t}{\zeta} \frac{\delta_r \xi}{2\Delta r} = \frac{P_t}{\zeta} \frac{(\xi_{j,i+1} - \xi_{j,i-1})}{2\Delta r} \quad (136)$$

$$\frac{\partial^2 P_t}{\partial z^2} \approx \frac{P_t}{\zeta} \left[\frac{\delta_z^2 \xi}{\Delta z^2} + \frac{(2+3\lambda_0)}{\zeta} \frac{(\delta_z \xi)^2}{4\Delta z^2} \right] = \frac{P_t}{\zeta} \left[\frac{(\xi_{j+1,i} + \xi_{j-1,i} - 2\xi_{j,i})}{\Delta z^2} + \frac{(2+3\lambda_0)}{\zeta} \frac{(\xi_{j-1,i} - \xi_{j+1,i})^2}{4\Delta z^2} \right] \quad (137)$$

$$\frac{\partial^2 P_t}{\partial r^2} \approx \frac{P_t}{\zeta} \left[\frac{\delta_r^2 \xi}{\Delta r^2} + \frac{(2+3\lambda_0)}{\zeta} \frac{(\delta_r \xi)^2}{4\Delta r^2} \right] = \frac{P_t}{\zeta} \left[\frac{(\xi_{j,i+1} + \xi_{j,i-1} - 2\xi_{j,i})}{\Delta r^2} + \frac{(2+3\lambda_0)}{\zeta} \frac{(\xi_{j,i+1} - \xi_{j,i-1})^2}{4\Delta r^2} \right] \quad (138)$$

Replacing the derivative by the equivalent finite difference operators in the Equation (105)

$$\begin{aligned} F = & \left[K_v \left\{ \frac{P_t}{\zeta} \left[\frac{\delta_r^2 \xi}{\Delta r^2} + \frac{\delta_z^2 \xi}{\Delta z^2} + \frac{2+3\lambda_0}{\zeta} \left(\frac{\delta_r \xi^2}{4\Delta r^2} + \frac{\delta_z \xi^2}{4\Delta z^2} \right) \right] - \frac{(2+3\lambda)}{\zeta^2} P_t \right. \right. \\ & \frac{\delta_r \xi^2}{4\Delta r^2} + \left(\frac{P_t}{\zeta} \frac{\delta_z \xi}{2\Delta z} - 1 \right) \left(\frac{2+3\lambda}{P_b} \frac{\partial P_b}{\partial z} + 3 \ln \left(\frac{P_b}{P_t} \right) \frac{\partial \lambda}{\partial z} - \frac{2+3\lambda}{\zeta} \frac{\delta_z \xi}{2\Delta z} \right) \\ & \left. + \frac{P_t}{r\zeta} \frac{\delta_r \xi}{2\Delta r} \right\} + \left(\frac{P_t}{\zeta} \frac{\delta_z \xi}{2\Delta z} - 1 \right) \frac{\partial K_v}{\partial z} \right]^{K+1} + \left[K_v \left\{ \frac{P_t}{\zeta} \left[\frac{\delta_r^2 \xi}{\Delta r^2} + \frac{\delta_z^2 \xi}{\Delta z^2} \right. \right. \right. \\ & \left. \left. + \frac{2+3\lambda_0}{\zeta} \left(\frac{\delta_r \xi^2}{4\Delta r^2} + \frac{\delta_z \xi^2}{4\Delta z^2} \right) \right] - \frac{(2+3\lambda)P_t}{\zeta^2} \frac{\delta_r \xi^2}{4\Delta r^2} + \left(\frac{P_t}{\zeta} \frac{\delta_z \xi}{2\Delta z} - 1 \right) \right. \\ & \left. \left(\frac{2+3\lambda}{P_b} \frac{\partial P_b}{\partial z} + 3 \ln \left(\frac{P_b}{P_t} \right) \frac{\partial \lambda}{\partial z} - \frac{2+3\lambda}{\zeta} \frac{\delta_z \xi}{2\Delta z} \right) + \frac{P_t}{r\zeta} \frac{\delta_r \xi}{2\Delta r} \right\} + \left(\frac{P_t}{\zeta} \frac{\delta_z \xi}{2\Delta z} - 1 \right) \right. \\ & \left. \frac{\partial K_v}{\partial z} \right]^K - \frac{2\eta\lambda(1-S_r)}{P_b^{2+2\lambda}} \frac{P_t^{2+2\lambda}}{\zeta} \left(\frac{\xi^{K+1} - \xi^K}{\Delta \tau} \right) = 0 \quad (139) \end{aligned}$$

in which $K+1$ subscript denotes the advance time step and K subscript denotes the current time step.

Let us use the square grid network, $\Delta s = \Delta r = \Delta z$ and multiply the above equation by ζ and $\Delta s^2 = \Delta r^2 = \Delta z^2$ to get the following equation:

$$\begin{aligned}
F = & \left[K_V \left\{ P_t \left[\delta_r^2 \xi + \delta_z^2 \xi + \frac{2+3\lambda_0}{\zeta} \left(\frac{\delta_r \xi^2}{4} + \frac{\delta_z \xi^2}{4} \right) \right] \right\} - \frac{(2+3\lambda)P_t}{\zeta} \frac{\delta_r \xi^2}{4} \right. \\
& + \left(P_t \frac{\delta_z \xi}{2} - \zeta \Delta s \right) \left(\frac{2+3\lambda}{P_b} \frac{\partial P_b}{\partial z} \Delta s + 3 \ln \left(\frac{P_b}{P_t} \right) \frac{\partial \lambda}{\partial z} \Delta s - \frac{2+3\lambda}{\zeta} \frac{\delta_z \xi}{2} \right) \\
& + \left. \frac{P_t}{r} \frac{\delta_r \xi}{2} \Delta s \right\} + \left(P_t \frac{\delta_z \xi}{2} - \zeta \Delta s \right) \frac{\partial K_V}{\partial z} \Delta s \Big]^{K+1} + \left[K_V \left\{ P_t \left[\delta_r^2 \xi \right. \right. \right. \\
& + \left. \left. \delta_z^2 \xi + \frac{2+3\lambda_0}{\zeta} \left(\frac{\delta_r \xi^2}{4} + \frac{\delta_z \xi^2}{4} \right) \right] \right\} - \frac{(2+3\lambda)P_t}{\zeta} \frac{\delta_r \xi^2}{4} + \left(P_t \frac{\delta_z \xi}{2} - \zeta \Delta s \right) \\
& \left(\frac{2+3\lambda}{P_b} \frac{\partial P_b}{\partial z} \Delta s + 3 \ln \left(\frac{P_b}{P_t} \right) \frac{\partial \lambda}{\partial z} \Delta s - \frac{2+3\lambda}{\zeta} \frac{\delta_z \xi}{2} \right) + \frac{P_t}{r} \frac{\delta_r \xi}{2} \Delta s \Big\} \\
& + \left. \left(P_t \frac{\delta_z \xi}{2} - \zeta \Delta s \right) \frac{\partial K_V}{\partial z} \Delta s \right]^K - \frac{2\eta\lambda(1-S_r)}{P_b^{2+2\lambda}} \frac{\Delta s^2}{\Delta \tau} P_t^{2+2\lambda} \\
& (\xi^{K+1} - \xi^K) = 0 \tag{140}
\end{aligned}$$

If subscripts j and i denote the space subscripts at axial and radial directions respectively, and subscript K denotes the time step such that:

$$j = 1 + (D-z)/\Delta s \tag{141}$$

$$i = 1 + \frac{r}{\Delta s} \tag{142}$$

$$K = 1 + \frac{\tau}{\Delta\tau} \quad (143)$$

The finite difference equation for the interior grid point is,

$$\begin{aligned}
F_{j,i} = & [K_v \{ P_t [(\epsilon_{j,i+1} + \epsilon_{j,i-1} - 2\epsilon_{j,i}) + (\epsilon_{j+1,i} + \epsilon_{j-1,i} \\
& - 2\epsilon_{j,i}) + \frac{2+3\lambda_0}{\zeta} \left(\frac{(\epsilon_{j,i+1} - \epsilon_{j,i-1})^2}{4} + \frac{(\epsilon_{j-1,i} - \epsilon_{j+1,i})^2}{4} \right)] \\
& - \left(\frac{(2+3\lambda)P_t}{\zeta} \frac{(\epsilon_{j,i+1} - \epsilon_{j,i-1})^2}{4} \right) + \left(P_t \frac{(\epsilon_{j-1,i} - \epsilon_{j+1,i})}{2} - \zeta \Delta s \right) \\
& \left(\frac{2+3\lambda}{P_b} \frac{\partial P_b}{\partial z} \Delta s + 3 \ln \left(\frac{P_b}{P_t} \right) \frac{\partial \lambda}{\partial z} \Delta s - \frac{(2+3\lambda)}{\zeta} \frac{(\epsilon_{j-1,i} - \epsilon_{j+1,i})}{2} \right. \\
& \left. + \left(\frac{P_t}{r} \frac{(\epsilon_{j,i+1} - \epsilon_{j,i-1})}{2} \Delta s \right) \right\} + \left(P_t \frac{(\epsilon_{j-1,i} - \epsilon_{j+1,i})}{2} - \zeta \Delta s \right) \\
& \frac{\partial K_v}{\partial z} \Delta s]^{K+1} + [K_v \{ P_t [(\epsilon_{j,i+1} + \epsilon_{j,i-1} - 2\epsilon_{j,i}) + (\epsilon_{j+1,i} \\
& + \epsilon_{j-1,i} - 2\epsilon_{j,i}) + \frac{2+3\lambda_0}{\zeta} \left(\frac{(\epsilon_{j,i+1} - \epsilon_{j,i-1})^2}{4} + \right. \\
& \left. \frac{(\epsilon_{j-1,i} - \epsilon_{j+1,i})^2}{4} \right)] - \left(\frac{(2+3\lambda)P_t}{\zeta} \frac{(\epsilon_{j,i+1} - \epsilon_{j,i-1})^2}{4} \right) + \\
& \left(P_t \frac{(\epsilon_{j-1,i} - \epsilon_{j+1,i})}{2} - \zeta \Delta s \right) \left(\frac{2+3\lambda}{P_b} \frac{\partial P_b}{\partial z} \Delta s + 3 \ln \left(\frac{P_b}{P_t} \right) \frac{\partial \lambda}{\partial z} \Delta s \right. \\
& \left. - \frac{(2+3\lambda)}{\zeta} \frac{(\epsilon_{j-1,i} - \epsilon_{j+1,i})}{2} + \left(\frac{P_t}{r} \frac{(\epsilon_{j,i+1} - \epsilon_{j,i-1})}{2} \Delta s \right) \right\} \\
& + \left(P_t \frac{(\epsilon_{j-1,i} - \epsilon_{j+1,i})}{2} - \zeta \Delta s \right) \frac{\partial K_v}{\partial z} \Delta s]^K - \frac{2\eta\lambda(1-S_r)}{P_b^{2+2\lambda}} \\
& \frac{\Delta s^2}{\Delta\tau} P_{ave}^{2+2\lambda} (\epsilon_{j,i}^{K+1} - \epsilon_{j,i}^K) = 0 \quad (144)
\end{aligned}$$

in which

$$P_{ave} = (P_{t,j,i}^{K+1} + P_{t,j,i}^K)/2 \quad (145)$$

Finite Difference Operators for Boundary

Grid Points

Operator for Boundary ① - ②.--Since the value of r equals zero at the axis of symmetry, the term, $\frac{P_t}{r} \frac{(\xi_{j,i+1} - \xi_{j,i-1})}{2} \Delta s$, in the flow equation will be undefined along the line singularity. This is the reason why an operator cannot be developed by combining the central difference approximation of $\frac{\partial \xi}{\partial r} = 0$ and replacing it with those in the flow equation to handle the nonexisting points $\xi_{j,i-1}$ (i.e., $\delta_r \xi = \xi_{j,2} - \xi_{j,0} = 0$). The boundary condition 1 - 2 in this problem has been handled by setting $\xi_{j,1} = \xi_{j,2}$ in the finite difference equation.

Operator for Boundary ② - ③.--The flux rate specified case (non Dirichlet type) leads to the condition that the axial component of velocity is constant over the boundary and equal to the infiltration rate. Therefore the boundary condition equation from Darcy's law is

$$W = -K \frac{\partial h_t}{\partial z} \quad (146)$$

$$h_t = z - P_t \quad (147)$$

in which W equals the axial component of seepage velocity, which is negative in magnitude being LT^{-1} in a downward direction; (input data is a positive value but the computer program adopts a different sign

convention, that is the minus sign of W is considered in developing the related function); K equals hydraulic conductivity, LT^{-1} ; h_t equals dimensionless hydraulic head; z equals dimensionless depth; and P_t equals the pressure head or capillary pressure, dimensionless.

$$W = -K \frac{\partial(z - P_t)}{\partial z} = K \left(\frac{\partial P_t}{\partial z} - 1 \right) \quad (148)$$

$$K = K_a K_v K_r \quad (149)$$

$$W = K_a K_v K_r \left(\frac{\partial P_t}{\partial z} - 1 \right) \quad (150)$$

$$\frac{W}{K_a K_v K_r} + 1 = \frac{\partial P_t}{\partial z} \quad (151)$$

$$\frac{\partial P_t}{\partial z} = \frac{P_t}{\zeta} \frac{\partial \xi}{\partial z} \quad (152)$$

Approximating $\frac{\partial \xi}{\partial z}$ with second order central differences centered on the boundary ($j=1$) will finally eliminate the value of ξ at a nonexistent grid point outside of the boundary ② - ③ by combining with the finite difference operation for interior grid points.

$$\frac{\zeta}{P_t} \left[\frac{W}{K_a K_v K_r} + 1 \right] = \frac{\partial \xi}{\partial z} = \frac{\xi_{j-1,i} - \xi_{j+1,i}}{2\Delta s} \quad (153)$$

$$2\Delta s \frac{\zeta}{P_t} \left[\frac{W}{K} + 1 \right] = \xi_{j-1,i} - \xi_{j+1,i} \quad (154)$$

The value of ξ for a nonexistent grid point outside of the boundary for $j=1$ from above equation is

$$\xi_{0,i} = \xi_{2,i} + 2\Delta s \frac{\zeta}{P_t} \left[\frac{W}{K} + 1 \right] \quad (155)$$

which combines with finite difference operator for interior grid points Equation (144) and results the following finite difference operator for the boundary (2) - (3) .

$$\begin{aligned}
F_{1,i} = & [K_V \{ P_t [(\xi_{1,i+1} + \xi_{1,i-1} - 2\xi_{1,i}) + 2(\xi_{2,i} + \Delta s \frac{\zeta}{P_t} (\frac{W}{K} + 1) \\
& - \xi_{1,i}) + \frac{2+3\lambda_0}{\zeta} (\frac{(\xi_{1,i+1} - \xi_{1,i-1})^2}{4} + \frac{[2\Delta s \frac{\zeta}{P_t} (\frac{W}{K} + 1)]^2}{4})] \\
& - (\frac{(2+3\lambda)P_t}{\zeta} \frac{(\xi_{1,i+1}, \xi_{1,i-1})^2}{4}) + [\frac{P_t}{2} (\xi_{2,i} + 2\Delta s \frac{\zeta}{P_t} (\frac{W}{K} + 1) - \xi_{2,i}) \\
& - \zeta\Delta s] (\frac{2+3\lambda}{P_b} \frac{\partial P}{\partial z} \Delta s + 3 \ln (\frac{P_b}{P_t}) \frac{\partial \lambda}{\partial z} \Delta s - \frac{(2+3\lambda)}{2\zeta} (\xi_{2,i} + 2\Delta s \frac{\zeta}{P_t} \\
& (\frac{W}{K} + 1) - \xi_{2,i})) + (\frac{P_t}{r} \frac{(\xi_{1,i+1} - \xi_{1,i-1})}{2} \Delta s) \} + (\frac{P_t}{2} \\
& (\xi_{2,i} + 2\Delta s \frac{\zeta}{P_t} (\frac{W}{K} + 1) - \xi_{2,i}) - \zeta\Delta s) \frac{\partial K_V}{\partial z} \Delta s]^{K+1} \\
& + [K_V \{ P_t [(\xi_{1,i+1} + \xi_{1,i-1} - 2\xi_{1,i}) + 2(\xi_{2,i} + \Delta s \frac{\zeta}{P_t} (\frac{W}{K} + 1) \\
& - \xi_{1,i}) + \frac{2+3\lambda_0}{\zeta} (\frac{(\xi_{1,i+1} - \xi_{1,i-1})^2}{4} + \frac{[2\Delta s \frac{\zeta}{P_t} (\frac{W}{K} + 1)]^2}{4})] \\
& - (\frac{(2+3\lambda)P_t}{\zeta} \frac{(\xi_{1,i+1}, \xi_{1,i-1})^2}{4}) + [\frac{P_t}{2} (\xi_{2,i} + 2\Delta s \frac{\zeta}{P_t} (\frac{W}{K} + 1) \\
& - \xi_{2,i}) - \zeta\Delta s] (\frac{2+3\lambda}{P_b} \frac{\partial P}{\partial z} \Delta s + 3 \ln (\frac{P_b}{P_t}) \frac{\partial \lambda}{\partial z} \Delta s - \frac{(2+3\lambda)}{2\zeta} \\
& (\xi_{2,i} + 2\Delta s \frac{\zeta}{P_t} (\frac{W}{K} + 1) - \xi_{2,i})) + (\frac{P_t}{r} \frac{(\xi_{1,i+1} - \xi_{1,i-1})}{2} \Delta s) \} \\
& + (\frac{P_t}{2} (\xi_{2,i} + 2\Delta s \frac{\zeta}{P_t} (\frac{W}{K} + 1) - \xi_{2,i}) - \zeta\Delta s) \frac{\partial K_V}{\partial z} \Delta s]^K
\end{aligned}$$

$$-\frac{2n\lambda(1-S_r)}{P_b^{2+2\lambda}} \frac{\Delta S^2}{\Delta \tau} P_{ave}^{2+2\lambda} (\xi_{1,i}^{K+1} - \xi_{1,i}^K) = 0 \quad (156)$$

Assume $\frac{W}{K_a}$ to be the dimensionless flux, VK

$$\frac{W}{K} = \frac{W}{K_a K_V K_r} = \frac{VK}{K_V K_r} \quad (157)$$

from Equation (45) we can write

$$\frac{W}{K} = \frac{VK}{K_V \left(\frac{P_b}{P_t} \right)^{2+3\lambda}} \quad (158)$$

The input data for parameter, W, is a positive number with units of LT^{-1} . The negative sign of the W is handled in the subroutine F1 and by multiplying the equation above by a minus sign. Upon simplifying the above equation, the finite difference operator for the boundary over which water is applied, ② - ③ is as follows:

$$\begin{aligned} F_{1,i} = & [K_V \{ P_t [(\xi_{1,i+1} + \xi_{1,i-1} - 2\xi_{1,i}) + 2(\xi_{2,i} + \Delta S \frac{\zeta}{P_t} \\ & (\frac{W}{K} + 1) - \xi_{1,i}) + \frac{2+3\lambda}{\zeta} \left(\frac{(\xi_{1,i+1} - \xi_{1,i-1})^2}{4} + [\Delta S \frac{\zeta}{P_t} (\frac{W}{K} + 1)]^2 \right) \\ & - \left(\frac{(2+3\lambda)P_t}{\zeta} \cdot \frac{(\xi_{1,i+1} - \xi_{1,i-1})^2}{4} \right) + (\zeta \Delta S \frac{W}{K}) \left(\frac{2+3\lambda}{P_b} \frac{\partial P_b}{\partial z} \Delta S \right. \\ & + 3 \ln \left(\frac{P_b}{P_t} \right) \frac{\partial \lambda}{\partial z} \Delta S - \frac{2+3\lambda}{P_t} \Delta S \left(\frac{W}{K} + 1 \right) \left. + \left(\frac{P_t}{r} \frac{\xi_{1,i+1} - \xi_{1,i-1}}{2} \right) \right. \\ & \left. \Delta S \right) \} + (\zeta \Delta S \frac{W}{K}) \frac{\partial K_V}{\partial z} \Delta S]^{K+1} + [K_V \{ P_t [(\xi_{1,i+1} + \xi_{1,i-1} - \end{aligned}$$

$$\begin{aligned}
& 2\xi_{1,i}) + 2(\xi_{2,i} + \Delta s \frac{\zeta}{P_t} (\frac{W}{K} + 1) - \xi_{1,i}) + \frac{2+3\lambda_0}{\zeta} \\
& \left(\frac{(\xi_{1,i+1} - \xi_{1,i-1})^2}{4} + [\Delta s \frac{\zeta}{P_t} (\frac{W}{K} + 1)]^2 \right) - \left(\frac{(2+3\lambda)P_t}{\zeta} \right. \\
& \left. \frac{(\xi_{1,i+1} - \xi_{1,i-1})^2}{4} \right) + \left(\zeta \Delta s \frac{W}{K} \right) \left(\frac{2+3\lambda}{P_b} \frac{\partial P_b}{\partial z} \Delta s + 3 \ln \left(\frac{P_b}{P_t} \right) \right. \\
& \left. \frac{\partial \lambda}{\partial z} \Delta s - \frac{2+3\lambda}{P_t} \Delta s \left(\frac{W}{K} + 1 \right) \right) + \left(\frac{P_t}{r} \frac{\xi_{1,i+1} - \xi_{1,i-1}}{2} \Delta s \right) \} + \\
& \left(\zeta \Delta s \frac{W}{K} \right) \frac{\partial K_v}{\partial z} \Delta s \left] - \frac{2\eta\lambda(1 - S_r)}{P_b^{2+2\lambda}} \frac{\Delta s^2}{\Delta \tau} P_{ave}^{2+2\lambda} (\xi_{1,i} - \xi_{1,i})^K = 0
\end{aligned}$$

for

$$i = 2 \dots N2X$$

(159)

where N2X is the number of points in radial direction to outer edge of circle of application.

Operator for Boundary ③ - ④.--Along this horizontal boundary the vertical component of seepage velocity is zero (no water application or evaporation from this surface). The finite difference operator for this boundary will be obtained by substituting W equals zero in the Equation (105). The operator for boundary ③ - ④ is as follows:

$$\begin{aligned}
F_{1,i} = & \left[K_v \left\{ P_t \left[(\xi_{1,i+1} + \xi_{1,i-1} - 2\xi_{1,i}) + 2(\xi_{2,i} + \Delta s \frac{S}{P_t} \right. \right. \right. \\
& \left. \left. \left. - \xi_{1,i}) + \frac{2+3\lambda_0}{\zeta} \left(\frac{(\xi_{1,i+1} - \xi_{1,i-1})^2}{4} + [\Delta s \frac{\zeta}{P_t}]^2 \right) \right] \right. \right. \\
& \left. \left. - \left(\frac{(2+3\lambda)}{\zeta} P_t \frac{(\xi_{1,i+1} - \xi_{1,i-1})^2}{4} \right) + \left(\frac{P_t}{r} \frac{(\xi_{1,i+1} - \xi_{1,i-1})}{2} \right) \right. \right.
\end{aligned}$$

$$\begin{aligned}
& \Delta s \}]^{K+1} + [K_V \{ P_t [(\xi_{1,i+1} + \xi_{1,i-1} - 2 \xi_{1,i}) + 2(\xi_{2,i} \\
& + \Delta s \frac{\xi}{P_t} - \xi_{1,i}) + \frac{2+3\lambda_0}{\xi} (\frac{(\xi_{1,i+1} - \xi_{1,i-1})^2}{4} + [\Delta s \frac{\xi}{P_t}]^2)] \\
& - (\frac{(2+3\lambda)}{\xi} P_t \frac{(\xi_{1,i+1} - \xi_{1,i-1})^2}{4}) + (\frac{P_t}{r} \frac{\xi_{1,i+1} - \xi_{1,i-1}}{2} \\
& \Delta s \}]^K - \frac{2\eta\lambda(1-S_r)}{P_b^{2+2\lambda}} \frac{\Delta s}{\Delta \tau} P_{ave}^{2+2\lambda} (\xi_{1,i} - \xi_{1,i}) = 0
\end{aligned}$$

for

$$\begin{aligned}
i &= N_{2X} + 1 \dots N_r - 1 \\
i &> (1 + \frac{r_a}{\Delta s})
\end{aligned} \tag{160}$$

where N_r equals subscript denoting number of grid lines from the axis of symmetry to the outside radius of the problem.

Operator for Boundary ④ - ⑤.--This boundary is assumed to be far enough from the source of water that no flow occurs in its vicinity. Thus, the values of hydraulic head do not change along boundary ④ - ⑤. No finite difference operator is needed (Dirichlet type).

$$\xi_0 = \xi$$

for

$$\begin{aligned}
j &= 1, N_z \\
i &= N_r
\end{aligned} \tag{161}$$

Operator for Boundary ⑤ - ①.--The finite difference equation for the bottom boundary (when unit saturation has not been

achieved, or is not of the Dirichlet type) is the same as the operator for boundary (3) - (4) in which the subscript $J=1$ is replaced by N_z and 2 by N_z-1 , ($i = 2, \dots, N_r - 1$), where N_z equals subscript denoting number of grid lines from the surface to the bottom boundary.

$$P_t = z - h_t \quad (162)$$

$$\frac{\partial P_t}{\partial z} = 1 \quad (163)$$

Also

$$\frac{\partial P_t}{\partial z} = \frac{P_t}{\zeta} \frac{\partial \xi}{\partial z} \quad (164)$$

at bottom boundary

$$j = N_z \quad (165)$$

$$\frac{\partial \xi}{\partial z} = \frac{\xi_{N_z-1,i} - \xi_{N_z+1,i}}{2\Delta s} \quad (166)$$

therefore

$$\frac{\partial P_t}{\partial z} = \frac{P_t}{\zeta} \cdot \frac{\xi_{N_z-1,i} - \xi_{N_z+1,i}}{2\Delta s} = 1 \quad (167)$$

Since N_z+1 is a nonexistant grid point, therefore, the value of $\xi_{N_z+1,i}$ can be replaced by:

$$\xi_{N_z-1,i} - \xi_{N_z+1,i} = 2\Delta s \frac{\zeta}{P_t} \quad (168)$$

$$\xi_{N_z+1,i} = \xi_{N_z-1,i} - 2\Delta s \frac{\zeta}{P_t} \quad (169)$$

Note this is the same as top boundary condition (soil surface), but $\xi_{2,i}$ is replaced by $\xi_{N_{z-1},i}$ and the sign of $\Delta s \frac{\zeta}{P_t} (\frac{W}{K} + 1)$ is changed and there is no flux, W , at this boundary.

Replacing the term $\xi_{N_{z+1},i} = \xi_{N_{z-1},i} - 2\Delta s \frac{\zeta}{P_t}$ in the general form of flow equation and considering $W = 0$, we have

$$\begin{aligned}
 F_{N_{z,i}} &= K_V \left\{ P_t \left[\delta_r^2 \xi + 2.0 \left(\xi_{N_{z-1},i} - \Delta s \frac{\zeta}{P_t} - \xi_{N_{z,i}} \right) \right. \right. \\
 &\quad \left. \left. + \frac{2+3\lambda_0}{\zeta} \left(\frac{\delta_r \xi^2}{4} + \left[\Delta s \frac{\zeta}{P_t} \right]^2 \right) \right] - \left(\frac{(2+3\lambda)P_t}{\zeta} \frac{\delta_r \xi^2}{4} + \left(\frac{P_t}{r} \frac{\sigma_r \xi}{2} \Delta s \right) \right\}^{K+1} \\
 &= \left[K_V \left\{ P_t \left[\delta_r^2 \xi + 2.0 \left(\xi_{N_{z-1},i} - \Delta s \frac{\zeta}{P_t} - \xi_{N_{z,i}} \right) \right. \right. \right. \\
 &\quad \left. \left. + \frac{2+3\lambda_0}{\zeta} \left(\frac{\delta_r \xi^2}{4} + \left[\Delta s \frac{\zeta}{P_t} \right]^2 \right) \right] \right. \\
 &\quad \left. - \left(\frac{(2+3\lambda)P_t}{\zeta} \frac{\delta_r \xi^2}{4} + \left(\frac{P_t}{r} \frac{\sigma_r \xi}{2} \Delta s \right) \right\}^K - \frac{2\eta\lambda(1-S_r)}{P_b^{2+2\lambda}} \frac{\Delta s^2}{\Delta \tau} \right. \\
 &\quad \left. P_{ave}^{2+2\lambda} (\xi_{N_{z,i}}^{K+1} - \xi_{N_{z,i}}^K) \right] = 0
 \end{aligned}$$

$$\text{for } i = 2, \dots, N_r - 1. \quad (170)$$

Method of Solution

Writing finite difference operators for all grid points (interior or boundary) produces a system of nonlinear algebraic equations for the unknown $\xi_{j,i}^{K+1}$. Since the coefficients involved, finite difference operators, are function of ξ , the produced system of equations is nonlinear. All values of ξ in the system of equation with superscript K are known, and within the region of computation, the number of equations is equal to the number of grid points. By solving the

system of nonlinear equations, the solution of the infiltration problem advances through one time step $\Delta\tau$.

For solving the finite difference equation, this study utilizes the scheme proposed by Jeppson (43) which in essence combines the line successive relaxation iterative method with the Newton-Raphson method, that is, an iteration is created within an iteration. The Newton-Raphson method starts with an estimate of the solution and iteratively computes better estimates. It has quadratic convergence, which means that each subsequent error at the $(m+1)$ iterate is proportional to square of the previous (m) th iterate error.

The iterative Newton-Raphson formula for a system of equations is:

$$(\xi^{k+1})^{m+1} = (\xi^{k+1})^m - (D^{-1})^m (\vec{F})^m \quad (171)$$

in which m equals iteration number; \vec{F} consists of the elements composed of the finite difference operators, $F_{j,i}$, when the solution is obtained $F_{j,i} = 0$; D equals the Jacobian matrix which consists of derivative elements, where in the case of three dimensional axisymmetric problem it is a banded matrix.

The elements of individual rows of this matrix are derivatives of that particular function, $F_{j,i}$, with respect to unknown vectors $\xi_{j,i}^{k+1}$ ($\xi_{j,i}^k$ is known). The rows and column corresponding to the known value of $\xi_{j,i}^{k+1}$ at the boundaries (Dirichlet type) are omitted. The innermost iteration solves for the values of ξ^{k+1} 's along a consecutive vertical lines from the system of equations resulting under the assumption that the ξ^{k+1} 's on the previous and next line are known. That is, two outer bands of matrix, D , were assumed zero,

consequently, the banded matrix reduced to a tridiagonal matrix. In this way for utilizing an inner iteration scheme considerable reduction in storage requirements and reduction in computer execution time will be achieved. The matrix is in tridiagonal form, so this system can be solved by a single pass through the runs with a Gaussian elimination to bring the terms below the diagonal of matrix to zero, then the unknown values of ξ^{K+1} 's are computed by back substitution. The inner most iteration will continue until the sum of absolute change in ξ 's along the line becomes less in magnitude than specified error (approximately 10^{-7}) term, then skips to next vertical line, and a pass through all lines constitutes an outer iteration, and provides values of ξ 's throughout the flow region which are close to those that would be obtained from one iteration by the Newton-Raphson method (Equation 171). During each outer iteration the sum of accumulated absolute changes in the values of ξ from the inner iterations along individual lines is accumulated. When this sum (SUMT) becomes less than a second error (error x 100), the iteration is terminated. However, when the Newton-Raphson iteration does not converge within a specified error and number of iterations, a message to this effect is printed and solution is terminated to another time step. The implementation of this solution method can be found in the listing of the FORTRAN program at Appendix II. The proposed method of solution referred as the Newton-Line-Relaxation method.

Since the division of a matrix is undefined, the D^{-1} in the Equation (171) is the inverse of matrix D, and for implementation of Newton-Raphson method the inverse is never obtained as Equation (171) implies. At the actual implementation of the Newton-Raphson method

the solution vector \vec{X} of the linear system $(D)^m \vec{X}^m = (\vec{F})^m$ is subtracted from the iterative vector of unknowns. Less computations are required in solving the linear system $(\vec{D})\vec{X}^m = (\vec{F})^m$ than computing the inverse of Jacobian matrix, D , thus the practical form of the Equation (171) is:

$$(\vec{\xi}^{K+1})^{m+1} = (\vec{\xi}^{K+1})^m - \vec{X}^m \quad (173)$$

A reasonably accurate guess of the unknown $(\xi^{K+1})^0$ is required to assure convergence. The initialization for $(\xi^{K+1})^0$ is obtained

$$\Delta \vec{\xi} = \vec{\xi}^{(K+1)} - \vec{\xi}^K \quad (174)$$

$$\vec{\xi}^{(K+1)} = \vec{\xi}^K - \Delta \vec{\xi} \quad (175)$$

by changing the values of ξ 's at each grid point by the amount which they changed during the previous time step.

Evaluating Derivatives of Jacobian D

(a) For The Soil Surface or First Row of Jacobian D.--

$$\begin{aligned} \frac{\partial F_{1,i}}{\partial \xi_{1,i}} = & K_V \left\{ \frac{\partial P_t}{\partial \xi_{1,i}} \left[\xi_{1,i+1} + \xi_{1,i-1} - 2\xi_{1,i} + 2\left(\xi_{2,i} + \Delta s \frac{\zeta}{P_t} \left(\frac{W}{K} + 1\right)\right. \right. \right. \\ & \left. \left. \left. - \xi_{1,i}\right) + \frac{2+3\lambda_0}{\zeta} \left(\frac{(\xi_{1,i+1} - \xi_{1,i-1})^2}{4} + \left(\Delta s \frac{\zeta}{P_t} \left(\frac{W}{K} + 1\right)\right)^2 \right) \right] \right. \\ & \left. + P_t \left[-2 + \left(2 \Delta s \left(\frac{W}{K} + 1\right) \frac{P_t \frac{\partial \zeta}{\partial \xi_{1,i}} - \zeta \frac{\partial P}{\partial \xi_{1,i}}}{P_t^2} - 2\right) + (2+3\lambda_0) \right. \right. \\ & \left. \left. \left(-\frac{1}{\zeta^2} \frac{\partial \zeta}{\partial \xi_{1,i}} \right) \left(\frac{(\xi_{1,i+1} - \xi_{1,i-1})^2}{4} + \left[\Delta s \frac{\zeta}{P_t} \left(\frac{W}{K} + 1\right)\right]^2 \right) \right] \right\} \end{aligned}$$

$$\begin{aligned}
& + \frac{2+3\lambda_0}{\zeta} (2) \left[\Delta s \frac{\zeta}{P_t} \left(\frac{W}{K} + 1 \right) \right]^1 (\Delta s) \left(\frac{W}{K} + 1 \right) \frac{P_t \frac{\partial \zeta}{\partial \xi_{1,i}} - \zeta \frac{\partial P_t}{\partial \xi_{1,i}}}{P_t^2} \Big] \\
& - \left(\frac{(2+3\lambda)(\xi_{1,i+1} - \xi_{1,i-1})}{4} \cdot \frac{\zeta \frac{\partial P_t}{\partial \xi_{1,i}} - P_t \frac{\partial \zeta}{\partial \xi_{j,i}}}{\zeta^2} \right) + \left(\Delta s \frac{W}{K} \right) \\
& \left[\left(\frac{\partial s}{\partial \xi_{1,i}} \right) \left(\frac{2+3\lambda}{P_b} \frac{\partial P_b}{\partial z} \Delta s + 3 \ln \left(\frac{P_b}{P_t} \right) \frac{\partial \lambda}{\partial z} \Delta s - \frac{2+3\lambda}{P_t} \Delta s \right. \right. \\
& \left. \left. \left(\frac{W}{K} + 1 \right) \right) + \zeta \left(- 3.0 \frac{\partial \lambda}{\partial z} \Delta s \cdot \frac{1}{P_t} \frac{\partial P_t}{\partial \xi_{1,i}} - (2+3\lambda) (\Delta s) \left(\frac{W}{K} + 1 \right) \cdot \right. \right. \\
& \left. \left. \left(- \frac{1}{P_t^2} \frac{\partial P_t}{\partial \xi_{1,i}} \right) \right) \right] + \left(\frac{\Delta s}{r} \frac{\xi_{1,i+1} - \xi_{1,i-1}}{2} \frac{\partial P_t}{\partial \xi_{1,i}} \right) \Big\} \\
& + \left(\Delta s \frac{W}{K} \right) \left(\frac{\partial \zeta}{\partial \xi_{1,i}} \right) \cdot \frac{\partial K_v}{\partial z} \Delta s - \frac{2\eta\lambda(1-S_r)}{P_b^{2+2\lambda}} \cdot \frac{\Delta s^2}{\Delta \tau} \cdot P_{ave}^{2+2\lambda} \\
& (\xi_{1,i}^{K+1} - \xi_{1,i}^K) (2+2\lambda) \left(\frac{1}{2} \right) (P_t) \left(\frac{1}{\zeta P_{ave}} \right) - \frac{2\eta\lambda(1-S_r)}{P_b^{2+2\lambda}} \frac{\Delta s^2}{\Delta \tau} \\
& \cdot P_{ave}^{2+2\lambda} = 0 \tag{176}
\end{aligned}$$

Upon simplifying, the following equation is obtained

$$\begin{aligned}
\frac{\partial F_{1,i}}{\partial \xi_{1,i}} &= K_v \left\{ \frac{P_t}{\zeta} \left[\xi_{1,i+1} + \xi_{1,i-1} - 2\xi_{1,i} + 2(\xi_{2,i} + \Delta s \frac{\zeta}{P_t} \left(\frac{W}{K} + 1 \right) \right. \right. \\
& \left. \left. - \xi_{1,i} \right) + \frac{2+3\lambda_0}{\zeta} \left(\frac{(\xi_{1,i+1} - \xi_{1,i-1})^2}{4} + \left(\Delta s \frac{\zeta}{P_t} \left(\frac{W}{K} + 1 \right) \right)^2 \right] \right. \\
& \left. + P_t \left[- 4 - \frac{2\Delta s \left(\frac{W}{K} + 1 \right) (2+3\lambda_0)}{P_t} + \frac{(2+3\lambda_0)(1+3\lambda_0)}{\zeta^2} \right] \right\}
\end{aligned}$$

$$\begin{aligned}
& \left(\frac{(\xi_{1,i+1} - \xi_{1,i-1})^2}{4} + (\Delta s \frac{\zeta}{P_t} (\frac{W}{K} + 1))^2 \right) - 2 \left(\frac{(2+3\lambda_0)(\Delta s)(\frac{W}{K} + 1)}{P_t} \right)^2 \Big] \\
& - \left(\frac{(2+3\lambda)}{\zeta^2} \cdot \frac{(\xi_{1,i+1} - \xi_{1,i-1})^2}{4} P_t (2+3\lambda_0) \right) + (\Delta s \frac{W}{K}) \\
& \left[(- (1+3\lambda_0)) \left(\frac{2+3\lambda}{P_b} \frac{\partial P_b}{\partial z} \Delta s + 3 \ln \left(\frac{P_b}{P_t} \right) \frac{\partial \lambda}{\partial z} \Delta s - \frac{2+3\lambda}{P_t} \Delta s \left(\frac{W}{K} + 1 \right) \right) \right. \\
& \left. + \left(- 3.0 \frac{\partial \lambda}{\partial z} \Delta s + \frac{(2+3\lambda)(\Delta s)(\frac{W}{K} + 1)}{P_t} \right) \right] + \left(\frac{\Delta s}{r} \cdot \frac{\xi_{1,i+1} - \xi_{1,i-1}}{2} \right. \\
& \left. \cdot \frac{P_t}{\zeta} \right) \Big] - \Delta s \frac{W}{K} (1+3\lambda_0) \frac{\partial K_r}{\partial z} \Delta s \\
& - \frac{2\eta\lambda(1-S_r)}{P_b^{2+2\lambda}} \frac{\Delta s^2}{\Delta \tau} P_{ave}^{2+2\lambda} (\xi_{1,i}^{K+1} - \xi_{1,i}^K) (2+2\lambda) \left(\frac{1}{2} \right) \cdot (P_t) \\
& \left(\frac{1}{\zeta P_{ave}} \right) - \frac{2\eta\lambda(1-S_r)}{P_b^{2+2\lambda}} \frac{\Delta s^2}{\Delta \tau} P_{ave}^{2+2\lambda} \tag{177}
\end{aligned}$$

$$\frac{\partial F_{1,i}}{\partial \xi_{2,i}} = 2 K_v P_t \tag{178}$$

$$\begin{aligned}
\frac{\partial F_{1,i}}{\partial \xi_{1,i+1}} &= K_v \left\{ P_t \left[1 + \frac{(2+3\lambda_0)}{4\zeta} (2 \xi_{1,i+1} - 2\xi_{1,i-1}) \right] - \frac{(2+3\lambda)P_t}{4\zeta} \right. \\
& \left. (2 \xi_{j,i+1} - 2\xi_{1,i-1}) + \frac{P_t}{r} \frac{\Delta s}{2} \right\} = K_v P_t \left[1 + \frac{2+3\lambda_0}{2\zeta} (\xi_{1,i+1} - \xi_{1,i-1}) \right. \\
& \left. - \frac{2+3\lambda}{2\zeta} (\xi_{1,i+1} - \xi_{1,i-1}) + \frac{\Delta s}{2r} \right] \tag{179}
\end{aligned}$$

$$\begin{aligned}
\frac{\partial F_{1,i}}{\partial \xi_{1,i-1}} &= K_V \left\{ P_t \left[1 + \frac{2+3\lambda_0}{4\zeta} (2\xi_{1,i-1} - 2\xi_{1,i+1}) \right] - \frac{(2+3\lambda)}{4\zeta} \right. \\
&\quad \left. (2\xi_{1,i-1} - 2\xi_{1,i+1}) - \frac{P_t}{r} \frac{\Delta s}{2} \right\} = K_V P_t \left[1 - \frac{2+3\lambda_0}{2\zeta} \right. \\
&\quad \left. (\xi_{1,i+1} - \xi_{1,i-1}) + \frac{2+3\lambda}{2\zeta} (\xi_{1,i+1} - \xi_{1,i-1}) - \frac{\Delta s}{2r} \right] \quad (180)
\end{aligned}$$

(b) For flow field or interior elements of Jacobian D.--

$$\begin{aligned}
\frac{\partial F_{j,i}}{\partial \xi_{j,i}} &= K_V \left\{ P_t \left[(-2 - 2) + (2+3\lambda_0) \left(\frac{(\xi_{j,i+1} - \xi_{j,i-1})^2}{4} + \right. \right. \right. \\
&\quad \left. \left. \frac{(\xi_{j-1,i} - \xi_{j+1,i})^2}{4} \right) \left(\frac{\partial(\frac{1}{\zeta})}{\partial \xi} \right) \right] + \frac{\partial P_t}{\partial \xi_{j,i}} \left[\frac{(\xi_{j,i+1} + \xi_{j,i-1} - 2\xi_{j,i})}{4} \right. \\
&\quad \left. + \frac{(\xi_{j+1,i} - \xi_{j-1,i} - 2\xi_{j,i})}{4} + \frac{2+3\lambda_0}{\zeta} \left(\frac{(\xi_{j,i+1} - \xi_{j,i-1})^2}{4} \right. \right. \\
&\quad \left. \left. + \frac{(\xi_{j-1,i} - \xi_{j+1,i})^2}{4} \right) \right] - \left(\frac{(2+3\lambda)(\xi_{j,i+1} - \xi_{j,i-1})^2}{4} \right. \\
&\quad \left. \cdot \frac{\zeta \frac{\partial P_t}{\partial \xi_{j,i}} - P_t \frac{\partial \zeta}{\partial \xi_{j,i}}}{\zeta^2} \right) \left. \right\} + \left(\frac{\partial P_t}{\partial \xi_{j,i}} \frac{\xi_{j-1,i} - \xi_{j+1,i}}{2} \right. \\
&\quad \left. - \frac{\partial \zeta}{\partial \xi_{j,i}} \Delta s \right) \left(K_V \frac{(2+3\lambda)}{P_b} \frac{\partial P_b}{\partial z} \Delta s + 3 K_V \ln \left(\frac{P_b}{P_t} \right) \frac{\partial \lambda}{\partial z} \Delta s \right. \\
&\quad \left. - \frac{K_V (2+3\lambda)}{\zeta} \frac{(\xi_{j,i+1} - \xi_{j,i-1})}{2} + \frac{\partial K_V}{\partial z} \Delta s \right) + \left(P_t \frac{(\xi_{j-1,i} - \xi_{j+1,i})}{2} \right. \\
&\quad \left. - \zeta \Delta s \right) \left(- 3 K_V \frac{\partial \lambda}{\partial z} \Delta s \frac{1}{\zeta} - K_V (2+3\lambda) \frac{(\xi_{j,i+1} - \xi_{j,i-1})}{2} \right)
\end{aligned}$$

$$\begin{aligned}
& \frac{\partial \left(\frac{1}{\zeta} \right)}{\partial \xi_{j,i}} \Big) + \left(\frac{\Delta s K_v}{r} \frac{\xi_{j,i+1} - \xi_{j,i-1}}{2} \frac{\partial P_t}{\partial \xi_{j,i}} \right) \\
& + \left(\frac{\xi_{j-1,i} - \xi_{j+1,i}}{2} \frac{\partial P_t}{\partial \xi_{j,i}} - \Delta s \frac{\partial \zeta}{\partial \xi_{j,i}} \right) \\
& - \frac{2n\lambda(1-S_r)}{p_b^{2+2\lambda}} \frac{\Delta s^2}{\Delta \tau} p_{ave}^{1+2\lambda} (\xi_{j,i}^{K+1} - \xi_{j,i}^K) \frac{\partial P_{ave}}{\partial \xi_{j,i}} - \\
& - \frac{2n\lambda(1-S_r)}{p_b^{2+2\lambda}} \frac{\Delta s^2}{\Delta \tau} p_{ave}^{2+2\lambda} \tag{181}
\end{aligned}$$

Since

$$\frac{\partial P_t}{\partial \xi_{j,i}} = \frac{P_t}{\zeta} \tag{182}$$

$$\frac{\partial \zeta}{\partial \xi_{j,i}} = - (1+3\lambda_0) \tag{183}$$

$$\frac{\partial \left(\frac{1}{\zeta} \right)}{\partial \xi_{j,i}} = \frac{- (- (1+3\lambda_0))}{\zeta^2} \tag{184}$$

$$\begin{aligned}
3.0 K_v \frac{\partial \lambda}{\partial z} \Delta s \frac{\partial (\ln \left(\frac{p_b}{P_t} \right))}{\partial \xi_{j,i}} &= 3.0 K_v \frac{\partial \lambda}{\partial z} \Delta s \frac{\partial (\ln p_b - \ln P_t)}{\partial \xi_{j,i}} \\
&= - 3.0 K_v \frac{\partial \lambda}{\partial z} \Delta s \frac{\partial (\ln P_t)}{\partial \xi_{j,i}} \\
&= - 3.0 K_v \frac{\partial \lambda}{\partial z} \Delta s \frac{\partial [1 - (1+3\lambda_0)\xi]}{\partial \xi_{j,i}} \\
&= - 3.0 K_v \frac{\partial \lambda}{\partial z} \Delta s \frac{1}{[1 - (1+3\lambda_0)\xi]} \\
&= - 3.0 K_v \frac{\partial \lambda}{\partial z} \Delta s \frac{1}{\zeta} \tag{185}
\end{aligned}$$

and making some algebraic manipulation the Equation (181) will be in the following form:

$$\begin{aligned}
\frac{\partial F_{j,i}}{\partial \xi_{j,i}} &= K_V \frac{P_t}{\zeta} [(\xi_{j,i+1} + \xi_{j,i-1} - 2\xi_{j,i}) + (\xi_{j+1,i} + \xi_{j-1,i} - 2\xi_{j,i}) \\
&+ \frac{2+3\lambda_0}{\zeta} (\frac{(\xi_{j,i+1} - \xi_{j,i-1})^2 + (\xi_{j-1,i} - \xi_{j+1,i})^2}{4}) - \frac{2+3\lambda}{\zeta} \\
&\frac{(\xi_{j,i+1} - \xi_{j,i-1})^2}{4}] + K_V P_t [-4. + \frac{(2+3\lambda)(1+3\lambda_0)}{\zeta^2} \\
&(\frac{(\xi_{j,i+1} - \xi_{j,i-1})^2 + (\xi_{i-1,i} - \xi_{j+1,i})^2}{4} - \frac{(2+3\lambda)(1+3\lambda_0)}{\zeta^2} \\
&\cdot \frac{(\xi_{j,i+1} - \xi_{j,i-1})^2}{4}] + [\frac{2+3\lambda}{P_b} \frac{\partial P_b}{\partial z} K_V \Delta s + 3. K_V \ln (\frac{P_b}{P_t}) \\
&\frac{\partial \lambda}{\partial z} \Delta s - \frac{K_V (2+3\lambda)}{\zeta} \frac{\xi_{j-1,i} - \xi_{j+1,i}}{2} + \frac{\partial K_V}{\partial z} \Delta s] (\frac{P_t}{\zeta} \\
&\frac{(\xi_{j-1,i} - \xi_{j+1,i})}{2} + (1+3\lambda_0) \Delta s) + (P_t \frac{(\xi_{j-1,i} - \xi_{i+1,i})}{2} \\
&- \zeta \Delta s) [- 3K_V \frac{\partial \lambda}{\partial z} \Delta s \frac{1}{\zeta} - \frac{K_V (2+3\lambda)(1+3\lambda_0)}{\zeta^2} \frac{(\xi_{j-1,i} - \xi_{j+1,i})}{2}] \\
&+ K_V \frac{P_t}{r\zeta} \frac{P_t}{r} \frac{(\xi_{j,i+1} - \xi_{j,i-1})}{2} \Delta s - \frac{2\eta\lambda(1-S_r)}{P_b^{2+2\lambda}} \frac{\Delta s^2}{\Delta \tau} P_{ave}^{(2+2\lambda)} \\
&(\xi_{j,i}^{K+1} - \xi_{j,i}^K) (2+2\lambda) (\frac{1}{2}) (P_t) \frac{1}{(\zeta P_{ave})} - \frac{2\eta\lambda(1-S_r)}{P_b^{2+2\lambda}} \\
&\frac{\Delta s^2}{\Delta \tau} P_{ave}^{(2+2\lambda)}
\end{aligned} \tag{186}$$

$$\begin{aligned}
\frac{\partial F_{j,i}}{\partial \xi_{j-1,i}} &= K_V P_t \left[1. + \frac{2+3\lambda_0}{2\zeta} (\xi_{j-1,i} - \xi_{j,i+1}) + \right. \\
&\quad \left. \left(\frac{2+3\lambda}{P_b} \frac{\partial P_b}{\partial z} \Delta s + 3 \ln \left(\frac{P_b}{P_t} \right) \frac{\partial \lambda}{\partial z} \Delta s - \frac{(2+3\lambda)}{\zeta} \frac{(\xi_{j-1,i} - \xi_{j+1,i})}{2} \right) \right] \\
&\quad + \frac{P_t}{2} \frac{\partial K_V}{\partial z} \Delta s - K_V \left(P_t \frac{(\xi_{j-1,i} - \xi_{j+1,i})}{2} - \zeta \Delta s \right) \frac{(2+3\lambda)}{2\zeta} \quad (187)
\end{aligned}$$

$$\begin{aligned}
\frac{\partial F_{j,i}}{\partial \xi_{j+1,i}} &= K_V P_t \left[1. - \frac{2+3\lambda_0}{2\zeta} (\xi_{j-1,i} - \xi_{j+1,i}) - \frac{1}{2} \left(\frac{2+3\lambda}{P_b} \right. \right. \\
&\quad \left. \left. \frac{\partial P_b}{\partial z} \Delta s + 3 \ln \left(\frac{P_b}{P_t} \right) \frac{\partial \lambda}{\partial z} \Delta s - \frac{2+3\lambda}{\zeta} \left(\frac{\xi_{j-1,i} - \xi_{j+1,i}}{2} \right) \right) \right] \\
&\quad - \frac{P_t}{2} \frac{\partial K_V}{\partial z} \Delta s + K_V \left(P_t \frac{(\xi_{j-1,i} - \xi_{j+1,i})}{2} - \zeta \Delta s \right) \frac{(2+3\lambda)}{2\zeta} \quad (188)
\end{aligned}$$

$$\begin{aligned}
\frac{\partial F_{j,i}}{\partial \xi_{j,i+1}} &= K_V P_t \left[1 + \frac{2+3\lambda_0}{2\zeta} (\xi_{j,i+1} - \xi_{j,i-1}) - \frac{2+3\lambda}{2\zeta} \right. \\
&\quad \left. (\xi_{j,i+1} - \xi_{j,i-1}) + \frac{\Delta s}{2r} \right] \quad (189)
\end{aligned}$$

$$\begin{aligned}
\frac{\partial F_{j,i}}{\partial \xi_{j,i-1}} &= K_V P_t \left[1 - \frac{2+3\lambda_0}{2\zeta} (\xi_{j,i+1} - \xi_{j,i-1}) + \frac{2+3\lambda}{2\zeta} \right. \\
&\quad \left. (\xi_{j,i+1} - \xi_{j,i-1}) - \frac{\Delta s}{2r} \right] \quad (190)
\end{aligned}$$

(c) For the Bottom Boundary or Bottom Row of Jacobian D.--

$$\begin{aligned}
 \frac{\partial F_{N_z, i}}{\partial \xi_{N_z, i}} &= K_V \left\{ \frac{P_t}{\zeta} \left[\xi_{N_z, i+1} + \xi_{N_z, i-1} - 2\xi_{N_z, i} + 2(\xi_{N_z-1, i} - \Delta s \frac{\zeta}{P_t} \right. \right. \\
 &\quad \left. \left. - \xi_{N_z, i} \right) + \frac{2+3\lambda_0}{\zeta} \left(\frac{(\xi_{N_z, i+1} - \xi_{N_z, i-1})^2}{4} + \left[\Delta s \frac{\zeta}{P_t} \right]^2 \right) \right] \\
 &\quad + P_t \left[-4. + \frac{2 \Delta s (2+3\lambda_0)}{P_t} + \frac{(2+3\lambda_0)(1+3\lambda_0)}{\zeta^2} \left(\frac{(\xi_{N_z, i+1} - \xi_{N_z, i-1})^2}{4} \right. \right. \\
 &\quad \left. \left. + \left[\Delta s \frac{\zeta}{P_t} \right]^2 \right) - 2 \left(\frac{(2+3\lambda_0) \Delta s}{P_t} \right)^2 \right] - \left(\frac{2+3\lambda}{\zeta^2} \right. \\
 &\quad \left. \frac{(\xi_{N_z, i+1} - \xi_{N_z, i-1})^2}{4} P_t (2+3\lambda_0) \right) + \left(\frac{\Delta s}{r} \frac{(\xi_{N_z, i+1} - \xi_{N_z, i-1})}{2} \right. \\
 &\quad \left. \frac{P_t}{\zeta} \right) - \frac{2\eta\lambda(1-S_r)}{P_b^{2+2\lambda}} \frac{\Delta s^2}{\Delta \tau} P_{ave}^{2+2\lambda} (\xi_{N_z, i}^{K+1} - \xi_{N_z, i}^K) (2+2\lambda) (.5) (P_t) \\
 &\quad \left(\frac{1}{\zeta P_{ave}} \right) - \frac{2\eta\lambda(1-S_r)}{P_b^{2+2\lambda}} \frac{\Delta s^2}{\Delta \tau} P_{ave}^{2+2\lambda} = 0 \tag{191}
 \end{aligned}$$

$$\frac{\partial F_{N_z, i}}{\partial \xi_{N_z-1, i}} = 2.0 K_V P_t \tag{192}$$

$$\begin{aligned}
 \frac{\partial F_{N_z, i}}{\partial \xi_{N_z, i+1}} &= K_V \left\{ P_t \left[1 + \frac{2+3\lambda_0}{\zeta} \frac{2\xi_{N_z, i+1} - 2\xi_{N_z, i-1}}{4} \right] - \left(\frac{2+3\lambda}{\zeta} P_t \right. \right. \\
 &\quad \left. \left. \cdot \frac{(2\xi_{N_z, i+1} - 2\xi_{N_z, i-1})}{4} \right) + \frac{P_t \Delta s}{r \cdot 2} \right\} \\
 &= K_V P_t \left[1 + \frac{2+3\lambda_0}{2\zeta} (\xi_{N_z, i+1} - \xi_{N_z, i-1}) - \frac{2+3\lambda}{2\zeta} \right. \\
 &\quad \left. (\xi_{N_z, i+1} - \xi_{N_z, i-1}) + \frac{\Delta s}{2r} \right] \tag{193}
 \end{aligned}$$

$$\begin{aligned}
\frac{\partial F_{N_z, i}}{\partial \xi_{N_z, i-1}} &= K_V \left\{ P_t \left[1 + \frac{2+3\lambda_0}{\zeta} \left(\frac{2\xi_{N_z, i-1} - 2\xi_{N_z, i+1}}{4} \right) \right] - \frac{2+3\lambda}{\zeta} P_t \right. \\
&\quad \cdot \left. \frac{(2\xi_{N_z, i-1} - 2\xi_{N_z, i+1})}{4} - \frac{P_t}{r} \frac{\Delta s}{2} \right. \\
&\quad = K_V P_t \left[1 - \frac{2+3\lambda_0}{2\zeta} (\xi_{N_z, i+1} - \xi_{N_z, i-1}) + \frac{2+3\lambda}{2\zeta} P_t \right. \\
&\quad \cdot \left. (\xi_{N_z, i+1} - \xi_{N_z, i-1}) - \frac{\Delta s}{2r} \right] \tag{194}
\end{aligned}$$

THE COMPUTER PROGRAM

Description and Structure of the Program

The program is written in FORTRAN IV language. A flow chart which describes the basic logic used in development of the program is given in Appendix I. The FORTRAN program consists of the main program, several subroutines and two function subroutines.

Main Program.-- Main program reads and calculates the following parameters to establish the dimensions and solution characteristics, initializes the problem and determines the manner of computation and outputting of the solution:

N2X	Number of grid points in the radial direction to outer edge of circle r_a over which water is applied
MX	Number of grid points in radial direction to outer radius of problem.
MY	Number of grid points in axial direction between top surface and bottom of problem.
NT	Number of time steps through which computation are to be completed.
HI	Value of the static equilibrium initial hydraulic head h_0 . (Minus must be punched into card).
DEPTH	The depth between top surface and bottom of the problem.
DELT	Size of dimensionless time step increments $\Delta\tau$ which are to be used in obtaining the solution.
SL	The characteristic length used to non dimensionalize all length parameters of the problem.

iteration. The individual line iterations are terminated when the absolute sum of change between consecutive iteration is less than ERR.

ERRT A parameter used to terminate Newton-Relaxation iteration in each time plane iteration when the absolute sum of change between consecutive iteration is less than ERRT (ERRT = 100 * ERR).

SATMAX Maximum saturation which can be attained in the soil surface which is used to transfer top boundary condition from specified application rate to specified saturation.

OMEGA Maximum saturation the soil can attain in the bottom boundary drain layer and moisture begins to build up in the soil profile. When OMEGA is less than computed saturation at the bottom boundary the $P_t = P_b$.

NRIT2 Number of regular time steps between which solution are printed.

NHSTAR If HNSTAR is less than zero only the values of the dependent variable ξ will be printed at the specified time steps. If NHSTAR = 0 the value of ξ , the saturation and hydraulic head will be printed at the specified time steps. If NHSTAR is greater than zero, values of ξ will not be printed, but values of saturation and hydraulic head will be printed.

MAX Maximum Newton-line iterations that will be allowed. The number of iterations on any time plane which will be allowed will be one-half this many.

MAXT The maximum number of iterations on any time plane that will not be allowed $MAXT = \frac{MAX}{2.0}$.

ISTEPB	An index when it is greater than one the first time step will be subdivided to some unequal but smaller time steps.
DELS	Dimensionless space increment Δs $DELS = \frac{HEIGHT}{MY-T}$.
R	Dimensionless radius of circle of application r_a , $R = DELS * FLOAT (N2X-1)$
AREAC	Dimensionless area of circle of application $AREAC = \pi * R * R$
Q	Application rate per area of the circle of application $Q = VK * AREAC$
TIME	Dimensionless time τ .
HO(J,I)	Values of pressure head at time = 0.0, $HO(J,I) = H(J,I)$.
HD(J,I)	Difference between pressure head at previous time step and current time step. $HD(J,I) = HO(J,I) - H(J,I)$.
H(J,I)	Values of pressure head at any time.
B(J,I)	Values of hydraulic head at any time.
D(I)	Values of saturation calculated from Brooks-Corey Equation
SATT	Magnitude of saturation on the circular water application rate. When SATT equals or is greater than the SATMAX the specified flux condition will be changed to specified saturation (NSSUR = 1) and pressure head will be calculated from the SSUR specified.
SI(I)	Initial saturation.

The main program specifies the problem and directs the order of computation and nature of output by calling subroutines and also changes the boundary condition. The program is capable of reading a

constant flux rate or an array of rainfall records (intensity and its time of occurrence). This condition defining the specified flux rate is true when the intake capacity of the soil is greater than the applied flux. When the intake capacity is exceeded, which is a normal phenomenon in the nature, the soil surface becomes fully saturated and the soil properties will govern infiltration. In this type of infiltration phenomenon, the boundary condition of soil surface ② - ③ changes to a specified saturation of about 90 percent and solution continues. Also data from a histogram can be read in to calculate and evaluate some dependent variables of infiltration. In the case of constant flux it is possible to obtain very useful information about flow from a trickle source or a low head sprinkler irrigation for example. For the flow of water from infiltrometers used to determine the infiltration rate of a soil, the program is capable of simulating this condition by setting a specified saturation at the beginning of the infiltration process. In the main program subroutines INITIA, DERV, TIMSTH, RITOUT are called, and a brief description of these subroutines is given in the following:

Subroutine INITIA.--Subroutine INITIA initializes the static equilibrium pressure head $H(J,I)$, dependent variable (ξ) $XI(J,I)$ and distribution of saturation in the soil profile by the following equations:

$$H(J,I) = HEIGT - DELS * FLOAT(J-L) - HIT \quad (195)$$

$$XI(J,I) = (H(J,I) * * ERR 1-1.) / ERRT \quad (196)$$

$$SI(J) = SR(J) + SR1(J) * (BB(J) / H(J,I) * * AMBDA(J) \quad (197)$$

But, whenever the saturation is specified the pressure head and ξ values for the boundary ② - ③ is obtained by the known saturation in this surface by the following equation:

$$H(1,I) = BB(1)/((SSUR - SR(1))/SR1(1)) * * (1./AMBDA(1)) \quad (198)$$

$$XI(1,I) = (H(1,I) * ERR1 - 1.) / ERR1 \quad (199)$$

for I = 1, N2X

Subroutine DERV.--In subroutine DERV the coefficient of the quadratic equations which will be used in defining the variation of pore size distribution exponent, λ , bubbling pressure, P_b , residual saturation, S_r , and porosity, η , saturated hydraulic conductivity was read. In this subroutine the magnitudes of all variables and their derivatives for each grid point and other parameters are determined and written out. The calculated values of each variable for every grid point passed through common statement which they will be used by the function subroutines F1 and F3 and one subroutine FJ. The quadratic distribution of soil parameters are as:

$$\lambda = AMBDA(J) = AL + (BL + CL * Z) * Z \quad (200)$$

$$K_v = VKS(J) = AKV + (BKV + CKV * Z) * Z \quad (201)$$

$$\eta = POR(J) = APOR + (BPOR + CPOR * Z) * Z \quad (202)$$

$$S_r = SR(J) = ASR + (BSR + CSR * Z) * Z \quad (203)$$

$$P_b = BB(J) = APB + (BPB + CPB * Z) + Z \quad (204)$$

in which

$$AKV = 1.0 - (BKV + CKV * HEIGT) * HEIGT \quad (205)$$

$$Z = HEIGT - DELS * FLOAT (J-1) \quad (206)$$

Subroutine TIMSTH.--Subroutine TIMSTH carries out the computation needed to advance one time step. This subroutine calls function subroutines F1 and F3 and subroutine FJ for the previous and current time steps. (K and K+1 time level) and subroutine FIBNOK. The major amount of computations take place in this subroutine. The function subroutine F3 will not be called unless the wetting front penetrates to the bottom boundary. When the values of the function F at each grid point are calculated in the flow region, the main computation will start by the Newton-Line-Relaxation method. In this method, as described before, iteration is created within an iteration. When the iteration numbers and error terms are satisfied, the process is terminated. The initial guess for $(\xi)^{\circ}$ in the Newton method is obtained by changing $H(J,I)$ or $XI(J,I)$ at each grid point by the amount they changed during the previous time step.

Function F1.--This function solves the function F1 and its derivatives P(1) and DP(1) at each grid point for both previous (NN=0) and current time step (NN \neq 0). The value of parameters which they are computed in subroutine DERV for J=1 are used in this subroutine to evaluate the equations F1, D(1) and DP(1). This subroutine calculates the value of F1 and its derivatives P(1) and DP(1) just for one grid point at soil surface when it is called.

Subroutine FJ.--For the interior portion of flow field subroutine FJ is used to solve the function F and its derivatives DM(J), D(J) and DP(J) by having the values of parameters which are determined in subroutine DERV for J=2 in MY-1.

Function F3.--The equation F3 which has been developed for the bottom boundary condition, and its derivatives equations D(MY) and DM(MY) are solved by this Function F3. Again values of parameters which have been evaluated in subroutine DERV for J=MY are used in this computation.

Subroutine FIBNOK.--Subroutine is called when $ERR1 * XI(J,I)$ is less than -0.99999. When the value of $ERR1 * XI(J,I)$ is less than or equal to -1.0, there is no solution for equation and computer will stop. For example, when the magnitude of $ERR1 * XI(J,I)$ is equal to -1.0 the computed pressure head will be $P_t = \infty$. In another case when the computed value of pressure head, P_t , is less than zero which is going to be used in functions F1, F3 and subroutine FJ to evaluate the term:

$$\log \left(\frac{P_b}{P_t} \right) \quad (235)$$

It is obvious that taking logarithm from a negative number is undefined. This subroutine then determines the root to each F by first squaring and then utilizing a Fibonacci search (117) to obtain the minimum of a squared function. After using the Fibonacci search iterative scheme for a few iterations, the solution process is again turned over to the Newton-Raphson iteration.

Subroutine RITOUT.--Subroutine RITOUT will print pressure head, hydraulic head and saturation at each grid point if specified through an input parameter. When the value of NM (NM = NHSTAR) is greater than zero only the values of saturation and hydraulic head will be

$$V_w^{K+1} - V_w^o = \sum_{j,i} 2\pi \eta \Delta s^3 (i-1) (S_{j,i}^{K+1} - S_{j,i}^o) \quad (218)$$

The values of dimensionless time τ and dimensionless volume of water which has infiltrated is recorded in each time step (TIM1 and WATC01). The average and instantaneous infiltration and infiltration per unit area is computed from

$$\text{Average Infiltration rate} = \frac{\text{WATCOT}}{\text{TIME}} \quad (219)$$

$$\text{Instantaneous Infiltration Rate} = \frac{\text{WATCOT} - \text{WATC01}}{\text{TIME} - \text{TIM1}} \quad (220)$$

$$\text{Instantaneous Infiltration per unit area} = \frac{\text{Inst. Infil. rate}}{\text{AREAC}} \quad (221)$$

in which WATCOT is the volume of water at current time step (dimensionless); WATC01 is the volume of water at previous time step (dimensionless); TIME is the actual dimensionless time; TIM1 is the magnitude of dimensionless time at previous time step; and AREAC is the dimensionless area circle of application.

DATA AND SPECIFICATION REQUIRED TO OBTAIN A SOLUTION

The required data and specifications of a problem are provided by means of several cards containing input data. The required data can be categorized as follows:

1. Establishing the dimensions of the problem.
2. Defining the physical properties of the soil.
3. Specifying the initial hydraulic head distribution and rainfall records.
4. Controlling the flow of computation including the type and amount of information printed out.

Establishing Dimensions for the Problem

The dimensions for the problem are established by specifying input data for soil depth (i.e. distance between the drained layer and the soil surface) and the number of grid lines to be used for the finite difference computations. The input data of the number of grid lines consists of number of lines radial from the axis of infiltrometer (circular area) to the outer boundary (MX), number of axial lines (MY) and the number of radial lines from the center of the infiltrometer to the edge of infiltrometer (circular water input area) N2X.

The incremental distance between adjacent grid lines in the axial direction, Δz , is obtained by dividing the depth of soil, D, by the number of axial grid lines minus one (minus one because the number of grid spaces is one less than the number of grid lines). Since the square

grid points are used in finite difference operators, the radial increment Δr is equal to the axial increment Δz . The radius of infiltrrometer is obtained by multiplying the increment ($\Delta r = \Delta z = \Delta s$) by specified number of grid lines to the infiltrrometer ring (or circular water entry zone) minus one $r_a = \Delta s \cdot (N2X - 1)$. The outer radius of the problem is determined by the following:

$$r_f = \Delta s \cdot (MX - 1) \quad (222)$$

and the number of grid lines from the axis of symmetry to the infiltrrometer ring of radius r_a is given by:

$$N2X = \left(\frac{MY - 1}{D} \right) \cdot r_a + 1 \quad (223)$$

In carrying out the computations required in the solution of flow equation, only those grid points within the region affected by infiltrating water are used during any time step, that is, the field over which the computations takes place is expanded gradually as required to be just ahead of the wetting front. Therefore, a solution to a problem not underlain by horizontal lower boundary can be accomplished by specifying a depth of soil greater than the depth through which the wetting front will penetrate. Generally, it is better to specify the number of grid lines to the outer boundary of the problem equal to the size of FORTRAN array dimensions corresponding to the radial lines. In this way there is less chance that the wetting front will penetrate laterally far enough to reach this outer boundary. But when a relatively shallow depth of soil is specified and computation is extended over a considerably longer time period, relatively much lateral movement occurs, then the wetting may reach

the outer boundary of the flow region and computation will be terminated.

Defining Hydraulic Properties of the Soil

The program utilizes the Brooks-Corey equations in the solution of the problem, requires that the following parameters and their variations be specified:

1. residual saturation, S_r
2. pore size distribution index, λ
3. bubbling pressure head, P_b
4. the soil porosity, η
5. saturated hydraulic conductivity, K_0

Residual Saturation.--The residual saturation is defined as the saturation at which water movement ceases. Brooks and Corey (9) reported that there was not too much difficulty in determination of residual saturation from desaturation curves. But when the wetting fluid is water and the medium is clay determination of the S_r is difficult. For example, clay soils, whose structure deteriorates on wetting, will not follow the typical S-shaped curve ($S-P_c$), and a residual saturation will not exist. Brooks and Corey (9) carefully removed all the clay from some sandstone cores and reduced the residual saturation almost to zero. Consequently, they reported high values of residual saturation for the sands containing some clay. Also they showed that the residual saturation is not entirely a function of clay content, perhaps the physical significance of residual

saturation can be explained in terms of a discontinuity in the distribution of pore sizes.

Pore-Size Distribution Exponent.--The pore size distribution exponent is the negative slope of the best-fit straight line drawn through effective saturation ($S-S_r$) and capillary pressure P_c data points plotted on log-log paper, Fig. 2. Sandy soils which have only a very narrow range of pore sizes have larger values of pore size distribution exponent, λ , than soils with structure and a larger range of pore sizes.

Bubbling Pressure Head.--The bubbling pressure is the capillary pressure at which air first begins to flow through the saturated porous media. Bower (5) defined the term critical tension as the capillary pressure head at the center of the range over which a permeability reduction occurs, which is similar to bubbling pressure head. Extrapolation of a straight line on log-log graph (Fig. 2) to the intercept of effective saturation $S_e = 1.0$ gives the value of bubbling pressure head, P_b . The values of parameters S_r , λ , and P_b can be obtained from a desaturation curve.

Soil Porosity.--Soil porosity is the ratio of volume of voids and total volume of the soil. For the single-grain materials, its value is smaller than for well developed soils.

Initialization of Hydraulic Head

The initial hydraulic head can be established by assigning all the values equal to a constant which is read in as one of input

parameters. The initialization with a constant hydraulic head represents a static equilibrium in which no external forces other than gravity are acting on the system. It is apparent that good judgment is required in specifying a problem to insure that all specifications are consistent with one another. For instance, specifying a flux rate which exceeds the infiltration capacity of the soil, or specifying an unrealistic initial hydraulic head, gives results that may not be valid in representing a physical condition. When the time increment $\Delta\tau$ is too large with respect to other features of the problem, this also will create difficulty in the numerical computation. Also smaller values of $\Delta\tau$ causes little difference in the value of hydraulic head and saturation to occur between the two consecutive time steps. Specifying a large infiltration rate creates some numerical computation difficulties. In order to obtain a solution to the problem, the infiltration rate is increased in magnitude during the first few time steps until a large rate is specified. Thereafter the infiltration rate can remain constant at a desired level for all other time steps.

Controlling the Flow of Computations

A number of parameters are required as input data which control whether or not specific computations are performed and the type and amount of output. These parameters serve to determine whether specified flux conditions or specified saturation is going to be used and when the flow of computation changes from one condition to another condition, and also those time steps when calculated values of hydraulic head, pressure head and saturation should be printed out.

saturation condition) of 90 percent. A horizontal lower boundary is assumed to exist at the bottom of the soil profile and no water will flow into the bottom boundary unless the soil at the bottom of the profile becomes fully saturated. The outer boundary is far enough from the source of water that the wetting front can not reach to this boundary.

2. Dimensions and Problem Specification

For all problems the dimensionless depth from soil surface to the bottom boundary was $D = 2.0$ and the dimensionless radius of circular area was taken as $r_a = 0.3$. A dimensionless time increment $\Delta\tau$ of .005 was used to start the solution. Thereafter value of $\Delta\tau$ are periodically multiplied by values larger than one to increase the efficiency and decrease the printout time. The solutions shown were terminated before the wetting front had penetrated to the bottom boundary or cylindrical outer boundary.

3. Methodology

To study the effect of heterogeneity of the soil a base solution for homogeneous soil in which all parameters are constant throughout soil profile and several solutions in which only one parameter in each is varied, were obtained. The variation of each parameter is a linear and continuous function of depth z . The variable z has a maximum value of 2 on the soil surface and $z = 0$ at drained layer. Except for variation of parameter K_v which is a dimensionless function of the depth, the other variations of parameter were chosen such that the average value of the parameter would be equal to its constant value in the homogeneous soil example.

Table 2 summarizes the specifications used in obtaining the solutions presented in the various figures hereafter. Subsequently, these solutions are referred to by the number in the first column of Table 2.

As the water moves into the soil filling a portion of the voids, the capillary pressure is increased (decreased in absolute magnitude) with a resulting increase in hydraulic head. Therefore, an examination of the variation of capillary pressure or head in the flow field reveals much about the nature of water movement. By noting the extent of the change from the initial capillary pressure in the lateral and vertical directions, an indication of the importance of soil heterogeneity effects on the flow pattern can be seen. Lines of constant capillary pressure head for different variables are shown in Figs. 9 through 13 for two dimensionless times, $\tau = 0.0$ and $\tau = 1.46$. The figures were drawn using the solution results from problems number 1 through 11 in Table 2. In each figure, a few lines of the constant capillary pressure head (iso-pressure head) lines have been plotted. The computer program defines the wetting front to be at a position where capillary pressure exceeds the initial hydraulic head by .0003 dimensionless units. The vertical position of the wetting front represents the depth of water penetration, and the difference between the maximum radial movement and the radius of the circle of the water application zone, r_a , equals the amount of lateral movement at that time step. Figs. 9 through 13 show the effect of soil heterogeneity on the position of wetting front since its position will lie just beyond the -7.0 ft curve. The distribution of dimensionless

TABLE 2.--Summary of Specification of Problems.

Problem Number	Soil Parameters				K_0 In Inches Per Hour	Initial Hydraulic Head, in Feet	Depth, in Feet	Flux, in Inches Per Hour	Surface Saturation, Percent	Radius of Circular Area in Feet	Characteristic Length, in Feet
	P'_b in Feet	λ	S_r	n							
(1)	(2)	(3)	(4)	(5)	(6)	(7)	(8)	(9)	(10)	(11)	(12)
1	1.0	1.0	0.15	0.40	1.0	-8.0	2.0	--	90	0.3	1.0
2	0.7+0.3z	1.0	0.15	0.40	1.0	-8.0	2.0	--	90	0.3	1.0
3	1.3-0.3z	1.0	0.15	0.40	1.0	-8.0	2.0	--	90	0.3	1.0
4	1.0	0.7+0.3z	0.15	0.40	1.0	-8.0	2.0	--	90	0.3	1.0
5	1.0	1.3-0.3z	0.15	0.40	1.0	-8.0	2.0	--	90	0.3	1.0
6	1.0	1.0	0.05+0.1z	0.40	1.0	-8.0	2.0	--	90	0.3	1.0
7	1.0	1.0	0.25-0.1z	0.40	1.0	-8.0	2.0	--	90	0.3	1.0
8	1.0	1.0	0.15	0.18+0.22z	1.0	-8.0	2.0	--	90	0.3	1.0
9	1.0	1.0	0.15	0.62-0.22z	1.0	-8.0	2.0	--	90	0.3	1.0
10	1.0	1.0	0.15	0.40	0.6+0.2z	-8.0	2.0	--	90	0.3	1.0
11	1.0	1.0	0.15	0.40	1.40-0.2z	-8.0	2.0	--	90	0.3	1.0
12	1.0	1.0	0.15	0.40	1.0	-4.0	2.0	--	90	0.30	1.0
13	1.0	1.0	0.15	0.40	1.0	-6.0	2.0	--	90	0.30	1.0
14	1.0	1.0	0.15	0.40	1.0	-8.0	2.0	0.10	--	0.30	1.0
15	1.0	1.0	0.15	0.40	1.0	-8.0	2.0	0.20	--	0.30	1.0
16	1.0	1.0	0.15	0.40	1.0	-8.0	2.0	0.30	--	0.30	1.0
17	1.0	1.0	0.15	0.40	1.0	-8.0	2.0	0.50	--	0.30	1.0
18	1.0	1.0	0.15	0.40	1.0	-8.0	2.0	0.70	--	0.30	1.0
19	1.0	1.0	0.15	0.40	1.0	-8.0	2.0	--	90	0.60	1.0
20	1.0	1.0	0.15	0.40	1.0	-8.0	2.0	--	90	0.90	1.0
21	1.0	1.0	0.15	0.40	1.0	-8.0	2.0	--	90	1.20	1.0

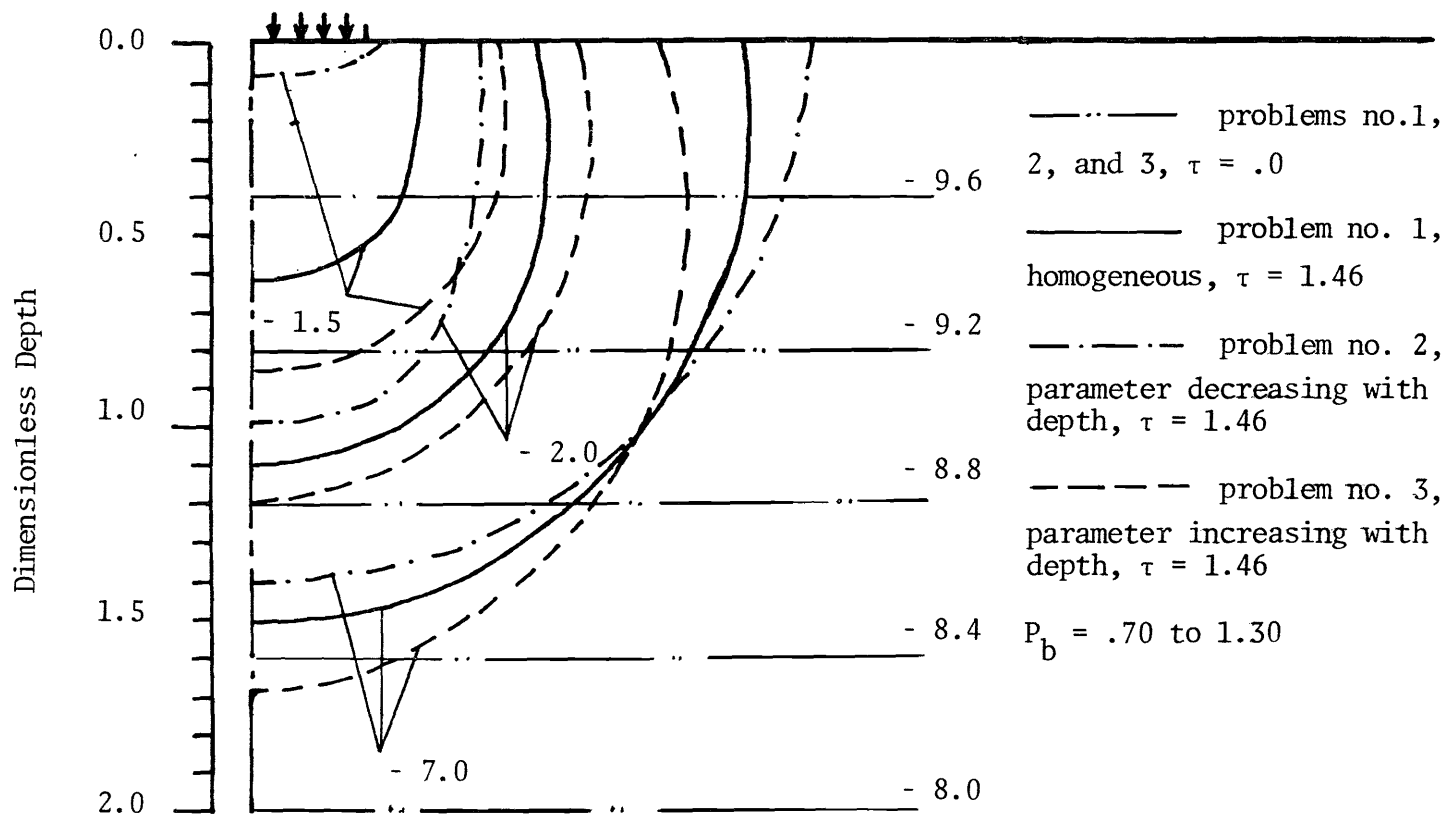


FIG. 9.--Effect of Variation of Bubbling Pressure, P_b , on Distribution of Dimensionless Capillary Pressure P_c Prior to Infiltration and at Dimensionless Time $\tau = 1.46$ from Maintaining the Surface Circle of Application at 90 Percent Saturation for Problems 1 through 3. The Values on the Curves Represent Capillary Pressure Head.

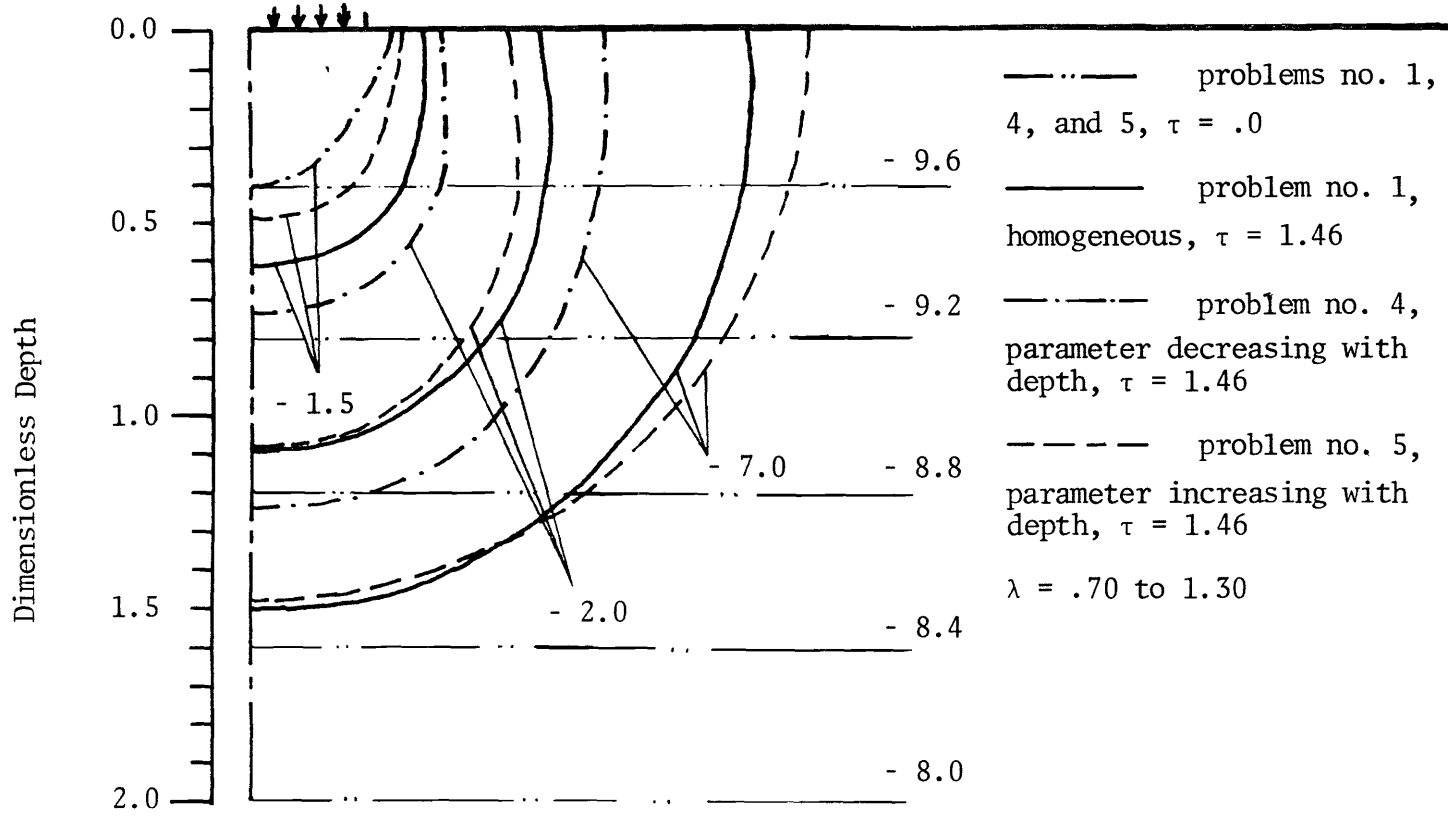


FIG. 10.--Effect of Variation of Pore Size Distribution Exponent, λ , on Distribution of Dimensionless Capillary Pressure P_c Prior to Infiltration and at Dimensionless Time $\tau = 1.46$ From Maintaining the Surface Circle of Application at 80 Percent Saturation for Problems 1, 4, and 5. The Values of the Curves Represent Capillary Pressure Head.

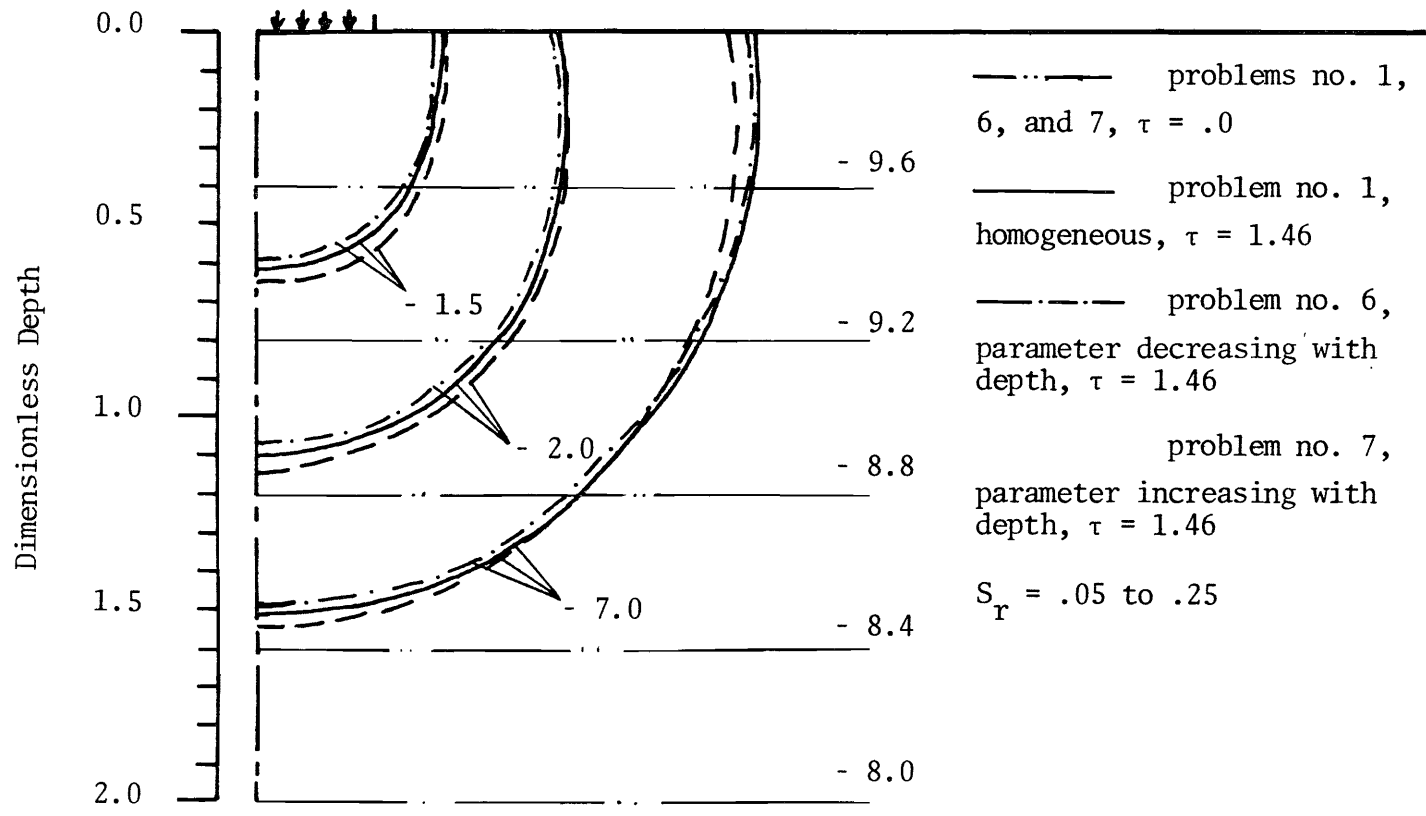


FIG. 11.--Effect of Variation of Residual Saturation, S_r , on Distribution of Dimensionless Capillary Pressure P_c Prior to Infiltration and at Dimensionless Time $\tau = 1.46$ From Maintaining the Surface Circle of Application at 90 Percent Saturation for Problems 1, 6, and 7. The Values of the Curves Represent Capillary Pressure Head.

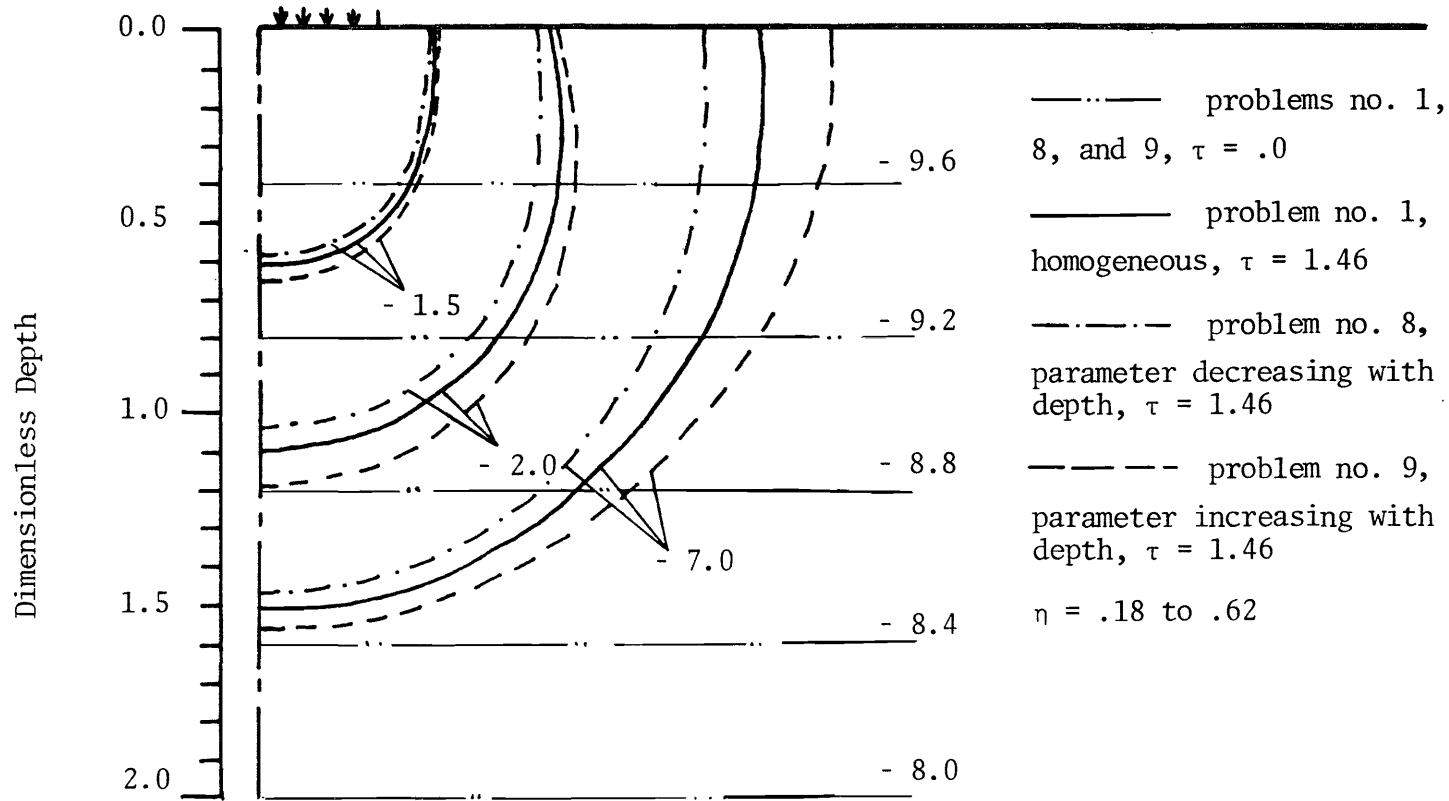


FIG. 12.--Effect of Variation of Porosity, η , on Distribution of Dimensionless Capillary Pressure P_c Prior to Infiltration and at Dimensionless Time $\tau = 1.46$ from Maintaining the Surface Circle of Application at 90 Percent Saturation for Problems 1, 8, and 9. The Values of the Curves Represent Capillary Pressure Head.

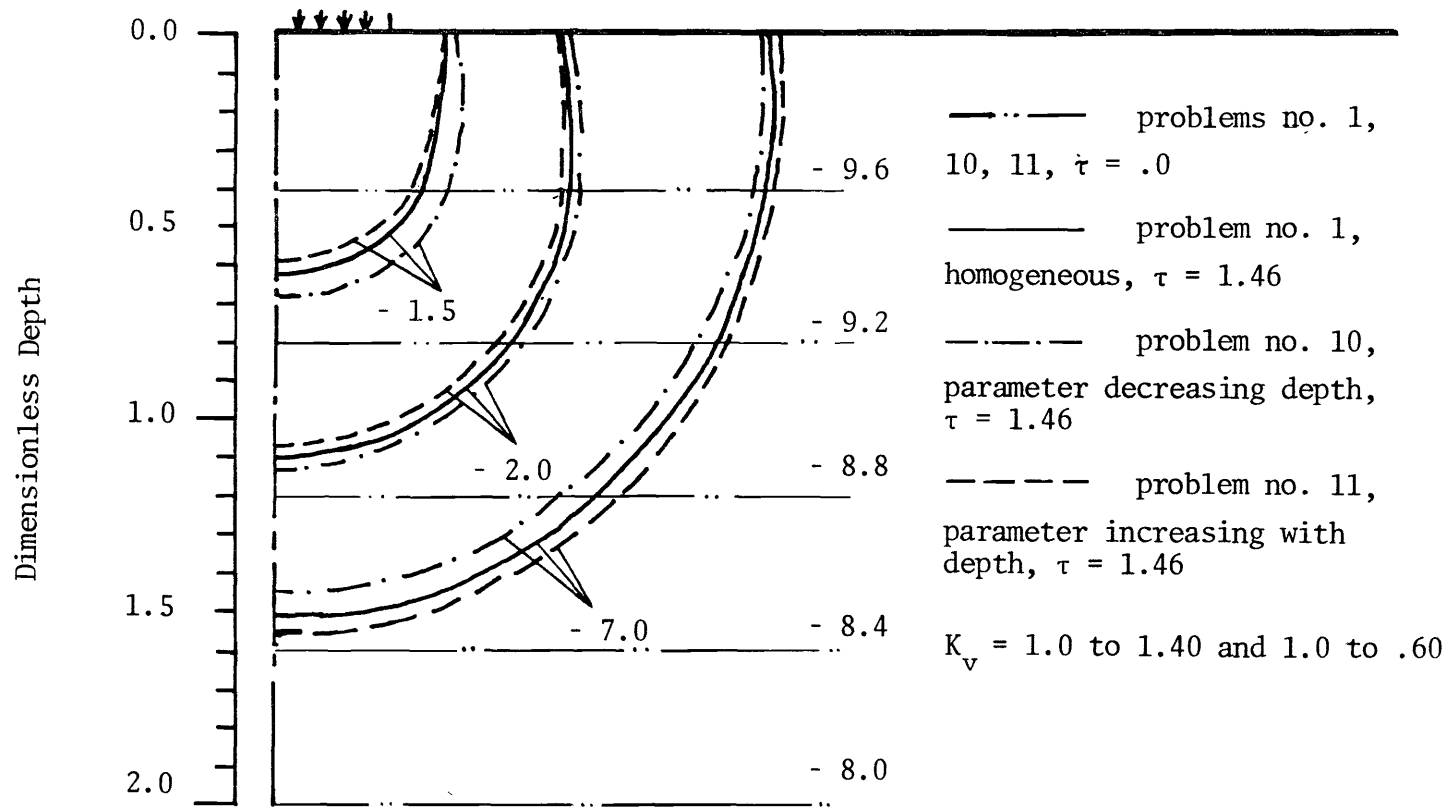
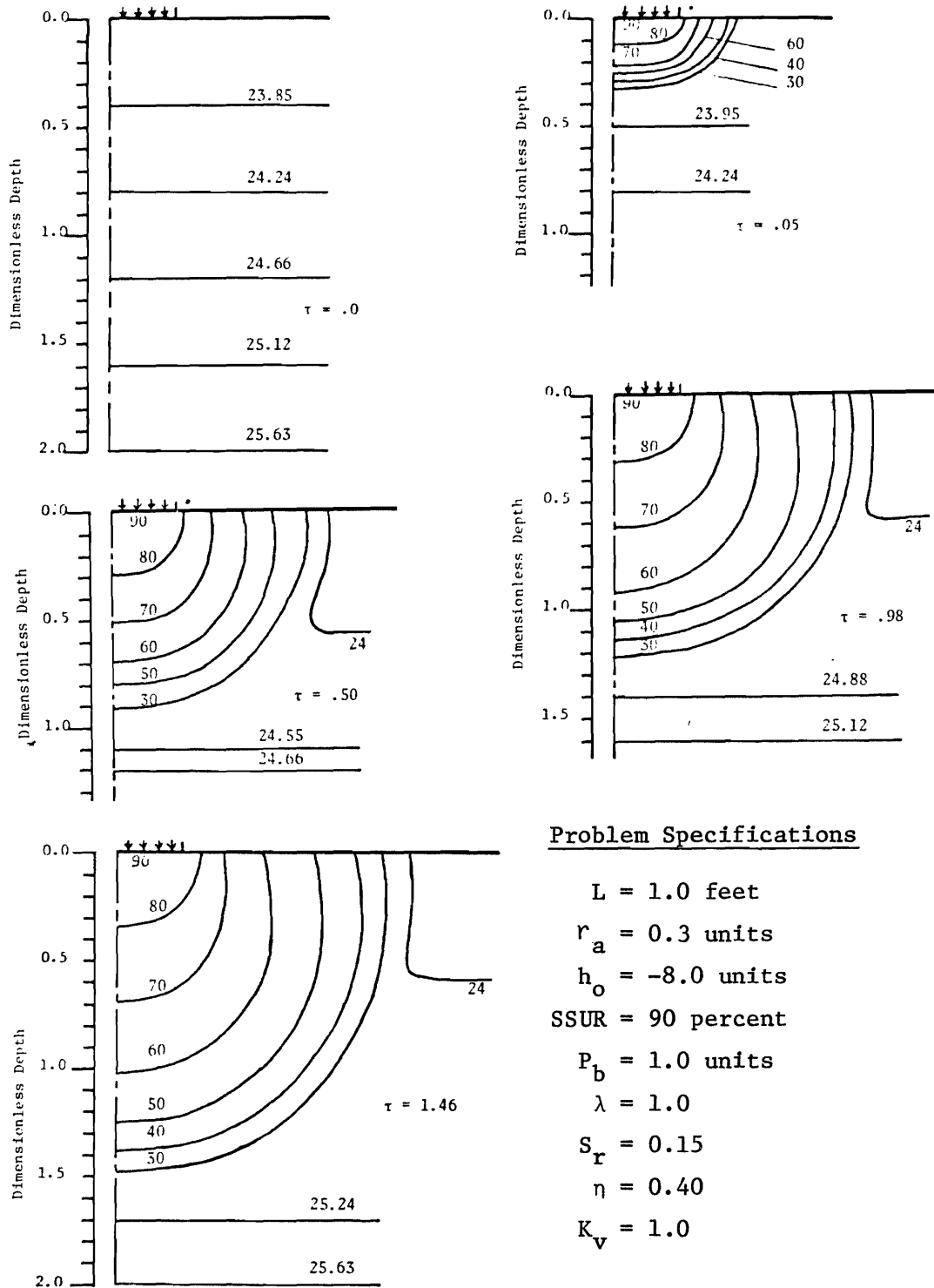


FIG. 13.--Effect of Variation of Saturated Hydraulic Conductivity, K_0 , on Distribution of Dimensionless Capillary Pressure P_c Prior to Infiltration and at Dimensionless Time $\tau = 1.46$ from Maintaining the Surface Circle of Application at 90 Percent Saturation for Problems 1, 10, and 11. The Values of the Curves Represent Capillary Pressure Head.

capillary pressure head prior to the start of the solution (i.e., initial capillary pressure head distribution, $\tau = 0.0$) is the same for all problems and is given by horizontal lines consisting of a long line and two dots. In order to find the difference between the results of the heterogeneous condition and the homogeneous condition, three solutions are plotted on the same graph for each varied parameter considered. In all figures presented hereafter, the dashed line gives solution results for the heterogeneity for which the magnitude of the variable parameter linearly increases with depth. The dash-dot-dash line is for heterogeneity where the magnitude of the variable parameter linearly decreases with depth. Finally, the homogeneous soil conditions where the soil parameters are constant, is shown by solid lines.

The increase in relative saturation in the soil from the beginning of water application is another item of interest. Distribution of saturation on a plane passing through the axis of symmetry at several time steps from results of the solutions in Table 2 are plotted in Figs. 14 through 24. The individual graphs show the vertical penetration and lateral movement of the wetting front at different dimensionless times.

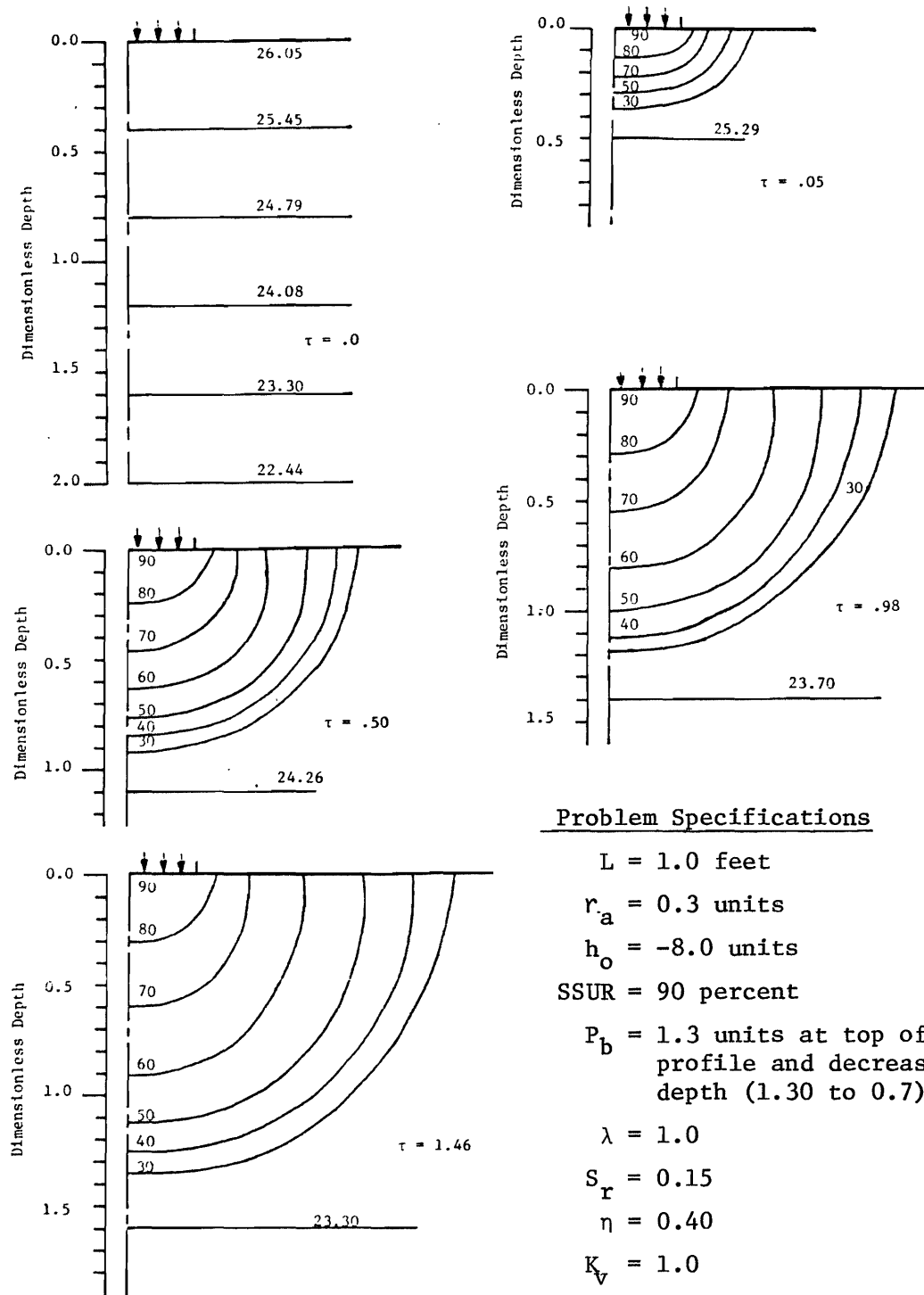
The resultant flow patterns from the solutions to the problems in Table 2 have been plotted for several dimensionless times, τ , in Figs. 25 through 31. These figures show how heterogeneity effects saturation with depth and how changes continue during the infiltration process. The saturation condition before there is water movement is shown for each problem at the right side of Figs. 25 through 31. Each different heterogeneity causes a different initialization of



Problem Specifications

- L = 1.0 feet
- r_a = 0.3 units
- h_o = -8.0 units
- SSUR = 90 percent
- P_b = 1.0 units
- λ = 1.0
- S_r = 0.15
- η = 0.40
- K_v = 1.0

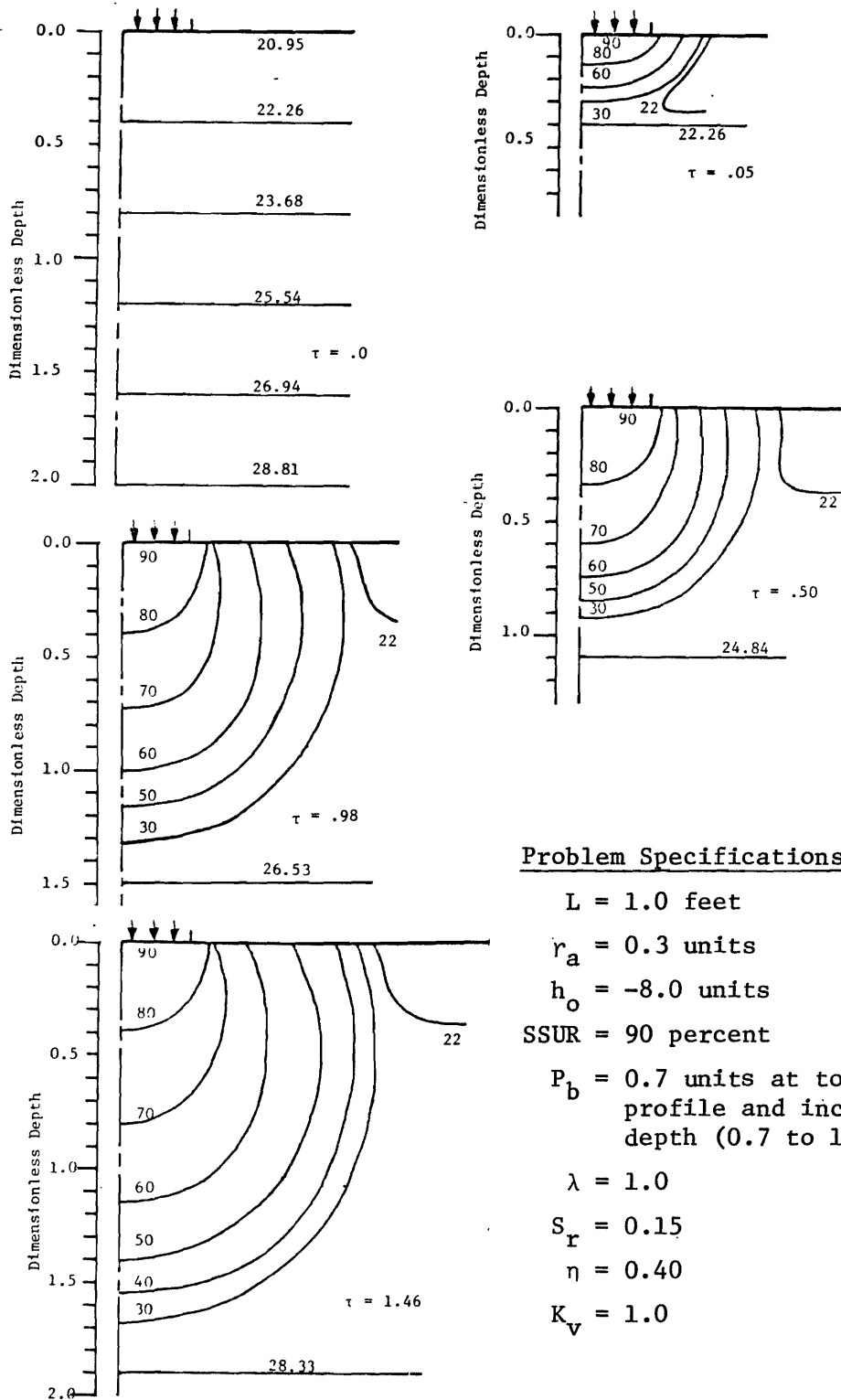
FIG. 14.--Distribution of Saturation at Several Dimensionless Times Resulting from Maintaining the Surface Circle of Application at SSUR = 90 Percent Saturation for Homogeneous Soils (Problem No. 1).



Problem Specifications

- $L = 1.0$ feet
- $r_a = 0.3$ units
- $h_o = -8.0$ units
- SSUR = 90 percent
- $P_b = 1.3$ units at top of soil profile and decreasing with depth (1.30 to 0.7)
- $\lambda = 1.0$
- $S_r = 0.15$
- $\eta = 0.40$
- $K_v = 1.0$

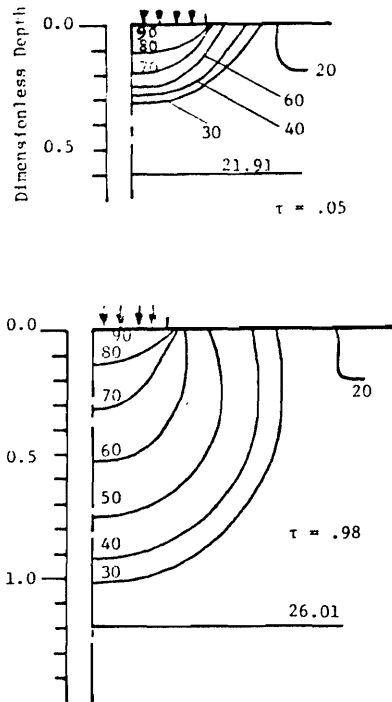
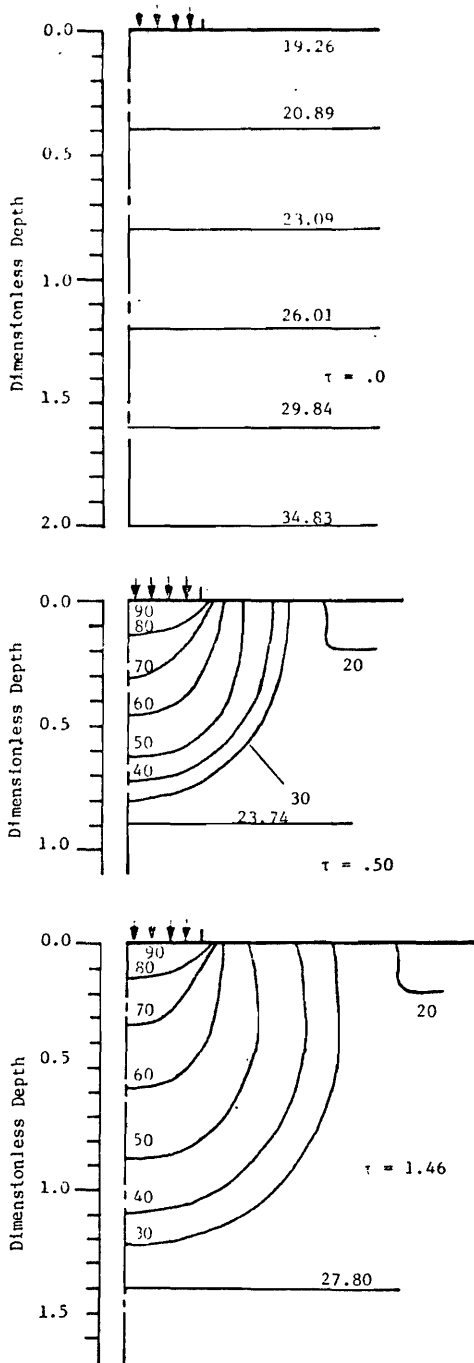
FIG. 15.--Distribution of Saturation at Several Dimensionless Times Resulting from Maintaining Surface Circle of Application at SSUR = 90 Percent Saturation for Heterogeneous Soil, Problem No. 2.



Problem Specifications

- L = 1.0 feet
- r_a = 0.3 units
- h_o = -8.0 units
- SSUR = 90 percent
- P_b = 0.7 units at top of soil profile and increasing with depth (0.7 to 1.3)
- λ = 1.0
- S_r = 0.15
- η = 0.40
- K_v = 1.0

FIG. 16.--Distribution of Saturation at Several Dimensionless Times Resulting from Maintaining Surface Circle of Application at SSUR = 90 Percent Saturation for Heterogeneous Soil, Problem No. 3.



Problem Specifications

- $L = 1.0$ feet
- $r_a = 0.3$ units
- $h_o = -8.0$ units
- SSUR = 90 percent
- $P_b = 1.0$ units
- $\lambda = 1.3$ at top of soil profile and decreasing with depth (1.3 to 0.7).
- $S_r = 0.15$
- $\eta = 0.40$
- $K_v = 1.0$

FIG. 17.--Distribution of Saturation at Several Dimensionless Times Resulting from Maintaining Surface Circle of Application at SSUR = 90 Percent Saturation for Heterogeneous Soil, Problem No. 4.

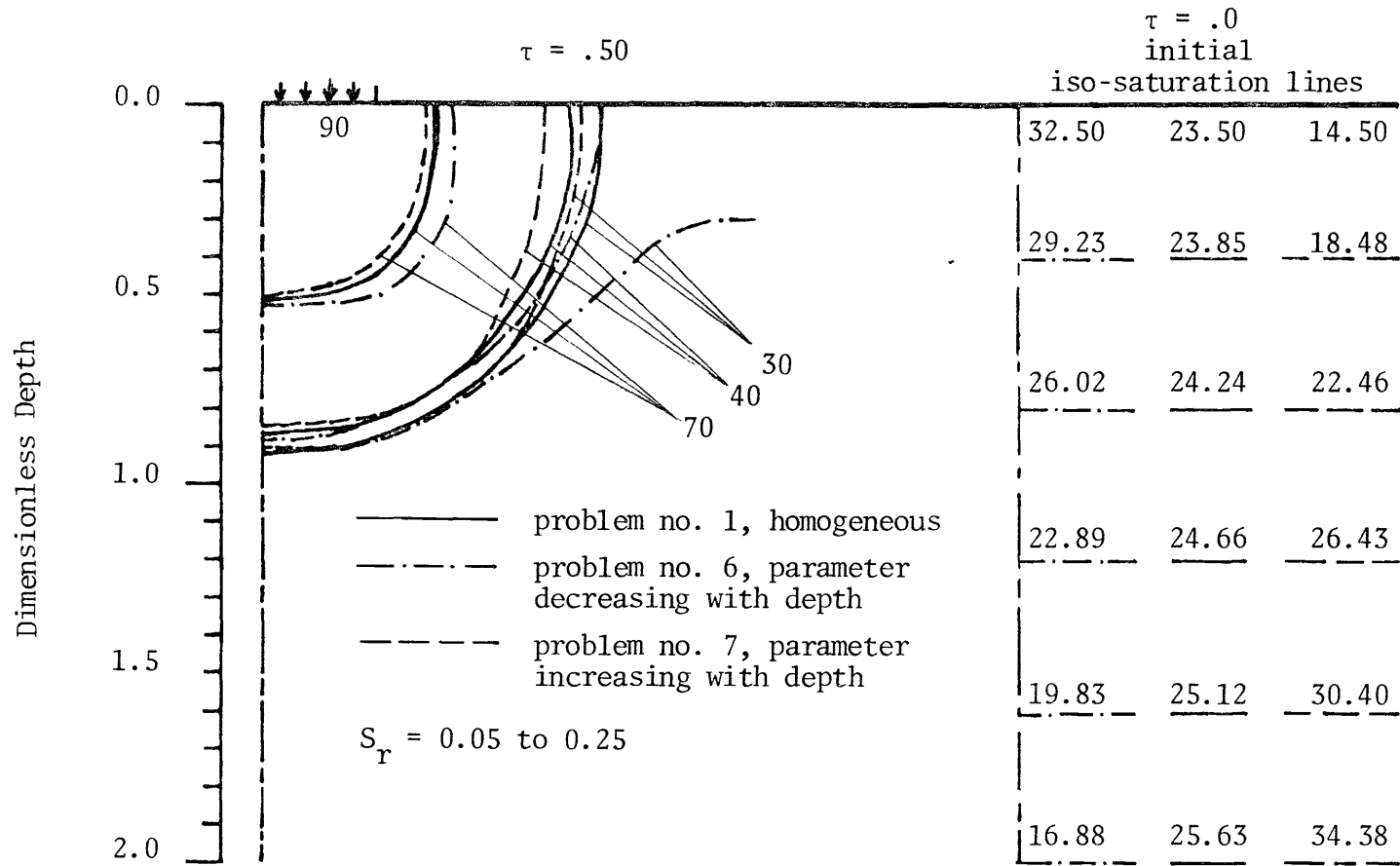


FIG. 28.--Effect of Variation of Residual Saturation, S_r , on Position of Iso-Saturation Lines Prior to Infiltration and at Dimensionless Time $\tau = .50$ from the Results of Solution of Problems 1, 6, and 7.

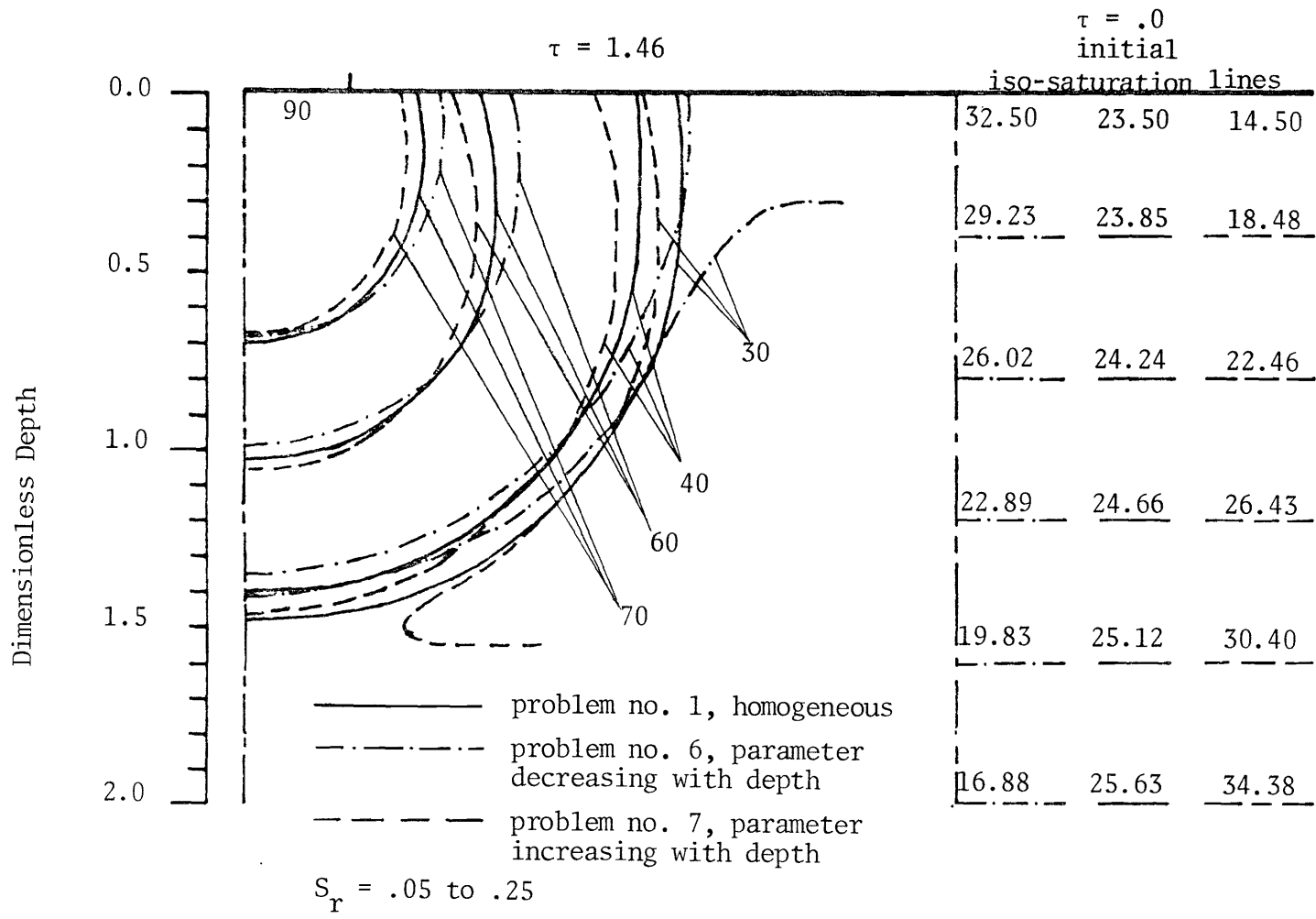


FIG. 29.--Effect of Variation of Residual Saturation, S_r , on Position of Iso-Saturation Lines Prior to Infiltration and at Dimensionless Time $\tau = 1.46$ From the Results of Solution of Problems 1, 6, and 7.

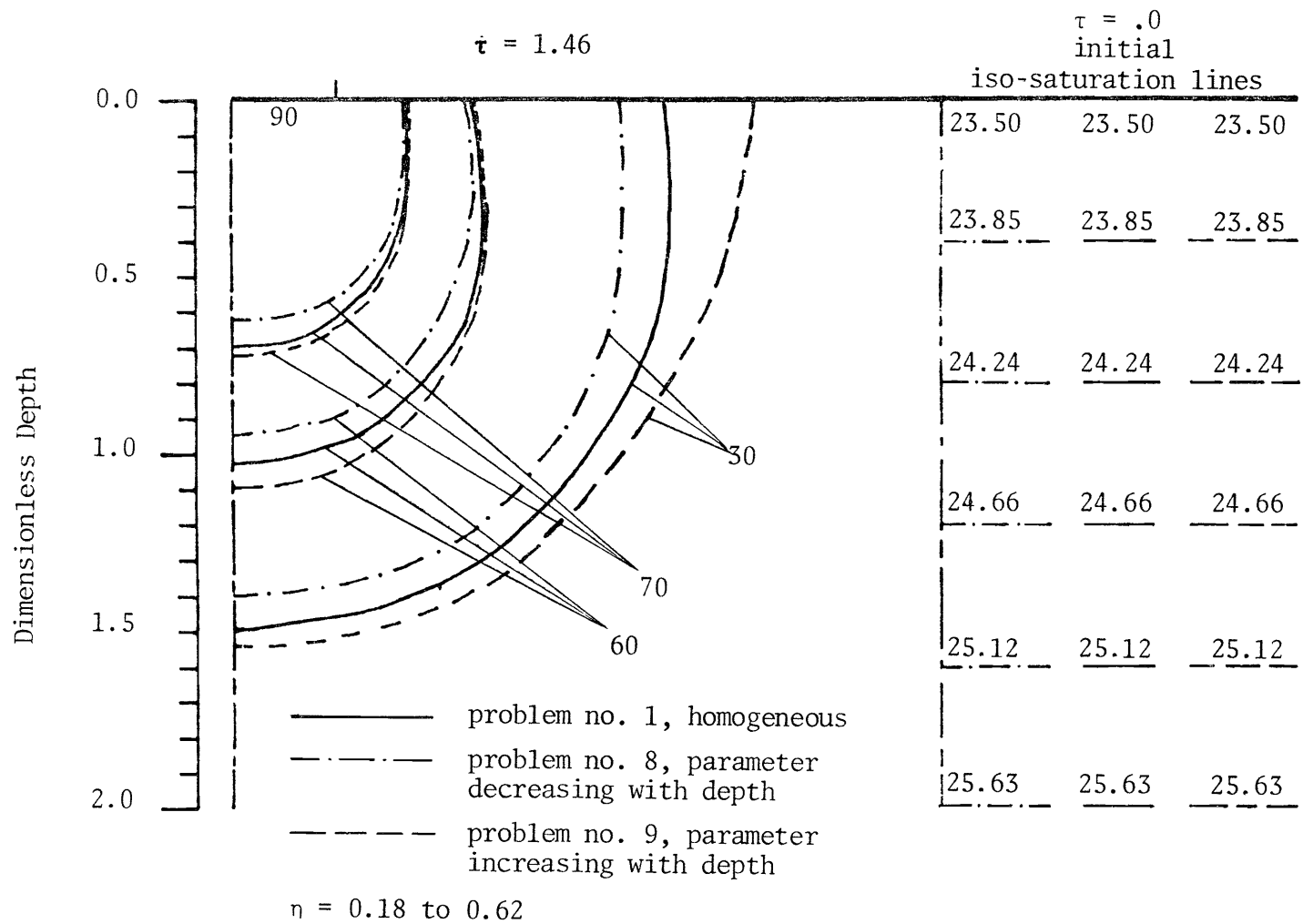


FIG. 30.--Effect of Variation of Porosity, η , on Position of Iso-Saturation Lines Prior to Infiltration and at Dimensionless Time $\tau = 1.46$ from the Results of Solution of Problems 1, 8, and 9.

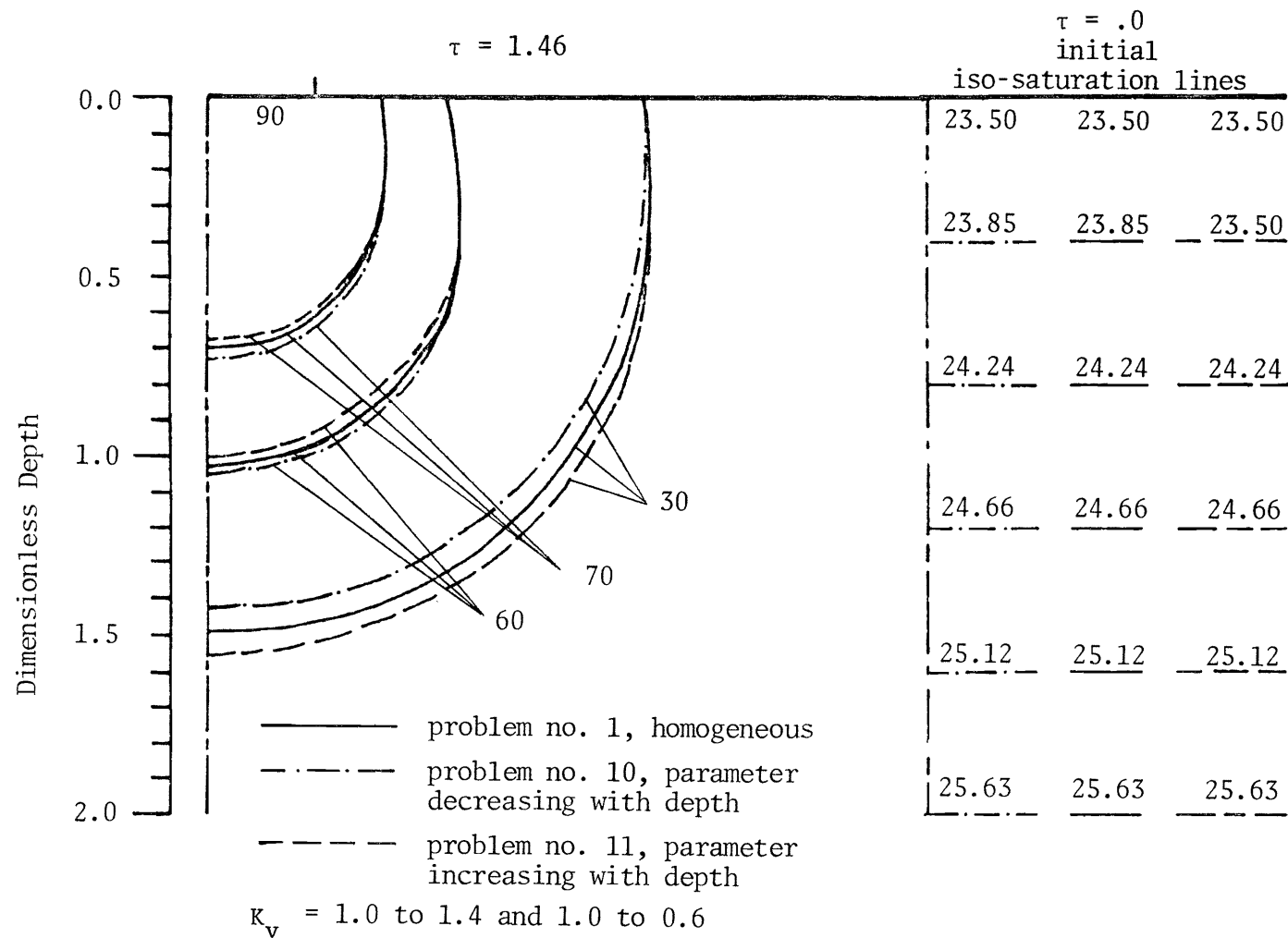


FIG. 31.--Effect of Variation Saturated Hydraulic Conductivity, K_0 , on Position of Iso-Saturation Lines Prior to Infiltration and at Dimensionless Time $\tau = 1.46$ From the Results of Solution of Problems 1, 10, and 11.

saturation except for the porosity, η , and saturated hydraulic conductivity, K_0 . For these two parameters the initial saturation is identical to the homogeneous case. In Fig. 25, the value of bubbling pressure used in solution of problem 1, the homogeneous case, is the average of the bubbling pressure heads of problems 2 and 3 ($\frac{.70 + 1.30}{2}$) = 1.0. Introducing this heterogeneity not only causes the initial saturation under no moisture movement ($\tau = 0.0$) to be different in each problem, but also influences the position of subsequent iso-saturation lines. Fig. 25 shows that the iso-saturation line of 30 percent at dimensionless time $\tau = 1.46$ has occurred at a depth of approximately 1.5 units for homogeneous soil (problem 1). For the same 30 percent iso-saturation line from problem 3, in which the bubbling pressure increases linearly with depth of soil, it is at a depth of 1.7 units. The lateral water movement for homogeneous and heterogeneous soil (Problems 1 and 3) is about 0.80 and 0.65 units, respectively, from the edge of the circular water application area. Where the bubbling pressure decreases linearly with depth (problem No. 2), at the same dimensionless time as $\tau = 1.46$, the vertical and lateral movement of the 30 percent iso-saturation line is 1.35 and 1.05, respectively (Fig. 25). Thus Fig. 25 shows that the rate of vertical penetration of the wetting front is more rapid and that lateral (or radial) movement of the wetting front is slower for soils with larger values of bubbling pressure near the surface, provided the other conditions and soil parameters are held constant. Small bubbling pressures generally correspond to coarse textured soils. Water applied to the surface of coarse soils will normally enter more rapidly than it does into fine soils. The pores are larger in coarse

soils and the movement of the free water is under less restriction than in the fine soils with smaller pores. In problem 2, where the soil texture becomes coarser with depth, i.e., P_b decreases, the wetting front has a tendency to spread laterally in the soil profile and the ratio of horizontal movement and vertical penetration is 0.83. Whereas this ratio for the problems 1 and 3 is 0.61 and 0.44, respectively.

The effects of variation of the pore size distribution exponent, λ , on the flow patterns for solutions of problems 1, 4, and 5 are shown in Figs. 26 and 27. The different distributions of saturation at the beginning of water application in Figs. 26 and 27 shows how λ affects the water movement patterns. Usually sandy soils which have a narrow range of pore sizes have larger values for pore size distribution exponent than soils with finer texture. That is, a larger range of pore sizes in a soil causes λ to be smaller. Fig. 26 shows that at dimensionless time $\tau = 0.50$, the iso-saturation line of 40 percent for homogeneous soil (problem no. 1) lies between the heterogeneous cases (problems No. 4 and 5) where the wetting front has not penetrated to the middle of the soil profile. The vertical penetration for the problems 1, 4, and 5 are 0.87, 0.72, and 0.94 and lateral movements are 0.42, 0.21, and 0.50, respectively. At later times, when the wetting front has passed the middle of the soil profile, the condition changes. For example, in Fig. 27 at dimensionless time $\tau = 1.46$, the 40 percent iso-saturation line for homogeneous soil (problem no. 1) has moved faster in the vertical direction and is ahead of the other 40 percent than lines from problems 4 and 5. Iso-saturation lines for problem 4 are always inside the iso-saturation

lines of the homogeneous soil (problem 1). The iso-saturation lines of the problem 5 in which the values of λ increase with depth, are crossed by the iso-saturation lines of homogeneous soil after the wetting front has passed the middle of the soil profile. In problem 5 the value of pore size distribution exponent, λ , increases linearly with depth ($\lambda = 0.70$ at soil surface) and at the middle of the soil profile its magnitude is $\lambda = 1.0$. The pore size distribution exponent affects the relative hydraulic conductivity as given by the Brooks-Corey's Equation (45). An examination of Equation (45) shows that smaller values of the, λ , will result in higher relative conductivity. Consequently, smaller values of λ , are related to a high hydraulic conductivity of the soil, and soil with larger values of, λ , may act as a hard pan.

Figs. 28 and 29 indicate the influence of the variation of residual saturation, S_r , on the water distribution before infiltration on and on the position of the iso-saturation lines during infiltration. The range of variation of the initial saturation (at $\tau = 0.0$) for problems 6 and 7 is larger than for all problems shown in Table 1. The magnitude of residual saturation directly affects the value of computed saturation from the Brooks-Corey Equation (1) and as Figs. 28 and 29 show, the vertical penetration of water has not been greatly affected. More effect can be seen in lateral water movement. For example, for time $\tau = 0.50$ (Fig. 28) and $\tau = 1.46$ (Fig. 29) the iso-saturation lines of 40 percent show that the difference between vertical penetration for the three problems 1, 6, and 7 is small and that this difference increases with time. Also, Figs. 28 and 29 show that the rate of vertical penetration of the

wetting front is decreased when the values of residual saturation are decreased. At dimensionless time $\tau = 0.50$ as Fig. 28 shows, the iso-saturation line of 40 percent for problem 1 lies between the iso-saturation lines of the problems 6, 7. Later on, at $\tau = 1.46$, the iso-saturation line of 40 percent of problems 6, 7 is shifted. In the lateral direction the water movement pattern is consistent at all times. Since the initial value of saturation is high (32.50 percent for the problem 6 on the soil surface) and decreases with depth, the wetting front moves more rapidly. Also the increasing residual saturation causes the wetting front to move more rapidly in the lower layers.

Variation of soil porosity does not affect the initial distribution of saturation because the computed saturation is independent of the porosity. Consequently, the initial saturation conditions of the homogeneous and heterogeneous cases are the same. An examination of Fig. 30 shows that for the three problems 1, 8, and 9 whose solutions are plotted, the 30 percent iso-saturation line for homogeneous soils lies between the heterogeneous solutions. This is caused by the linear variation of the porosity, η with depth. In the case where the porosity decreases with depth, the volume of wetted soil is smaller than for both the homogeneous and the heterogeneous case in which porosity increases linearly with depth. Soils with high porosity at the upper layers have larger water storage capacity and therefore the rate of advance of wetting front is smaller. A longer time is required to fill the pore spaces.

The positions of the iso-saturation lines from solution of problems 1, 10, and 11 are shown in Fig. 31. The heterogeneity is

caused by linear variation of saturated hydraulic conductivity with depth. Since the values of the computed saturation are independent of the magnitude of the saturated hydraulic conductivity, K_0 , the saturation at the beginning of the solution (at $\tau = 0.0$) for the problems 10 and 11 is the same as for homogeneous soil (problem 1). The saturated hydraulic conductivity is defined as the product of a constant, K_a , with units of velocity and a dimensionless function of the depth, K_v , [$K_0(z) = K_a K_v(z)$]; in which the constant K_a is taken to be equal to the saturated hydraulic conductivity on the soil surface. Therefore, on the soil surface the value of K_v is always equal to one for all problems and linearly decreases or increases with depth. The magnitudes of all soil parameters on soil surface (λ , P_b , S_r , η , and K_0) are the same in problems 1, 10, and 11. For this reason the rate of lateral movement near the soil surface is the same for all cases. It can be concluded that the heterogeneity caused by variations of the saturated hydraulic conductivity does not have a significant effect on the resulting flow patterns in the upper layers. The distribution of iso-saturation lines in Fig. 30 for variable porosity, the 30 percent iso-saturation line for homogeneous soil lies between the lines for the heterogeneous soils (problems 10 and 11). Also Fig. 31 indicates that as saturated hydraulic conductivity increases with depth, the wetting front moved faster than when its magnitude decreased with depth. But the difference between the vertical penetration of the iso-saturation lines for heterogeneous cases and homogeneous cases are not great. These differences may be greater for a greater range of variation of saturated hydraulic conductivity. Otherwise, the properties of the soil near the surface

is governing the resulted water flow patterns. Since near the soil surface these properties are almost the same, it is expected that an almost unique iso-saturation line would exist for three problems 1, 10, and 11.

The changes in soil saturation at different times at the centerline and at a radial distance of 0.4 beyond the circle of application are shown on Figs. 32 through 42. Comparison of the individual curves on these figures indicates how the initialization of saturation in the soil profile, rate of penetration and spreading of wetting front, and distribution of saturation are affected by the heterogeneity defined by variation of the indicated soil hydraulic property. Fig. 32 (problem No. 1, homogeneous soil) shows that at the centerline and at a radial distance of 0.7 units, the wetting front has penetrated to a dimensionless depth of approximately 1.8 and 1.6 units, respectively, at dimensionless time of $\tau = 2.0$. Figs. 33 through 42 (problems 2 to 11, heterogeneous soils) show how rates of penetration of wetting front and distributions of saturation differ for different problem specifications. For example, in the homogeneous soil (Fig. 32) at $\tau = 2.0$, the bottom boundary saturation has not yet been changed by the movement of the wetting front. Whereas, when bubbling pressure increases with depth (Fig. 34) at $\tau = 2.0$ the saturation at the bottom has increased by 6 percent. As another example, the degree of saturation at depth 0.90 units below soil surface at time $\tau = 0.60$ is 32.5 percent, whereas when there is an increasing of porosity with depth, for the same time, and depth, the saturation is approximately 50 percent. Large values of bubbling pressure, P_b , at the soil surface (heavy soils) caused the moisture to spread more laterally but not to

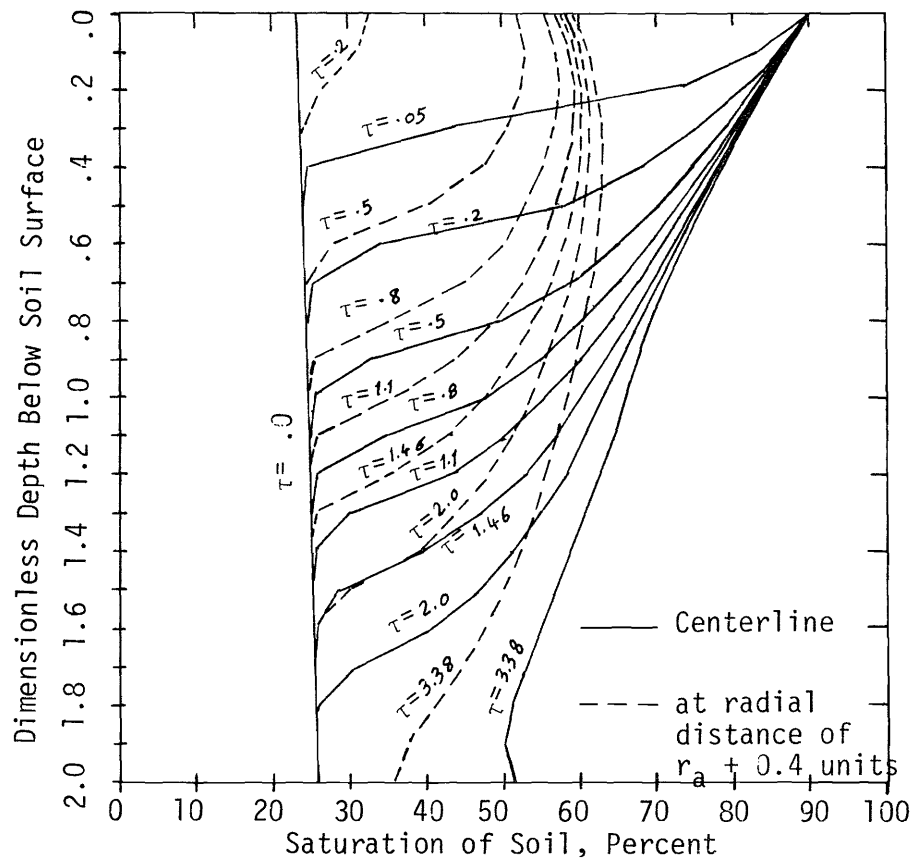


FIG. 32.--Distribution of Saturations with Depth at Several Dimensionless Times at the Centerline and at a Radial Distance from the Centerline Equal to $r = r_a + 0.4 = 0.7$ Units for Problem No. 1 (Homogeneous Soil).

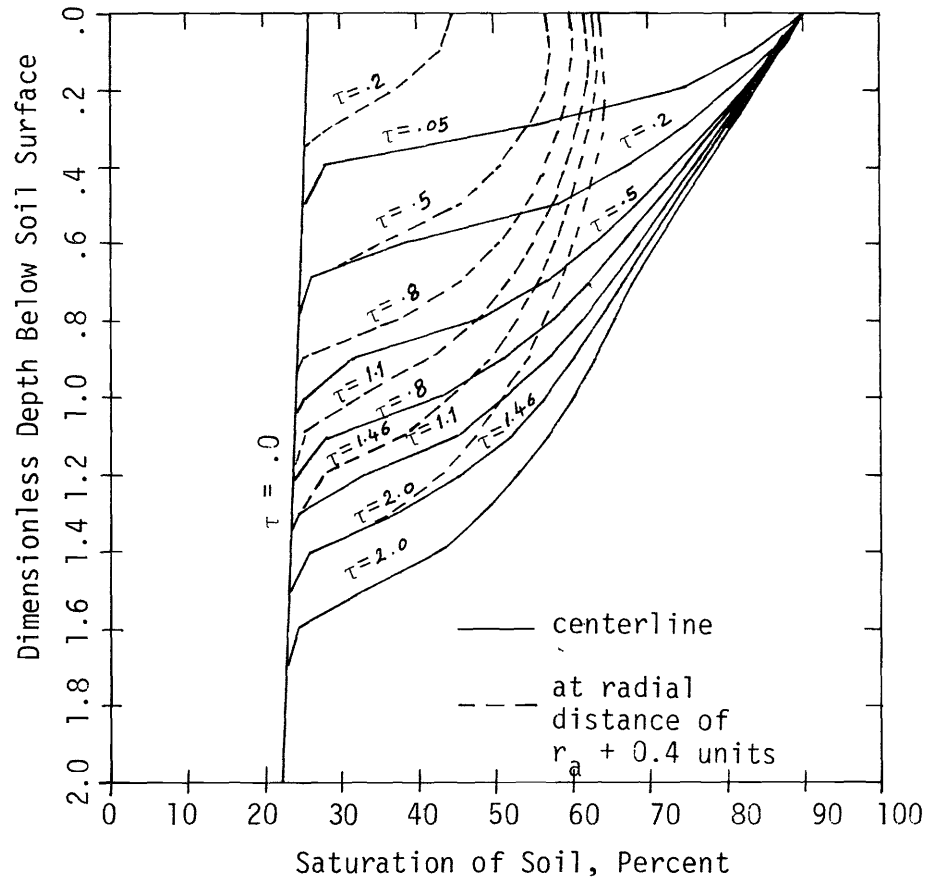


FIG. 33.--Distribution of Saturations with Depth at Several Dimensionless Times at the Centerline and at a Radial Distance from the Centerline Equal to $r = r_a + 0.4 = 0.7$ Units for Problem No. 2 (Magnitude of Dimensionless Bubbling Pressure, P_b , Linearly Decreasing with Depth, 1.30 to 0.70).

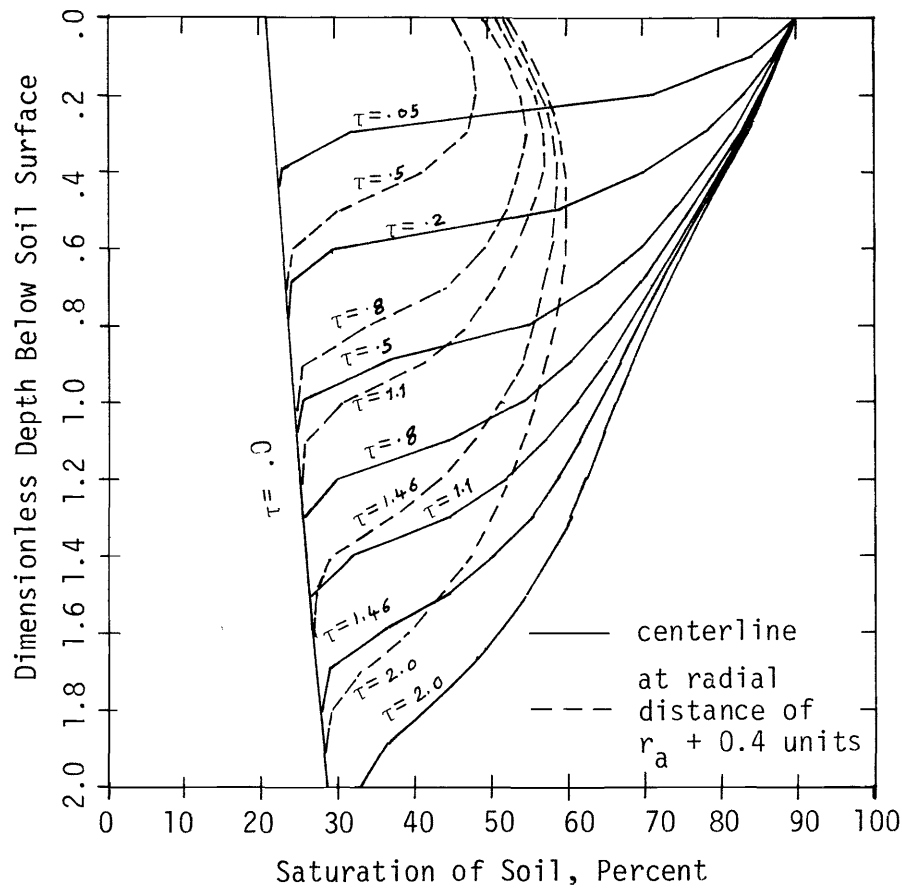


FIG. 34.--Distribution of Saturations with Depth at Several Dimensionless Times at the Centerline and at a Radial Distance from the Centerline Equal to $r = r_a + 0.4 = 0.7$ Units for Problem No. 3 (Magnitude of Dimensionless Bubbling Pressure, P_b , Linearly Increasing with Depth, 0.70 to 1.30).

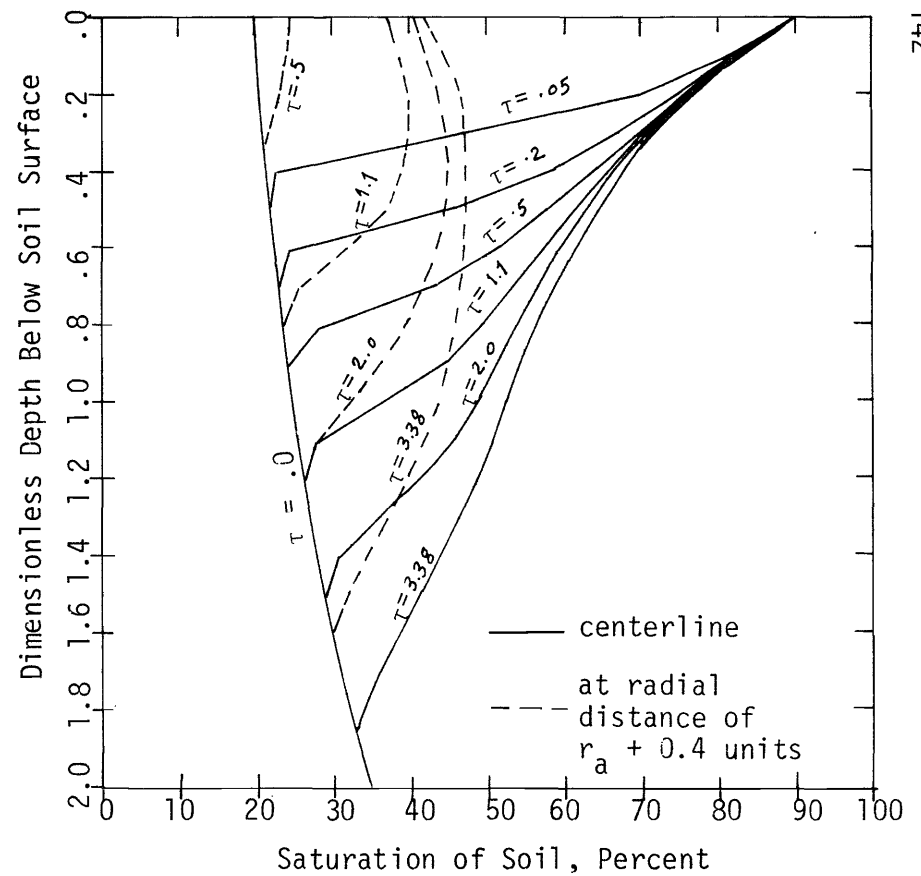


FIG. 35.--Distribution of Saturations with Depth at Several Dimensionless Times at the Centerline and at a Radial Distance from the Centerline Equal to $r = r_a + 0.4 = 0.7$ Units for Problem No. 4 (Magnitude of Pore Size Distribution Exponent, λ , Linearly Decreasing with Depth, 1.30 to 0.70).

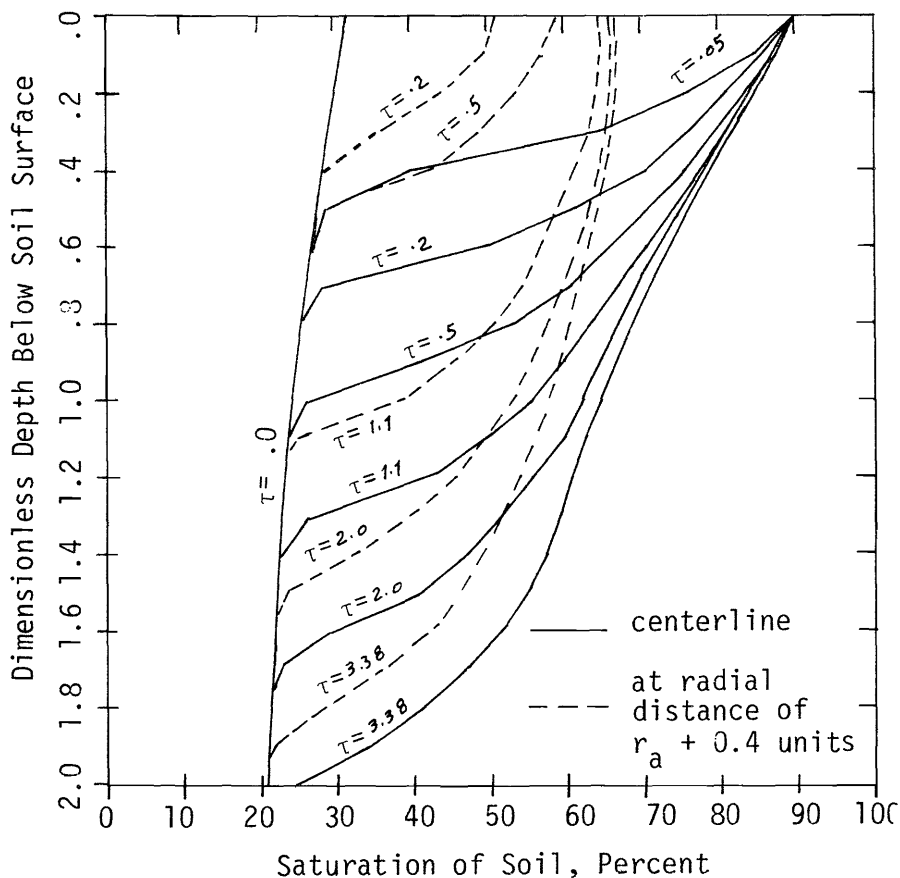


FIG. 36.--Distribution of Saturations with Depth at Several Dimensionless Times at the Centerline and at a Radial Distance from the Centerline Equal to $r = r_a + 0.4 = 0.7$ Units for Problem No. 5 (Magnitude of Pore Size Distribution Exponent, λ , Linearly Increasing with Depth, 0.70 to 1.30).

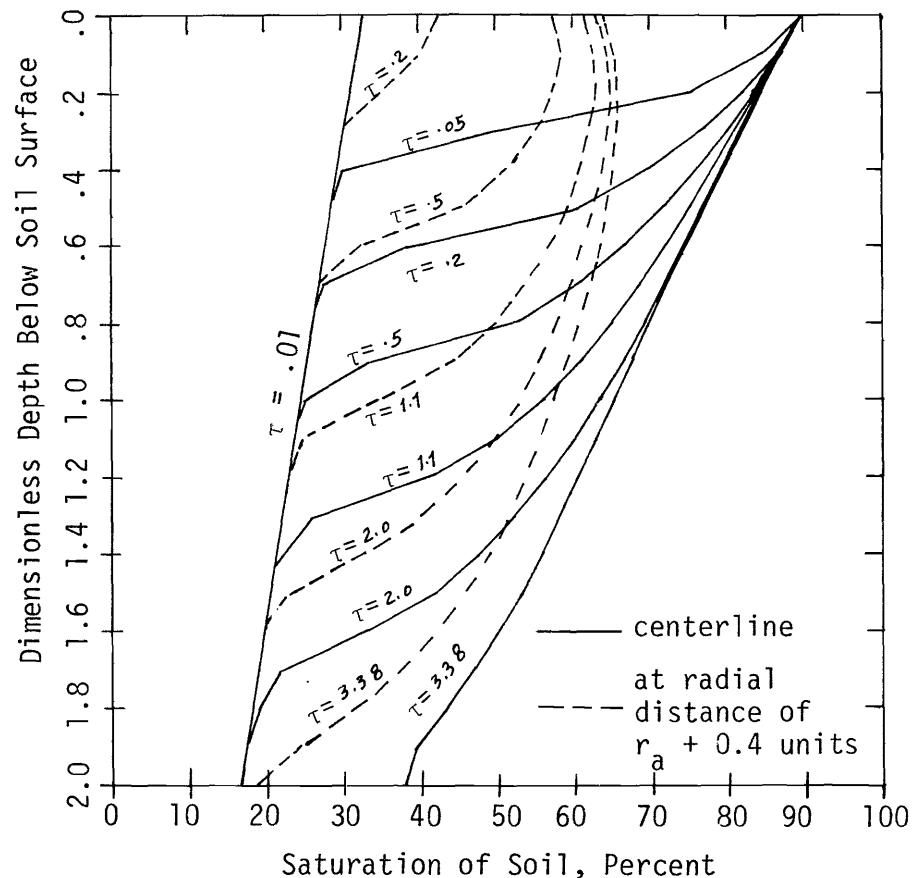


FIG. 37.--Distribution of Saturations with Depth at Several Dimensionless Times at the Centerline and at a Radial Distance from the Centerline Equal to $r = r_a + 0.4 = 0.7$ Units for Problem No. 6 (Magnitude of Residual Saturation, S_r , Linearly Decreasing with Depth, 0.25 to 0.05).

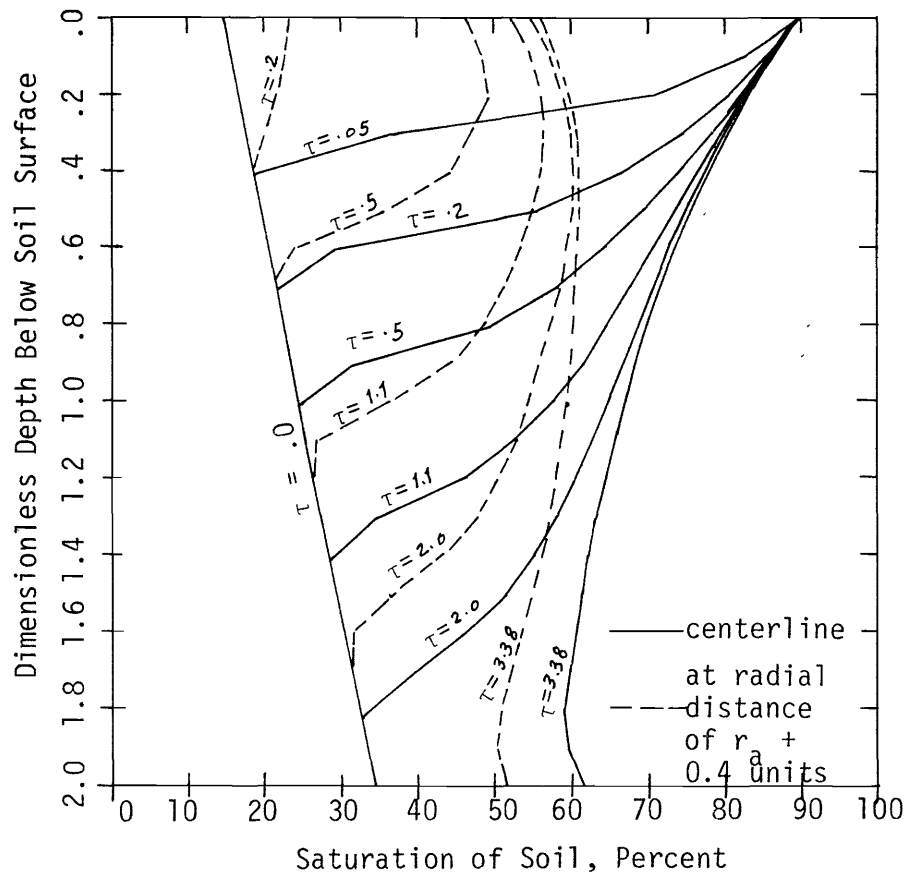


FIG. 38.--Distribution of Saturations with Depth at Several Dimensionless Times at the Centerline and at a Radial Distance from the Centerline Equal to $r = r_a + 0.4 = 0.7$ Units for Problem No. 7 (Magnitude of Residual Saturation, S_r , Linearly Increasing with Depth, 0.05 to 0.25).

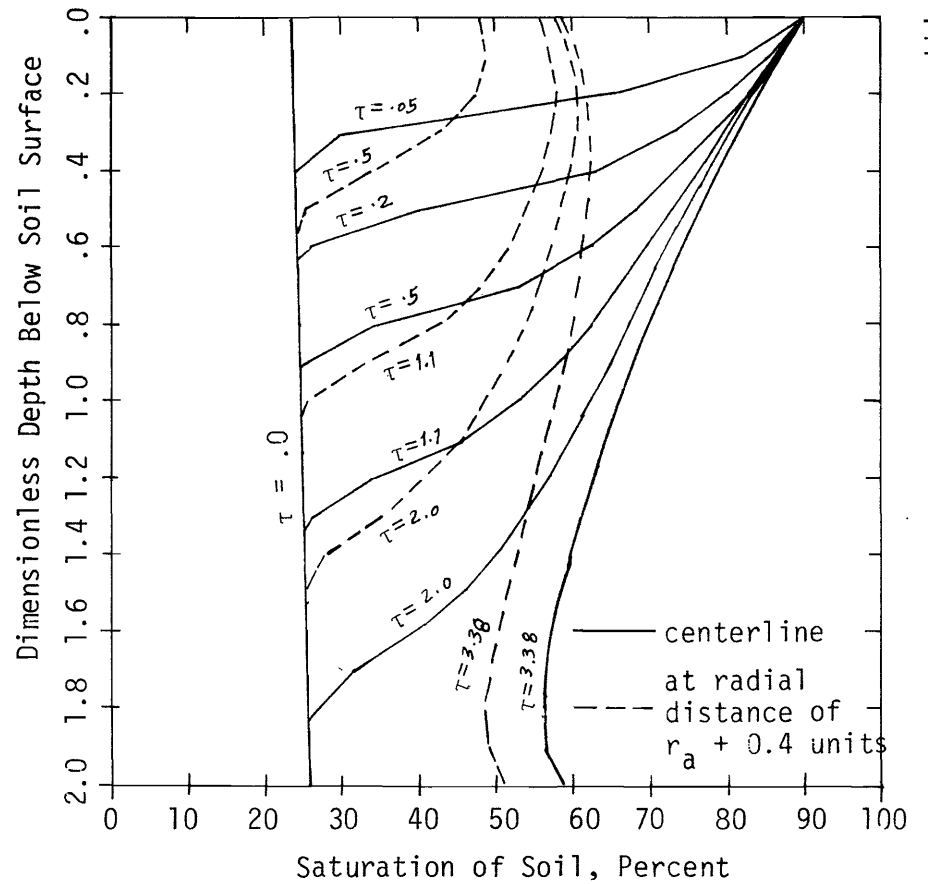


FIG. 39.--Distribution of Saturations with Depth at Several Dimensionless Times at the Centerline and at a Radial Distance from the Centerline Equal to $r = r_a + 0.4 = 0.7$ Units for Problem No. 8 (Magnitude of Soil Porosity, η , Linearly Decreasing with Depth, 0.62 to 0.18).

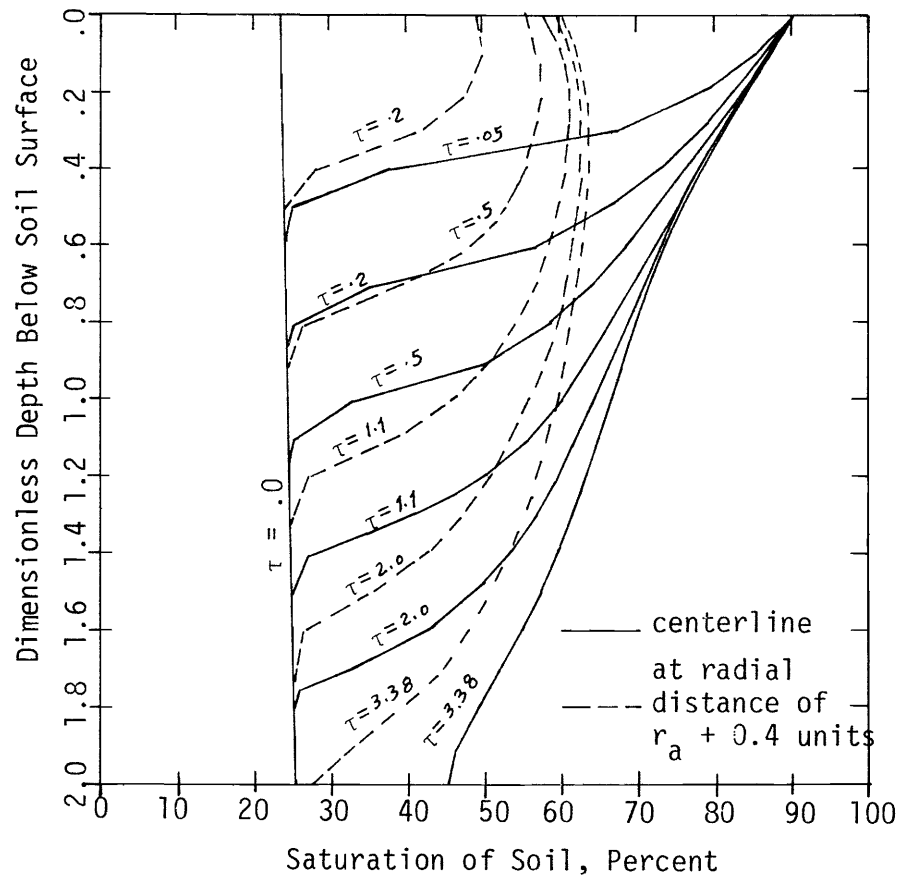


FIG. 40.--Distribution of Saturations with Depth at Several Dimensionless Times at the Centerline and at a Radial Distance from the Centerline Equal to $r = r_a + 0.4 = 0.7$ Units for Problem No. 9 (Magnitude of Soil Porosity, η , Linearly Increasing with Depth, 0.18 to 0.62).

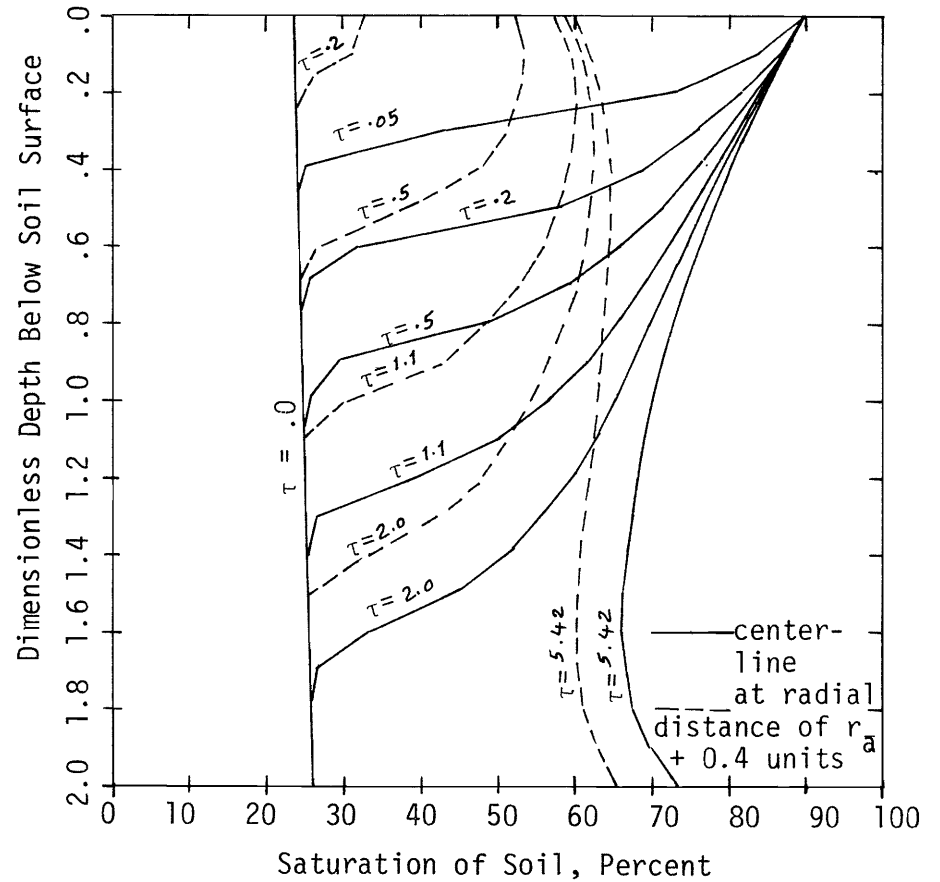


FIG. 41.--Distribution of Saturations with Depth at Several Dimensionless Times at the Centerline and at a Radial Distance from the Centerline Equal to $r = r_a + 0.4 = 0.7$ Units for Problem No. 10 (Magnitude of Saturated Hydraulic Conductivity, K_0 , Linearly Decreasing with Depth, 1.0 to 0.60).

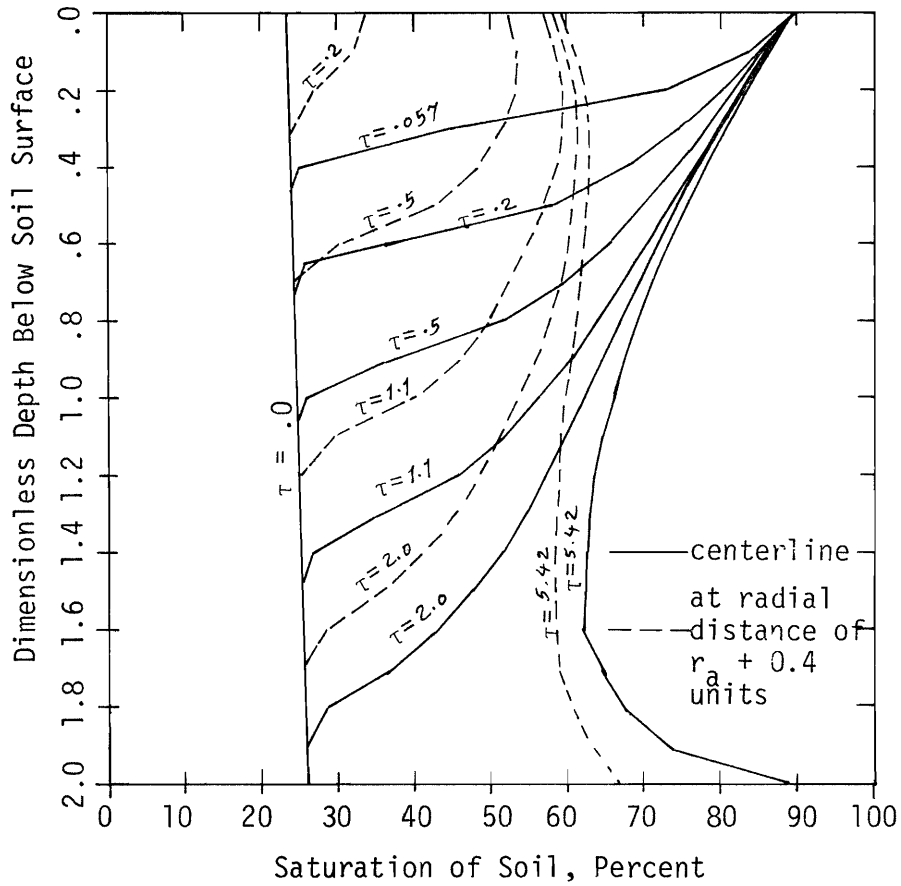


FIG. 42.--Distribution of Saturations with Depth at Several Dimensionless Times at the Centerline and at a Radial Distance from the Centerline Equal to $r = r_a + 0.4 = 0.7$ Units for Problem No. 11 (Magnitude of Saturated Hydraulic Conductivity, K_0 , Linearly Increasing with Depth, 1.0 to 1.40).

move as deep. At dimensionless time of $\tau = 0.2$ and a radial distance of 0.7 units, the soil is not affected by moisture movement when P_b is small at the soil surface (Fig. 34). However, for larger values of P_b , at the soil surface the wetting front has penetrated beyond a radial distance of 0.7 units (Fig. 33). Further comparison of Figs. 33 and 34 indicates that the wetting front has moved deeper when the value of P_b is small at the soil surface.

Brooks and Corey's data show that when a soil contains a wide range of pore sizes its value of pore size distribution, λ , is small. In general, sandy soils have only a very narrow range of pore sizes, have higher hydraulic conductivities and have larger values of λ . Fig. 35 indicates that larger values of λ on the soil surface with its magnitude decreasing with depth inhibits the infiltration process throughout the soil profile. However, when λ is small at soil surface and increasing with depth, infiltration rates are larger (Fig. 36).

The effect of heterogeneity caused by the decreasing and increasing residual saturation with depth are shown in Figs. 37 and 38. These figures indicate that at both the centerline and radial distance of 0.7 units, the soil profile becomes saturated more rapidly when the value of, S_r , is increased with depth. For example at dimensionless time $\tau = 3.38$, saturation at the bottom boundary is 63 percent for the case in which S_r increases with depth, whereas for the decreasing case, saturation at the bottom boundary is 37 percent at the same relative time.

When the porosity is assumed to be small at the soil surface, water is spread on the soil surface more rapidly as revealed by noting that at a radial distance of 0.7 units the saturation increases much

sooner than when the soil has a large value of porosity. For example, Fig. 39 shows at time 0.20 the wetting front has not reached to a radial distance of 0.7 units whereas in Fig. 40 which has smaller values of porosity on the soil surface, the radial distance of 0.7 has been reached and there are changes in saturation at that distance.

Similarly, when the value of saturated hydraulic conductivity increases with depth, the wetting front moved deeper than when its magnitude is decreased, Figs. 41 and 42.

The variation of infiltration rate with time for the solution of the problems in Table 2 have been plotted in Figs 43 through 47. Each figure contains three curves; one for homogeneous soil, one for heterogeneity in which the indicated parameter increases with depth and the last in which the same parameter decreases with depth. The figures show the well known trend of declining rate of infiltration with time. For almost all of the solutions (with one exception, solution for variation of λ) the average rate of infiltration from $\tau = .0$ to any time resulting from decreasing and increasing the magnitude of each parameter with depth, is almost equal to the infiltration rate obtained for homogeneous soil. Varying the pore size distribution exponent, λ , has a larger effect on the rate of infiltration, particularly in cases where its value is large at the soil surface and decreases with depth, (Fig. 44). A study by Jeppson (45) showed that for the same soil specifications, when the value of λ increases (homogeneous soil) the rate of infiltration decreases. The phenomena on Fig. 44 reflects this same conclusion since the surface soils exert a greater influence on infiltration rates than do the deeper soils.

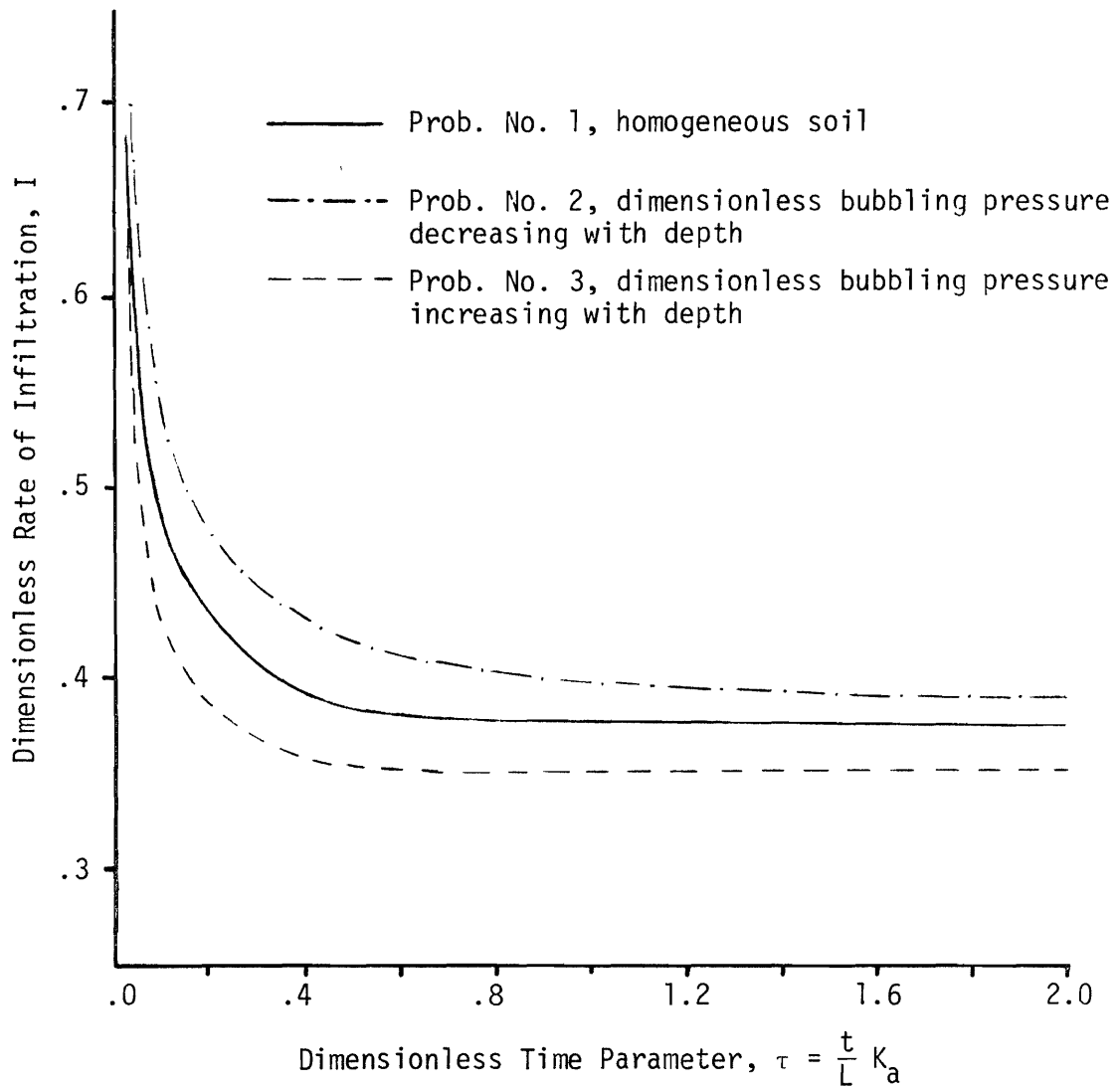


FIG. 43.--Effect of Variation of Dimensionless Bubbling Pressure, P_b , on Infiltration Capacity Curves Obtained From Solutions of Problems 1 through 3.

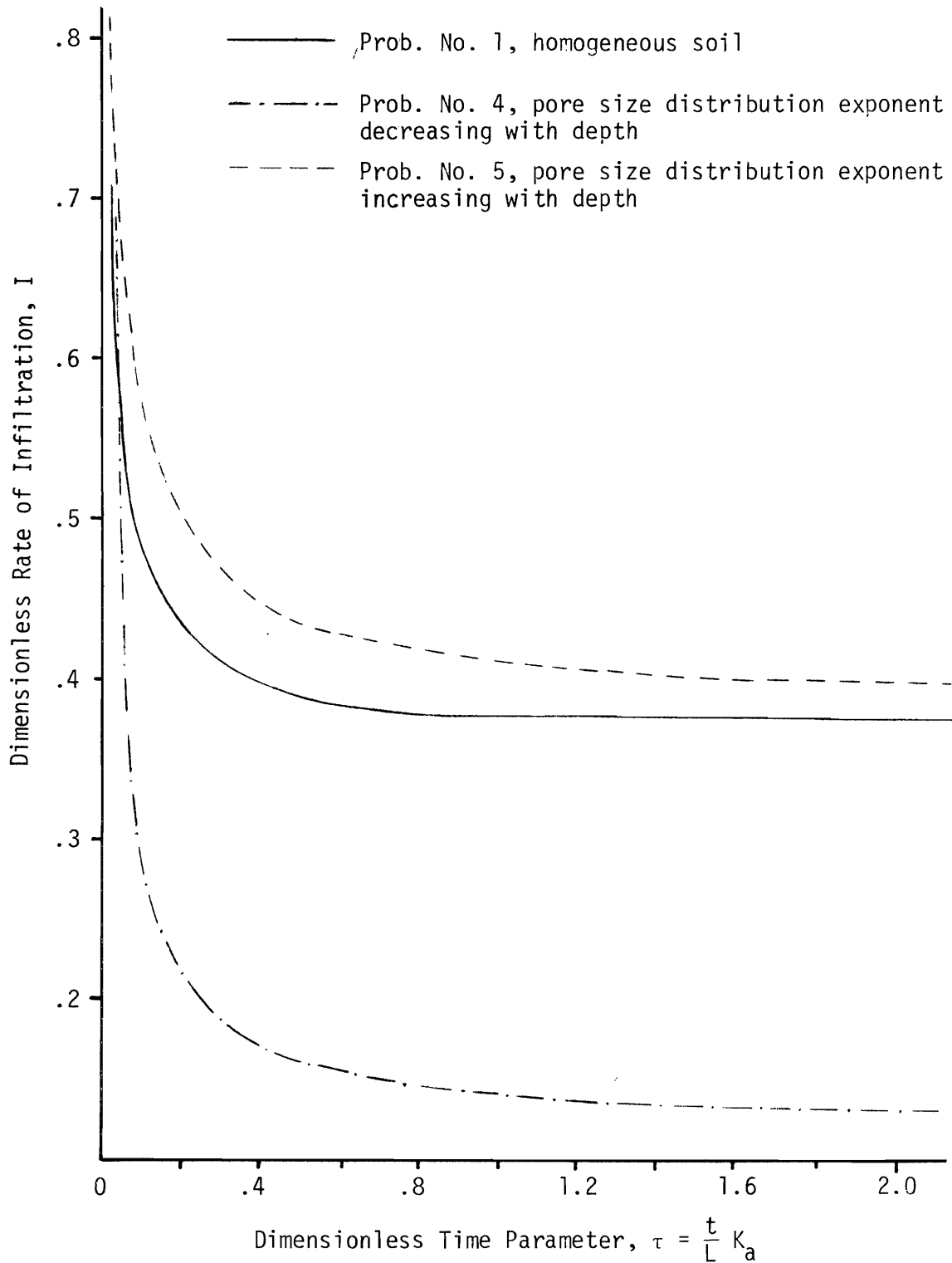


FIG. 44.--Effects of Variation of Pore Size Distribution, λ , on Infiltration Capacity Curves Obtained from Solutions of Problem 1, 4, and 5.

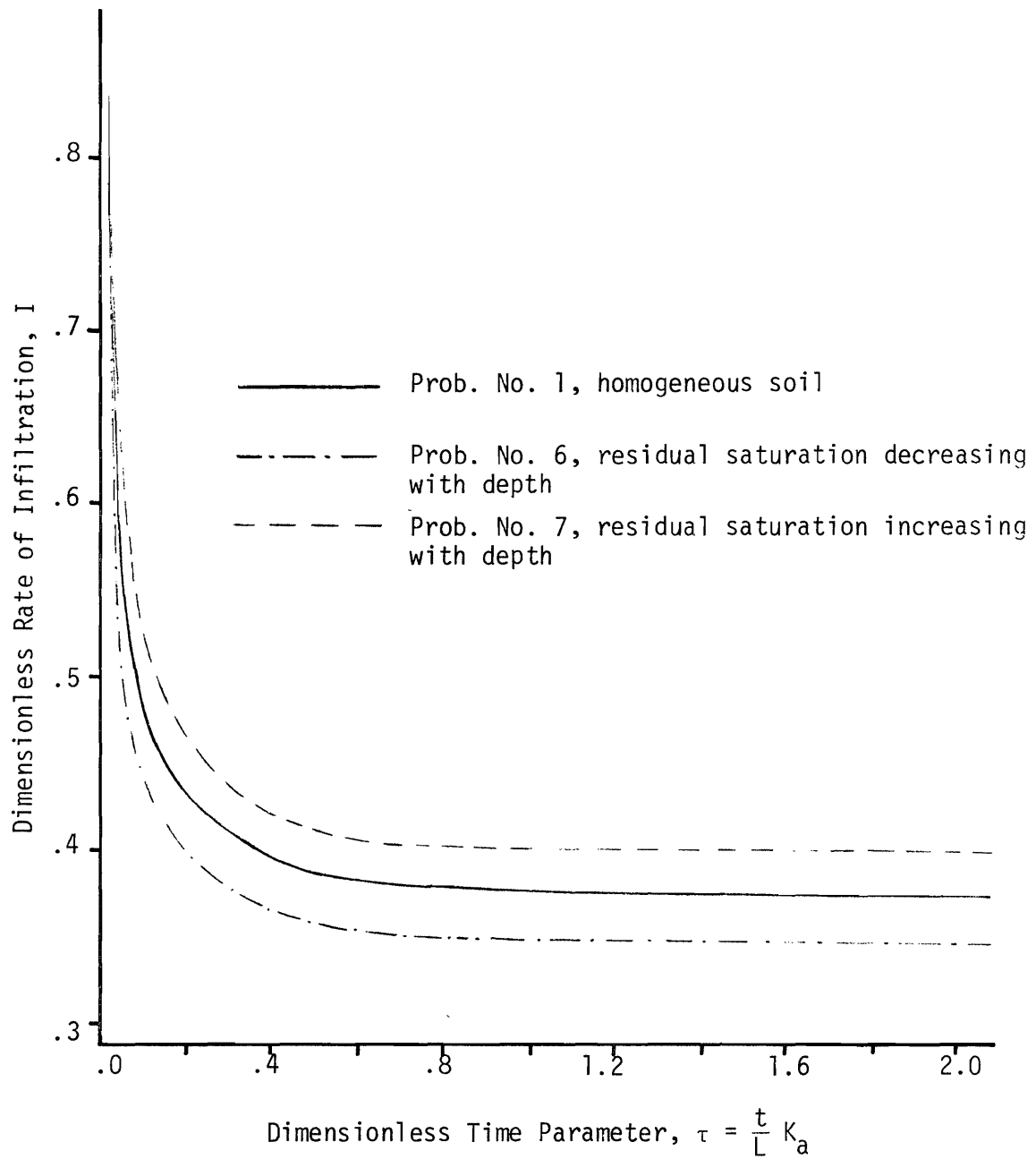


FIG. 45.--Effect of Variation of Residual Saturation, S_r , on Infiltration Capacity Curves Obtained from Solution of Problems 1, 6, and 7.

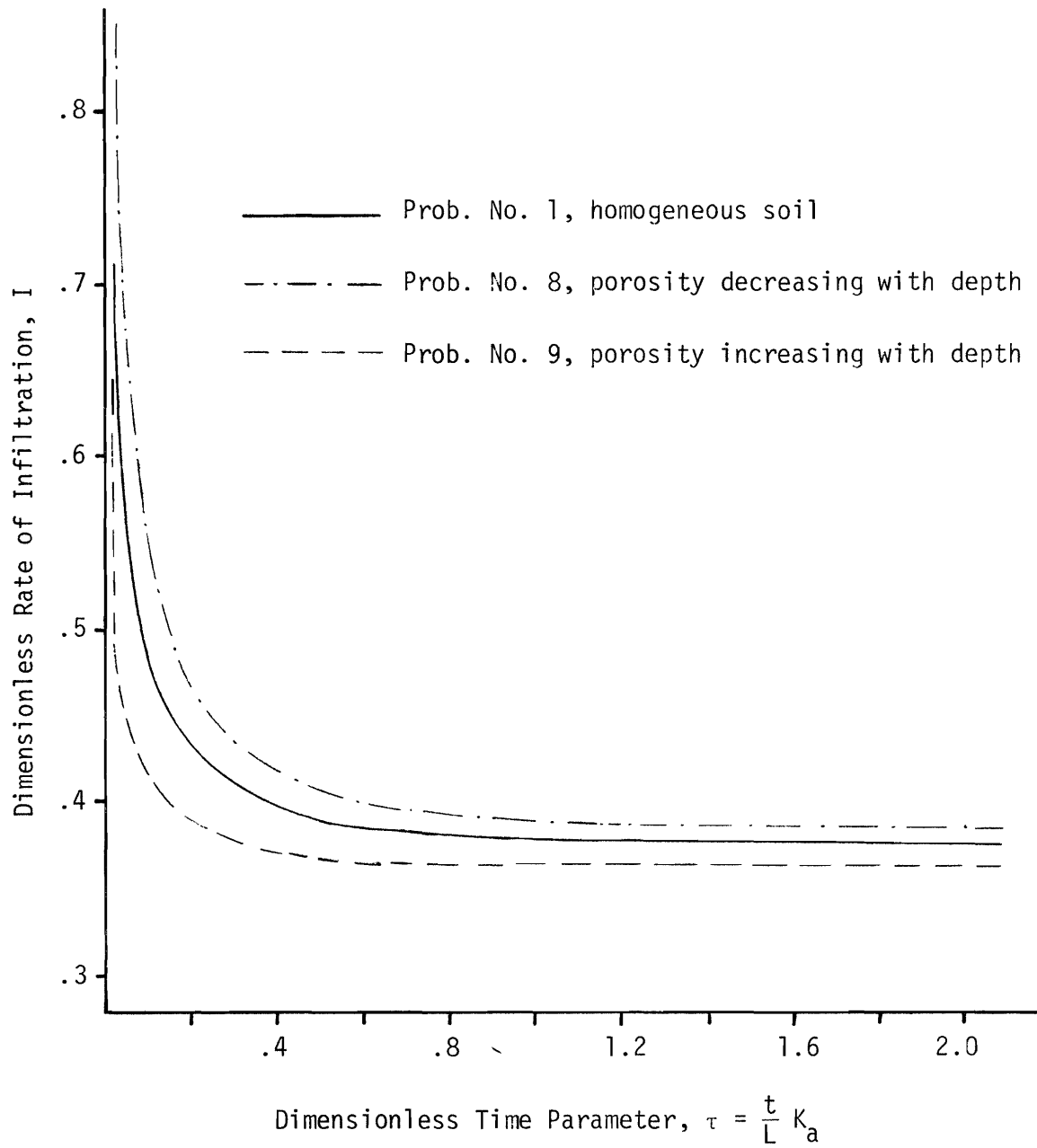


FIG. 46.--Effect of Variation of Porosity, η , on Infiltration Capacity Curves Obtained From Solutions of Problems 1, 8, and 9.

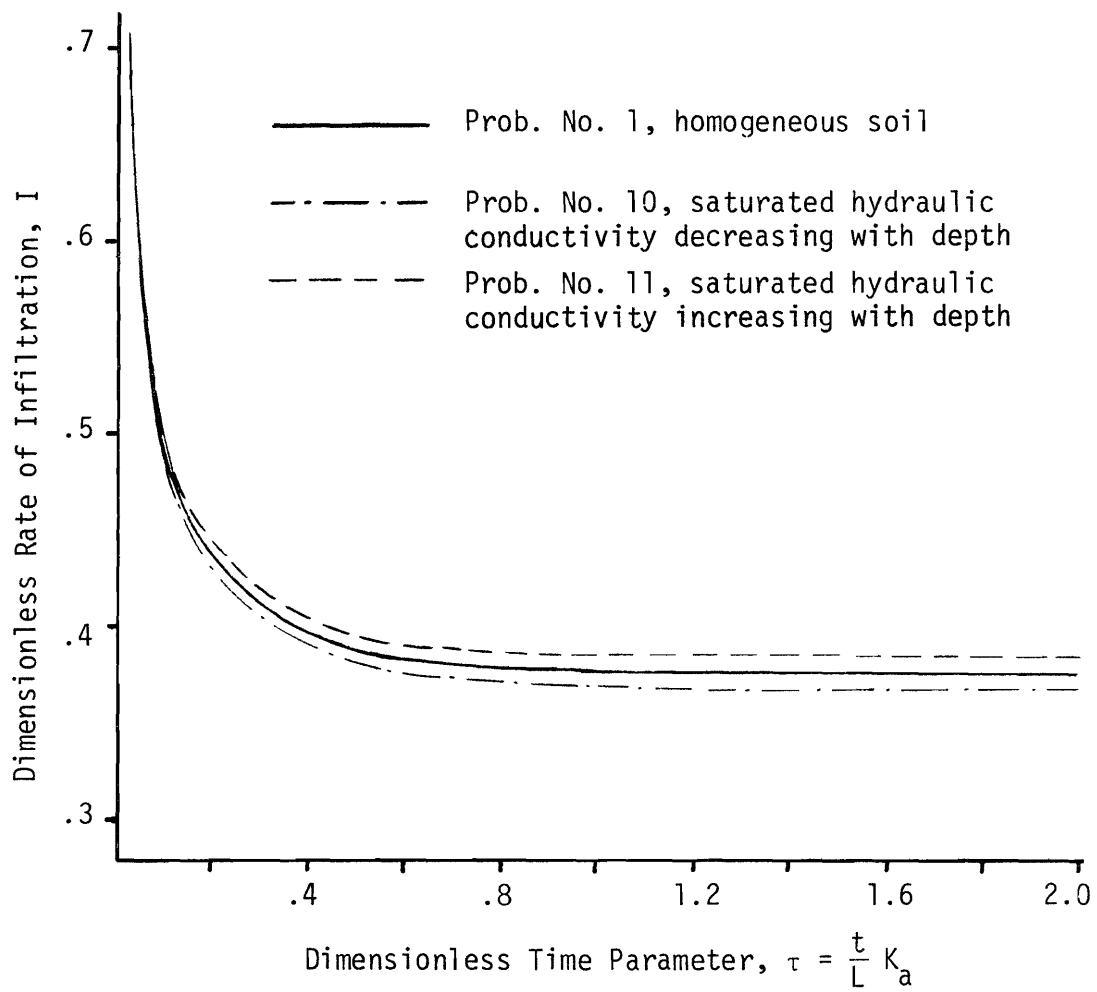


FIG. 47.--Effect of Variation of Saturated Hydraulic Conductivity, K_0 , on Infiltration Capacity Curves Obtained from Solutions of Problems 1, 10, and 11.

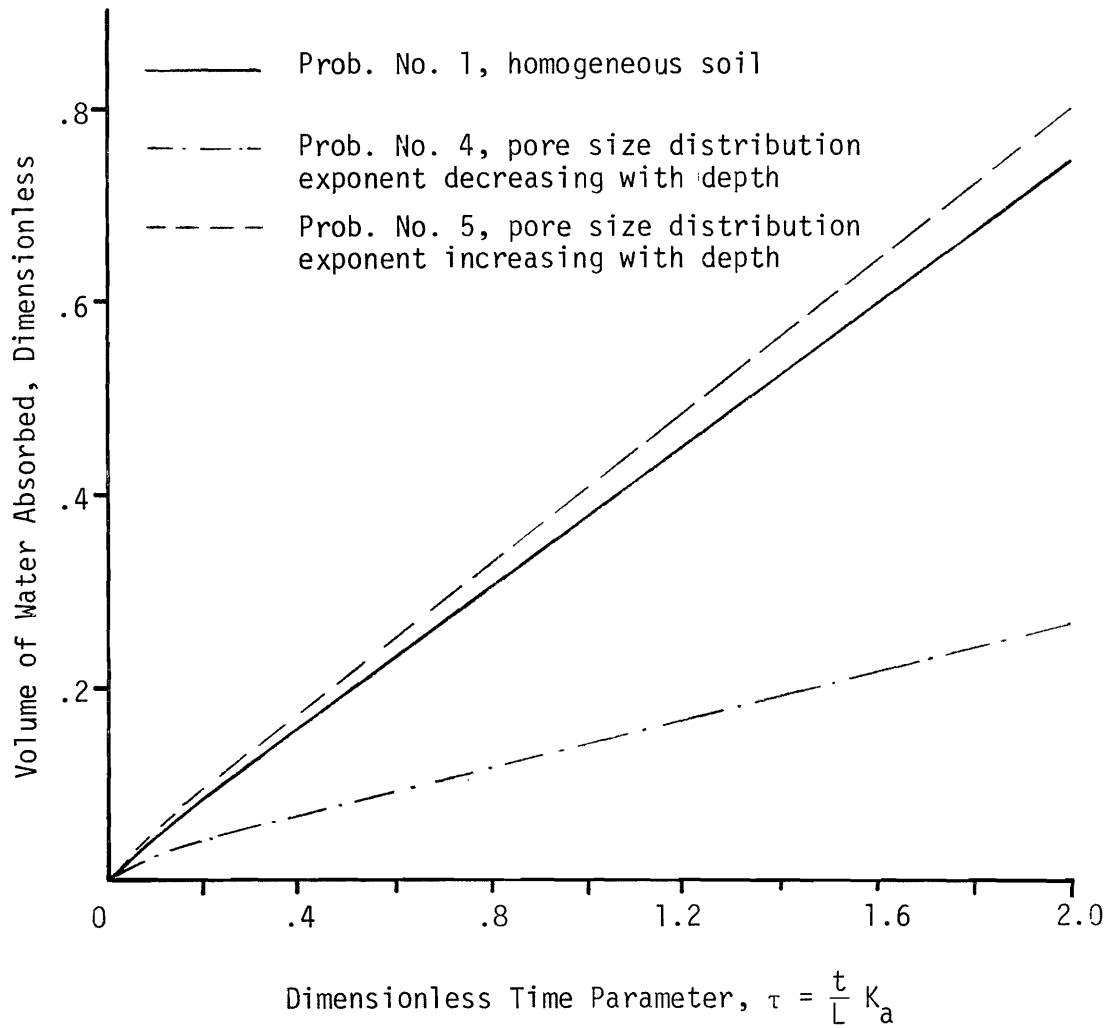


FIG. 49.--Effect of Variation of Pore Size Distribution Exponent, λ , on Volume of Water Absorbed With Time as Obtained From Solutions of Problems 1, 4, and 5.

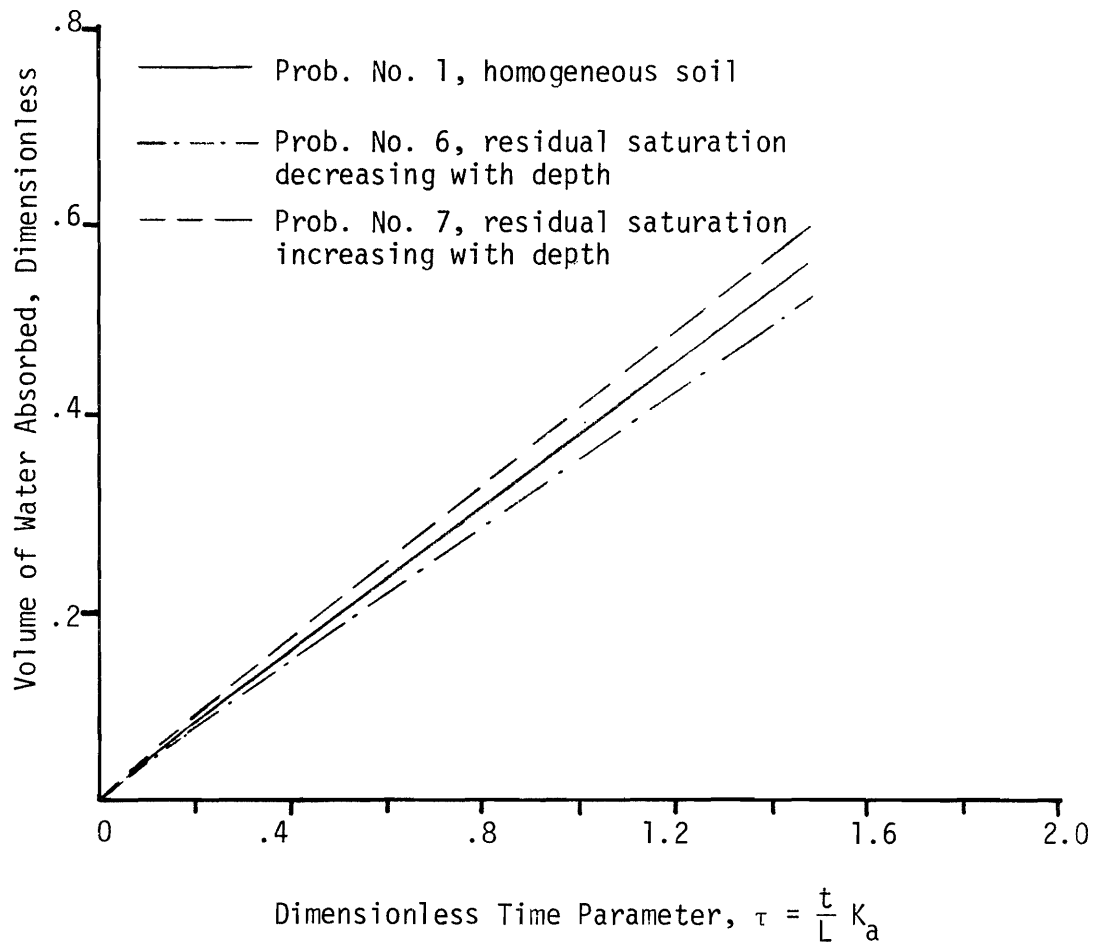


FIG. 50.--Effect of Variation of Residual Saturation, S_r , on Volume of Water Absorbed With Time as Obtained from Solution of Problems 1, 6, and 7.

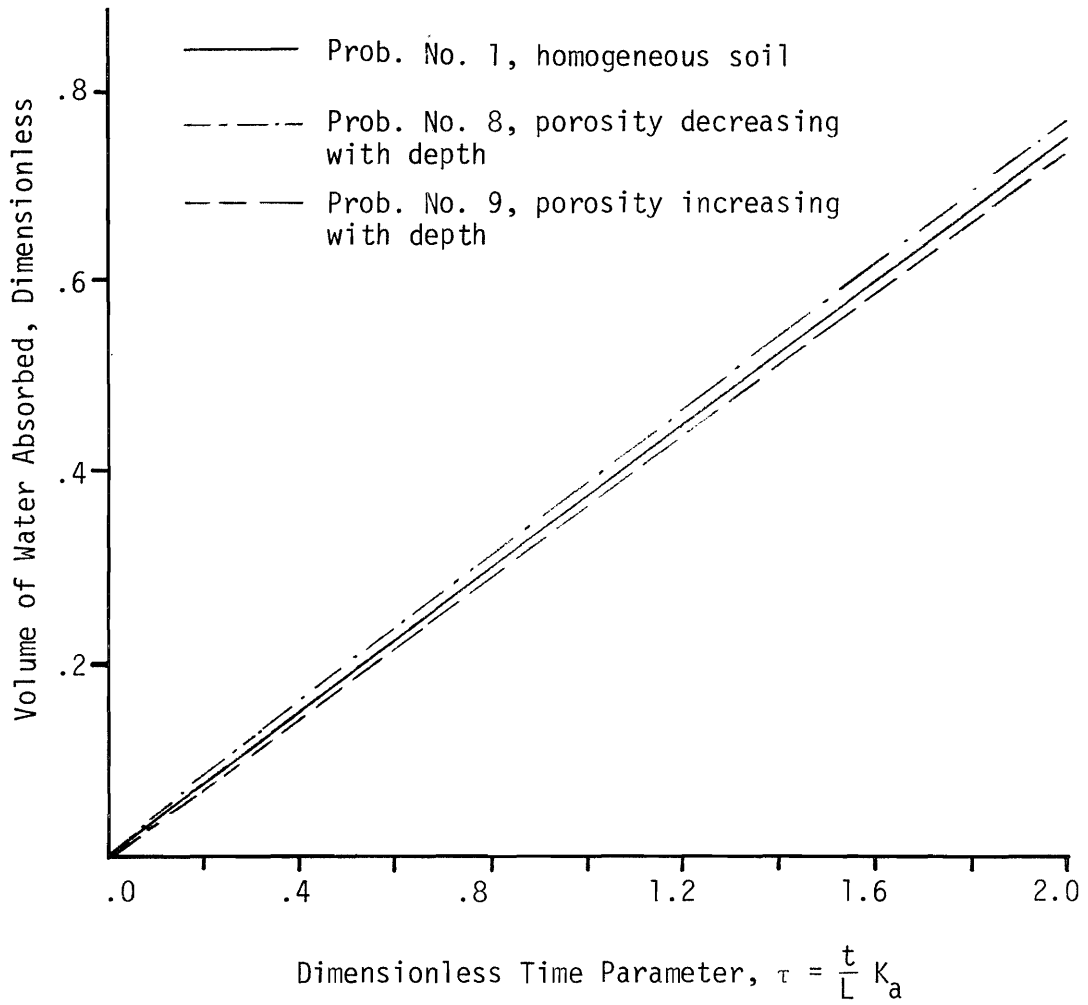


FIG. 51.--Effect of Variation of Porosity, η , on Volume of Water Absorbed With Time as Obtained From Solutions of Problems 1, 8, and 9.

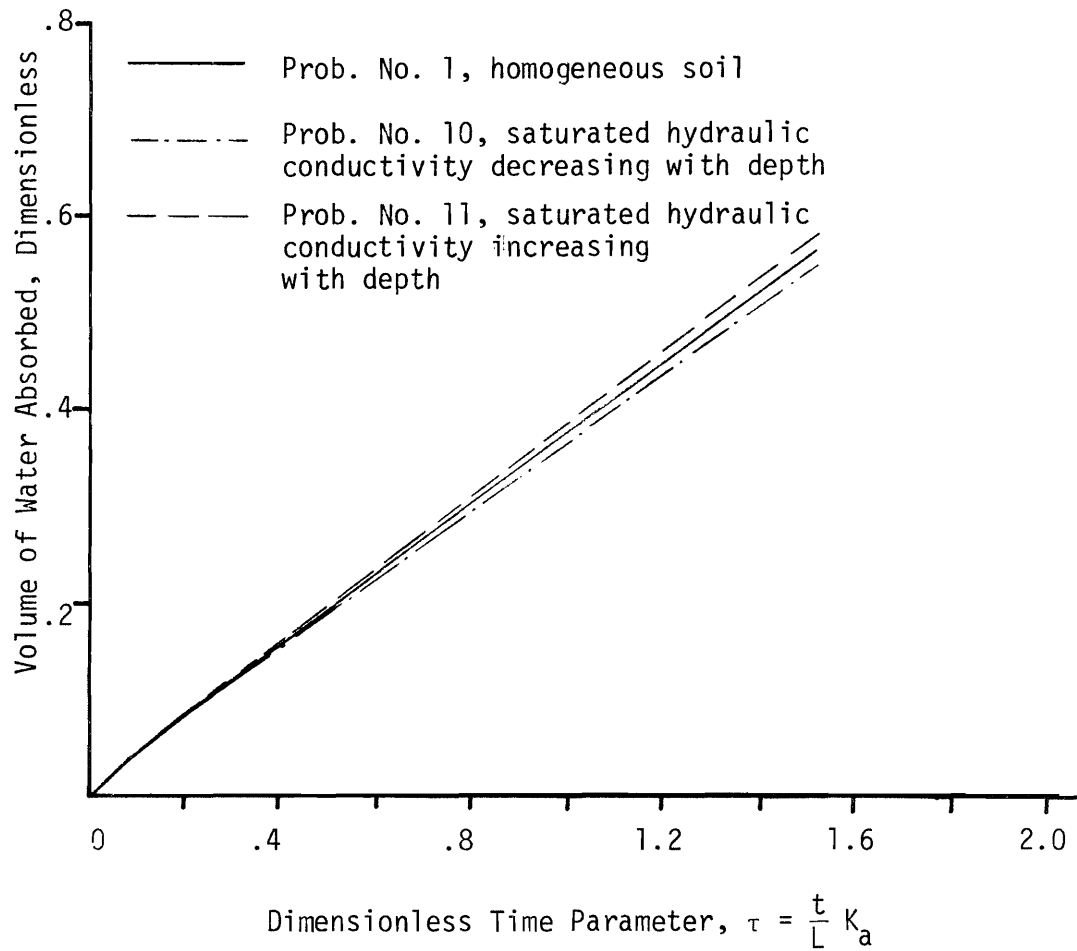


FIG. 52.--Effect of Variation of Saturated Hydraulic Conductivity, K_s , on Volume of Water Absorbed With Time as Obtained From Solutions of Problems 1, 10, and 11.

movement of moisture in the vertical direction have been plotted against the dimensionless time parameter, τ , in Figs. 53 through 57. All of the figures indicate that the wetting front has penetrated to the bottom boundary before the solution was terminated at $\tau = 3.38$. The time at which the wetting front first penetrates to the bottom boundary is different for the various problem specifications. For example, Fig. 57, which gives the results when saturated hydraulic conductivity, K_0 , increases with depth, shows that the wetting front penetrates to the bottom boundary at time $\tau = 1.76$, whereas it took $\tau = 2.30$ when K_0 decreases with depth. The results for homogeneous soil indicates the time of penetration of the wetting front to the bottom boundary is $\tau = 1.94$. An examination of Figs. 53 through 57 shows that increasing bubbling pressure with depth causes the wetting front to move faster, while decreasing its value with depth resulted in slower movement of wetting front in the vertical direction than for all other variations of parameters, λ , S_r , K_v , η and the homogeneous condition.

The radial movement of the wetting front at any time is also of interest and how this position is related to hydraulic properties and heterogeneity of the soil. The Figs. 58 through 62 shows the maximum radial movement of the wetting front beyond the circle of water application for the problems in Table 1.

The figures indicate the vertical heterogeneity caused by variation of residual saturation, Fig. 60, and saturated hydraulic conductivity, (dimensionless function of depth, K_v) Fig. 62 has a small effect on the spreading of wetting front. The effect of the other three variables λ , P_b and η is significant. For example, in

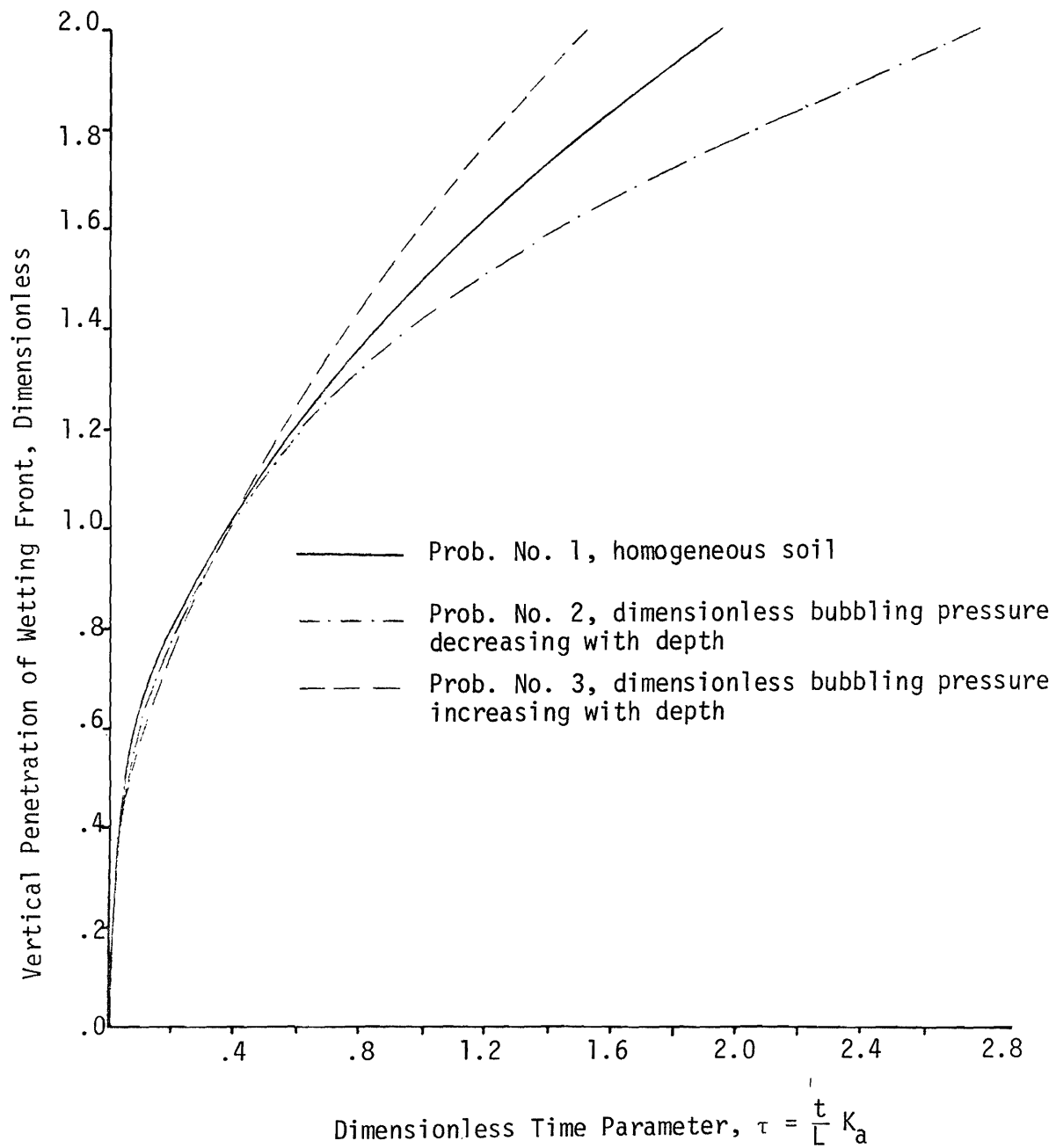


FIG. 53.--Effect of Variation of Dimensionless Bubbling Pressure, P_b , on Vertical Depth of Penetration of Wetting Front with Time Obtained from Solutions of Problems 1 through 3.

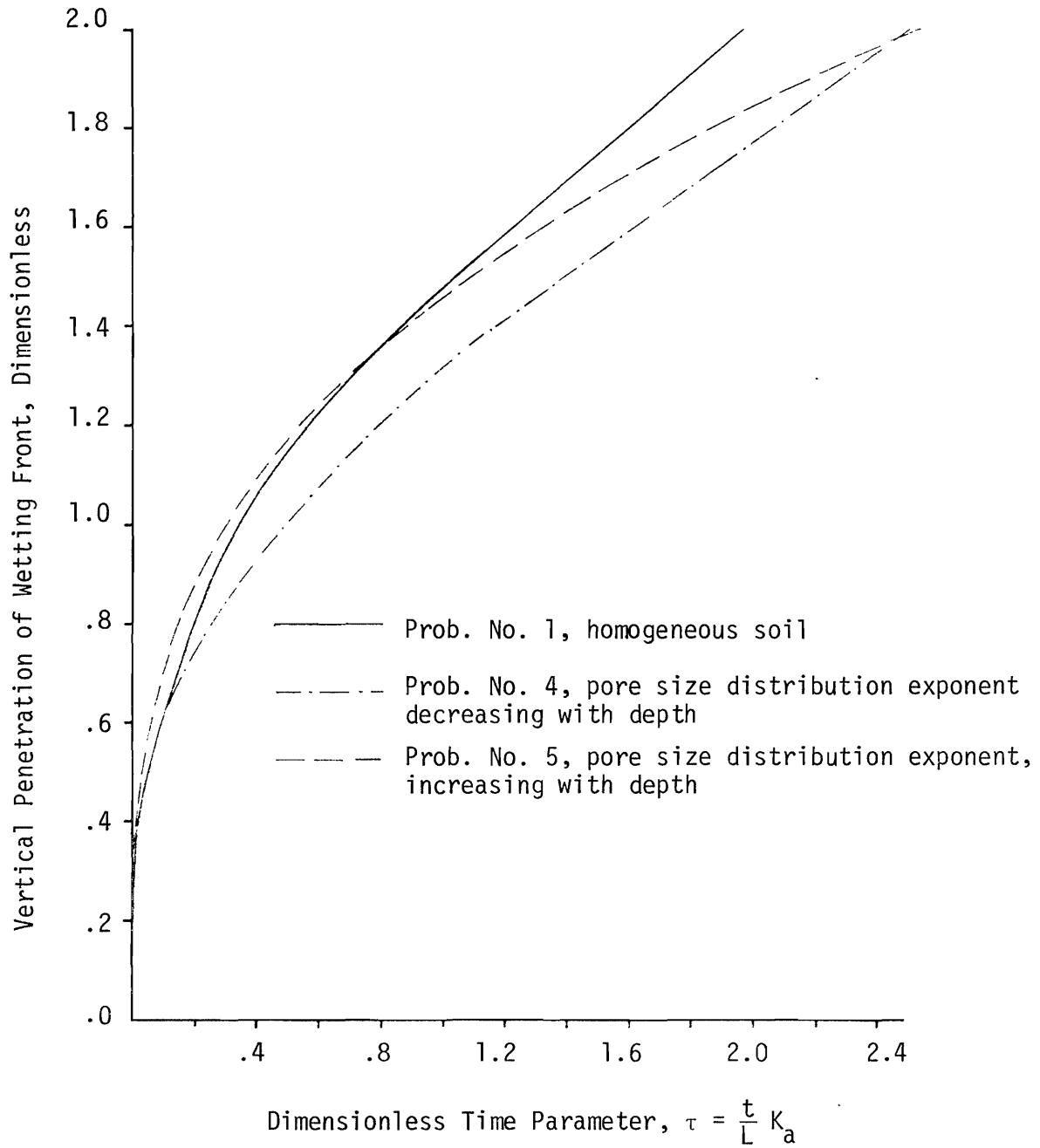


FIG. 54.--Effect of Variation of Pore Size Distribution Exponent, λ , on Vertical Depth of Penetration of Wetting Front with Time Obtained from Solutions of Problems 1, 4, and 5.

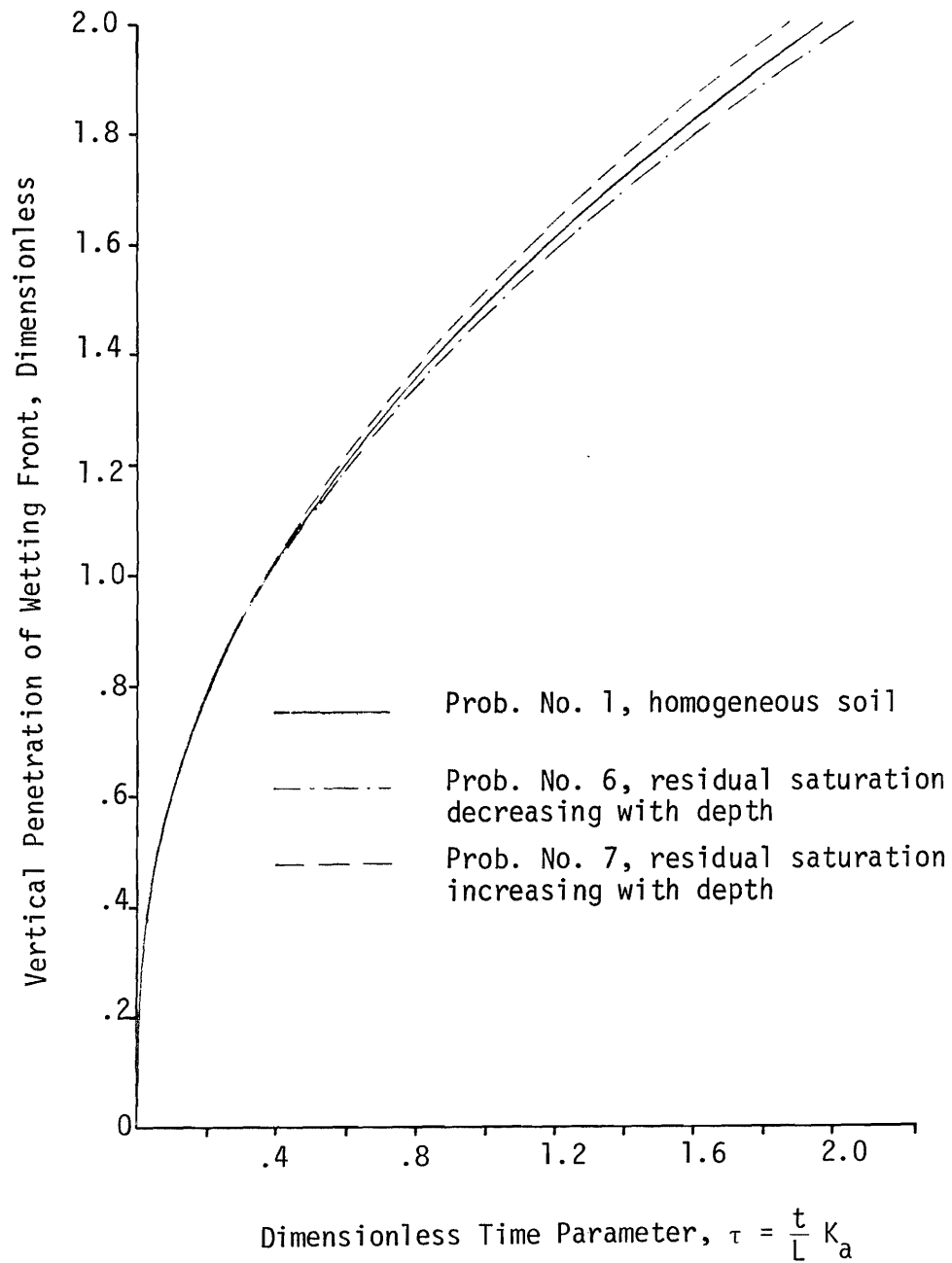


FIG. 55.--Effect of Variation of Residual Saturation, S_r , on Vertical Depth of Penetration of Wetting Front With Time Obtained From Solutions of Problems 1, 6, and 7.

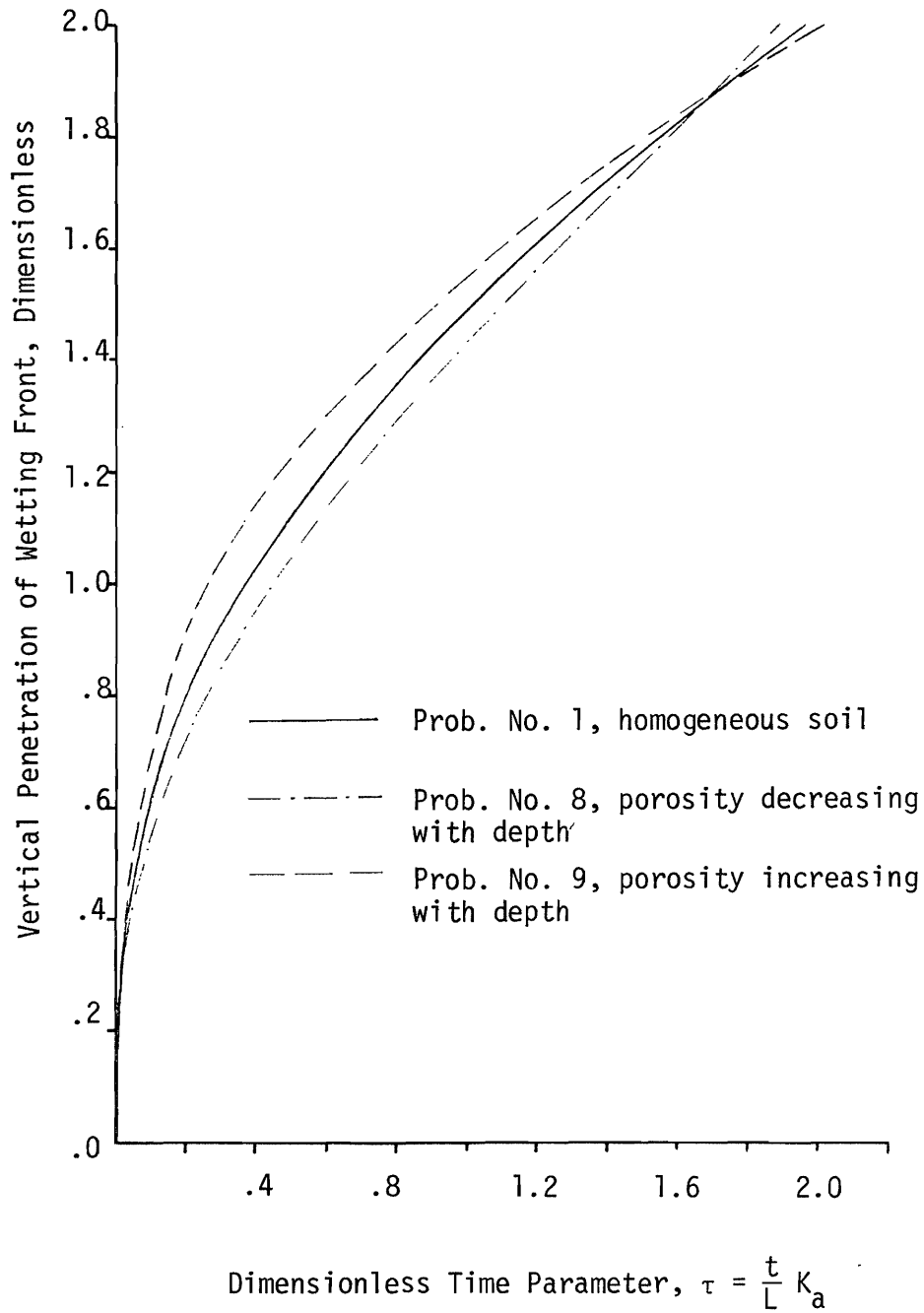


FIG. 56.--Effect of Variation of Porosity, η , on Vertical Depth of Penetration of Wetting Front With Time Obtained From Solutions of Problems 1, 8 and 9.

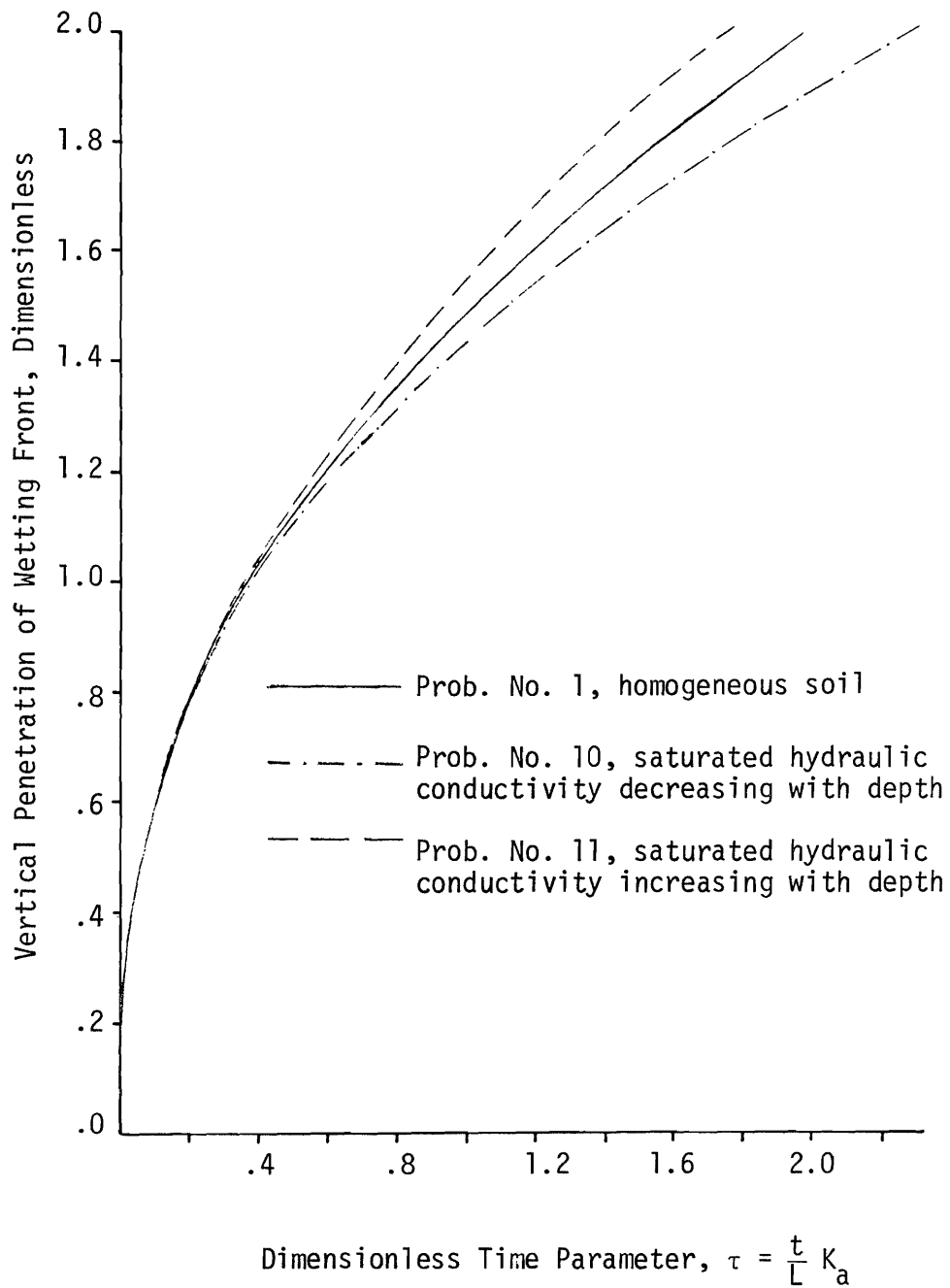


FIG. 57.--Effect of Variation of Saturated Hydraulic Conductivity, K_s , on Vertical Depth of Penetration of Wetting Front with Time Obtained from Solutions of Problems 1, 10, and 11.

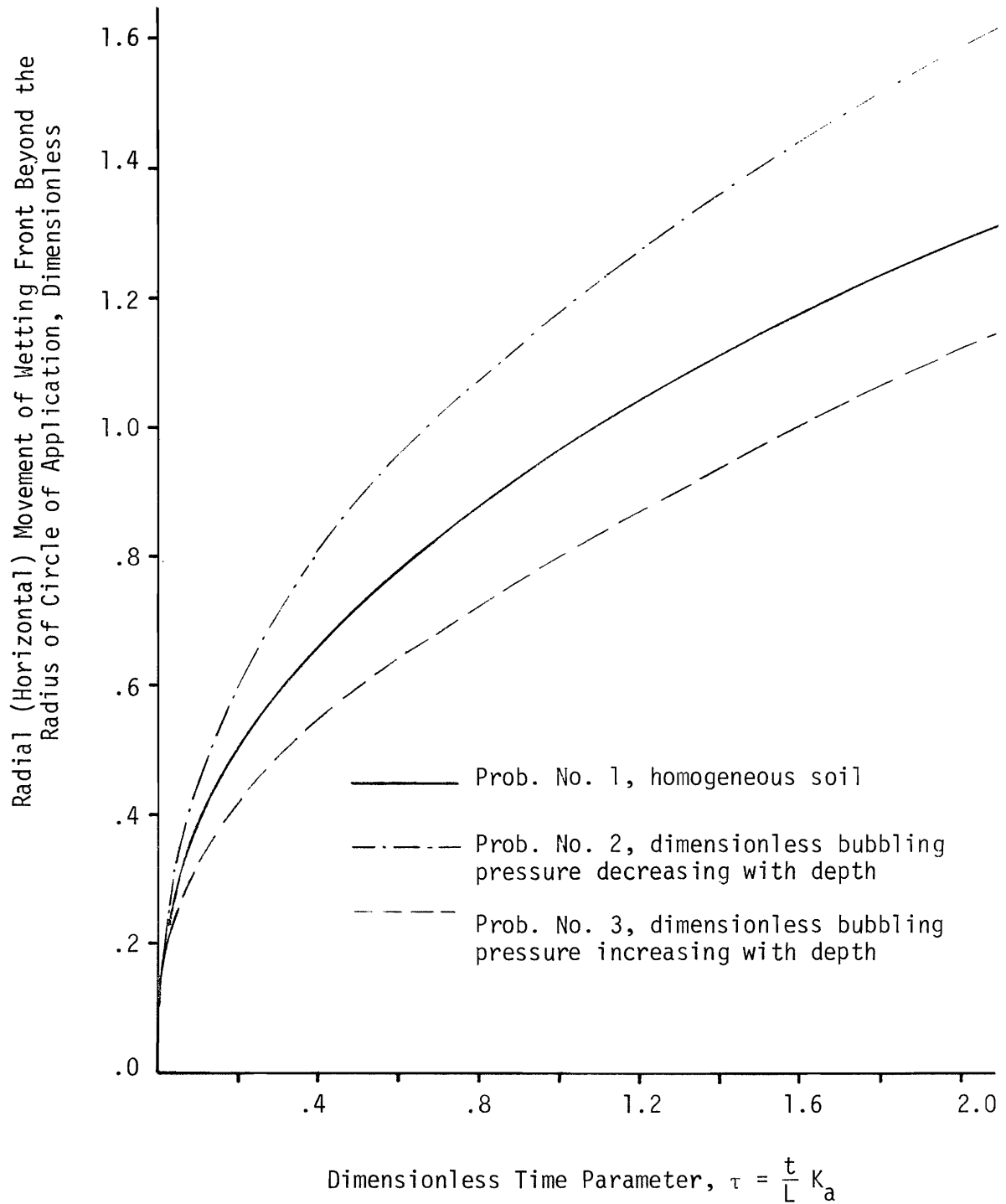


FIG. 58.--Effect of Variation of Dimensionless Bubbling Pressure, P_b , on Lateral Movement of Wetting Front with Time for Problems 1 through 3.

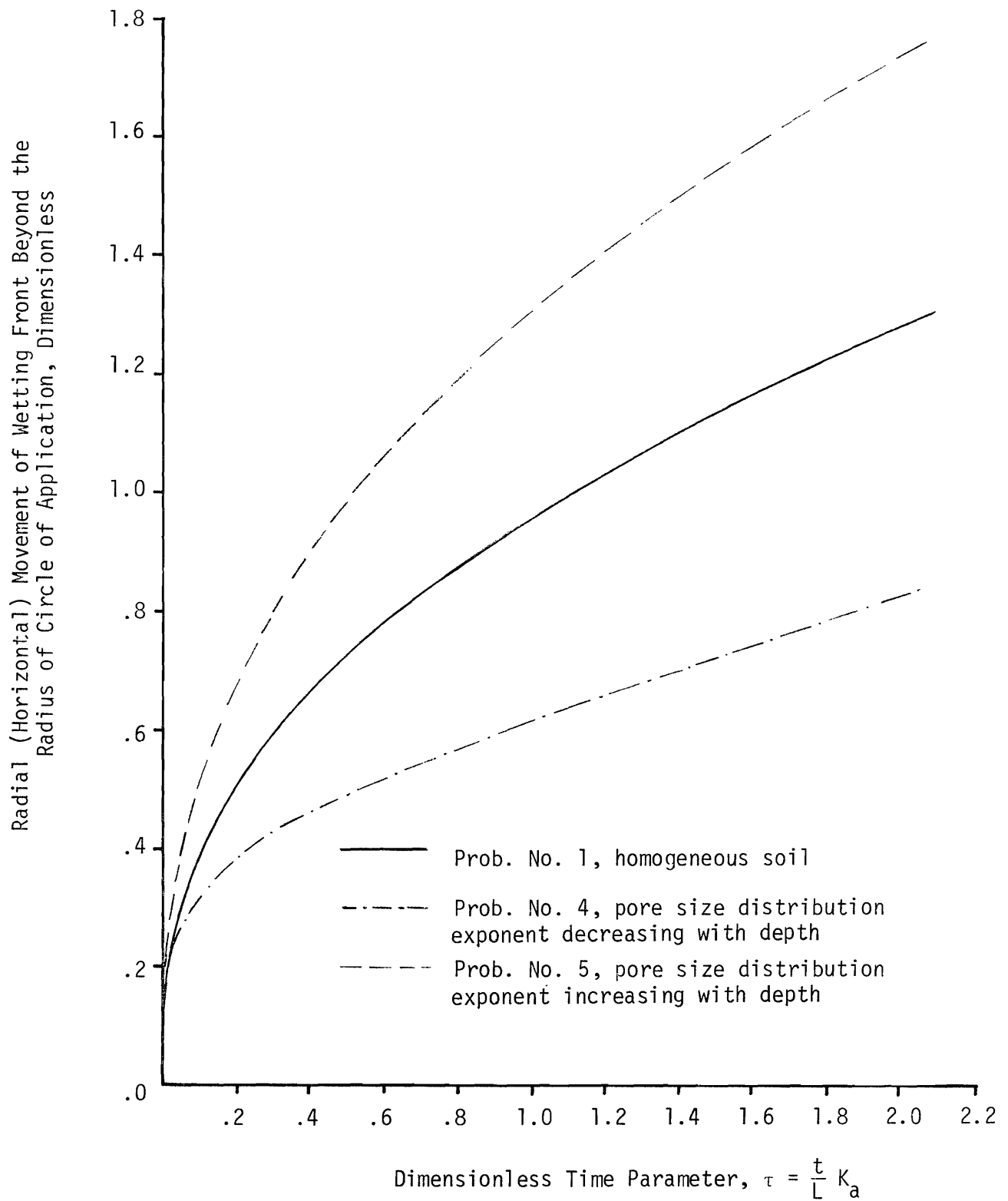


FIG. 59.--Effect of Variation of Pore Size Distribution Exponent, λ , on Lateral Movement of Wetting Front with Time for Problems 1, 4, and 5.

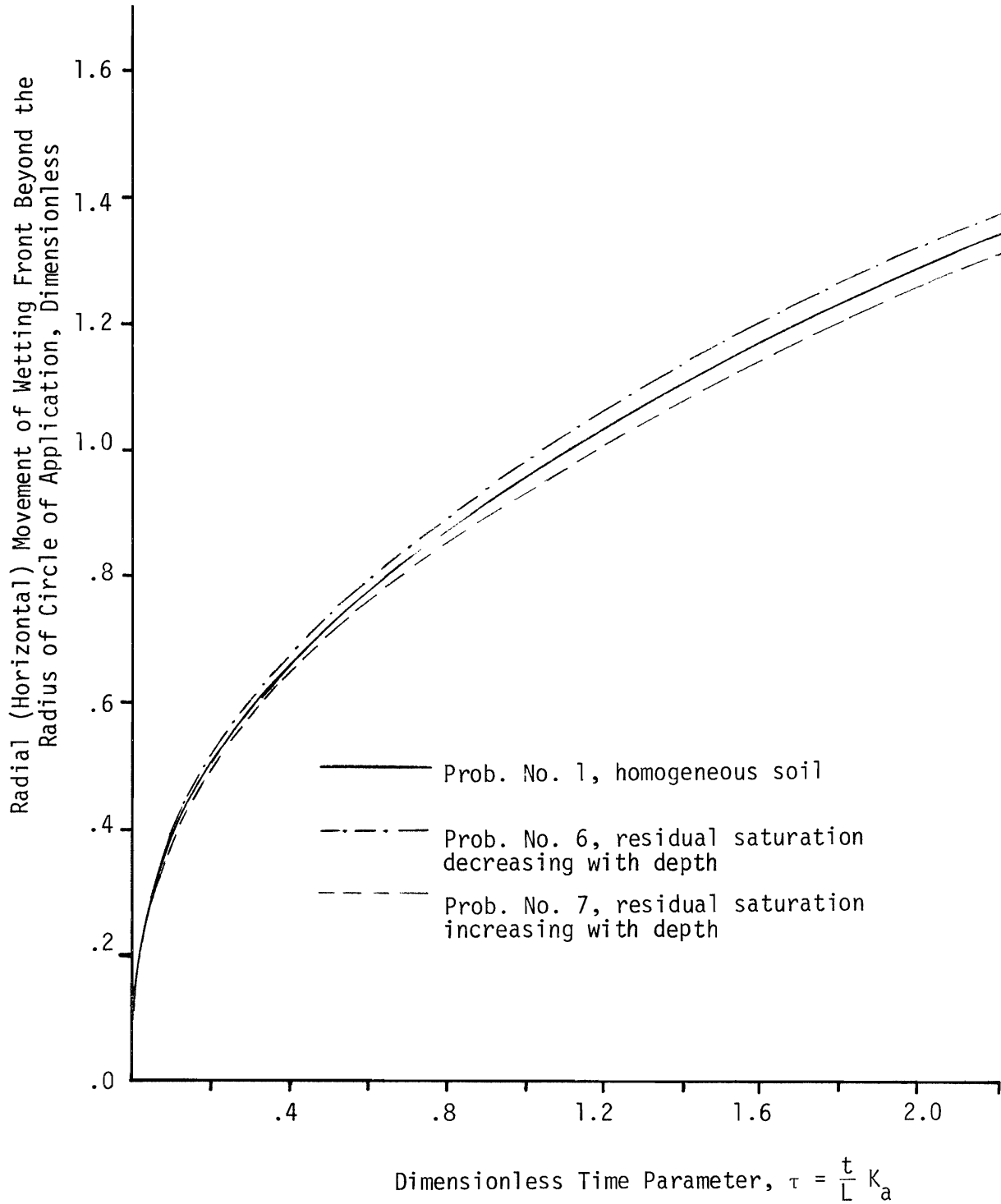


FIG. 60.--Effect of Variation of Residual Saturation, S_r , on Lateral Movement of Wetting Front with Time for Problems 1, 6, and 7.

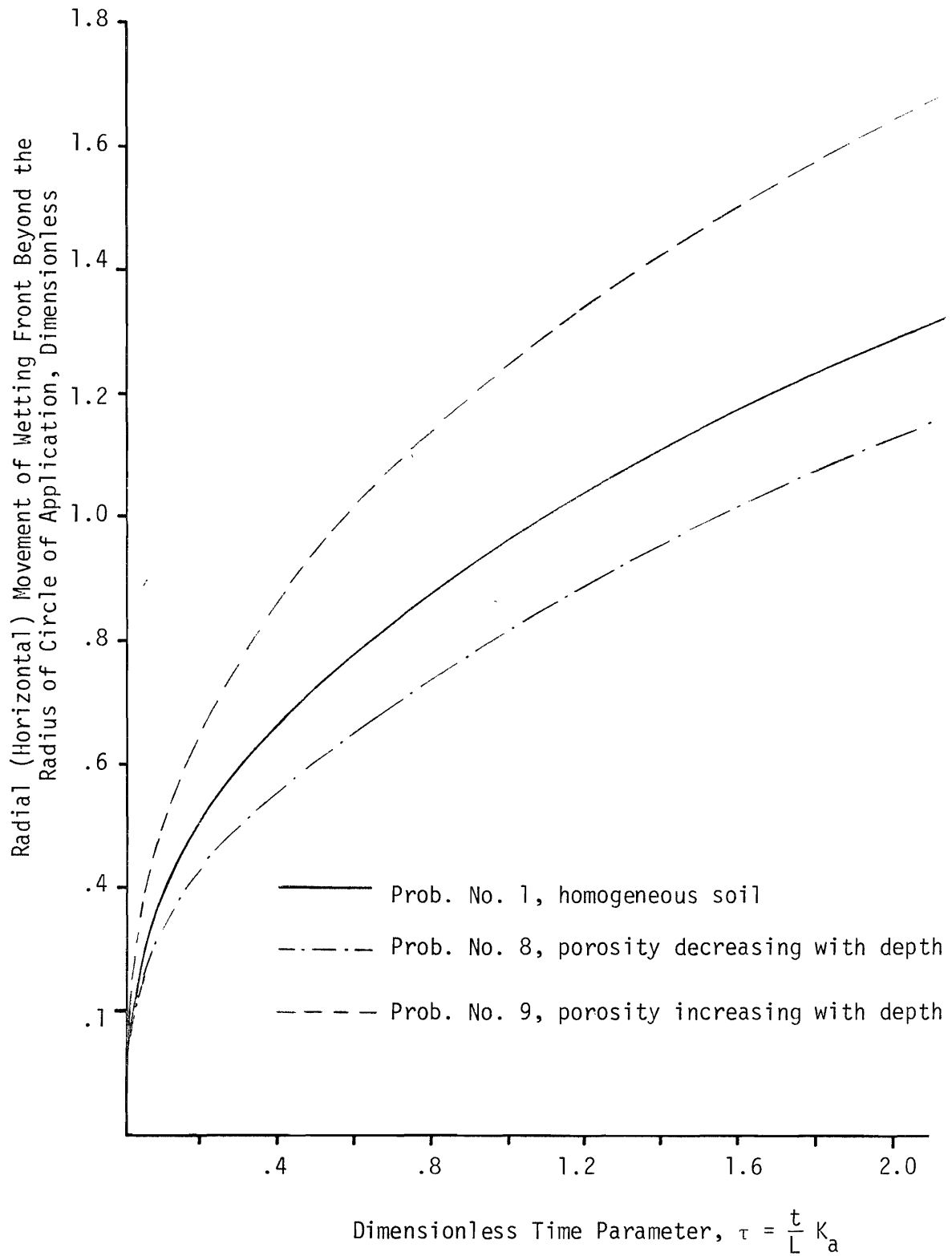


FIG. 61.--Effect of Variation of Porosity, n , on Lateral Movement of Wetting Front with Time for Problems 1, 8, and 9.

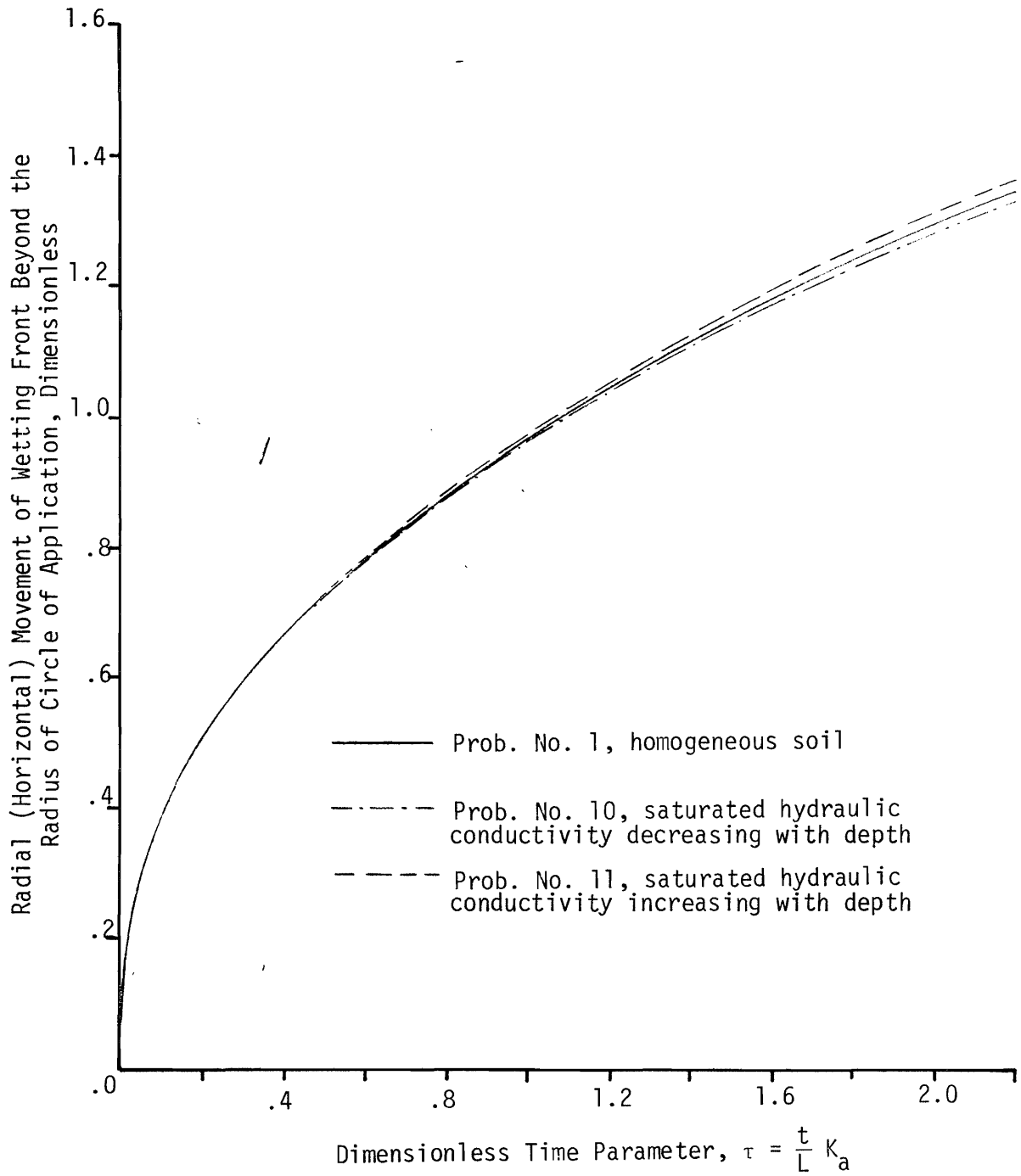


FIG. 62 .--Effect of Variation of Saturated Hydraulic Conductivity, K_s , on Lateral Movement of Wetting Front with Time for Problems 1, 10, and 11.

Fig. 59 which shows the results of heterogeneity caused by variation of λ , the radial movement of the wetting front is approximately twice as great for λ increasing with depth as for λ decreasing with depth. At $\tau = 2.22$ the wetting front passed the point 1.8 units beyond the circle of application, but for the decreasing case it was at distance 0.8 units beyond the radius of circle of application after the same time.

Solutions of problems 1, 12, and 13 indicate the effect of different magnitude of hydraulic head, h_0 , used in the initialization of the problem on the flow patterns. All specifications are assumed to be identical and constant (homogeneous) except initial hydraulic head, h_0 . Figs. 63 and 64 are the variation of infiltration rate and volume of water infiltrated with time, respectively. Fig. 63 shows that the rate of infiltration is larger for the soil with the smaller initial hydraulic head. The infiltration capacity curve for the same specification at an initial hydraulic head of -4.0 feet lies above the curve for the problem of initial hydraulic head of -6.0 feet and the curve for the higher hydraulic head of -8.0 is the lower curve. After ($\tau = 2.50$) the infiltration rate of the three soils becomes almost a constant value of about 0.38. Therefore, the initial hydraulic head or static equilibrium condition of the soil has no significant effect on infiltration rate, particularly after a longer time. This observation confirms Jeppson's (42) conclusion.

The effect of initial hydraulic head on the variation of vertical movement of the wetting front with depth is shown in Fig. 65. As the figure shows, water moves more rapidly in wet soils than in a dry soil. When the soil has an initial hydraulic head of -4.0 at $\tau = 1.12$ the

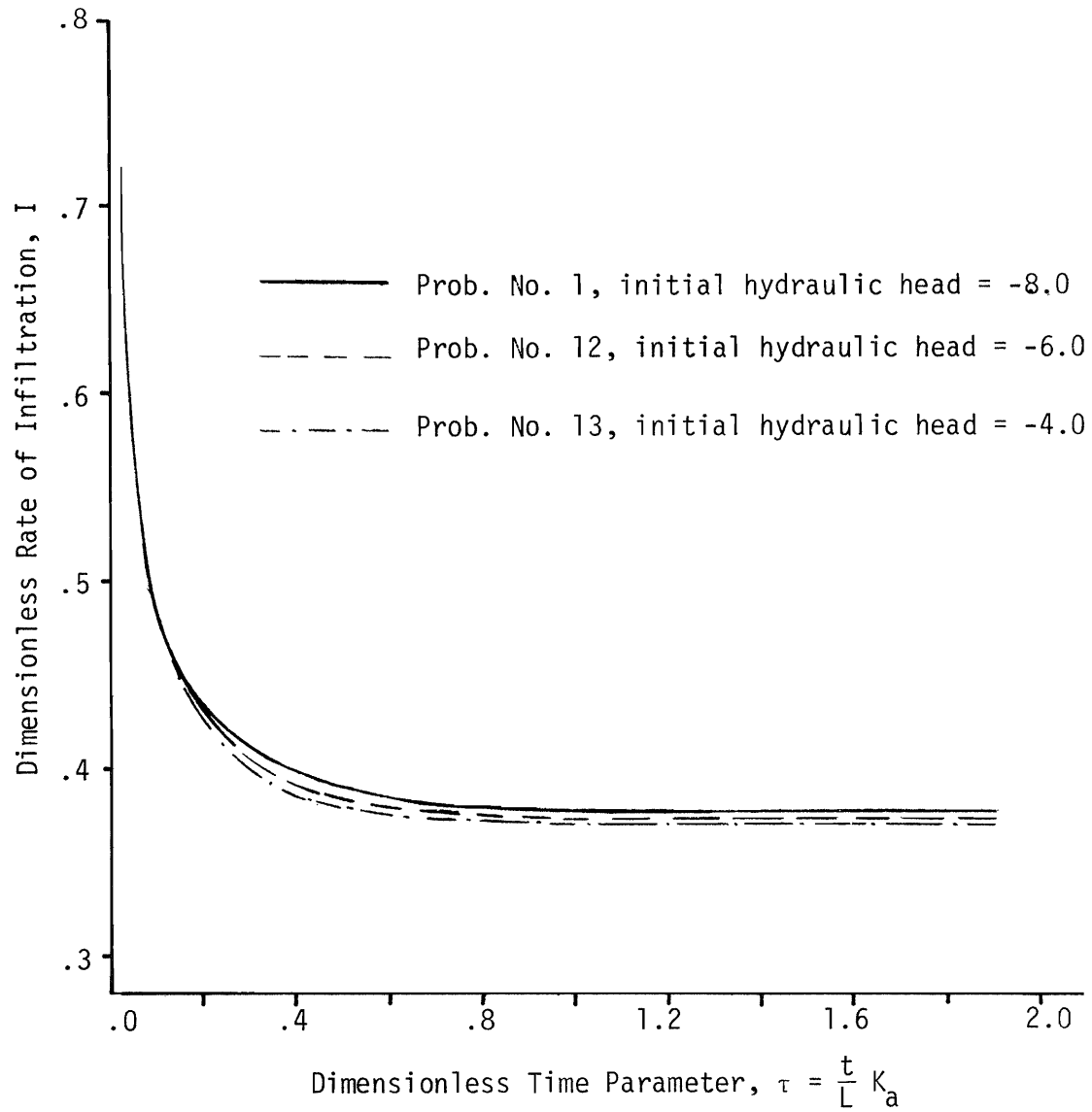


FIG. 63.--Effect of Different Values of Dimensionless Initial Hydraulic Head, h_0 , on Infiltration Capacity Curve Obtained From Solutions of Problems 1, 2, and 13.

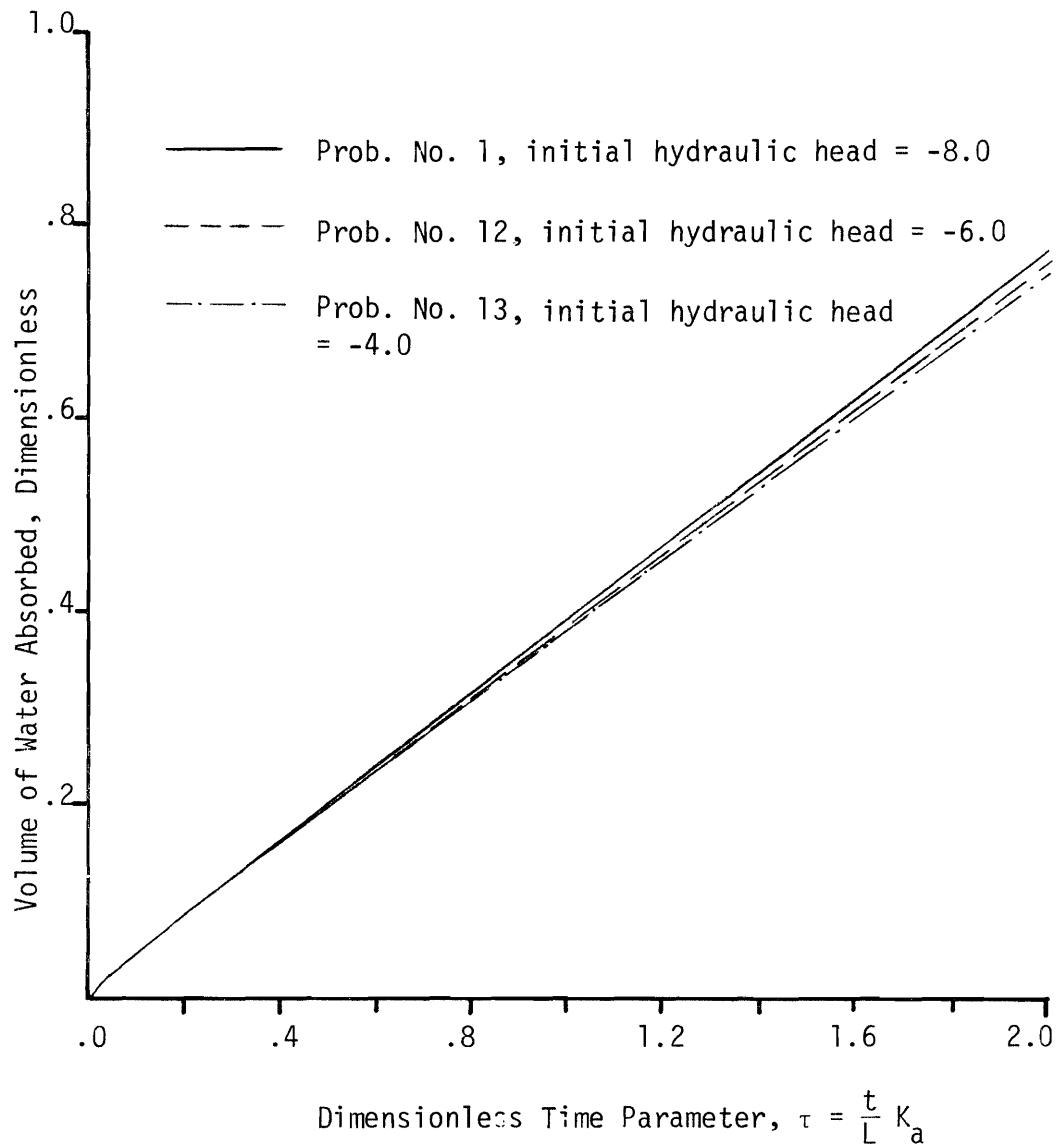


FIG. 64.--Effect of Different Values of Dimensionless Initial Hydraulic Head, h_0 , on Volume of Water Absorbed as Obtained from Solutions of Problems 1, 12, and 13.

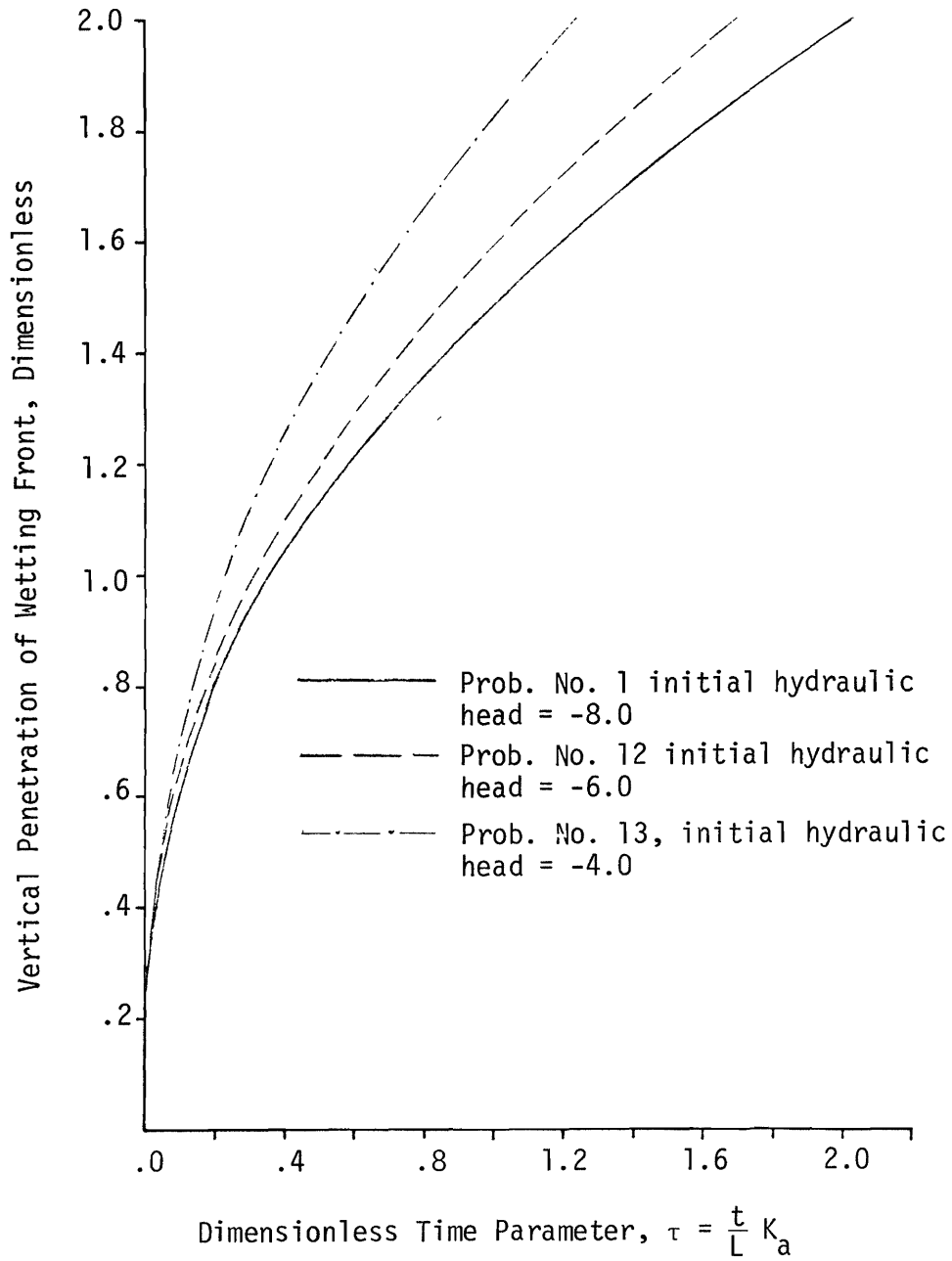


FIG. 65.--Effect of Different Values of Dimensionless Initial Hydraulic Head, h_0 , on Vertical Depth of Penetration of Wetting Front with Time for Problems 1, 12, and 13.

wetting front reaches the bottom boundary whereas for soil of hydraulic head of -8.0 it reached the bottom boundary at $\tau = 1.98$. Lateral movement of the wetting front in wet soil is much faster than the dry soil. For example, Fig. 66 shows that at $\tau = 2.20$ the lateral movement in wet soil ($h_0 = -4$) is 1.75 units and in drier soil (-8.0) at the same time it is 1.375 units beyond the circle of water application area.

The increase in saturation at any time is also of interest. The variation of saturation of the soil on the centerline at 0.4 unit depth and on soil surface at 0.3 units beyond the circle of application with time parameter, τ , has been plotted in Figs. 67 and 68. A comparison of these curves reveals that a change of the initial hydraulic head has no noticeable effect on the saturation at any point in the flow field, particularly after a period of time. The difference between the curves exists from $\tau = .0$ and is a consequence of the initial saturation at the beginning of infiltration.

Solutions to Problems 14 through 18 show the effect of different application rates on the flow patterns, and other dependent functions of infiltration. Figs. 69 and 70 show the effect of specified application rates on the penetration of the wetting front in both vertical and lateral directions for the same soil type (homogeneous soil), respectively. As the application rate increases, the vertical and lateral movement, and consequently the volume of wetted soil, increases. For the same flux the lateral movement of wetting front is less than the vertical penetration. This difference is a consequence of a constant gravitational gradient of unity in the vertical direction. Figs. 71 and 72 are plotted to show how the dimensionless application

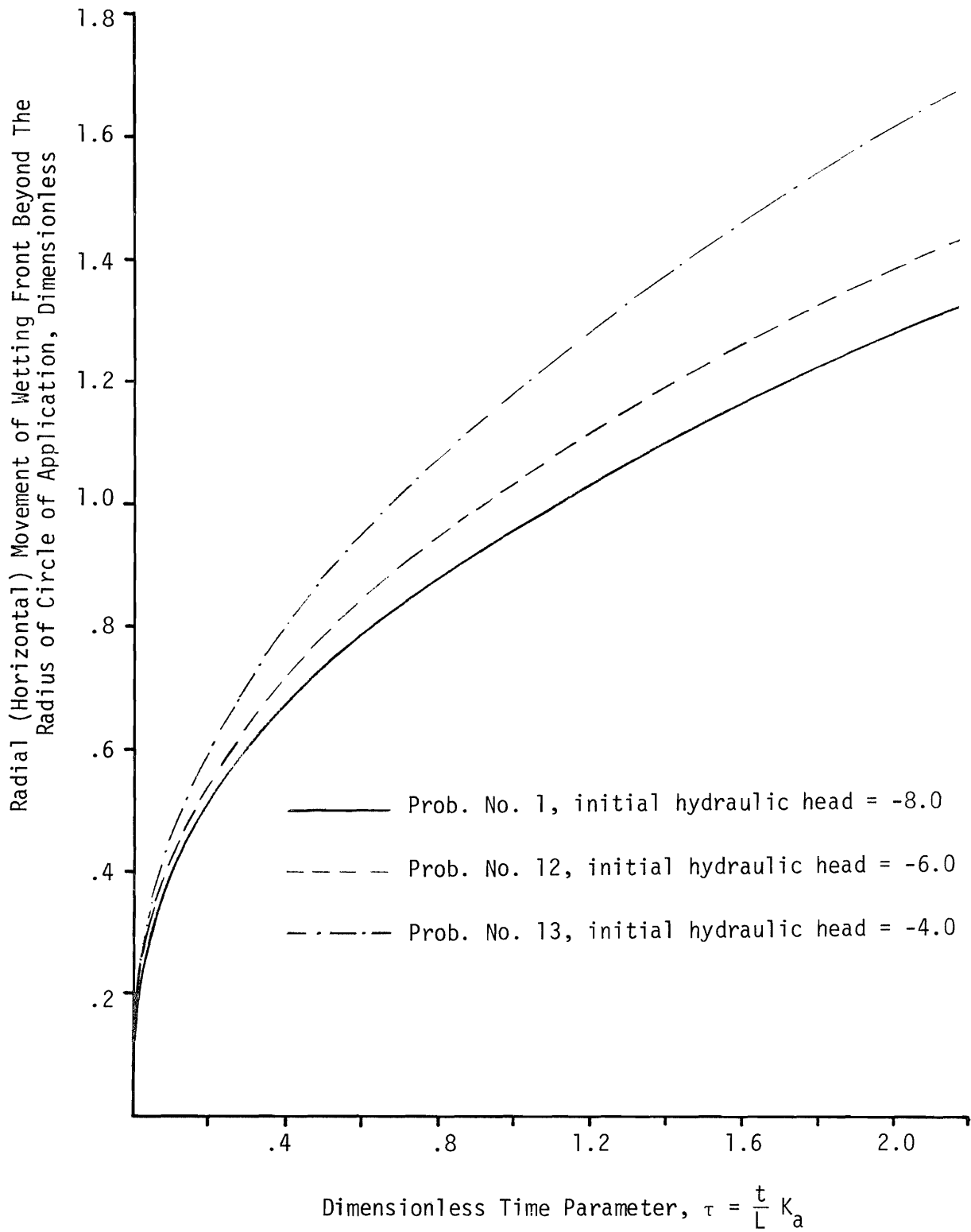


FIG. 66.--Effect of Different Values of Dimensionless Initial Hydraulic Head, h_0 , on Lateral Movement of Wetting Front With Time for Problems 1, 12, and 13.

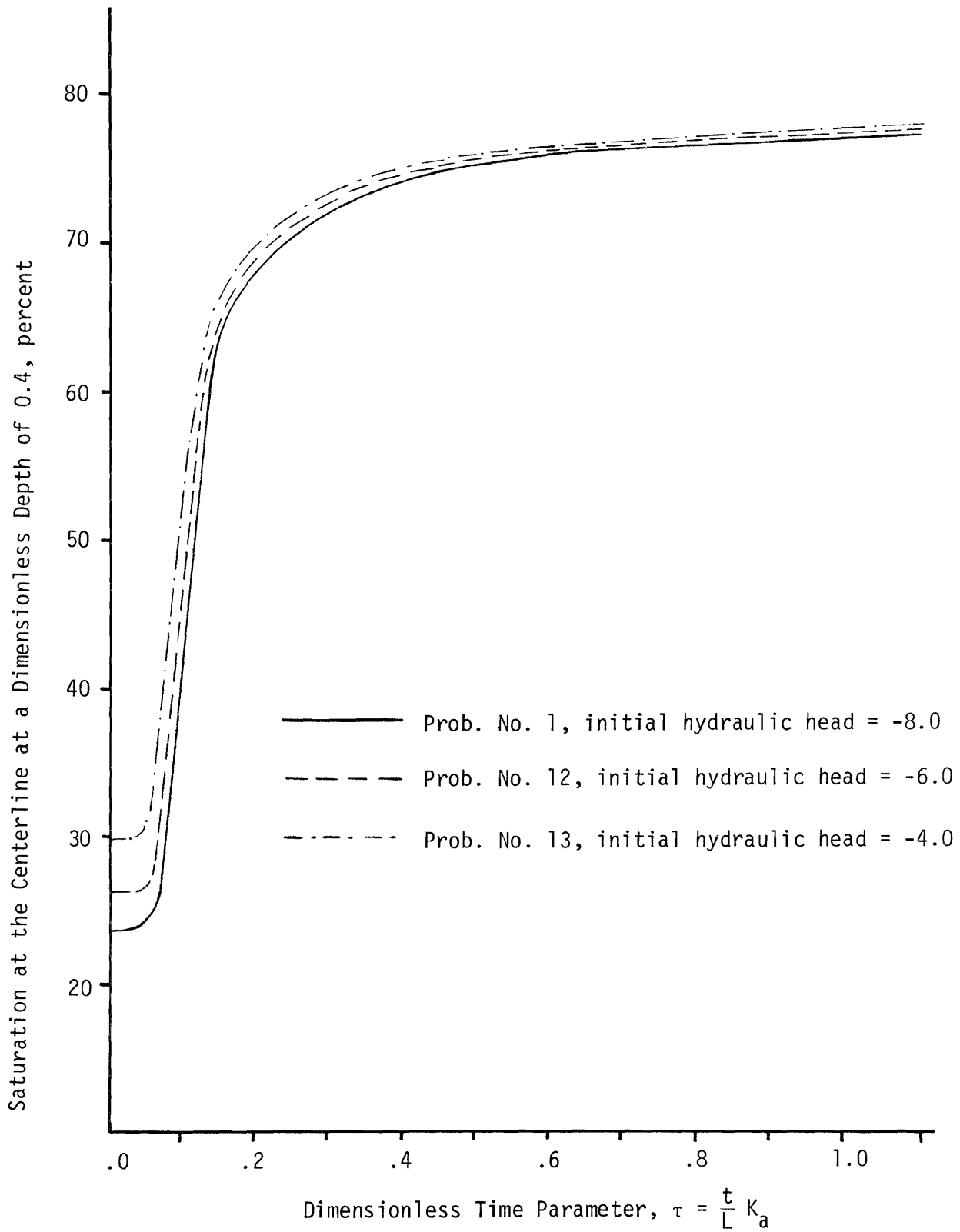


FIG. 67.--Changes in Saturation at the Centerline at a Dimensionless Depth of 0.4 Units as Obtained from Solutions to Problems 1, 12, and 13 in Different Values of Dimensionless Initial Hydraulic Head, h_0 .

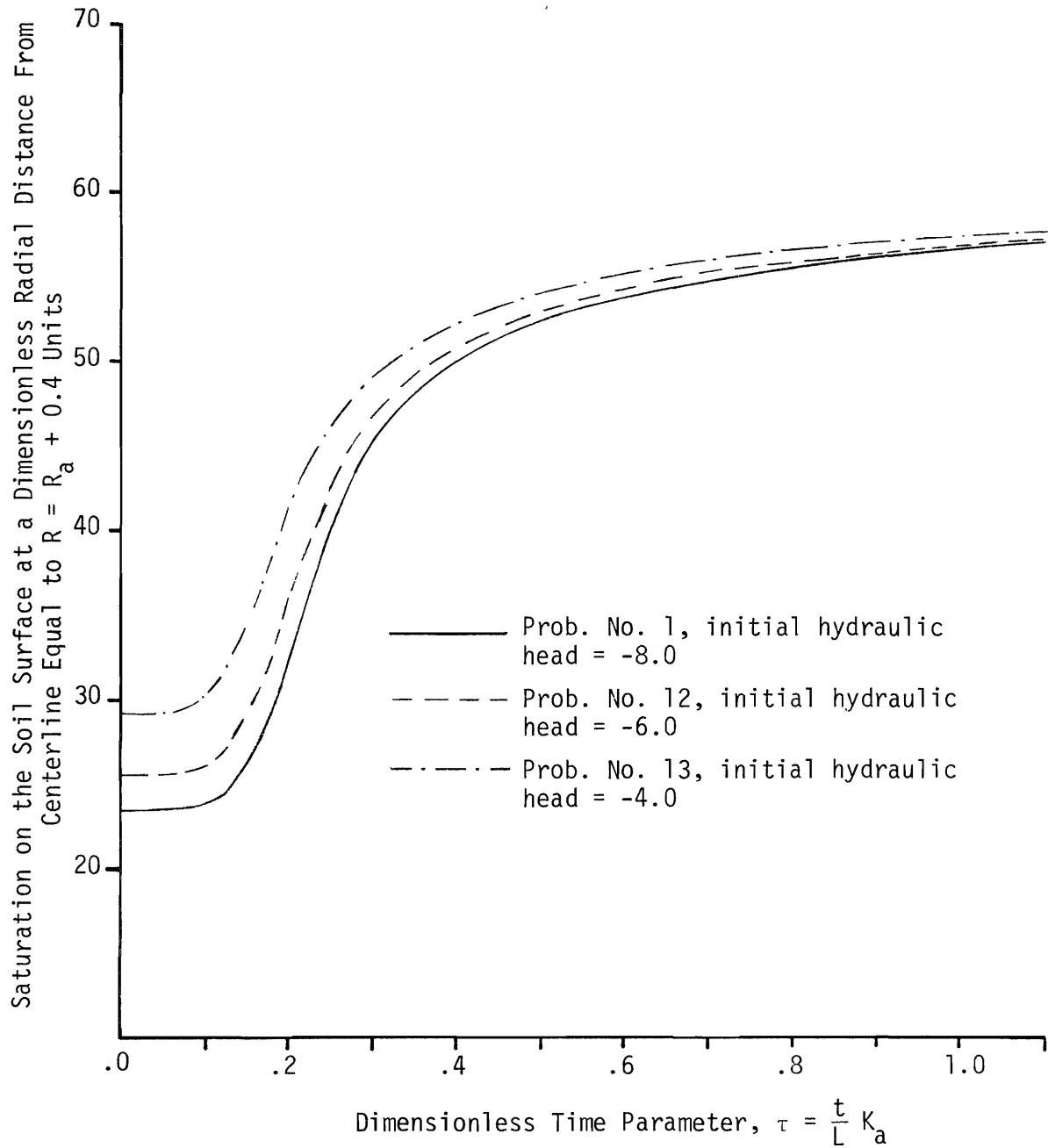


FIG. 68.--Changes in Saturation on the Soil Surface at a Dimensionless Radial Distance from Centerline Equal to $r = r_a + 0.4$ Units as Obtained From Solutions to Problems 1, 12, and 13 with Different Values of Dimensionless Initial Hydraulic Head, h_0 .

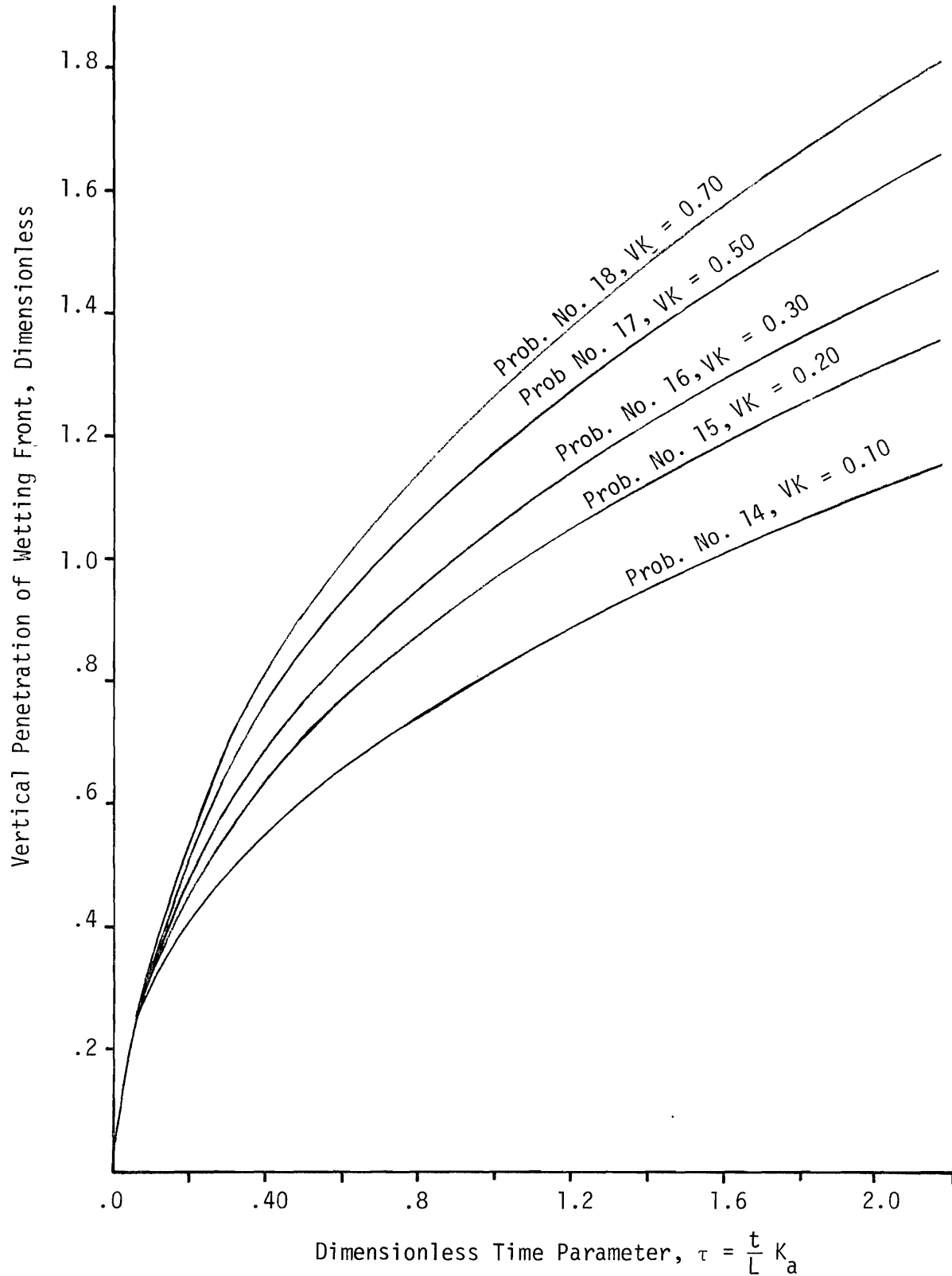


FIG. 69.--Effect of Different Values of Dimensionless Application Rate, VK , on Vertical Depth of Penetration of Wetting Front with Time for Problems 14 through 18.

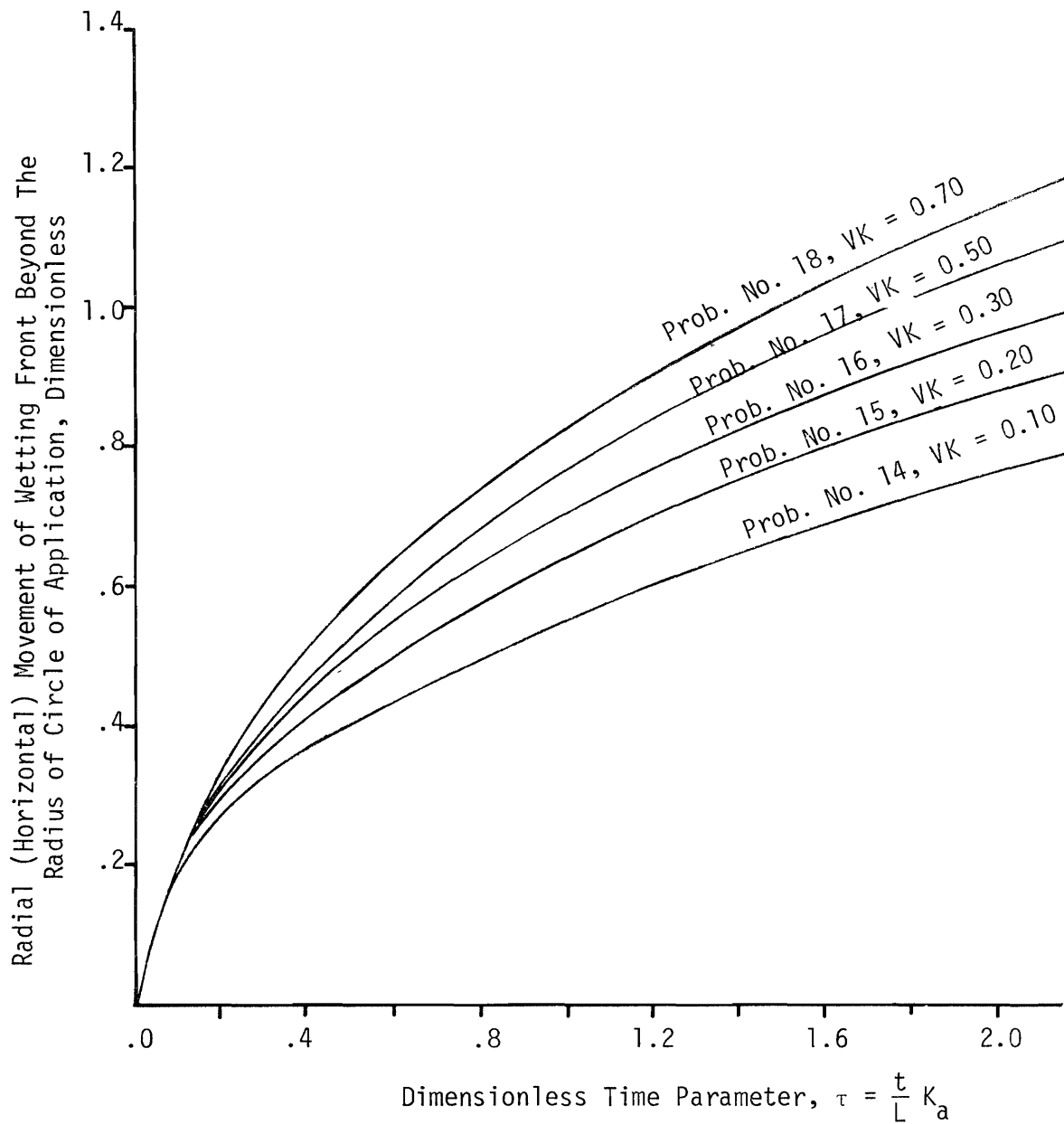


FIG. 70.--Effect of Different Values of Dimensionless Application Rate, VK, on Lateral Movement of Wetting Front with Time for Problems 14 through 18.

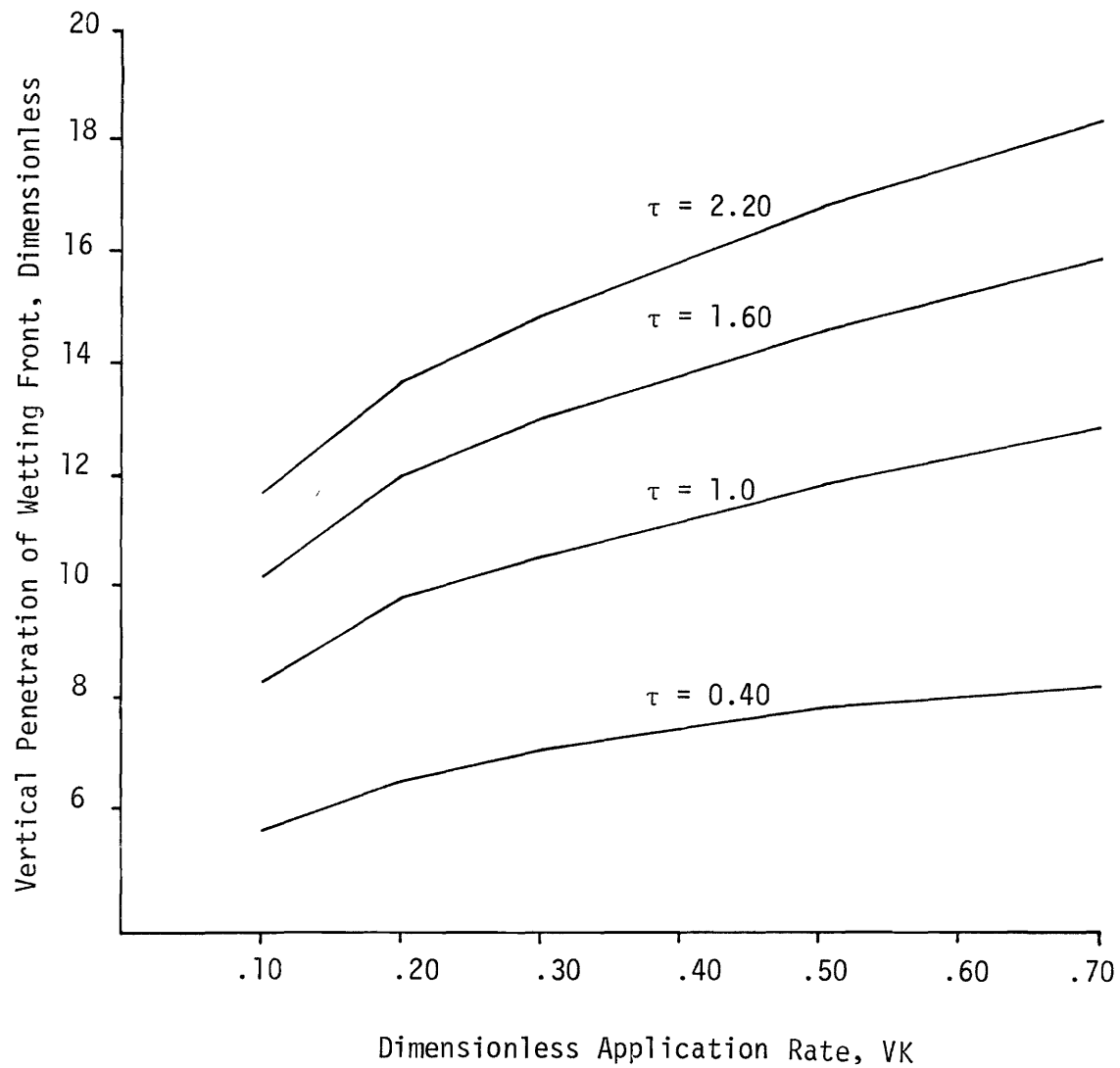


FIG. 71.--Changes in Vertical Depth of Penetration of Wetting Front with Dimensionless Application Rate, VK, for Different Dimensionless Time Parameter, τ , as Obtained From Solutions of Problems 14 through 18.

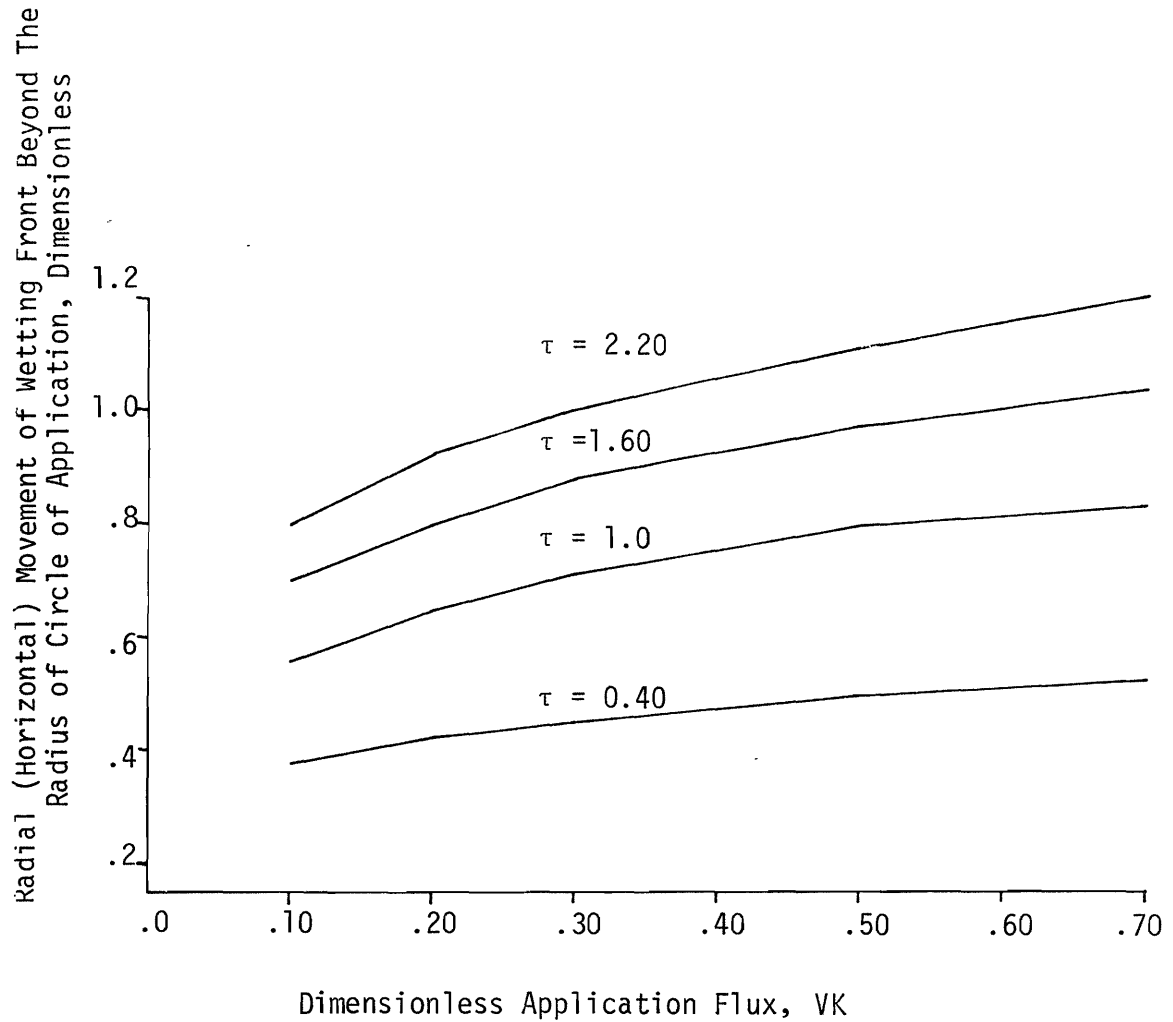


FIG. 72.--Changes in Lateral Movement of Wetting Front Beyond the Radius of Circle of Application with Dimensionless Application Flux, v_3 , for Different Dimensionless Time Parameter, τ , as Obtained From Solutions of Problems 14 through 18.

rate VK is related to the depth of penetration and lateral movement of wetting front.

Change in saturation at several points for different application rates is also of interest. The variation of saturation on the surface centerline, on the surface at 0.4 units beyond the circle of application and at 0.4 units depth on centerline are shown in Figs. 73, 74 and 75, respectively. The figures indicate for the same time, τ , saturation increases with increasing rate of water application. The increase in the saturation in vertical direction is more than in the lateral direction. For example the initial (at $\tau = 0.0$) saturation for depth 0.4 units below soil surface on axis of symmetry (Fig. 75) was about 24.0 percent and after time $\tau = 1.0$ increased 42.0 percent for the application rate 0.1, (change in saturation = $42 - 24 = 18$) whereas for the same soil, time, and application rate the change in saturation of the soil surface at 0.4 units beyond circle of application (Fig. 74) was about $26 - 23.5 = 5.5$ percent. This is also true for the higher values of application rate (see Figs. 74 and 75). Further, the Fig. 74 shows up to time $\tau = 0.25$ there is no change in saturation on the 0.4 unit beyond the circle of application for all application rates. At $\tau = 0.70$ there are noticeable changes in saturation for higher application rates while for a low application rate of 0.1, the saturation is almost at the initial saturation, (Fig. 72).

Another item of interest is the effect of the radius of circle of application, r_a , on the infiltration rate and other dependent functions of infiltration. Several solutions were obtained in which all of the parameters were identical except the radius of water

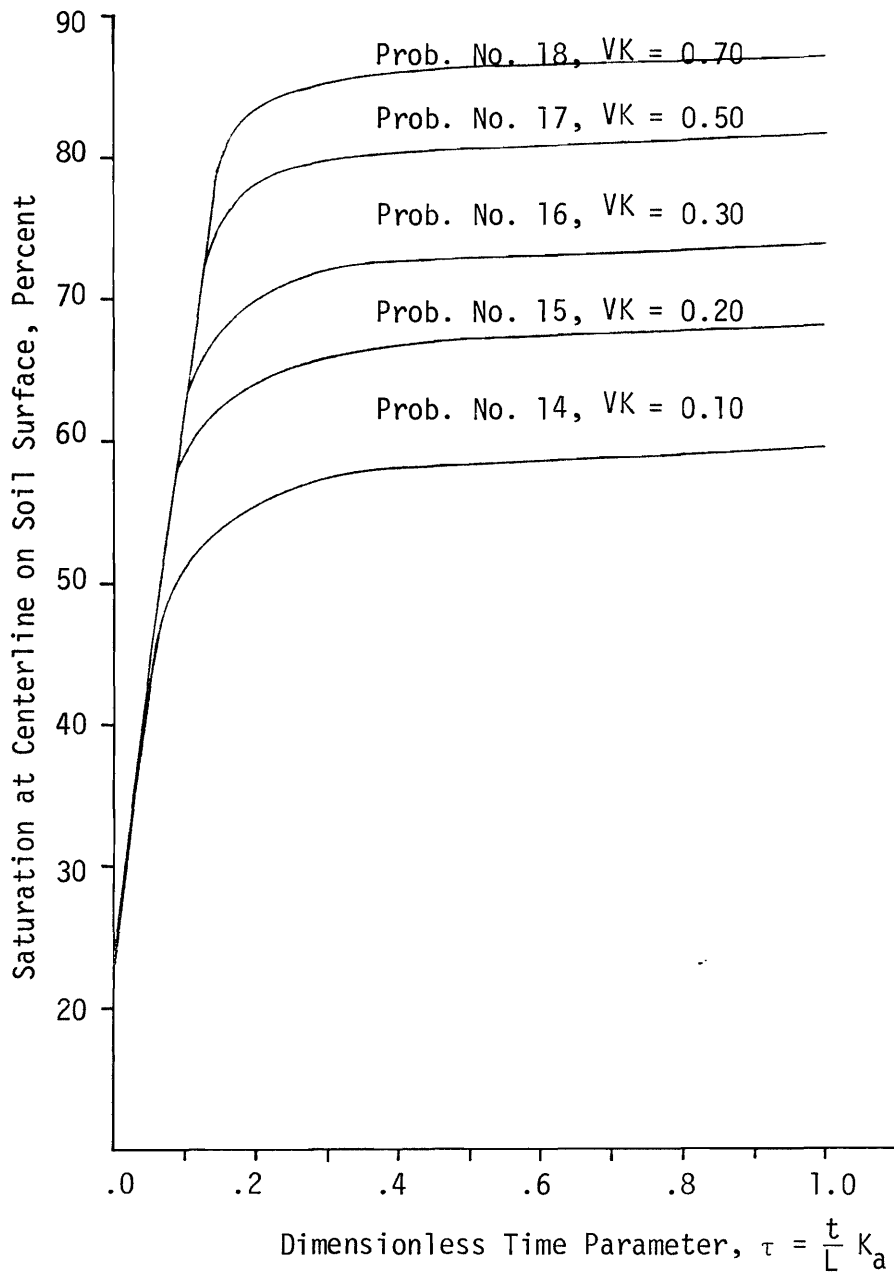


FIG. 73.--Changes in Saturation at Centerline on Soil Surface with Time for Different Values of Dimensionless Application Rate, VK, as Obtained from Solutions of Problems 14 through 18.

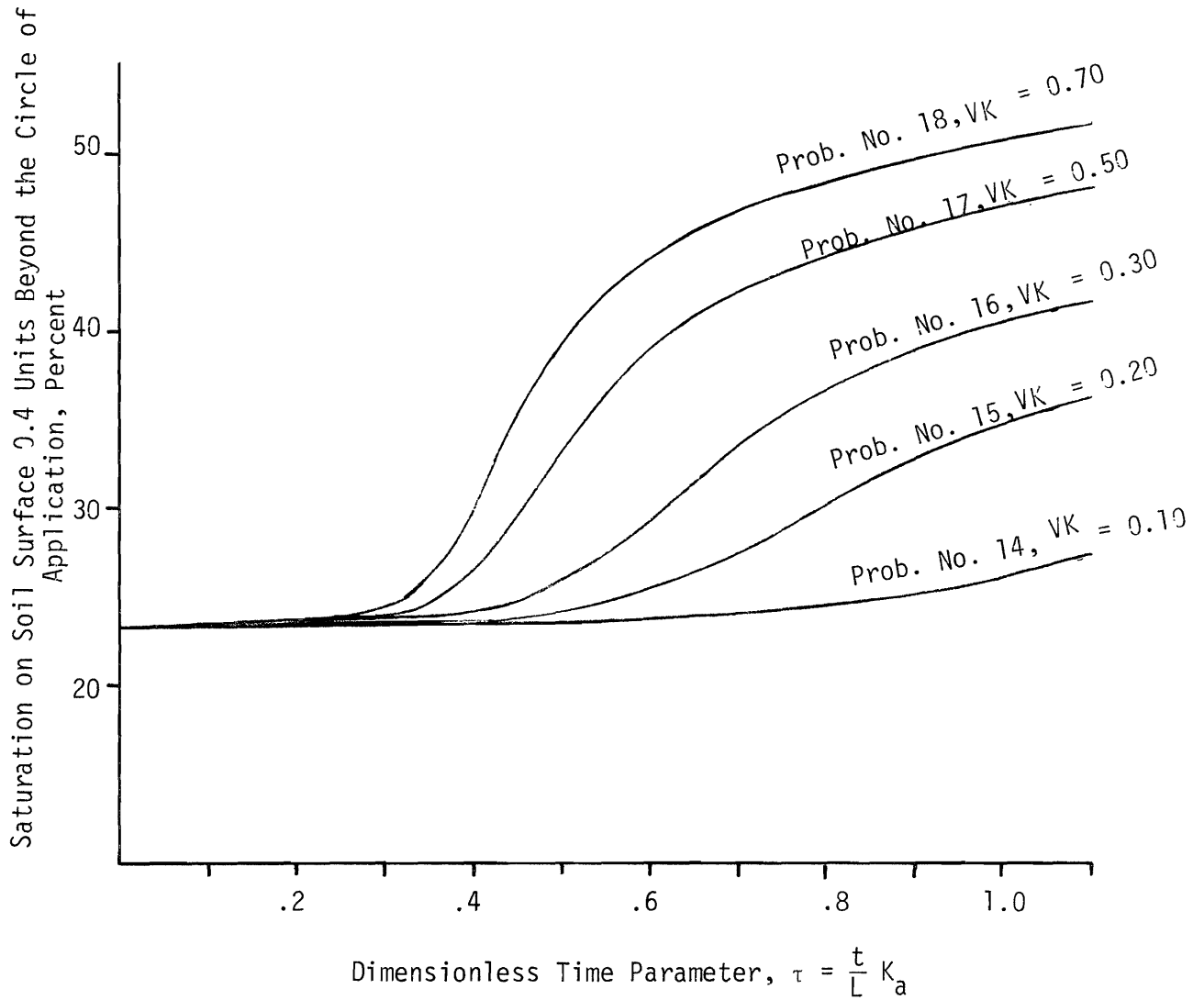


FIG. 74.--Changes in Saturation on Soil Surface 0.4 Units Beyond the Circle of Application with Time, for Different Values of Dimensionless Application Rate, VK, as Obtained From Solutions of Problems 14 through 18.

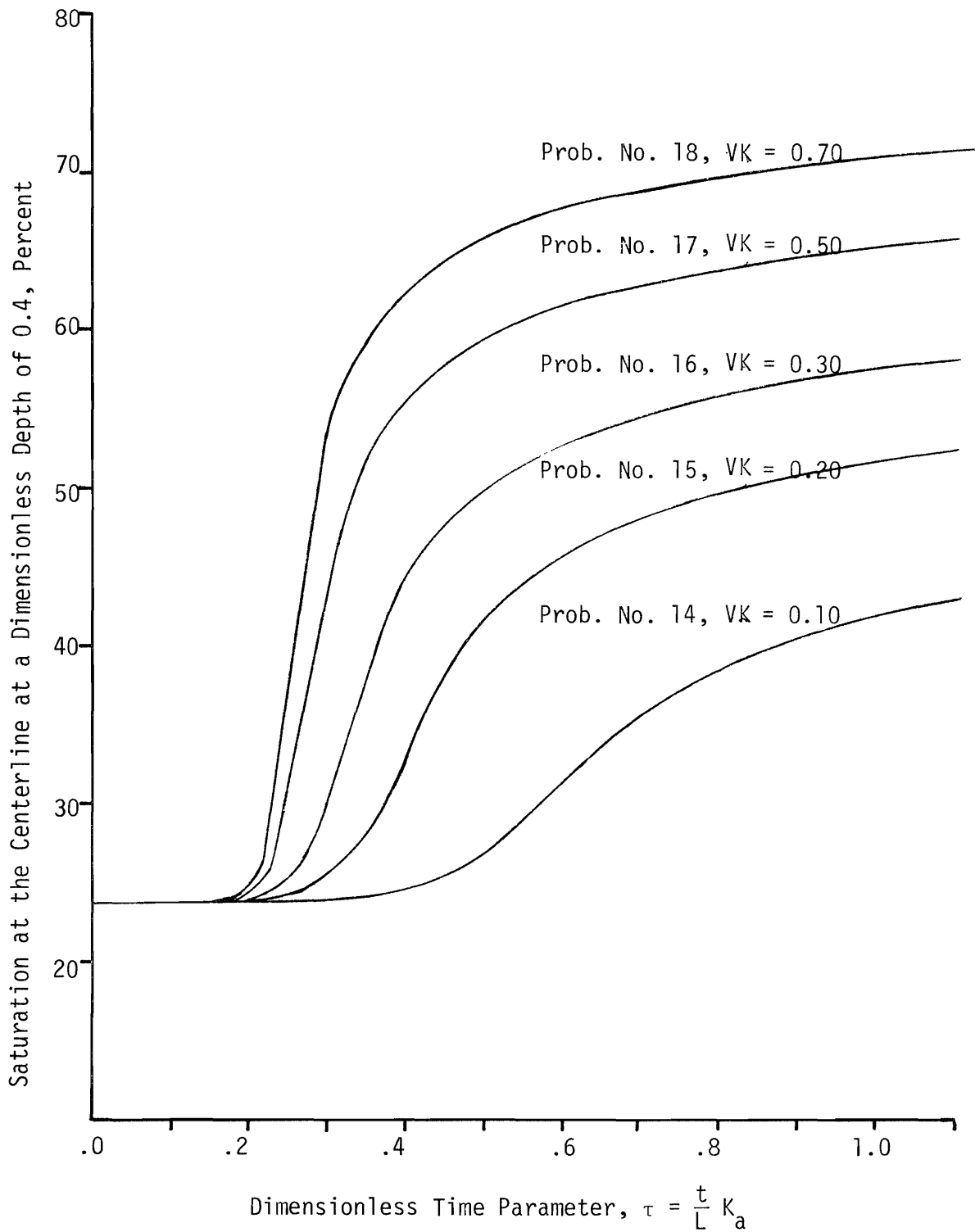


FIG.75 .--Changes in Saturation at the Centerline at a Dimensionless Depth of 0.4 Units with Time for Different Values of Application Rate, VK , as Obtained from Solutions of Problems 14 through 18.

application r_a (problems 19 through 22). The infiltration capacity curves obtained from this solution are shown in Figs. 76 and 77 in which Fig. 76 is the infiltration rate from the entire circular area and Fig. 77 indicates the infiltration rate per unit surface area. An examination of Fig. 76 and 77 shows that infiltration increases with decreasing radius of water application area. For example the infiltration rate at $\tau = 1.4$ from circular area of radius $r_a = 0.3$ unit is about 1.14 and for a circular area of radius 1.2 is approximately 0.60 for the same soil and at the same time. This relationship of the radius, r_a , and infiltration rate can provide a quantitative measure of how much the infiltration rate as measured from a small radius infiltrometer, should be reduced to predict rainfall intake capacity which is occurring in one dimension.

Fig. 78 which is a result from Figs. 76 and 77 indicates that more water infiltrated from unit area of a smaller circular area than larger area at the same time. For example, the dimensionless volume of water infiltrated from a circular area of radius 0.30 at the time $\tau = 1.4$ is approximately 1.6 whereas at the same time and soil this value is about 0.775 for an area of radius 1.2 (see Fig. 78). The variation of saturation at the centerline for the several radii of application is shown in Fig. 79. The figure shows at the beginning of infiltration, the rate of increase in saturation is almost the same for all radii r_a , thereafter a rapid change in saturation occurs in the vicinity of the wetting front. Thereafter the saturation changes a decreasingly small amount and approaches constant saturation. Since the saturations are smaller for small radii of application, r_a , it is obvious that the hydraulic gradients are substantially increased by the lateral movement

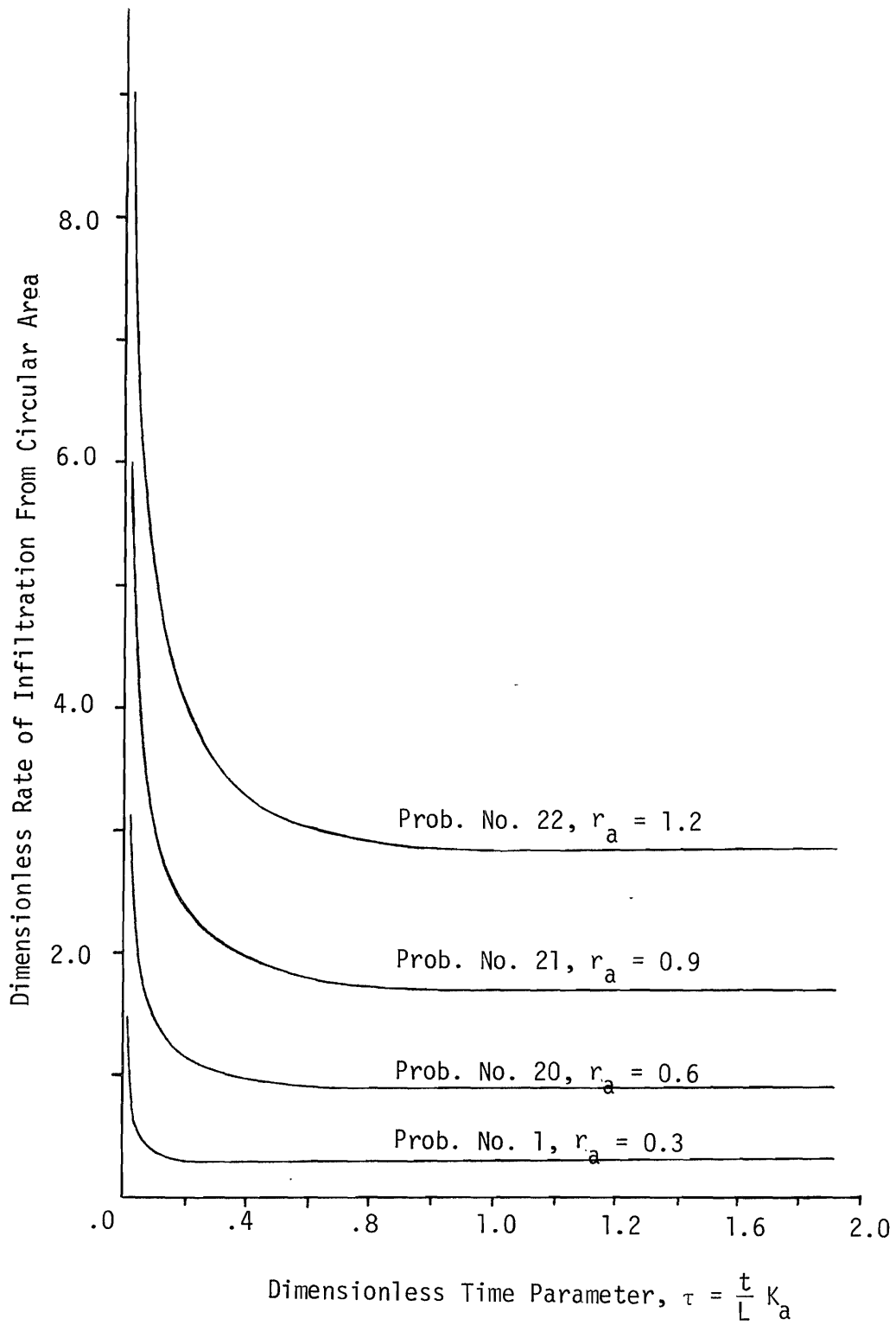


FIG. 76.--Infiltration Capacity Curves per Total Area as Obtained From Solutions of Problems 1 and 19 through 21 in Which Dimensionless Radius of Application r_a , was Varied.

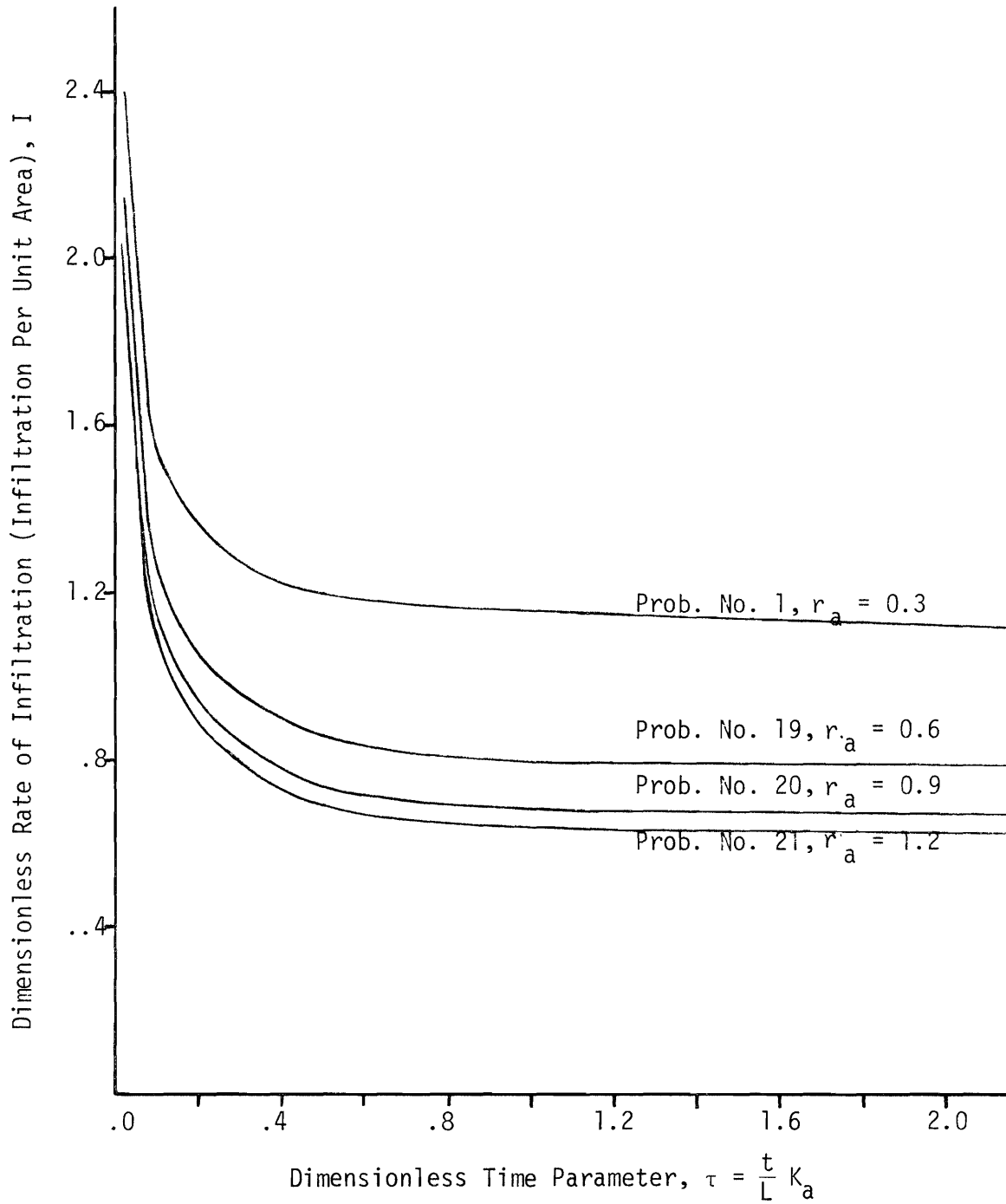


FIG. 77.--Infiltration Capacity Curves Obtained From Solutions of Problems 1 and 19 through 21 in Which Dimensionless Radius of Application, r_a , Was Varied.

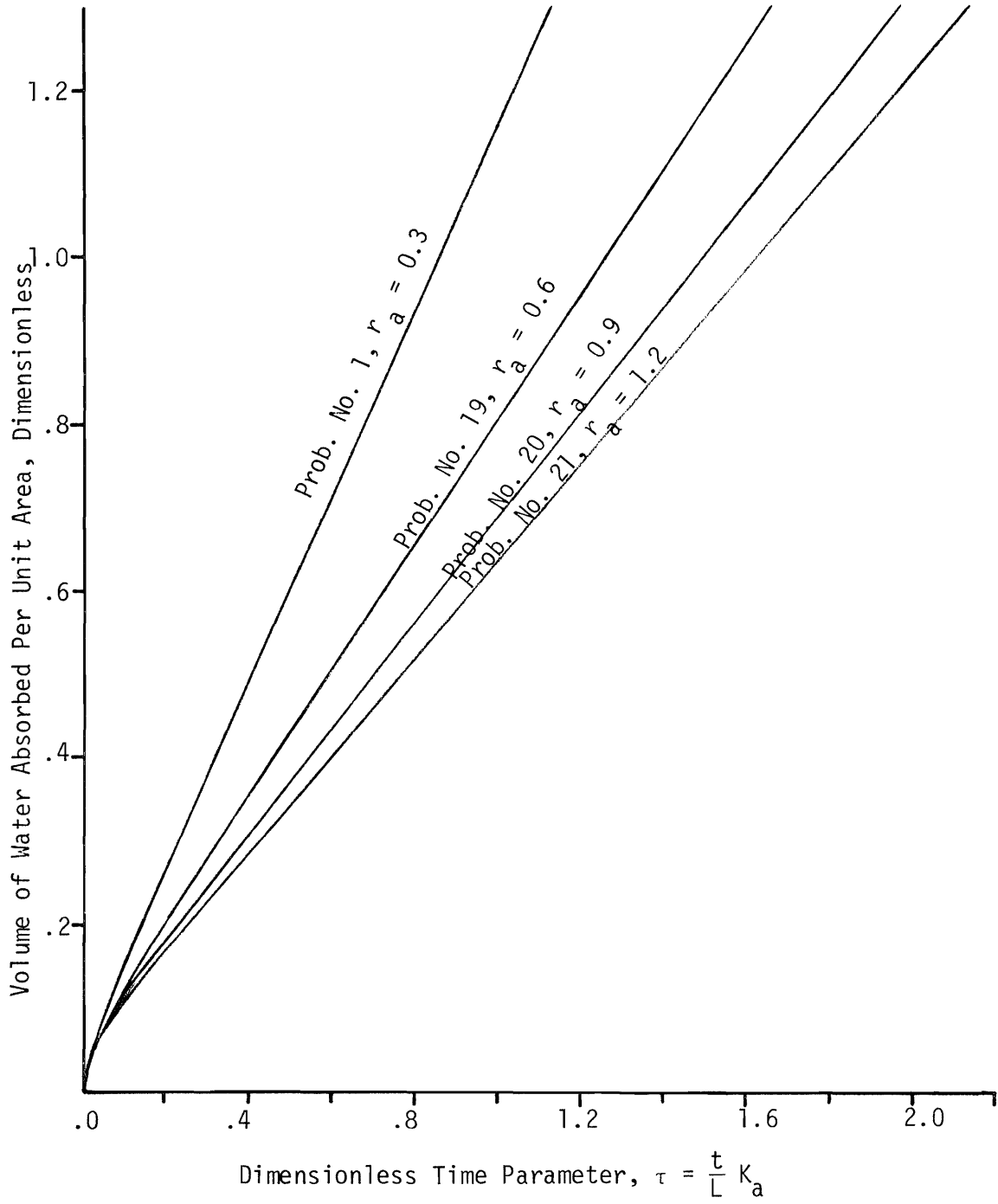


FIG. 78.--Volume of Water Absorbed Curves Obtained From Solutions of Problems 1 and 19 through 21, in which Dimensionless Radius of Application r_a , was varied.

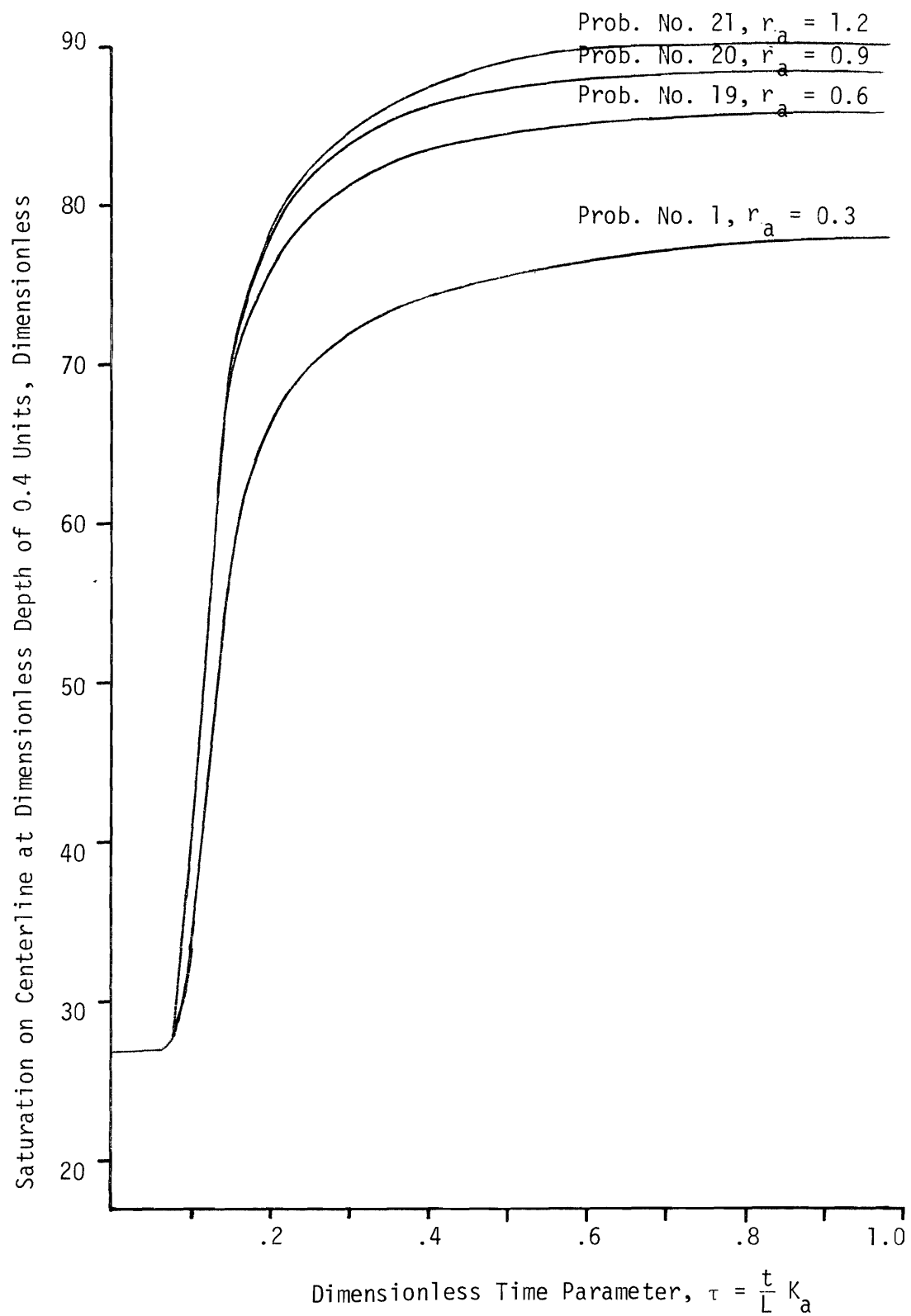


FIG. 79.--Changes in Saturation at 0.4 Units Depth on Centerline with Time for Different Radii of the Circle of Application as Obtained from Solutions of Problems 1 and 19 Through 21.

of water. The gradient developed by the lateral movement is larger than the gradients that exist for water movement only in vertical direction. Because not only saturations are less for a smaller area of application, but also quantity of infiltration water per unit area is also larger (see Fig. 78).

Coaxial Graphs

The qualitative illustration of how various types of heterogeneity effects infiltration are given in previous section. In order to quantify and define the relationship between varying soil parameters and dependent variables of the infiltration process data obtained from the numerical solutions were fitted by linear regression analyses. For these analyses, data were obtained from solutions to problems 1 through 11 at the following dimensionless times, τ : 0.2, 0.5, 1.0, and 1.5. The independent variables for these analyses are the B coefficient (in Eq. 227, 228, and 229) of all five soil parameters and τ , and differences between homogeneous and heterogeneous infiltration rates; the depth of penetration and radial movement are dependent variables. The regression program has the capability that the independent variable could either have its actual value or a transformation of it. For example, $(BPB)^2$, $(BL)^2$ are transformations of B coefficients of bubbling pressure, and pore size distribution exponent. Several analyses were made for different transformations of independent variables. The best fit was found to be a quadratic relationship for all five soil variables and cubic relationships for the time, τ . The coefficients for general equations to fit a curve through data for 13 independent variables and one dependent variable

were computed. The general expressions relate the difference between the dependent variable of infiltration for homogeneous and heterogeneous case or

$$\Delta I = I_{\text{homo.}} - I_{\text{hetero.}} \quad (224)$$

$$\Delta D = D_{\text{homo.}} - D_{\text{hetero.}} \quad (225)$$

$$\Delta R = R_{\text{homo.}} - R_{\text{hetero.}} \quad (226)$$

to the soil parameters and time, in which I is the dimensionless infiltration rate; D is the dimensionless vertical penetration of wetting front, and R is the dimensionless lateral movement of wetting front.

The resulting regression equations are:

$$\begin{aligned} \Delta I = & - .003658 + .03855(\text{BKV}) - .00075(\text{BKV})^2 + .2777(\text{BSR}) + .2110(\text{BSR})^2 \\ & - .0882(\text{BPB}) - .00844(\text{BPB})^2 + .45487(\text{BL}) + 1.0393(\text{BL})^2 \\ & - .08291(\text{BPOR}) + .018182(\text{BPOR})^2 + .0080363(\tau) - .0051842(\tau)^2 \\ & + .0014946(\tau)^3 \quad (R^2 = 0.98) \quad (227) \end{aligned}$$

$$\begin{aligned} \Delta D = & - .014 + .232(\text{BKV}) - .155(\text{BKV})^2 + .173(\text{BSR}) - .03(\text{BSR})^2 \\ & + .23567(\text{BPB}) - .12111(\text{BPB})^2 + .23367(\text{BL}) + .83444(\text{BL})^2 \\ & + .28864(\text{BPOR}) - .12397(\text{BPOR})^2 + .038548(\tau) - .033138(\tau)^2 \\ & + .010726(\tau)^3 \quad (R^2 = 0.92) \quad (228) \end{aligned}$$

$$\begin{aligned} \Delta R = & .0070762 + .0185(\text{BKV}) + .0125(\text{BKV})^2 - .18900(\text{BSR}) - .15(\text{BSR})^2 \\ & - .55(\text{BPB}) - .27778(\text{BPB})^2 + .99667(\text{BL}) - .10(\text{BL})^2 \\ & - .85455(\text{BPOR}) - 1.2479(\text{BPOR})^2 - .024151(\tau) + .028802(\tau)^2 \\ & - .011772(\tau)^3 \quad (R^2 = 0.98) \quad (229) \end{aligned}$$

in which BKV, BSR, BPB, BL, and BPOR represent the B coefficients of K_v , S_r , P_b , λ , and η , respectively. The above three equations, (227), (228), and (229) are solved by the three coaxial graphs, Figs. 80, 81, and 82, respectively. Each coaxial graph provides the magnitude of dependent variables ΔI , ΔD , and ΔR , and shows how time, τ , and rate of change of η , P_b , λ , S_r , and K_0 effect them.

In using the coaxial graphs, first take a specific dimensionless time parameter, τ , next select appropriate B coefficient for each soil parameter, then enter each individual plots with these coefficients in the order shown by the line with an arrow, until the axis for ΔI , ΔD , or ΔR is reached. On each figure the homogeneous case is solved.

The values of ΔI , ΔD , and ΔR can be considered as correction factors in obtaining infiltration rate, vertical penetration and lateral movement of the wetting front when homogeneous assumptions are made. For example, ΔI can be obtained from coaxial graph, Fig. 80, or can be computed from Equation (227), for any known soil (i.e., the magnitude of soil parameters and their variation are known).

Thus

$$I_{\text{hetero}} = I_{\text{homo}} - \Delta I_{\text{hetero}} \quad (230)$$

Because of the following assumptions, caution should be exercised in using the coaxial graphs.

1. The regression equation used in developing these graphs assumes no interaction of the soil parameters.
2. The problems that have been solved and compared herein are based on a single soil parameter, varying in a given case.

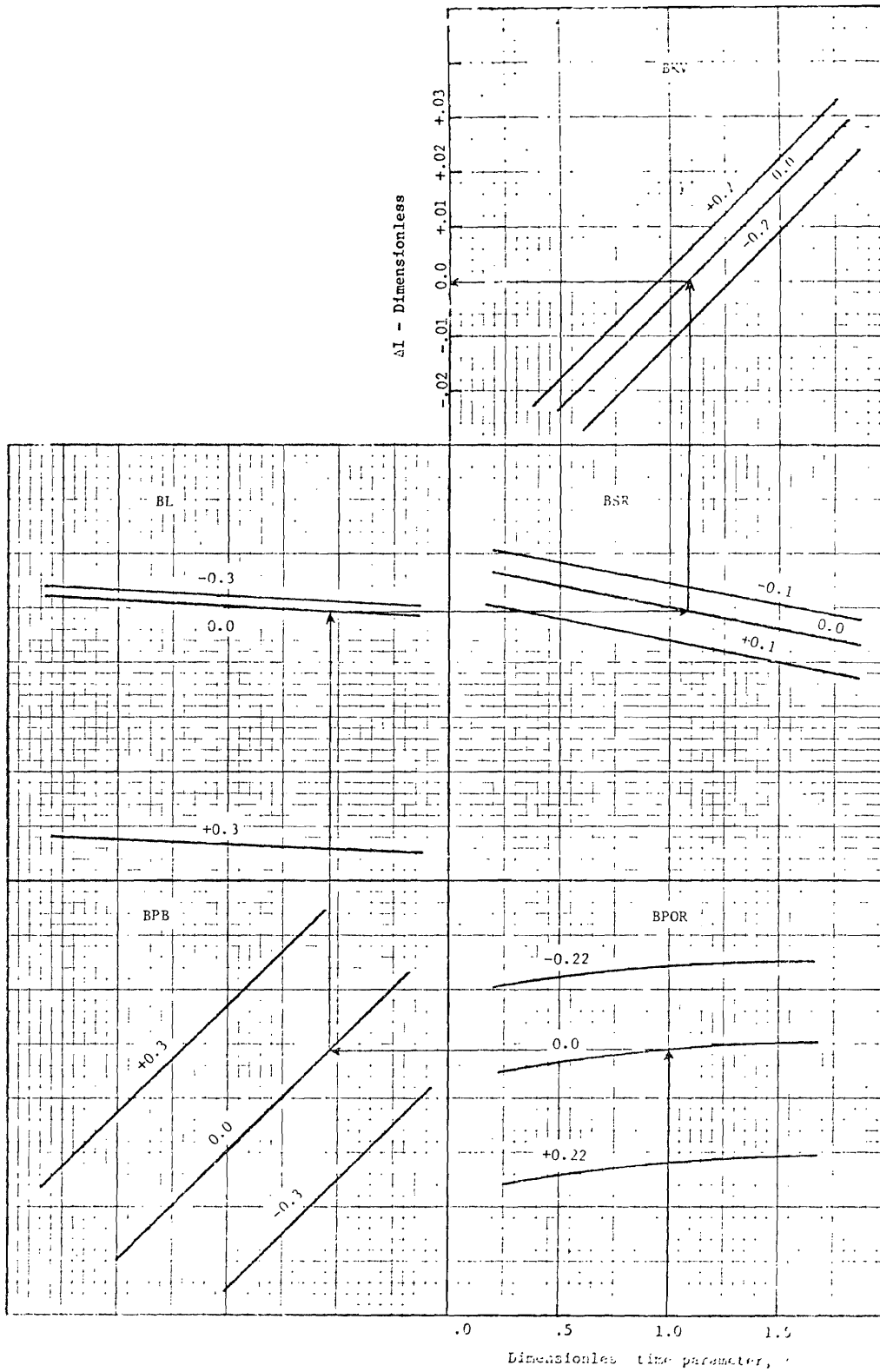


FIG. 80.--Graphical Solution Giving the Difference between the Instantaneous Infiltration Rate for Homogeneous and Heterogeneous Soil, ΔI ; Based upon Linear Coefficients which Describe Heterogeneity as a Function of Depth.

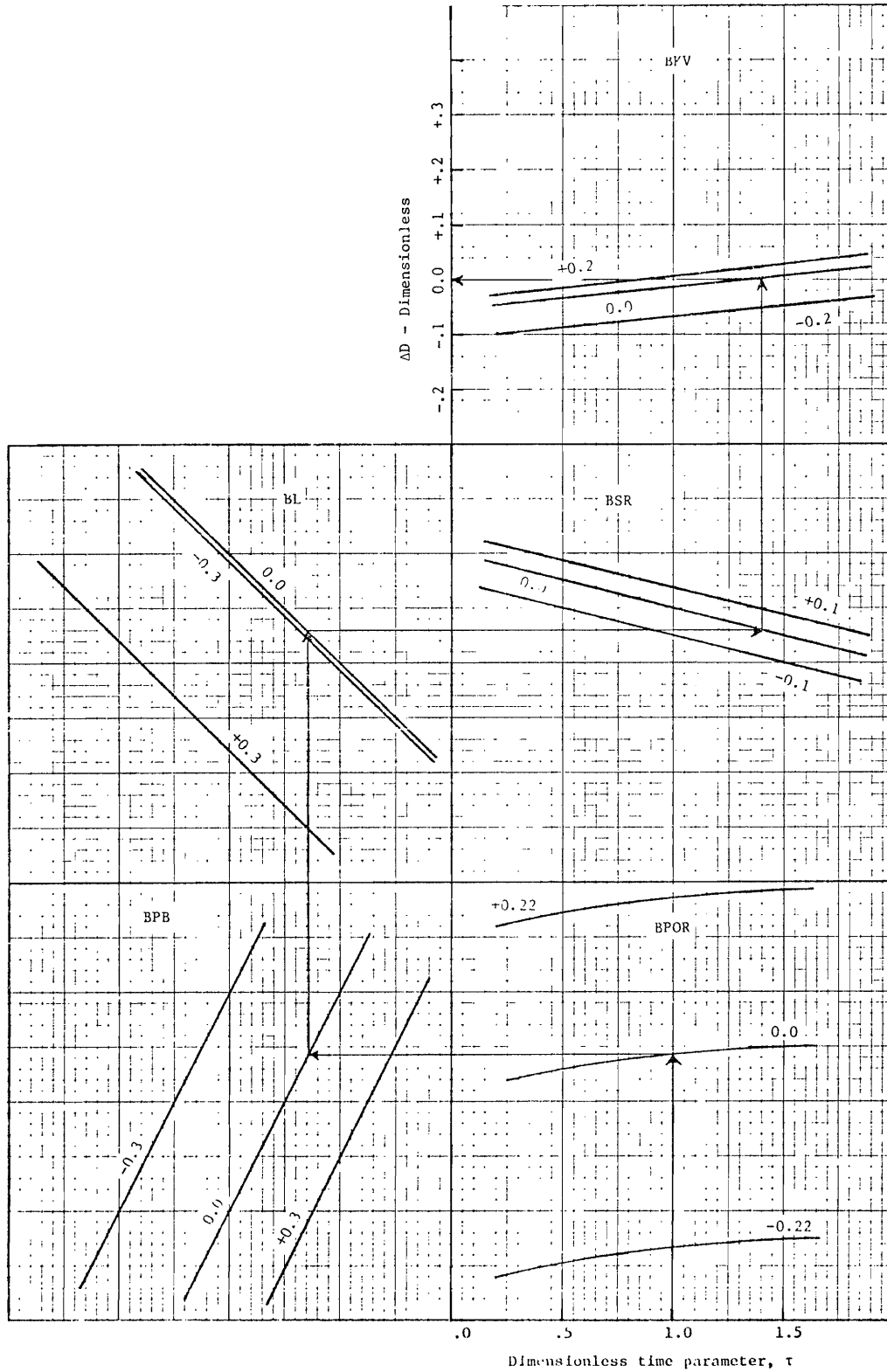


FIG. 81.--Graphical Solution Giving the Difference Between the Vertical Penetration of Wetting Front for Homogeneous and Heterogeneous Soil, ΔD . Based Upon Linear Coefficients Which Describe Heterogeneity as a Function of Depth.

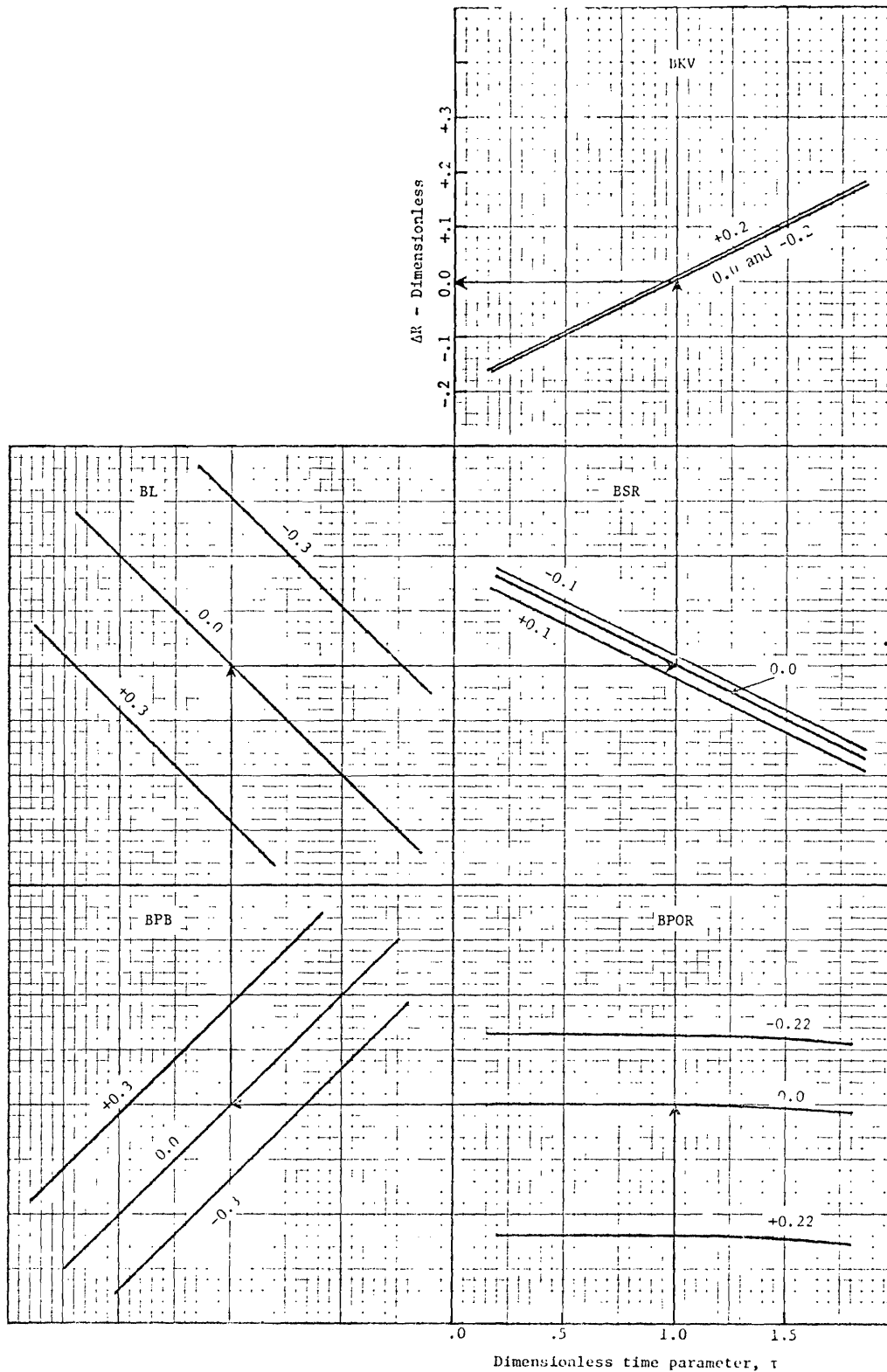


FIG. 82.--Graphical Solution Giving the Difference Between the Lateral Movement of Wetting Front for Homogeneous and Heterogeneous Soil, ΔR . Based Upon Linear Coefficients Which Describe Heterogeneity as a Function of Depth.

3. Other analyses for axisymmetric infiltration, in which actual or more realistic interactions between soil parameters are made, are needed to evaluate parameter interaction effects.

Comparison of Results with the Results
of a One Dimensional Infiltration

Jeppson (45) developed a computer program which solves the problem of unsaturated, unsteady one dimensional infiltration through heterogeneous soil. Problems 1 through 11 were solved using this one dimensional model. In order to show the difference between the results of three-dimensional and one-dimensional infiltration problems the infiltration rate per unit area and saturation at several points in flow field are compared. Fig. 83 gives the difference between three-dimensional axisymmetric and one-dimensional infiltration at a specific time, τ , for different soils. The plotted points on log-log graph paper are essentially straight lines. As the figure indicates this difference, $\Delta I = I_3 - I_1$, is constant for the variation of pore size distribution exponent, λ . For the other problems the following form can be suggested:

$$\Delta I = a'(\tau - 0.1)^{b'} \quad (231)$$

Since the slope of the separate straight lines on Fig. 83 is nearly constant except the curve for $BL = -.3$, the exponent b' in Equation (231) will be the same for all lines and is equal to 0.0625. The intercept a' is equal to ΔI when the time $(\tau - 0.1)$, is unity.

Differences between the three-dimensional and one-dimensional saturation at a dimensionless depth of 0.4 on center line, and at a given radial distance, r_a , are presented in Fig. 84. These figures

show that the difference of saturation for three and one-dimensional infiltration decreases with time, except for variation of pore size distribution exponent and when bubbling pressure is decreasing with depth (see Fig. 84a).

Therefore for the same soil properties and other specifications, the comparison between three-dimensional and one-dimensional infiltration reveals that:

1. Infiltration per unit area in a three dimensional infiltration situation is higher than for a one-dimensional case for all cases of heterogeneity investigated.

2. At the same time the increase in relative saturation is higher for one-dimensional infiltration than for three-dimensional axisymmetric infiltration for all problems.

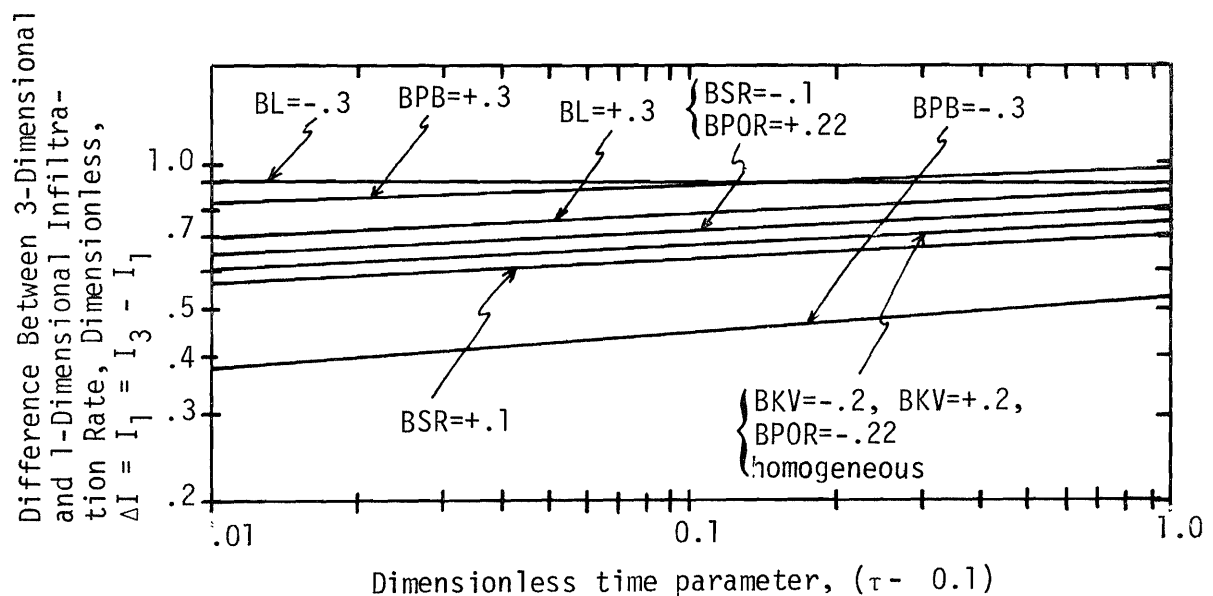
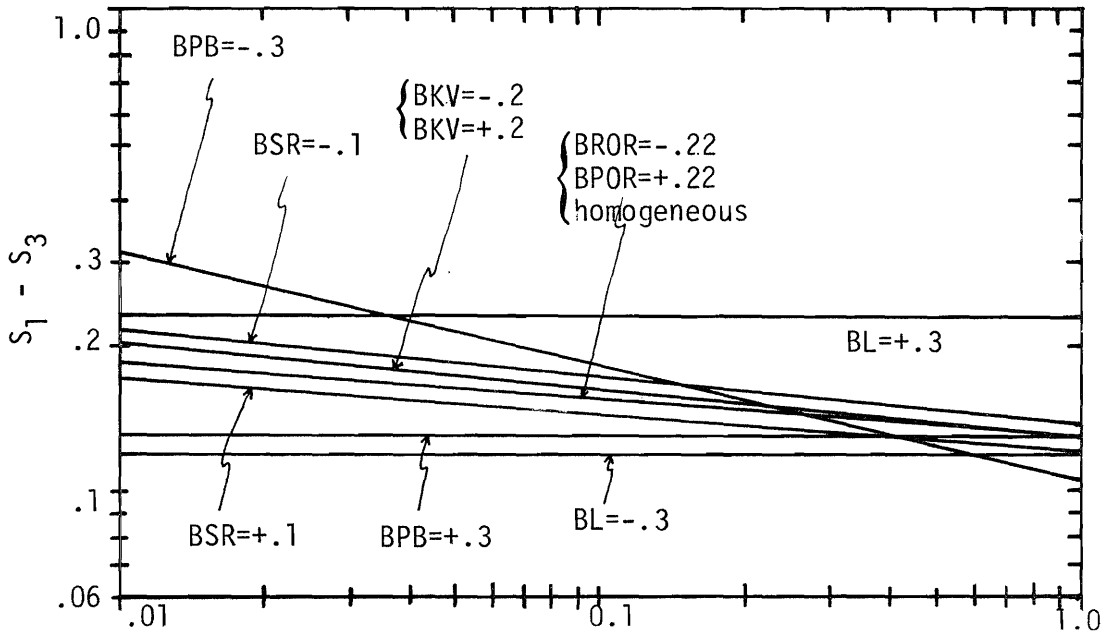
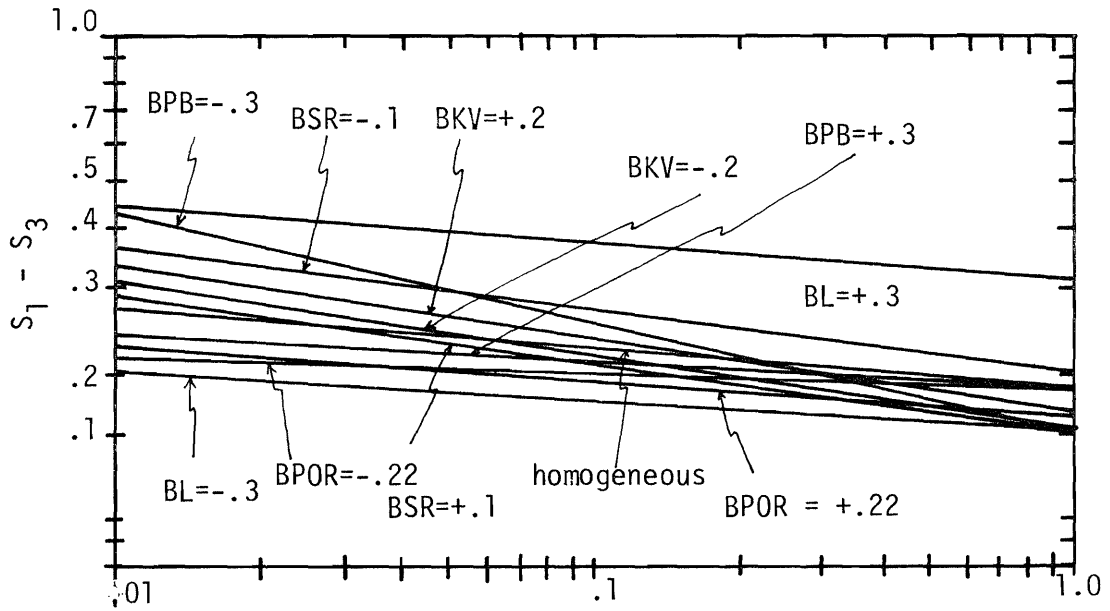


FIG. 83.--Additional Infiltration Rate Due to Applying Water Over a Finite Circular Area.



a) Dimensionless Time Parameter, ($\tau - 0.1$)



b) Dimensionless Time Parameter ($\tau - 0.1$)

FIG. 84.--Difference Between One-Dimensional and Three-Dimensional Axisymmetric Saturation at a Dimensionless Depth of 0.4 Units at (a) The Centerline and (b) Radial Distance, r_a .

3. The wetting front movement in vertical direction is more rapid than for three-dimensional infiltration.

Since the water flows radially as well as vertically in the three-dimensional infiltration, the items 2 and 3 above are due to spreading of flow patterns.

Comparison of Numerical Solutions and Field Data

Field data used in this study were obtained from Lower Sheep Creek, at the Reynolds Creek Experimental Watershed in Southwestern Idaho. Field equipment included a portable rainfall simulator, gamma probe, and tensiometers, which are used to control surface application of water, and to monitor water content of soil and pressure during infiltration. The rainfall simulator was able to apply water to a plot of 6-by-6 foot (1.83-by-1.83 m) in intensities from 0.15 to 0.8 inches per hour (3.8 to 203.2 mm per hour). Soil information and physical data for this site, equipment, and methods for collecting of data are described by Jeppson et al. (46).

In simulation of field tests, the mathematical specifications such as geometry, hydraulic properties, and external boundary influences must describe the field conditions.

In this experiment the water was applied over a 6-by-6 foot (1.83-by-1.83-m) square plot, whereas surface geometry of the mathematical model over which water is applied is a circular area. Even though the field data is obtained from the center of the plot, this inconsistency in water entry zone geometry seems to have an insignificant effect on the magnitude of collected data.

Jeppson et al. (46) used a matching procedure which consists of obtaining a series of numerical solutions, based on different values of W/K_a , and selected the solution that both duplicates best the saturation-time curves measured in the field and agrees with the field application rate. With this technique the saturated hydraulic conductivity of $K_0 = K_a = 1.665$ inches per hour (4.23 cm/hr) is obtained.

The porosity, η , at different depths of soil profile has been measured and is given as about 0.50.

Since the field data did not measure the residual saturation, S_r , pore size distribution exponent, λ , and bubbling pressure head, P_b , directly reasonable values for each parameter were obtained by matching the field saturation data with solution to problem 1 through 11.

Saturation at the 2-in (5.08-cm) depth from the field data are plotted in Fig. 85 versus time, t , as well as the saturation at 2-inches-depth from the numerical solution for application rate of $W = 0.70$ inches per hour, estimated soil properties. The field application rate was 0.70 inches per hour (1.78 cm/hr), or $\frac{W}{K_a} = \frac{0.70}{1.665} = 0.42$, which is the dimensionless application rate specified in the numerical solution. When the values of saturation at 2-inches depth on the centerline did not agree with the field data in Fig. 85, another numerical solution with a different variation of P_b , λ , and S_r or some combination of these parameters were obtained to examine whether better agreement could be achieved. A comparison of capillary pressure variation with the field data for 2 inches depth is shown in Fig. 86.

Table 3 shows various specifications which are used in comparing saturation and pressure from numerical solution with field data.

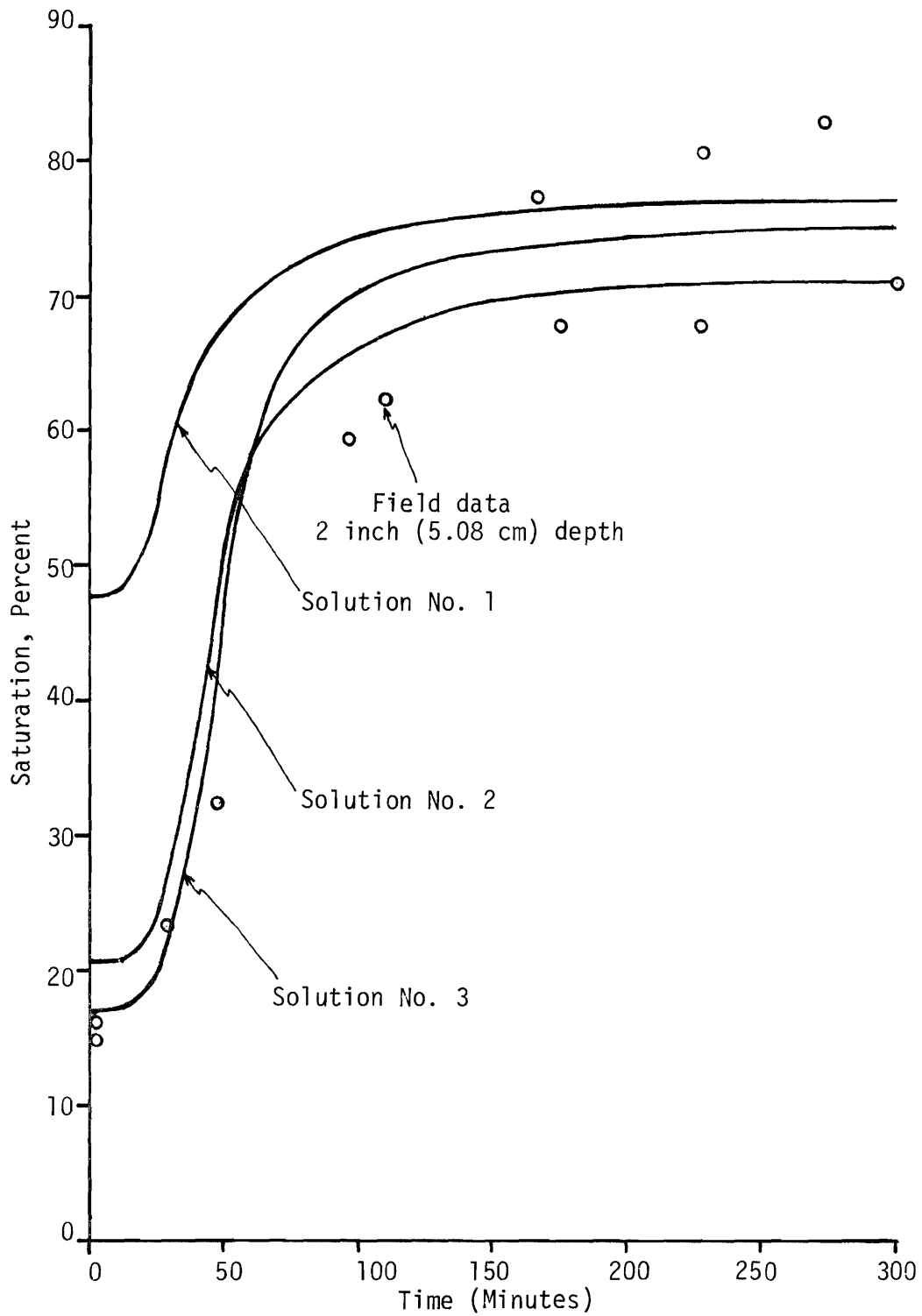


FIG. 85.--Variation of Saturation with Time at 2 Inch Depth in The Soil at Lower Sheep Creek Beneath an Axisymmetric Infiltrator.

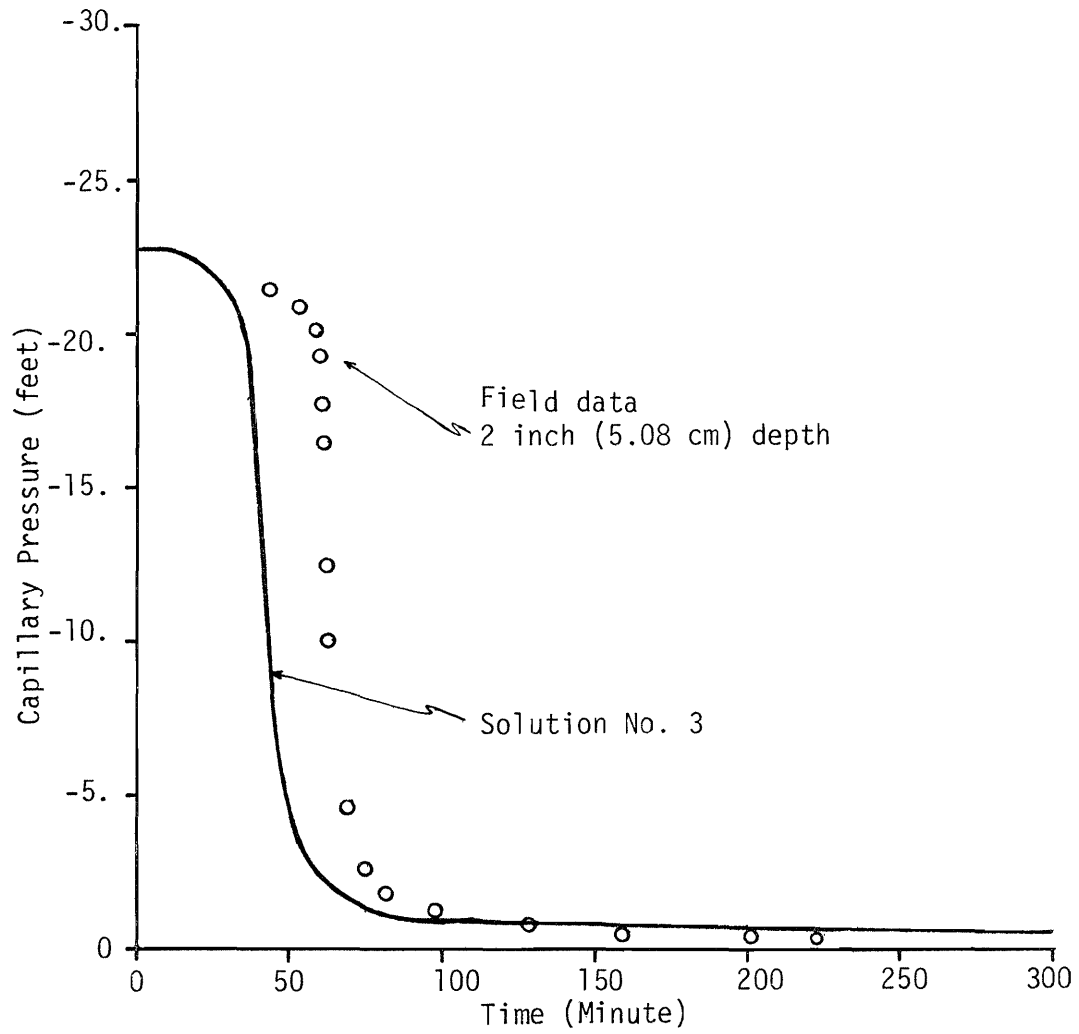


FIG. 86.--Variation of Capillary Pressure with Time at 2-inch Depth in the Soil at Lower Sheep Creek Beneath an Axisymmetric Infiltrator.

TABLE 3.--Values of Hydraulic Properties of Soil Used in Matching.

Solution	W	$\frac{W}{K_a}$	P_b	λ	S_r	η	K_o
(1)	(2)	(3)	(4)	(5)	(6)	(7)	(8)
1	.7	.42	1.0-2.5z	.4-.1z	.25-.1z	.55	1.665-.3325z
2	.7	.42	1.10-.4z	.9-.1z		.50	1.665-.3325z
3	.7	.42	1.0-.25z	.8-.1z		.50	1.665-.3325z

SUMMARY AND CONCLUSIONS

Solutions for the problem of transient three-dimensional axisymmetric unsaturated flow through heterogeneous soils from water applied over a horizontal circular area have been obtained. The needed relationships of saturation and relative hydraulic conductivity to capillary pressure are defined by Brooks and Corey (9) equations. The mathematical model permits any vertical heterogeneity of the soil to be specified and describes the heterogeneity so that all the pertinent hydraulic properties of the soil can vary continuously as a function of depth. Kirchhoff-Transformation is used to transform the dependent variable P_t in the partial differential Equation (81) to a new variable ξ which changes much less abruptly across the wetting front than capillary pressure P_t . The Crank-Nicolson method is used to difference the partial differential Equation (105) to produce a system of nonlinear algebraic equations. The system of nonlinear algebraic equations obtained therefrom are solved by Newton-Line-Relaxation method to advance the solution through each time step.

For solving the problem a FORTRAN IV program has been written. To a typical problem such as those presented in this dissertation it requires approximately 1600 seconds of execution time and about 10 second input-output time on a Burroughs 6700 digital computer to obtain a solution. The computer output gives the values of saturation, capillary pressure, hydraulic head, volume of water applied, infiltration rate, and instantaneous infiltration rate from time zero to any time.

From computer solutions of 21 different problems, the distribution of saturation, the capillary pressure magnitude, the lateral and vertical penetration of wetting front, and the magnitude and characteristics of intake capacities have been analyzed to show their relationship with soil heterogeneity and other problem specifications. The results from the analyses are presented in a number of graphs.

General qualitative conclusions derived therefrom are summarized in Table 4. The entries in Table 4 show the difference between a base or standard homogeneous soil condition solution and the solution of the problem with a single variable described in column 1. The homogeneous soil (problem no. 1) and soil with initial hydraulic head of $h_0 = -6.0$ (problem No. 13), and problems with having application rate of $W = 0.3$ and $r_a = 0.9$ are the selected as base solutions.

Positive or negative sign in the table indicates that the magnitude of this quantity is greater or less than in the base problem solution. A zero entry indicates there is not a difference between the solutions from base and actual problems.

The nomographs, Figs. 80, 81, and 83, provide more detail regarding the magnitudes of the plus or minus difference given in Table 4.

TABLE 4.--Summary of Results and Conclusions. Table Shows the Difference Between a Base Solution and the Solution From the Problem Described in Column 1 (Base Problem - Problem in Column 1).

Infiltration Variable	Initial Saturation		Saturation During Infiltration			Wetting Front Penetration		Infiltration Rate	Volume of Water Absorbed Per Unit Surface Area
	Problem Specification	On Soil Surface	On Bottom Boundary	At Centerline on Soil Surface	On Soil Surface at Radial Distance $r_a + 0.4$	At Centerline At a Depth of 0.4	Vertical		
Heterogeneous Soil	P_b decreasing with depth (1.3 to 0.7)	-	+	0	-	+	+	-	-
	P_b increasing with depth (0.7 to 1.3)	+	-	0	+	-	-	+	+
	λ decreasing with depth (1.3 to 0.7)	+	-	0	+	+	+	+	+
	λ , increasing with depth (0.7 to 1.30)	-	+	0	-	- then +	- then +	-	-
	S_r decreasing with depth (0.25 to 0.05)	-	+	0	-	-	+	-	+
	S_r increasing with depth (0.05 to 0.25)	+	-	0	+	+	-	+	-
	n decreasing with depth (0.62 to 0.18)	0	0	0	+	+	+ then -	+	-
	n increasing with depth (0.18 to 0.62)	0	0	0	-	-	- then +	-	+
	K decreasing with depth (1.0 to 0.60)	0	0	0	0	-	+	0 then +	+
	K_0 increasing with depth	0	0	0	0	+	-	0 then -	-

TABLE 4.--Continued.

	Initial hydraulic head, $h_0 = - 3.0$	+	+	0	+ close to zero	+ close to zero	-	- close to zero	- close to zero	- close to zero
	Initial hydraulic head, $h_0 = - 4.0$	-	-	0	- close to zero	- close to zero	+	+ close to zero	+ close to zero	+ close to zero
Homogeneous Soil	Radius of water application area, $r_a = 1.2$	0	0	0	- close to zero	-	-	0	+	+
	Radius of water application area, $r_a = 0.6$	0	0	0	+ close to zero	+	+	0	-	-
	Application rate, $W = 0.1$	0	0	+	+	+	+	+	+	+
	Application rate, $W = 0.7$	0	0	-	-	-	-	-	-	-

LITERATURE CITED

1. Ames, W. F., Nonlinear Partial Differential Equations in Engineering, Academic Press, 1965.
2. Amerman, C. R., "Soil Water Modeling I: A Generalized Simulator of Steady, Two Dimensional Flow." Composite, Vol. 19, No. 3, 1976, pp. 466-471.
3. Ashcroft, Gaylong, March, Donald D., Evans, D. D., and Boersma, Larry, "Numerical Method for Solving the Diffusion Equation: I. Horizontal Flow in Semi-Infinite Media," Soil Science Society of America, Proceedings, Vol. 26, 1962, pp. 522-525.
4. Bear, J., Zaslavsky, D., and Irmay, S., "Physical Principles of Water Percolation and Seepage," United Nations Educational, Scientific and Cultural Organization (UNESCO), Paris, France, 1968, 465 p.
5. Bouwer, H., "Theoretical Aspects of Unsaturated Flow in Tile Drainage of Shallow Homogeneous Soil," Proceedings, Soil Science Society of America, Vol. 23, No. 4, July-August, 1959, pp. 260-263.
6. Brandt, A., Bresler, E., Diner, N., Ben-Asher, I., and Heller, J. "Infiltration from a Trickle Source: I. Mathematical Models." Soil Science Society of America Proceedings, Vol. 35, 1971, pp. 675-682.
7. Bresler, E., Heller, J., Diner, N., Ben-Acher, I., Brandt, A., and Goldberg, D., "Infiltration from a Trickle Source: II. Experimental Data and Theoretical Predictions," Soil Science Society of America Proceedings, Vol. 35, 1971, pp. 683-689.
8. Brooks, R. H., and Corey, A. T., "Hydraulic Properties of Porous Media," Hydrology Paper No. 3., Colorado State University, Fort Collins, Colorado, 1964, 27 p.
9. Brooks, R. H., and Corey, A. T., "Properties of Porous Media Affecting Fluid Flow," Journal of the Irrigation and Drainage Division, ASCE, Vol. 92, No. IR2, 1966, pp. 61-88.
10. Brutsaert, Wilfried, "The Adaptability of an Exact Solution to Horizontal Infiltration," Water Resources Research, Vol. 4, 1968, pp. 785-789.

11. Brutsaert, Willem F., "A Functional Iteration Technique for Solving the Richards Equation Applied to Two-Dimensional Infiltration Problems," Water Resources Research, Vol. 7, 1971, pp. 1583-1596.
12. Brutsaert, Willem F., Breitenback, E. Allen, and Sunada, Daniel K., "Computer Analysis of Free Surface Well Flow," American Society of Civil Engineers, Journal of the Irrigation and Drainage Division, Vol. 97, No. IRI, 1971, pp. 405-420.
13. Buckingham, Edgar., "Studies on the Movement of Soil Moisture," United States Department of Agriculture, Bureau of Soils, Bulletin No. 38, 1907, 61 p.
14. Burdine, N. T., "Relative Permeability Calculations from Pore Size Distribution Data," Transactions, American Institute of Mining and Metallurgical Engineers, Vol. 198, 1953, pp. 71-78.
15. Burejev, L. N., and Burejeva, Z. M., "Some Numerical Methods for Solving Problems of Non-Steady Seepage in Non-Homogeneous Anisotropic Soils, pp. 500-503, In P. E. Ritjetma, and H. Wassink (ed.) Water in the Unsaturated Zone, Proceedings of the Wageningen Symposium, UNESCO.
16. Childs, E. C., An Introduction to the Physical Basis of Soil Water Phenomena, John Wiley and Sons., Ltd., London, 1969, 493 p.
17. Childs, E. C. and Collis-George, N., "The Permeability of Porous Materials," Proceedings, Royal Society of London, 201A, 1950, pp. 392-405.
18. Cooley, Richard L., "A Finite Difference Method for Unsteady Flow in Variably Saturated Porous Media: Application to a Single Pumping Well," Water Resources Research, Vol. 7, 1971, pp. 1607-1625.
19. Darcy, H., Les Fontaines Publiques de la Ville de Dijon, Dalmont, Paris, 1956.
20. Day, Paul R., and Luthin, James N., "A Numerical Solution of the Differential Equation of Flow for a Vertical Drainage Problem," Soil Science Society of America Proceedings, Vol. 20, 1956, pp. 443-447.
21. Douglas, Jim Jr., "A Survey of Numerical Methods for Parabolic Differential Equations," pp. 1-54, In Franz, L., Alt. (ed.), Advance in Computers, Vol. 2, Academic Press, New York, 1961, 434 p.

22. Fok, Yu-Si., "A Comparison of the Green-Ampt and Philip Two Term Infiltration Equations," Journal of Irrigation and Drainage Division, Proceedings of the American Society of Civil Engineers Vol. 93, 1975, pp. 139-141.
23. Forsythe, George E., and Wasaow, Wolfgang R., Finite Difference Methods for Partial Differential Equations, John Wiley and Sons, Inc., New York, 1960, 444 p.
24. Freeze, R. Allan, "The Mechanics of Natural Ground Water Recharge and Discharge, I. One Dimensional, Vertical, Unsteady Flow Above a Recharging or Discharging Groundwater Flow System," Water Resources Research, Vol. 5, 1969, pp. 153-171.
25. Freeze, R. Allan, "Influence of the Unsaturated Flow Domain on Seepage Through Earth Dams," Water Resources Research, Vol. 7, 1971, pp. 929-941.
26. Freeze, R. Allan, and Witherspoon, P. A., "Theoretical Analysis of Regional Groundwater Flow: I. Analytical and Numerical Model," Water Resources Research, Vol. 2, 1966, pp. 641-656.
27. Gardner, W. R., "Some Steady-State Solutions of the Unsaturated Moisture Flow Equation with Application to Evaporation From a Water Table," Soil Science, Vol. 85, 1958, pp. 228-232.
28. Gardner, W. R., and Mayhugh, M. S., "Solutions and Tests of the Diffusion Equation for the Movement of Water in Soil," Proceedings of Soil Science Society of America, Vol. 22, No. 2, 1958, pp. 197-201.
29. Green, W. H., and Ampt., G. A., "Studies on Soil Physics, 1. The Flow of Air and Water Through Soils," Journal of Agriculture Science, Vol. 4, No. 1, 1911, pp. 1-24.
30. Green, Don W., Dabiri, Hassan, and Weinang, Charles F., "Numerical Modeling of Unsaturated Ground Water Flow and Comparison of the Model with Field Experiment," Water Resources Research, Vol. 6, 1970, pp. 862-874.
31. Hall, Warren A., "An Analytical Derivation of the Darcy Equation," Transactions, American Geophysical Union, Vol. 37, No. 2, 1956, pp. 185-188.
32. Hanks, R. J., and Bowers, S. A., "Numerical Solution of Moisture Flow Equation for Infiltration Into Layered Soils," Soil Science Society of America Proceedings, Vol. 26, 1962, pp. 530-534.
33. Hanks, R. J., Klute, A., and Bresler, E., "A Numerical Method for Estimating Infiltration, Redistribution, Drainage and Evaporation of Water from Soil," Water Resources Research, Vol. 5, 1969, pp. 1064-1069.

34. Hornberger, George M., Ebert, Janet, and Remson, Irwin, "Numerical Solution of the Boussinesq Equation for Aquifer-Stream Interaction," Water Resources Research, Vol. 6, 1970, pp. 601-608.
35. Hornberger, George M., Remson, Irwin and Fungarolli, A. A., "Numeric Studies of a Composite Soil Moisture Groundwater System," Water Resources Research, Vol. 5, 1969, pp. 797-802.
36. Horton, R. E., "An Approach Towards a Physical Interpretation of Infiltration Capacity," Soil Science Society of America Proceedings, Vol. 5, 1940, pp. 399-417.
37. Hubbert, M. K., "Darcy's Law and the Field Equations of the Flow of Underground Fluids," Transactions, American Institute of Mining, Metallurgical and Petroleum Engineers, Vol. 207, Petroleum Branch, 1956, pp. 222-239.
38. Ibrahim, Hassan Ali, and Brutsaert, Wilfried, "Intermittent Infiltration into Soils with Hysteresis," American Society of Civil Engineers, Journal of the Hydraulic Division, Vol. 94, No. HY1, 1968, pp. 113-137.
39. Irmay, S., "On the Hydraulic Conductivity of Unsaturated Soils," Transactions, American Geophysical Union, Vol. 35, 1954, pp. 463-467.
40. Isherwood, J. D., "Water-table Recession in Tile Drained Land," Journal of Geophysical Research, Vol. 64, 1959, pp. 795-804.
41. Jeppson, Roland W., "Personal Communications and a Computer File Copy," Utah Water Research Laboratory, Utah State University, Logan, Utah, 1975.
42. Jeppson, Roland W., "Transient Flow of Water From Infiltrimeters-Formulation of Mathematical Model and Preliminary Numerical Solutions and Analyses of Results," Report No. PRWG-59c-2, Utah Water Research Laboratory, Utah State University, Logan, Utah, 1970, 50 p.
43. Jeppson, Roland W., "Limitations of Some Finite Difference Methods in Solving the Strongly Nonlinear Equation of Unsaturated Flow in Soils," Report No. PRWG-59-c-8, Utah Water Research Laboratory, Utah State University, Logan, Utah, 1972, 50 p.
44. Jeppson, Roland W., "Axisymmetric Infiltration in Soils, I. Numerical Techniques for Solution," Journal of Hydrology, Vol. 23, 1974, pp. 111-130.
45. Jeppson, Roland W., "Axisymmetric Infiltration in Soils, II. Summary of Infiltration Characteristics Related to Problem Specifications," Journal of Hydrology, Vol. 23, 1974, pp. 191-202.

46. Jeppson, Roland W., et al., "Use of Axisymmetric Infiltration Model and Field Data to Determine Hydraulic Properties of Soils," Water Resource Research, Vol. II, No. 2, February, 1975, pp. 127-138.
47. Jeppson, Roland W., and Nelson, R. William, "Inverse Formulation and Finite Difference Solution to Partially Saturated Seepage From Canals," Soil Science Society of America Proceedings, Vol. 34, 1970, pp. 9-14.
48. Jeppson, Roland W., and Schreiber, David L., "Solution of a Two-Dimensional, Steady-State Watershed Flow System, Part I. Description of Mathematical Model," Transactions of the ASAE, Vol. 15, No. 13, 1972, pp. 457-470.
49. King, L. G., "Description of Soil Characteristics for Partially Saturated Flow," Soil Science Society of America Proceedings, Vol. 29, 1965, pp. 359-362.
50. Kirkham, Don, and Gaskell, R. E., "The Falling Water Table in Tile and Ditch Drainage," Soil Science Society of America Proceedings, Vol. 15, 1950, pp. 37-42.
51. Klute, A., "A Numerical Method for Solving the Flow Equations for Water in Unsaturated Materials," Soil Science, Vol. 73, 1952, pp. 105-116.
52. Klute, A., "Laboratory Measurement of Hydraulic Conductivity of Unsaturated Soil," In C. A. Black, et al., (ed.) Methods of Soil Analysis, Part 1, Agronomy, Vol. 9, 1973, pp. 253-261.
53. Klute, A., Whisler, F. D., and Scott, E. J., "Numerical Solution of the Nonlinear Diffusion Equation for Water Flow in a Horizontal Soil Column of Finite Length," Soil Science Society of America Proceedings, Vol. 29, 1965, pp. 353-358.
54. Kobayashi, H., "A Theoretical Analysis and Numerical Solutions of Unsaturated Flow in Soils," pp. 429-439, In P. E. Rijtema, and H. Wassink (ed.), Water in the Unsaturated Zone, Proceedings of the Wageningen Symposium, UNESCO, Paris, France, 1966.
55. Kostiaikov, A. N., "On the Dynamics of the Coefficient of Water Percolation in Soils and on the Necessity for Studying it from a Dynamic Point of View for Purposes of Amelioration," Transactions of the Sixth Committee International Society of Soil Science, Russian, Part A., 1932, pp. 17-21.
56. Liakopoulos, A. C., "Theoretical Solution of the Unsteady Unsaturated Flow Problems in Soils," International Association of Science Hydrologic Bulletin, Vol. 10, 1965, pp. 5-39.

57. Lin, Chang L., "Digital Simulation of the Boussinesq Equation for a Water Table Aquifer," Water Resources Research, Vol. 8, 1972, pp. 691-698.
58. Lin, Chang L., "Digital Simulation of an Outwash Aquifer," Ground Water, Vol. 11, No. 2, 1973, pp. 38-43.
59. Luthin, James N., and Day, Paul R., "Lateral Flow Above a Sloping Water Table," Soil Science Society of America Proceedings, Vol. 19, 1955, pp. 406-410.
60. Luthin, James N., and Gaskell, R. E., "Numerical Solutions for Tile Drainage of Layered Soils," Transactions, American Geophysical Union, Vol. 31, No. 4, 1950, pp. 595-602.
61. Luthin, James N., and Scott, V. H., "Numerical Analysis of Flow Through Aquifers Towards Wells," Agricultural Engineering, Vol. 33, pp. 279-282.
62. Luthin, James N., and Taylor, G. S., "Computer Solutions for Drainage of Sloping Land," American Society of Agricultural Engineers, Transactions, Vol. 9, No. 4, 1966, pp. 546-549.
63. Millington, R. J., and Quirk, M. P., "Permeability of Porous Solids," Transactions Faraday Society, Vol. 57, 1961, pp. 1200-1209.
64. Millington, R. J. and Quirk, J. P., "Formation Factor and Permeability Equations," Nature, Vol. 202, No. 4928, 1964, pp. 143-145.
65. Moody, William T., "Nonlinear Differential Equation of Drain Spacing," American Society of Civil Engineers, Journal of Irrigation and Drainage Division, Vol. 92, No. IR2, 1966, pp. 1-9.
66. Moore, R. E., "Water Conduction from Shallow Water Tables," Hilgardia, Vol. 12, 1939, pp. 383-426.
67. Muskat, M., The Flow of Homogeneous Fluids Through Porous Media, McGraw-Hill Book Company, Inc., New York, 1937, 763 p.
68. Nelson, R. W., "Steady Darcian Transport of Fluids in Heterogeneous Partially Saturated Porous Media, Part I. Mathematical and Numerical Formulation," Atomic Energy Commission, Research and Development Report No. HW-72335 Pt. 1, Hanford Atomic Products Operation, Richland, Washington, 1962.
69. Olsen, H. W., "Deviations from Darcy's Law in Saturated Clays," Soil Science Society of America Proceedings, Vol. 29, No. 2, 1965, pp. 135-140.

70. Olsen, H. W., "Darcy's Law in Saturated Kaolinite," Water Resources Research, Vol. 2, No. 2, 1966, pp. 287-295.
71. Philip, J. R., "Numerical Solution of Equations of the Diffusion Type with Diffusivity Concentration-Dependent," Transactions Faraday Society, Vol. 51, 1955, pp. 885-892.
72. Philip, J. R., "The Theory of Infiltration: 1. The Infiltration Equation and Its Solution," Soil Science, Vol. 83, No. 5, 1957, pp. 345-357.
73. Philip, J. R., "Discussion to Session IIa," Proceedings UNESCO-Netherlands Symposium, "Water in the Unsaturated Zone," Wageningen, The Netherlands, 1966.
74. Philip, J. R., Theory of Infiltration, in Advances in Agronomy, Academic Press, New York, 1968.
75. Philip, J. R., "Steady Infiltration from Buried Point Sources and Spherical Cavities," Water Resources Research, Vol. 4, No. 5, 1968, pp. 1039-1047.
76. Philip, J. R., "Theory of Infiltration," pp. 215-295, In Ven Te Chow (ed.) Advance in Hydroscience, Academic Press, New York, Volume 5, 1969.
77. Philip, J. R., "Steady Infiltration from Buried, Surface and Perched Point and Line Sources in Heterogeneous Soils: 1. Analysis," Proceedings of Soil Science Society of America, Vol. 36, 1972, pp. 268-273.
78. Raats, P. A. C., "Steady Infiltration from Point Sources, Cavities and Basins," Soil Science Society of America, Proceedings, Vol. 35, 1971, pp. 689-694.
79. Reisenauer, A. E., "Methods for Solving Problems of Multi-Dimensional, Partially Saturated Steady Flow in Soils," Journal of Geophysical Research, Vol. 68, 1963, pp. 5725-5733.
80. Reisenauer, A. E., Nelson, R. W., and Knudsen, C. N., "Steady Darcian Transport of Fluids in Heterogeneous Partially Saturated Porous Media, Part 2. The Computer Program," Atomic Energy Commission, Research and Development Report No. HW-72335, Part 2., Hanford Atomic Products Operation, Richland, Washington, 1963.
81. Remson, Irwin, Drake, Ronald L., McNeary, Samuel S., and Wall, Edward M., "Vertical Drainage of an Unsaturated Soil," American Society of Civil Engineers, Journal Hydraulics Division, Vol. 91, No. HY1, 1965, pp. 55-74.

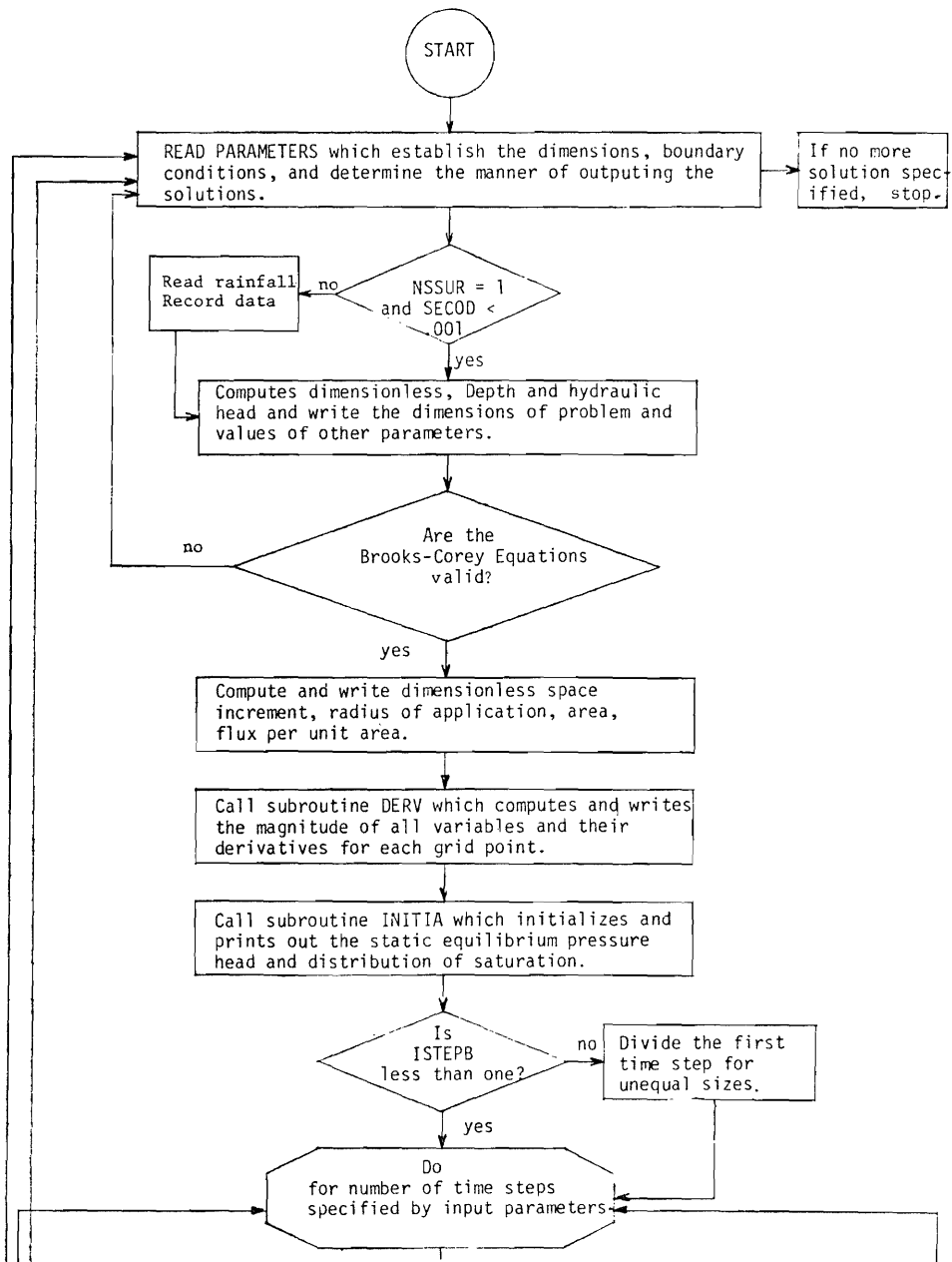
82. Remson, Irwin, Fungareli, A. Alexander, and Hornberger, George M., "Numerical Analysis of Soil Moisture Systems," American Society of Civil Engineers, Journal of Irrigation and Drainage Division, Vol. 93, No. IR3, 1967, pp. 153-166.
83. Remson, Irwin, Hornberger, George M., and Molz, Fred J., "Numerical Methods in Subsurface Hydrology," Wiley-Interscience, John Wiley and Sons, Inc., New York, 1971, 389 p.
84. Remson, Irwin, Resnicoff, Morton, and Scott, B. B., "Numerical Studies of Drainage of Unsaturated Soils," American Society of Agricultural Engineers, Transactions, Vol. 10, No. 3., 1967, pp. 388-390.
85. Richards, L. A., "Capillary Conduction of Liquids Through Porous Mediums," Physics, Vol. 1, 1931, pp. 318-333.
86. Richtmyer, Robert D., Difference Methods for Initial-Value Problems, Interscience Publishers, Inc., New York, 1957, p. 238.
87. Rubin, J., "Numerical Analysis of Poned Rainfall Infiltration," Symposium on Water in the Unsaturated Zone, UNESCO, Paris, France, 1966.
88. Rubin, J., "Numerical Method for Analyzing Hysteresis-Affected, Post-Infiltration Redistribution of Soil Moisture," Soil Science Society of America Proceedings, Vol. 31, 1967, pp. 13-20.
89. Rubin, J., "Theoretical Analysis of Two-Dimensional, Transient Flow of Water in Unsaturated and Partly Saturated Soils," Soil Science Society of America Proceedings, Vol. 32, 1968, pp. 607-615.
90. Samadi, S. A., "The Effect of Heterogeneity Due to Variation of Soil Parameters on the Solution of the Flow Equation," M. S. Thesis, Utah State University, Logan, Utah, 1975, 123 p.
91. Scott, V. H. and Corey, A. T., "Pressure Distribution During Steady Flow in Unsaturated Sands," Soil Science of America, Proceedings, Vol. 25, No. 4, 1961, pp. 270-274.
92. Scott, E. J. and Hanks, R. J., "Solution of the One Dimensional Diffusion Equation for Exponential and Linear Diffusivity Functions by Power Series Applied to Moisture Flow in Soils," Soil Science, Vol. 94, No. 5, 1962, pp. 314-322.
93. Scott, E. J., Hanks, R. J., and Peters, D. B., and Klute, A., "Power Series Solution of the One-Dimensional Diffusion Equations for Exponential and Linear Diffusivity Function," USDA, ARS, 41-64, September, 1962.

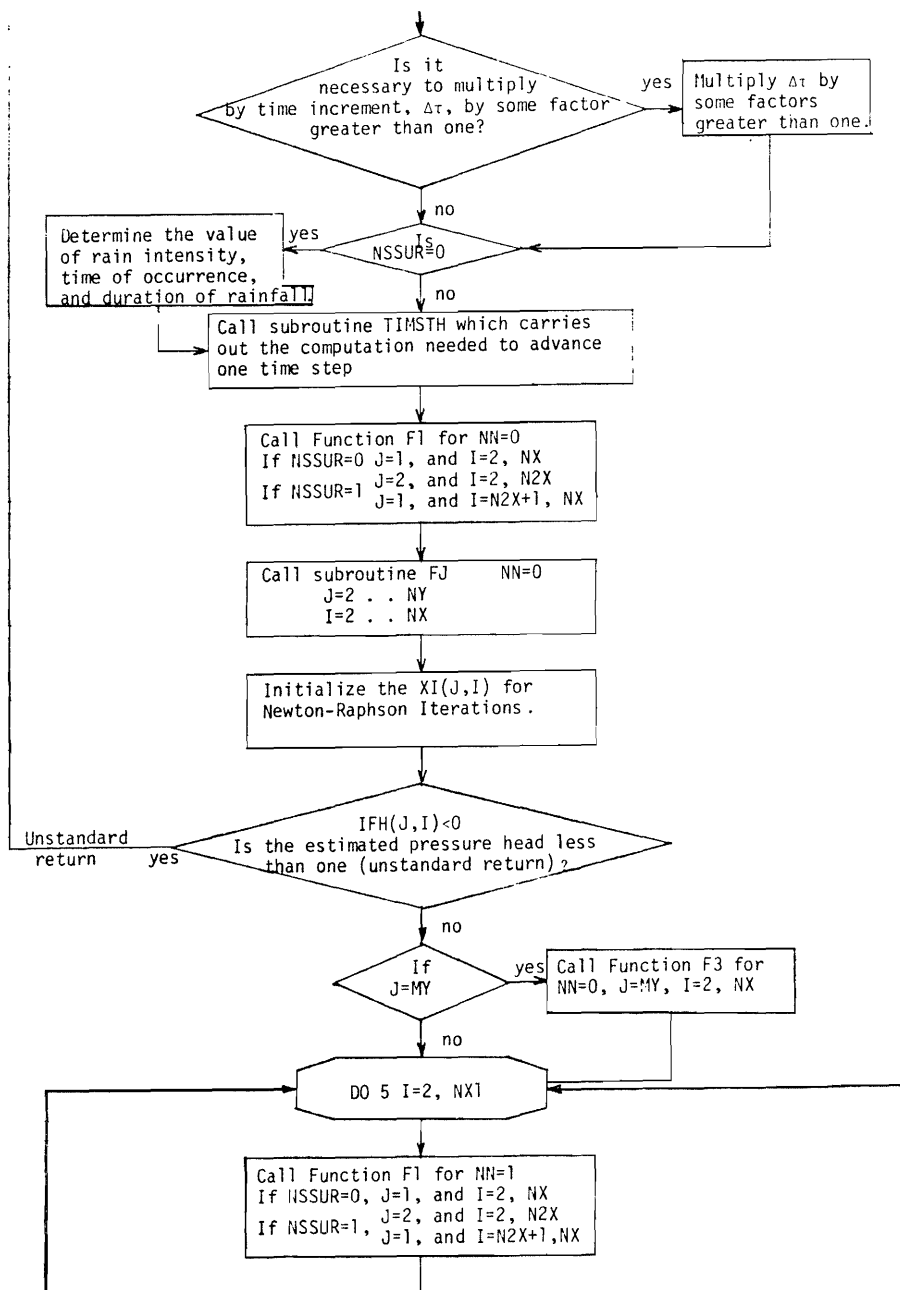
94. Selim, H. M., and Kirkham, Don, "Unsteady Two-Dimensional Flow of Water in Unsaturated Soils Above an Impervious Barrier," Soil Science Society of America, Proceedings, Vol. 37, 1973, pp. 389-495.
95. Sewell, John I., and van Schilfgaarde, Jan., "Digital Computer Solutions of Partially Saturated, Steady State Drainage and Subirrigation Problems," American Society of Agricultural Engineers, Transactions, Vol. 6, No. 4, 1963, pp. 292-296.
96. Staple, W. J., "Infiltration and Redistribution of Water in Vertical Columns of Loam Soil," Soil Science Society of America Proceedings, Vol. 30, 1966, pp. 553-558.
97. Swartzendruber, D., "Modification of Darcy's Law for the Flow of Water in Soils," Soil Science, Vol. 93, January-June, 1962, pp. 23-29.
98. Swartzendruber, D., "Non-Darcy Flow Behavior in Liquid Saturated Porous Media," Journal of Geophysical Research, Vol. 67, No. 13, December, 1962, pp. 5205-5213.
99. Swartzendruber, Dale, "Non-Darcy Behavior and the Flow of Water in Unsaturated Soil," Soil Science Society of America, Proceedings, Vol. 27, 1963, pp. 491-495.
100. Su, Charles, Brooks, R. H., "Hydraulic Functions of Soils From Physical Experiments and Their Applications," Report No. WRR1-41, Oregon State University, Corvallis, Oregon, 1976, p. 130.
101. Taylor, George S., and Luthin, J. N., "The Use of Electronic Computers to Solve Subsurface Drainage Problems," Hilgardia, Vol. 34, 1963, pp. 543-558.
102. Taylor, George S., and Luthin, James N., "Computer Methods for Transient Analysis of Water Table Aquifers," Water Resources Research, Vol. 5, 1969, pp. 144-152.
103. Thomas, Adrian W., Kruse, Gordon E., Duke, Harold R., "Steady Infiltration from Line Sources Buried in Soil," Transactions of American Society of Agricultural Engineers, Vol. 17, No. 1, 1974, pp. 125-128.
104. Todsén, Marius, "On the Solution of Transient Free Surface Flow Problems in Porous Media by Finite Difference Methods," Journal of Hydrology, Vol. 12, No. 3, 1971, pp. 177-210.
105. van Bavel, C. H. M., "The Three-Phase Domain in Hydrology," p. 23-30, In P. E. Rijtema, and H. Wassink (ed.) Water in the Unsaturated Zone, Proceedings of the Wageningen Symposium, UNESCO, Paris, France, 1969.

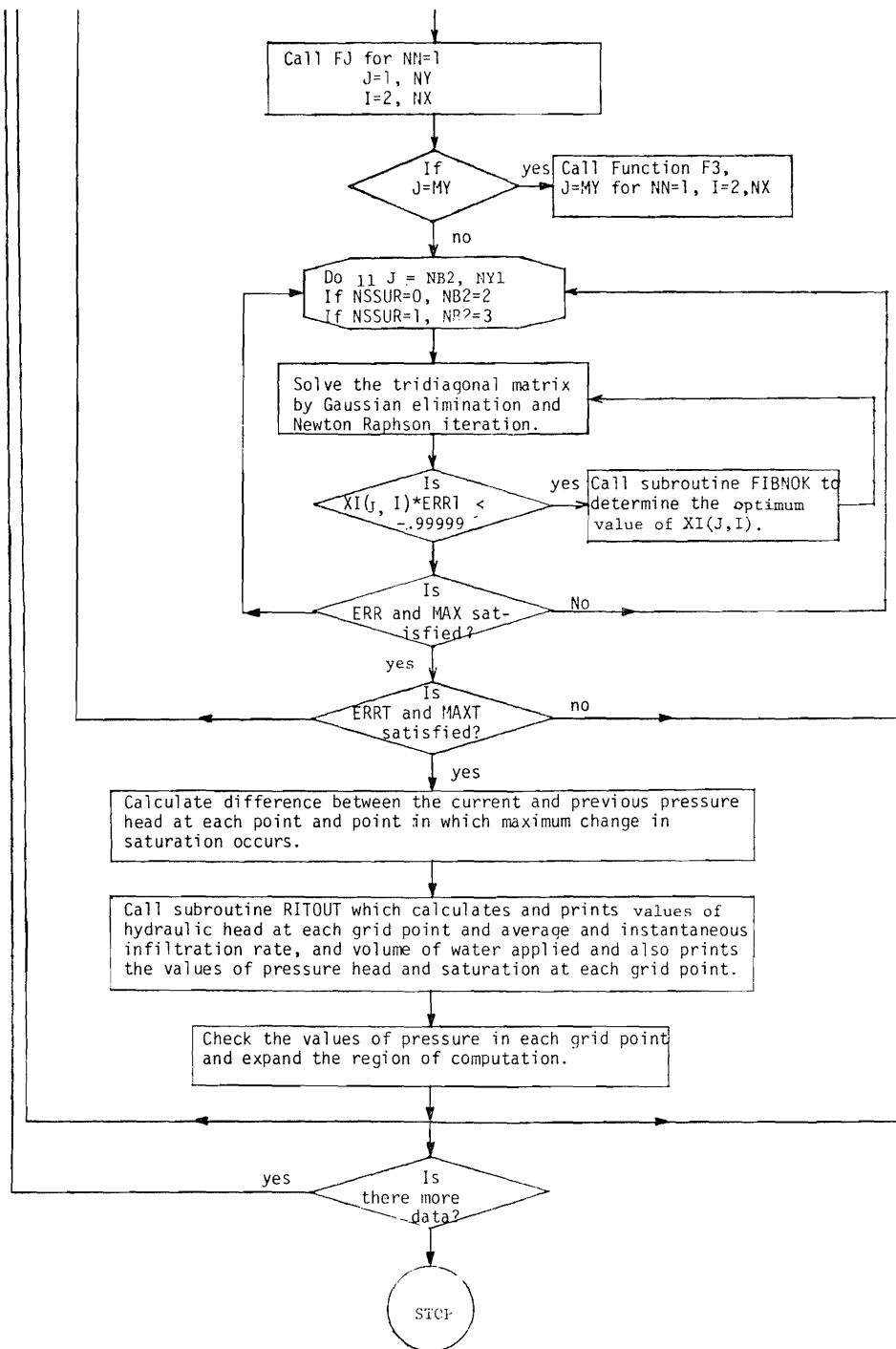
106. van der Ploeg, R. R. and Benecke, P., "Unsteady-Unsaturated nondimensional Moisture Flow in Soil: A Computer Simulation Program," Proceedings of Soil Science of America, Vol. 38, No. 6, 1974, pp. 881-885.
107. Wang, Flora Chu, Hassan, Nabil A., and Franzini, Joseph B., "A Method of Analyzing Unsteady Unsaturated Flow in Soils," Journal of Geophysical Research, Vol. 69, 1964, pp. 2569-2577.
108. Warrick, A. W., "Time-Dependent Linearized Infiltration, I. Point Sources," Soil Science Society of America Proceedings, Vol. 38, 1974, pp. 383-386.
109. Watson, K. K. and Whisler, F. D., "Numerical Analysis of Drainage of a Heterogeneous Porous Medium," Soil Science Society of America Proceedings, Vol. 36, 1972, pp. 251-256.
110. Wei, Chi-Yuan, and Jeppson, R. W., "Finite Difference Solutions of Axisymmetric Infiltration Through Partially Saturated Porous Media," Report No. PRWG-59c-6, Utah Water Research Laboratory, Utah State University, Logan, Utah 1971, 64 p.
111. Wesseling, J. and Wit, K. E., "An Infiltration Method for the Determination of Capillary Conductivity of Undisturbed Soil Cores, p. 223-234, In P. E. Rijtema, and H. Wassink (ed.) Water in the Unsaturated Zone, Proceedings of the Wageningen Symposium UNESCO, Paris, France, 1966.
112. Whisler, F. D., and Bower, H., "Comparison of Methods for Calculating Vertical Drainage and Infiltration for Soils," Journal of Hydrology, Vol. 10, 1970, pp. 1-19.
113. Whisler, F. D., and Klute, A., "The Numerical Analysis of Infiltration Considering Hysteresis, Into a Vertical Soil Column at Equilibrium Under Gravity," Soil Science Society of America Proceedings, Vol. 29, 1965, pp. 489-494.
114. Whisler, F. D., and Klute, A., "Analysis of Infiltration into Stratified Soil Columns, pp. 451-470, In P. E. Rijtema, and H. Wassink (ed.) Water in the Unsaturated Zone, Proceedings of the Wageningen Symposium, UNESCO, Paris, France, 1966.
115. Whisler, F. D., and Klute, A., "Rainfall Infiltration Into a Vertical Soil Column," American Society of Agricultural Engineers, Transactions, Vol. 10, No. 3, 1967, pp. 391-395.
116. Whisler, Frank D., and Watson, Keith K., "Analysis of Infiltration into Draining Porous Media," American Society of Civil Engineers, Journal of the Irrigation and Drainage Division, Vol. 95, No. IR4, 1969, pp. 481-491.

117. Wilde, D. J., and Beightler, C. S., Foundations of Optimization, Prentice-Hall, London, 1967, 480 p.
118. Wooding, R. A., "Steady Infiltration from a Circular Pond," Water Resources Research, Vol. 4, 1968, pp. 1259-1273.
119. Youngs, E. G., "Moisture Profiles During Vertical Infiltration," Soil Science, Vol. 84, 1957, pp. 283-290.

Appendix I
Flow Chart







Appendix IIFortran Program Listing Typical Input Data and Sample Solutions

```

C *****
C * A PROGRAM TO SOLVE THE PROBLEM OF TRANSIENT THREE- *
C * DIMENSIONAL AXISYMMETRIC UNSATURATED FLOW THROUGH *
C ***** HETEROGENEOUS SOILS *****
C *****
C
C N2X = NUMBER OF GRID POINTS IN THE RADIAL DIRECTION TO OUTER EDGE OF
C CIRCLE RA OVER WHICH WATER IS APPLIED.
C MX = NUMBER OF GRID POINTS IN RADIAL DIRECTION TO OUTER RADIUS OF
C PROBLEM.
C MY = NUMBER OF GRID POINTS IN AXIAL DIRECTION BETWEEN TOP SURFACE
C AND BOTTOM OF PROBLEM.
C NT = NUMBER OF TIME STEPS THROUGH WHICH COMPUTATION ARE TO BE
C COMPLETED.
C HI = VALUE OF THE STATIC EQUILIBRIUM INITIAL HYDRAULIC HEAD
C (MINUS MUST BE PUNCHED INTO CARD).
C DEPTH = THE DEPTH BETWEEN TOP SURFACE AND BOTTOM OF THE PROBLEM.
C DELT = SIZE OF DIMENSIONLESS TIME STEP INCREMENTS WHICH ARE TO
C BE USED IN OBTAINING THE SOLUTION.
C SL = THE CHARACTERISTIC LENGTH USED TO NONDIMENSIONALIZE ALL LENGTH
C PARAMETERS OF THE PROBLEM.
C SSUR = IF THE UPPER SURFACE BOUNDARY CONDITION IS TO BE USED WHICH
C SPECIFIES THE APPLICATION RATE, SSUR MUST BE GIVEN A VALUE OF ZERO.
C IF THE CONDITION SPECIFYING THE SURFACE SATURATION IS TO BE USED SSUR
C EQUALS THE DECIMAL SURFACE SATURATION.
C SECOD = AN INDEX WHEN ITS VALUE IS GREATER THAN .001 THE RAIN=FALL
C RECORD WILL BE READ.
C IMAXJ = THE NUMBER OF GRID POINT IN VERTICAL DIRECTION WHICH THE
C MAXIMUM CHANGE IN SATURATION IS OCCURRED.
C TIM1 = MAGNITUDE OF DIMENSIONLESS TIME IN PREVIOUS TIME STEP USED TO
C COMPUTE THE INSTANTANEOUS INFILTRATION RATE.
C WATCOT = MAGNITUDE OF WATER CONTENT IN PREVIOUS DIMENSIONLESS TIME
C STEP USED TO COMPUTE THE INSTANTANEOUS INFILTRATION RATE.
C NFAC = NUMBER OF FACTORS TFAC(I) USED TO INCREASE THE VALUE
C DIMENSIONLESS TIME INCREMENT DELT.
C TFAC(1) = MAGNITUDES OF THE FACTORS USED TO BE MULTIPLIED BY DELT
C A SPECIFIED TIME STEP IMFAC(I).
C IMFAC(1) = IN THIS TIME STEP THE DIMENSIONLESS TIME INCREMENT DELT
C MULTIPLIED BY THE TFAC(I).
C NSSUR = AN INDEX WHICH IS USED TO CHANGE THE CONDITION OF THE TOP
C BOUNDARY CUNDITION 2=3. WHEN NSSUR=0 UPPER BOUNDARY CONDITION
C APPLICATION RATE IS SPECIFIED, IN OTHER CASE (NASSUR=1) SURFACE
C SATURATION IS SPECIFIED.
C KTIM2 = COUNTER INDEX FOR THE MUBER OF RAIN FALL RATES AT DIFFERENT
C DIMENSILESS TIMES, AND SUMS UP TO KTIM2 = NRAIN
C KKT1 = COUNTER INDEX USED IN TO CHANGE VALUE OF IMFAC(I), AND SUMS
C UP TO KKT1 = NFAC
C NSKIP = AN INDEX WHEN ITS VALUE IS ONE THE SOLUTION TO OTHER PROBLEMS
C WILL BE PRINTED ON ANOTHER PAGE.
C NRAIN = NUMBER OF RAIN FALL RECORDS
C QK(I) = INTENSITY OF RAIN FALL IN INCHES PER HOUR. WHEN NSWIT(I)=1,
C QK(I) IS EQUALS TO THE DECIMAL SURFACE SATURATION.
C TIMH(1) = DIMENSLESS TIME WHICH IN THAT TIME THE INTENSITY OF RAIN
C IS QK(I).
C NS*IT(1) = AN INDEX SIMILAR TO NSSUR WHICH CHANGES THE CONDITION OF
C TOP BOUNDARY CONDITION 2=3. WHEN ITS VALUE IS ZERO THE CONDITION
C OF TOP SURFACE IS SPECIFIED APPLICATION RATE AND WHEN IT VALUE IS
C EQUAL TO ONE THE SURFACE SATURATION IS SPECIFIED AT THAT PARTICULAR
C DIMENSIONLESS TIME.

```

```

C
C VK = FORTWAN VARIABLE USED TO SHOW THE RAINFALL RATE OR APPLICATION
C FLUX WHICH IS USED ONLY WHEN NSSUR=0. IT HAS A DIMENSIONS OF INCHES
C PER HOUR WHEN VK = QK(I) AND IN DIMENSIONLESS FORM VK = QK(I)/AK IN
C WHICH AK IS THE SATURATED HYDRAULIC CONDUCTIVITY ON THE SOIL SURFACE
C UNITS OF LENGTH PER TIME.
C HEIGT = DIMENSIONLESS DEPTH BETWEEN TOP SURFACE AND BOTTOM OF THE
C PROBLEM (DEPTH/SL)
C HIT = DIMENSIONLESS STATATIC EQUILIBRIUM HYDRAULIC HEAD (HI/SL)
C AK = SATURATED HYDRAULIC CONDUCTIVITY ON THE SOIL SURFACE USED TO
C NONDIMENSIONALIZE THE APPLICATION RATE, OR RAIN FALL RATE.
C EXPAND = A PARAMETER TO EXPAND THE NUMBER OF GRID POINTS AT WHICH
C VALUES ARE COMPUTED AT NEW TIME STEPS. WHEN H(J,I) CHANGES FROM THE
C INITIAL CONDITIONS BY AN AMOUNT GREATER THAN EXPAND THE NUMBER OF
C GRID POINTS IN EITHER THE RADIAL AND AXIAL DIRECTIONS IS EXPANDED.
C ERR = A PARAMETER USED TO TERMINATE THE NEWTON-RELAXATIUN METHOD
C ITERATION. THE INDIVIDUAL LINE ITERATIONS ARE TERMINATED WHEN THE
C ABSOLUTE SUM OF CHANGE BETWEEN CONSECUTIVE ITERATION IS LESS THAN
C ERR.
C ERRT = A PARAMETER USED TO TERMINATE NEWTON-RELAXATION ITERATION IN
C EACH TIME PLANE ITERATION WHEN THE ABSOLUTE SUM OF CHANGE BETWEEN
C CONSECUTIVE ITERATION IS LESS THAN ERRT (ERRT=100*ERR).
C SATMAX = MAXIMUM SATURATION WHICH CAN BE ATTAINED IN THE SOIL
C SURFACE WHICH IS USED TO TRANSFER TOP BOUNDARY CONDITION FROM
C SPECIFIED APPLICATION RATE TO SPECIFIED SATURATION.
C OMEGA = MAXIMUM SATURATION THE SOIL CAN ATTAIN IN THE BOTTOM
C BOUNDARY DRAIN LAYER AND MOISTURE BEGINS TO BUILD UP IN THE SOIL
C PROFILE. WHEN OMEGA IS LESS THAN COMPUTED SATURATION AT THE BOTTOM
C BOUNDARY H(MY,I)=BB(MY).
C NHITZ = NUMBER OF REGULAR TIME STEPS BETWEEN WHICH SOLUTIONS ARE
C PRINTED.
C NHSTAR = IF NHSTAR IS LESS THAN ZERO ONLY THE VALUES OF THE
C INDEPENDENT VARIABLE XI(J,I) WILL BE PRINTED A THE SPECIFIED TIME
C STEPS. IF NHSTAR=0 THE VALUE OF XI(J,I) THE SATURATION AND
C HYDRAULIC HEAD WILL BE PRINTED AT THE SPECIFIED TIME STEPS. IF
C NHSTAR IS GREATER THAN ZERO, VALUES OF XI(J,I) WILL NOT BE PRINTED,
C BUT VALUES OF SATURATION AND HYDRAULIC HEAD WILL BE PRINTED.
C MAX = MAXIMUM NEWTON-LINE ITERATIONS THAT WILL BE ALLOWED. THE
C NUMBER OF ITERATIONS ON ANY TIME PLANE WHICH WILL BE ALLOWED
C WILL BE ONE-HALF THIS MANY.
C MAXT = THE MAXIMUM NUMBER OF ITERATIONS ON ANY TIME PLANE THAT WILL
C BE ALLOWED MAXT=MAX/2.0
C ISTEPB = AN INDEX WHEN IT IS GREATER THAN ONE THE FIRST TIME STEP
C WILL BE SUBDIVIDED TO SOME UNEQUALL BUT SMALLER TIME STEPS.
C DELS = DIMENSIONLESS SPACE INCREMENT (DELS=HEIGT/MY=1).
C R = DIMENSILESS RADIUS OF CIRCLE OF APPLICATION RA (R=DELS*FLOAT
C (N2X-1)).
C AREAC = DIMENSIONLESS AREA OF CIRCLE OF APPLICATION AREAC=3.14*R*R
C G = APPLICATION RATE PER AREA OF THE CIRCLE OF APPLICATION.
C TIME = DIMENSIONLESS TIME.
C HO(J,I) = VALUES OF PRESSURE HEAD AT TIME = 0,0, HO(J,I)=H(J,I).
C HD(J,I) = DIFFERENCE BETWEEN PRESSURE HEAD AT PREVIOUS TIME STEP AND
C CURRENT TIME STEP. HO(J,I)-HO(J,I)=H(J,I)
C H(J,I) = VALUES OF PRESSURE HEAD AT ANY TIME.
C B(J,I) = VALUES OF HYDRAULIC HEAD AT ANY TIME.
C D(I) = VALUES OF SATURATION CALCULATED FROM BROOKS-COREY EQUATION.
C SATT = MAGNITUDE OF SATURATION ON THE CIRCULAR WATER APPLICATION
C AREA. WHEN SATT EQUALS OR GREATER THAN THE SATMAX THE SPECIFIED FLUX
C CONDITION WILL BE CHANGED TO SPECIFIED SATURATION(NSSUR=1). AND
C PRESSURE HEAD WILL BE CALCULATED FROM THE SSUR SPECIFIED.
C SI(I) = INITIAL SATURATION
C AVERAGE INFILTRATION RATE = WATCOT/TIME

```



```

108  FORMAT(' RADIUS OVER WHICH INFILTRATION OCCURS',F10.5,
      S'INFILTRATION FLUX=',F9.4,'DELS=',F8.3,'AREA=',F8.3)
7    TIME=0.0
    CALL DERV
    NX1=NX-1
    NY1=NY-1
    FY=NY1
    NX2=NX-2
    NY2=NY-2
    CALL INITIA
    FAC1=MEIGT=HIT
    DO 49 I=1, MX
    HO(1,I)=FAC1
49   HO(1,I)=HO(1,I)-H(1,I)
    DO 53 J=2, MY
    DO 53 I=1, MX
    IJK=1
    HO(J,I)=0.0
53   HO(J,I)=H(J,I)
    IF(NSSUR,EQ,1) GO TO 13
    DO 12 I=1, MX
    IJK=1
    FAC2=0.2 * HO(1,I) * VK
12   HO(1,I)=FAC2
13   DO 43 I=1, MX
    IJK=1
    FAC3=0.20* HO(1,I)
43   HO(2,I)=FAC3
    NT1=1
    IF(ISTEPB,LT,1) GO TO 17
    NT1=2
    I1=0
    DO 14 I=1, ISTEPB
14   I1=I1+I
    ARG1=I1
    IF(NSSUR,EQ,1) GO TO 27
    DELS2(1)=D(1)

    MX1=MX-1
    DO 71 I=2, NX1
    D(2)=HO(1,I)
    HO(1,I)=HO(1,I)
    D(3)=HO(2,I)
28   DELS2(1) = ARG1*D(1)
    XI1I=(HO(1,I)**ERR1-1.)/ERR1
    XI1IP=(HO(1,I+1)**ERR1-1.)/ERR1
    XI1IM=(HO(1,I-1)**ERR1-1.)/ERR1
    XI2I=(HO(2,I)**ERR1-1.)/ERR1
    ARG = F1(HO(1,I),XI(1,I),XI(1,I+1),XI(1,I-1),XI(2,I),0)+F1
    S(HO(1,I),XI(1,I),XI(1,I+1),XI(1,I-1),XI(2,I),1)
    DELS2(1)=D(1)
    IF (ARG,LT, 0.0) GO TO 29
    ISTEPB = ISTEPB +1
    ARG1 = ARG1 + FLOAT (ISTEPB)
    WRITE(6,255) ISTEPB,ARG,ARG1
255  FORMAT(' PRELIMINARY TIME STEPS HAVE BEEN INCREASED TO',I5,3E13.6)
    IF(ISTEPB,LT,50) GO TO 28
    IF (ISTEPB,EQ,50) STOP
29   HO(1,I)=D(2)
71   HO(2,I)=D(3)
27   ARG=0.0

```

```

DETT = DELT/ARG1
DO 15 I=1, ISTEPB
KK=I
22  ARG = ARG + FLOAT(I)
    FAC = ARG1/ARG
    DO 16 K=1, NY
16  DELS2(K) = FAC * DELS2(K)
    ARG1 = ARG
    TIME = TIME + DETT * FLOAT(I)
    CALL TIMSTH(810)
    CALL RITOUT(NHSTAR,KK)
19  NY2 = NY-2
    IF (H(NY2,2),GT,HO(NY2,MX)=EXPAND,OR,NY,EQ,MY) GO TO 18
    NY = NY+1
    GO TO 19
18  NY1 = NY-1
    NY2=NY-2
    FY=NY1
61  NX4=NX-4
    IF(H(1,NX4),GT,HO(1,MX)=EXPAND,OR,NX,EQ,MX) GO TO 81
    NX=NX+1
    GO TO 61
81  NX1=NX-1
15  NX2=NX-2
17  IF(NSSUR ,EQ, 1) GO TO 177
    VK=QK(1)/AK
177  DO 2 I=NT1,NT
    IJK=1
    IF(IMFAC(KKT1) ,NE, 1) GO TO 24
    DELT=DELT*FAC(KKT1)
    DO 661 JK=1,MY
661  DELS2(JK)=DESS*POR(JK)*AMBDA(JK)*SR1(JK)/(BB(JK)**AMBDA(JK)*DELT)
    KKT1=KKT1+1
24  IF(NSSUR,EQ,1) GO TO 23
    DO 567 KK=1,N2X
    SATT=SR(1)+SR1(1)*(BB(1)/H(1,KK))**AMBDA(1)
    IF(SATT ,GE, SATMAX) NSSUR=1
567  CONTINUE
    IF(NSSUR ,EQ, 0) GO TO 568
    SSUR=SATMAX*.05
    NB1=2
    NB2=3
    MB2=N2XP
    MB3=MB2+1
    DO 569 K=1,N2X
    H(1,K)=BB(1)/((SSUR=SR(1))/SR1(1))** (1./AMBDA(1))
569  XI(1,K)=(H(1,K)**ERR1-1.)/ERR1
    GO TO 23
568  IF(TIMH(KTIM2),GT,TIME,OR,KTIM2,EQ,NRAIN) GO TO 23
    KTIM2=KTIM2+1
    IF(NSWIT(KTIM2) ,EQ,0) GO TO 54
    IF(NSWIT(KTIM2)=1) ,EQ, NSWIT(KTIM2)) GO TO 56
    NSSUR = 1
    NB1=2
    NB2=3
    MB2=N2XP
    MB3=MB2+1
56  SSUR=QK(KTIM2)
    DO 566 K=1,N2X
    H(1,K)=BB(1)/((SSUR=SR(1))/SR1(1))** (1./AMBDA(1))
566  XI(1,K)=(H(1,K)**ERR1-1.)/ERR1

```

```

GO TO 23
54 IF(N8WIT(KTIM2=1) .EQ. N8WIT(KTIM2)) GO TO 55
N8SUR=0
NB1=1
NB2=2
NB3=N2XP
NB3=NB2+1
55 VK=QK(KTIM2)/AK
23 N8SR=0
NRR=MOD(I,NRIT2)
CALL TIMSTH(&I0)
TIME=TIME+DELT
IF(NRR.GT.0) GO TO 3
CALL RITOUT(NHSTAR,I)
3 NY2=NY-2
IF (H(NY2,2).GT.HO(NY2,MX)=EXPAND.OR,NY.EQ,MY) GO TO 4
NY=NY+1
GO TO 3
4 NY1=NY-1
NY2=NY-2
FY=NY1
5 NX4=NX-4
IF (H(1,NX4).GT.HO(1,MX)=EXPAND.OR,NX.EQ,MY) GO TO 6
NX=NX+1
GO TO 5
6 NX1=NX-1
NX2=NX-2
2 CONTINUE
NSKIP=1
GO TO 10
99 STOP
END

```

SUBROUTINE TIMSTH CARRIES OUT THE COMPUTATIONS NEEDED TO ADVANCE ONE TIME STEP.

```

SUBROUTINE TIMSTH(*)
COMMON M(32,32),HO(32,32),B(32,32),OM(32),D(32),DP(32),F(32),S1(32
$),VK8(33),AMBDA(32),DELS2(32),AMB32(32),AMB1(32),POR(32),8R(32),
$SR1(32),DVKS(32),DAMBDA(32),PAVK(32),B8(32),DPB(32),VK,MEIGT,AK
$,DEPTH,SL,DELT,DELS,MI,HIT,ERR,ERRT,ERR1,RRERR1,TIME,DES2,DELM,$SUR
$,OMEGA,WATCO1,TIM1,XI(32,32),XIM(32,32),XIO(32),MY1,NY,NY11,NY2,
$NHSR,MY,NSAT,NSSUR,NB1,NB2,MAX,HAXT,NX,NX1,NRX,N5,N6,JJ,JM,JP,M1,
$M2,IMAXJ,IMAXM,IMAX2,ITIME,IM,IP,DAMBK(32),DELS2(32),DCUB(32),
$DELS2(32),DCUB5(32),HD(32,32),Q,R,N2X,MX,MB2,MB3,IIJ,N2XP
RERR1=1./ERR1
LOGICAL NTURN
VVK=VK
NY1=NY11
NX=NX1
NY=NY1
IF(NX .EQ. MX) NNX=MX
IF(NY .EQ. MY) NNY=MY
DO 2 I=MB2,NX1
IIJ=I
IF(I .EQ. N2XP) VK=0.0

```

```

IP=I+1
IM=I-1
2 B(1,I)=F1(H(1,I),XI(1,I),XI(1,IP),XI(1,IM),XI(2,I),0)
DO 3 I=2,NX1
IIJ=I
IP=I+1
IM=I-1
DO 3 J=2,NY1
JJ=J
JM=J-1
JP=J+1
CALL FJ(H(J,I),XI(J,I),XI(JM,I),XI(JP,I),XI(J,IP),XI(J,IM),
$FF,0)
3 B(J,I)=FF
NBT=NB1
DO 26 I=2,NNX
IIJ=I
IF(N8SUR .GT. 0 .AND. I .EQ. N2XP) NB1=1
DO 31 J=NB1,NNY
JJ=J
ARG=H(J,I)
FAC=1.
IF(J .EQ. IMAXJ) GO TO 32
IF(J .LT. IMAXJ) GO TO 29
IF(J .GT. IMAX2) GO TO 166
FAC=1./I
IF(J .LT. 4) FAC=.1
H(J,I)=ARG-FAC*HD(J,I)
GO TO 13
29 IF(J .LT. IMAXM) GO TO 166
IF(J .EQ. IMAXM) GO TO 33
H(J,I)=ARG-.65*HD(J,I)
GO TO 13
33 FAC=.85
H(J,I)=ARG-FAC*HD(J,I)
GO TO 13
32 FAC=.25
IF(J .LT. 3) FAC=.15
H(J,I)=ARG-FAC*HD(J,I)
GO TO 13
166 H(J,I)=ARG=HD(J,I)
13 HD(J,I)=ARG
IF(H(J,I) .LT. 0.0) RETURN 1
XI(J,I)=(H(J,I)**ERR1-1.)/ERR1
31 XIM(J,I)=(ARG**ERR1-1.)/ERR1
26 CONTINUE
NB1=NBT
IF(NY .LT. MY) GO TO 15
DO 16 I=2,NX1
IIJ=I
IP=I+1
IM=I-1
16 B(MY,I)=F3(H(MY,I),XI(MY,I),XI(MY,IP),XI(MY,IM),XI(MY1,I),0)
15 NCOUNT=0
VK=VVK
4 SUMT=0.0
MNCT=0
NBB2=NB2
DO 5 I=2,NX1
IIJ=I
NTURN= .FALSE.

```

```

NY1=NY11
SATB=SR(MY)+SR1(MY)*(BB(MY)/H(MY,I))*AMBDA(MY)
IF(SATB .LT. OMEGA) GO TO 288
NY1=MY1
H(MY,I)=BB(MY)
XI(MY,I)=(H(MY,I)**ERR1-1.)/ERR1
NTURN=.TRUE.
288 IP=I+1
IM=I-1
NCT=0
6 IF(NSSUR .GT. 0 .AND. I .LT. N2XP) GO TO 8
IF(I .EQ. N2XP) VK=0.0
IF(H(1,I) .LT. BB(1)) H(1,I)=BB(1)
ARG=F1(H(1,I),XI(1,I),XI(1,IP),XI(1,IM),XI(2,I),1)
F(1)=ARG+B(1,I)
8 DO 9 J=2,NY1
JJ=J
JP=J+1
JM=J-1
CALL FJ(H(J,I),XI(J,I),XI(JM,I),XI(JP,I),XI(J,IP),XI(J,IM),
$FF,1)
9 F(J)=FF+B(J,I)
IF(NY .LT. MY) GO TO 10
IF(NTURN) GO TO 10
NY1=MY
ABG=F3(H(MY,I),XI(MY,I),XI(MY,IP),XI(MY,IM),XI(MY1,I),1)
F(MY)=ABG+B(MY,I)
10 IF(I .EQ. N2XP) NB2=2
DO 11 J=NB2,NY1
JJ=J
JM=J-1
ARG=DM(J)/D(JM)
F(J)=F(J)-ARG+F(JM)
11 D(J)=D(J)-ARG+DP(JM)
J=NY1
DIF=F(J)/D(J)
XI(J,I)=XI(J,I)-DIF
IF(J .EQ. MY .AND. XI(MY,I) .GT. XIO(MY)) XI(MY,I)=XIO(MY)
H(J,I)=(1.+ERR1*XI(J,I))*REERR1
SUM=ABS(DIF)
12 J=J-1
DIF=(F(J)-DP(J)*DIF)/D(J)
XITP=XI(J,I)-DIF
IF(XITP .LT. XIH(J,I)) GO TO 54
IF(ERR1*XITP .GT. -.99999) GO TO 154
CALL F18NOK(XI(J-1,I),XI(J+1,I),XITP,I,J)
GO TO 155
154 XITP=XIH(J,I)-1.E=11
155 DIF=0.0
54 H(J,I)=(1.+ERR1*XITP)**REERR1
XI(J,I)=XITP
53 SUM=SUM+ABS(DIF)
IF(J .GE. NB2) GO TO 12
IF(NCT .EQ. 0) SUMT=SUMT+SUM
NCT=NCT+1
IF(SUM .GT. ERR .AND. NCT .LT. MAXT) GO TO 6
IF(NCT .GT. MNCT) MNCT=NCT
5 CONTINUE
NB2=NB2
DO 47 J=1,NNY
H(J,1)=H(J,2)

```

```

47 XI(J,1)=XI(J,2)
NCOUNT=NCOUNT+1
VK=VVK
IF(MNCT .LT. 3) GO TO 46
IF(SUMT .GT. ERRT .AND. NCOUNT .LT. MAX ) GO TO 4
IF(NCOUNT .EQ. MAXT) WRITE(6,100) NCT,NCOUNT,SUMT
100 FORMAT(1H ,I3, ' DID NOT CONVERGE IN ALLOWABLE NUMBER OF
$ITERATIONS',I3, ' SUMT='E15.8)
46 SUM=0.0
NBT=NB1
DO 24 I=1,NX1
IIJ=I
IF(NSSUR .GT. 0 .AND. I .EQ. N2XP) NB1=1
DO 24 J=NB1,NY1
JJ=J
DIF=HD(J,I)-H(J,I)
IF(DIF .LT. SUM) GO TO 24
SUM=DIF
IMAXJ=J
24 HD(J,I)=DIF
VK=VVK
NB1=NBT
IMAX2=IMAXJ+2
IMAXM=IMAXJ-2
RETURN
END

```

C
C
C
C
C
C
C
C
C
C
C

SUBROUTINE RITOUT COMPUTES SATURATION ,AVERAGE INFILTRATION RATE,
INSTANTENOUS INFILTRATION RATE ,VOLUME OF WATER APPLIED, HYDRAULIC
HEAD AND PRINTS PRESSURE HEAD, HYDRAULIC HEAD, SATURATION, AVERAGE
INFILTRATION RATE, INSTANTENOUS INFILTRATION RATE, VOLUME OF WATER
APPLIED AT EACH GRID POINT, AT ANY TIME STEP.

```

SUBROUTINE RITOUT(NM,ITIME1)
COMMON H(32,32),HO(32,32),B(32,32),DM(32),D(32),DP(32),F(32),S1(32
$),VKS(33),AMBDA(32),DELS2(32),AMB32(32),AMB01(32),POR(32),SR(32),
$SR1(32),DVKS(32),DAMBDA(32),PAVK(32),BB(32),DPB(32),VK,HEIGT,AK
$,DEPTH,SL,DELTA,DELS,HI,HIT,EKR,ERRT,ERR1,RERR1,TIME,DES2,DELM,SSUR
$,OMEGA,WATCO1,TIM1,XI(32,32),XIH(32,32),XIO(32),MY1,NY,NY1,NY2,
$SNHSR,MY,NSAT,NSSUR,NB1,NB2,MAX,MAXT,NX,NX1,NRX,NS,N6,J,JP,JP1,
$SM2,IMAXJ,IMAXM,IMAX2,ITIME,IM,IP,DAMBK(32),DELS2(32),DCUB(32),
$DELS2(32),DCUB5(32),HD(32,32),Q,R,N2X,MX,MB2,MB3,I,N2XP,AREAC
NM1=1
IF(NM .GT. 0) GO TO 35
NM2=16
1 IF(NM2 .GT. NX) NM2=NX
WRITE(6,105) ITIME1,TIME
105 FORMAT('0 VALUES OF PRESSURE FOR TIME STEP',I5,' TAU='F9.4)
WRITE(6,101) (I, I=NM1,NM2)
101 FORMAT(3H ,I5,15I8)
DO 2 J=1,NY
2 WRITE(6,100) J,(H(J,I), I=NM1,NM2)
100 FORMAT(1H ,I2,16F8.4)
IF(NM2 .EQ. NX) GO TO 3
NM1=NM1+16
NM2=NM2+16
GO TO 1

```



```

$,OMEGA,WATCO1,TIM1,XI(32,32),XIH(32,32),XIO(32),MY1,NY,NY1,NY2,
SNHSR,MY,NSAT,NSUR,NB1,NB2,MAX,MAXT,NX,NX1,NRX,N5,N6,J,JM,JP,M1,
SM2,IMAXJ,IMAXM,IMAX2,ITIME,IM,IP,DAMBK(32),DELS2(32),DCUB(32),
$DELS2(32),DCUB5(32),HD(32,32),Q,R,N2X,MX,MB2,MB3,I,N2XP
PT#MJI
DRI=.5*(XI1IP-XI1IM)
D2RI=XI1IP+XI1IM-2.*XI1I
ARG#1,+ERR1*XI1I
DLWK=VK*(BB(1)/PT)**AMB32(1)/VKS(1)
VKS#VKS(J)*PT
DRIS=DRI*DR1
SSPK#DELS*ARG*DLWK
SSPKE=(DELS*ARG/PT)*(DLWK+1,0)
FT1=(D2RI+2.0*(XI2I+SSPKE=XI1I)+(DM(1)/ARG)*(DRIS+(SSPKE**2)))
FT2#AMB32(1)*PT*DRIS/ARG
BRACT#DPB(1)+DAMBK(1)*ALOG(BB(1)/PT)+AMB32(1)*DELS*(DLWK+1,0)/PT
FIT#PT*DR1/FLOAT(I-1)
FT3#SSPK*DVKS(1)
F1=VKS(1)*((PT*FT1)+FT2+SSPK*BRACT+FIT)+FT3
IF(NN.EQ.0) RETURN
HDA=(1,+ERR1*XIH(1,I))**RERR1
PAV=.5*(PT+HDA)
TS2#DELS2(1)*PAV**AMB01(1)
TS3#TS2*(XI1I=XIH(1,I))
F1#F1-TS3
DFT4#-4.0+2.0*DELS*(DLWK+1,0)*DM(1)/PT-(DM(1)*ERR1/(ARG*ARG))*
$(DRIS+SSPKE**2)-2.0*(DM(1)*DELS*(DLWK+1,0)/PT)**2)
DFT2#FT2*DM(1)/ARG
BRACT2#AMB32(1)*DELS*(DLWK+1,0)/PT+DAMBK(1)
DFT#FIT/ARG
DFT3#DELS*DLWK*ERR1*DVKS(1)
D(1)=VKS(1)*((PT/ARG)*FT1)+PT*DFT4+DFT2+DELS*DLWK*(ERR1+
$BRACT-BRACT2)+DFT1-DFT3-TS3*AMB01(1)*0.5*PT/(ARG*PAV)-TS2
DP(1)=2.0*VKS(1)*PT
RETURN
END

```

SUBROUTINE FJ IS CALLED TO EVALUATE THE FUNCTION AND ITS DERIVATIVES FOR THE INTERIOR PORTION OF FLOW FIELD.

```

SUBROUTINE FJ(MJI,XIJI,XIJMI,XIJPI,XIJIP,XIJIM,FF,NN)
COMMON H(32,32),HO(32,32),B(32,32),DM(32),D(32),DP(32),F(32),S1(32
$),VKS(32),AMBDA(32),DELS2(32),AMB32(32),AMB01(32),POR(32),SR(32),
$SR1(32),DVKS(32),DAMBDA(32),PAVK(32),BB(32),DPB(32),VK,HEIGHT,AK
$,DEPTH,SL,DELT,DELS,HI,HIT,ERR,ERRT,ERR1,RERR1,TIME,DES2,DELM,SSUR
$,OMEGA,WATCO1,TIM1,XI(32,32),XIH(32,32),XIO(32),MY1,NY,NY1,NY2,
SNHSR,MY,NSAT,NSUR,NB1,NB2,MAX,MAXT,NX,NX1,NRX,N5,N6,J,JM,JP,M1,
SM2,IMAXJ,IMAXM,IMAX2,ITIME,IM,IP,DAMBK(32),DELS2(32),DCUR(32),
$DELS2(32),DCUB5(32),HD(32,32),Q,R,N2X,MX,MB2,MB3,I,N2XP
PT#MJI
DRI=.5*(XIJMI-XIJPI)
D2RI=.5*(XIJIP-XIJIM)
D2XI=XIJPI+XIJMI-2.*XIJI
D2KI=XIJIP+XIJIM-2.*XIJI
ARG#1,+ERR1*XIJI
DPDL#PT*DXI-DELS*ARG
VKS#VKS(J)*PT

```

```

FI#VKS*DR1/FLOAT(I-1)
DXIS#DXI*DXI
DRIS#DRI*DR1
BRAC=(DPB(J)+(DAMBDA(J)/VKS(J))*ALOG(BB(J)/PT)+AMB32(J)*DXI/ARG)
$*VKS(J)
FJ2=(DM(1)*(DXIS+DRIS)+AMB32(J)*DRIS)/ARG
FJ1#VKS*(D2XI+D2RI+FJ2)
FF#FJ1+DPDL*(BRAC+DVKS(J))+FI
IF(NN.EQ.0) RETURN
HDA=(1,+ERR1*XIH(J,I))**RERR1
PAV=.5*(PT+HDA)
TS2#DELS2(J)*PAV**AMB01(J)
TS3#TS2*(XIJI=XIH(J,I))
FF#FF-TS3
DMM#DM(1)*DXI/ARG+.5*(BRAC/VKS(J))
DMP=.5*(PT+DVKS(J)+VKS(J)*DPDL*AMB32(J)/ARG)
DM(J)=VKS*(1,+DMM)+DMP
DP(J)=VKS*(1,-DMM)-DMP
D(J)=FJ1/ARG-VKS*(FJ2*ERR1/ARG+4.)+(BRAC+DVKS(J))*PT*DXI/ARG-
$ERR1*DELS*DPDL*(DAMBDA(J)+PAVK(J)*ERR1*DXI/ARG)/ARG+FI/ARG-TS3*
$AMB01(J)*.5*PT/(ARG+PAV)-TS2
RETURN
END

```

FUNCTION F3 = IS CALLED WHEN THE WETTING FRONT HAS REACHED TO DRAINED OR WATER TABLE AND COMPUTES THE VALUE OF FUNCTION AND ITS DERIVATIVES ON THIS BOUNDARY.

```

FUNCTION F3(HMYI,XIMYI,XIMYIP,XIMYIM,XIMY1I,NN)
COMMON H(32,32),HO(32,32),B(32,32),DM(32),D(32),DP(32),F(32),S1(32
$),VKS(32),AMBDA(32),DELS2(32),AMB32(32),AMB01(32),POR(32),SR(32),
$SR1(32),DVKS(32),DAMBDA(32),PAVK(32),BB(32),DPB(32),VK,HEIGHT,AK
$,DEPTH,SL,DELT,DELS,HI,HIT,ERR,ERRT,ERR1,RERR1,TIME,DES2,DELM,SSUR
$,OMEGA,WATCO1,TIM1,XI(32,32),XIH(32,32),XIO(32),MY1,NY,NY1,NY2,
SNHSR,MY,NSAT,NSUR,NB1,NB2,MAX,MAXT,NX,NX1,NRX,N5,N6,J,JM,JP,M1,
SM2,IMAXJ,IMAXM,IMAX2,ITIME,IM,IP,DAMBK(32),DELS2(32),DCUB(32),
$DELS2(32),DCUB5(32),HD(32,32),Q,R,N2X,MX,MB2,MB3,I,N2XP
PT#HMYI
DRI=.5*(XIMYIP-XIMYIM)
D2RI=XIMYIP+XIMYIM-2.*XIMYI
ARG#1,+ERR1*XIMYI
VKS#VKS(MY)*PT
DRIS#DRI*DR1
SSPKE#DELS*ARG/PT
FT1=(D2RI+2.0*(XIMYI-SSPKE=XIMYI)+(DM(1)/ARG)*(DRIS+(SSPKE
$**2)))
FT2#AMB32(MY)*PT*DRIS/ARG
FIT#PT*DR1/FLOAT(I-1)
F3#VKS(MY)*((PT*FT1)+FT2+FIT)
IF(NN.EQ.0) RETURN
HDA=(1,+ERR1*XIH(MY,I))**RERR1
PAV=.5*(PT+HDA)
TS2#DELS2(MY)*PAV**AMB01(MY)
TS3#TS2*(XIMYI=XIH(MY,I))
F3#F3-TS3
DFT4#-4.+2.*DELS*DM(1)/PT-(DM(1)*ERR1/(ARG*ARG))*(DRIS+SSPKE**2
$)-2.*(DM(1)*DELS/PT)**2)

```

C
C
C
C
C
C
C
C
C
C

C
C
C
C
C
C
C
C
C
C

```

DFT2=FT2*DM(1)/ARG
DFIT=FIT/ARG
DCMY)=VK(S(MY))*((PT/ARG)*FT1)+PT*DFT4+DFT2+DFIT)=TS3*AMBDA1(MY)*
S,5*PT/(ARG*PAV)=TS2
DM(MY)=2.0*VK(S(MY))*PT
RETURN
END

```

```

SUBROUTINE DERV -IN THIS SUBROUTINE THE MAGNITUDE OF ALL VARIABLES AND
AND THEIR DERIVATIVES FOR EACH GRID POINT ARE DETERMINED AND WRITTEN
OUT.

```

```

SUBROUTINE DERV
COMMON H(32,32),HO(32,32),B(32,32),DM(32),D(32),DP(32),F(32),S1(32
S),VK(S(32),AMBDA(32),DELS2(32),AMB32(32),AMB01(32),POR(32),SR(32),
SR1(32),DVKS(32),DAMBDA(32),PAVK(32),BB(32),DPB(32),VK,HEIGHT,AKK
S,DEPTH,SL,DEL,DELS,HI,HIT,ERR,ERRT,ERR1,RERR1,TIME,DES2,DELM,SSUR
S,OMEGA,WATCO1,TIM1,XI(32,32),XIH(32,32),XIO(32),MY1,NY,NY1,NY2,
SNH8R,MY,NSAT,NSSUR,NB1,NB2,MAX,MAXT,NX,NX1,NRX,N5,N6,J,JM,JP,M1,
SM2,IMAXJ,IMAXM,IMAX2,ITIME,IM,IP,DAMBK(32),DELS2(32),DCUB(32),
SDELS2(32),DCUBS(32),HD(32,32),Q,R,N2X,MX,MB2,MB3,I,N2XP
READ(5,100) AL,BL,CL,BK,CK,AS,BB,CB,AP,BP,CP,APB,BPB,CPB
100 FORMAT(8F10.5)
DESS=DES2*DELS
AK=1.-(BK+CK*HEIGHT)*HEIGHT
CL2=2.*CL
CK2=2.*CK
CPB2=2.*CPB
AMBMIN=100.
DO 1 J=1,MY
Z=HEIGHT-DELS*FLOAT(J-1)
AMBDA(J)=AL+(BL+CL*Z)*Z
IF (AMBDA(J) .LT. AMBMIN) AMBMIN=AMBDA(J)
AMB01(J)=2.+2.*AMBDA(J)
AMB32(J)=-2.-3.*(AL+(BL+CL*Z)*Z)
VK(S(J))=AK+(BK+CK*Z)*Z
DVKS(J)=(BK+CK*Z)*DELS
DAMBK(J)=3.0*(BL+CL*Z)+DELS
DAMBDA(J)=3.*VK(S(J))*(BL+CL*Z)*DELS
PAVK(J)=VK(S(J))*AMB32(J)
POR(J)=AP+(BP+CP*Z)*Z
DELS2(J)=6.2831853*POR(J)*DELS**3
DCUB(J)=.758398*POR(J)*DELS**3
SR(J)=AS+(BS+CS*Z)*Z
SR1(J)=1.-SR(J)
BB(J)=APB+(BPB+CPB*Z)*Z
DPB(J)=-DELS*(BPB+CPB*Z)/BB(J)*AMB32(J)
BB(J)=BB(J)/SL
1 DELS2(J)=DESS*POR(J)*AMBDA(J)+SR1(J)/(BB(J))*AMB01(J)*DEL
DELS2(1)=.5*DELS2(1)
DCUBS(1)=.5*DCUB(1)
DELS2(MY)=.5*DELS2(MY)
DCUBS(MY)=.5*DCUB(MY)
DM(1)=2.+3.*AMBMIN
ERR1=1.-DM(1)
WRITE(6,102) AMBMIN,ERR1,DM(1)
102 FORMAT(' REF. LAMBDA=',3F10.4)

```

```

WRITE(6,101) (BB(J),J=1,MY)
WRITE(6,101) (AMBDA(J),J=1,MY)
WRITE(6,101) (AMB01(J),J=1,MY)
WRITE(6,101) (AMB32(J),J=1,MY)
WRITE(6,101) (POR(J),J=1,MY)
WRITE(6,101) (VK(S(J),J=1,MY)
WRITE(6,101) (SR(J),J=1,MY)
WRITE(6,101) (SR1(J),J=1,MY)
WRITE(6,101) (DELS2(J),J=1,MY)
WRITE(6,101) (DAMBDA(J),J=1,MY)
WRITE(6,101) (PAVK(J),J=1,MY)
WRITE(6,101) (DAMBK(J),J=1,MY)

```

```

101 FORMAT(1H ,13F10.5)
RETURN
END

```

```

SUBROUTINE FIBNOK IS CALLED TO OPTIMIZE THE VALUES OF TRANSFORMED
PRE88RE HEAD (XI(J,I)).

```

```

SUBROUTINE FIBNOK(X1,X2,X,II,II)
COMMON H(32,32),HO(32,32),B(32,32),DM(32),D(32),DP(32),F(32),S1(32
S),VK(S(32),AMBDA(32),DELS2(32),AMB32(32),AMB01(32),POR(32),SR(32),
SR1(32),DVKS(32),DAMBDA(32),PAVK(32),BB(32),DPB(32),VK,HEIGHT,AKK
S,DEPTH,SL,DEL,DELS,HI,HIT,ERR,ERRT,ERR1,RERR1,TIME,DES2,DELM,SSUR
S,OMEGA,WATCO1,TIM1,XI(32,32),XIH(32,32),XIO(32),MY1,NY,NY1,NY2,
SNH8R,MY,NSAT,NSSUR,NB1,NB2,MAX,MAXT,NX,NX1,NRX,N5,N6,J,JM,JP,M1,
SM2,IMAXJ,IMAXM,IMAX2,ITIME,IM,IP,DAMBK(32),DELS2(32),DCUB(32),
SDELS2(32),DCUBS(32),HD(32,32),Q,R,N2X,MX,MB2,MB3,IK,N2XP
X2=X22
IF (ERR1*X2 .LT. -.9999) X2=-.9999/ERR1
KEY=-1
ITER=12
J=0
K=1
RERR1=1./ERR1
HJI=(1.+ERR1*X1)**RERR1
IF (JJ .GT. 1) GO TO 3
XIJJ=XI(JJ,II+1)
XIJIM=XI(JJ,II-1)
GO TO 4
3 XIJJ=(H(JJ-1,II+1)**ERR1-1.)/ERR1
XIJIM=(H(JJ-1,II-1)**ERR1-1.)/ERR1
4 CALL FJ(HJ1,XIJM1,XIJI1,XIJP1,XIJIP,XIJIM,FF,100)
F1=(FF+B(JJ,II))**2
HJI=(1.+ERR1*X2)**RERR1
XIJJ=(H(JJ+1,II+1)**ERR1-1.)/ERR1
XIJIM=(H(JJ+1,II-1)**ERR1-1.)/ERR1
CALL FJ(HJ1,XIJP1,XIJI1,XIJM1,XIJIP,XIJIM,FF,100)
F2=(FF+B(JJ,II))**2
Y1=1.
Y2=1.
DO 10 I=1,ITER
TEMP=Y2
Y2=Y2+Y1
10 Y1=TEMP
XA=X1+(X2-X1)*Y1/(Y1+Y2)
X=XA

```

```

20 HJI=(1.+ERR1*X)**ERR1
   XIJIP=(H(JJ,II+1)**ERR1-1)/ERR1
   XIJIM=(H(JJ,II-1)**ERR1-1)/ERR1
   CALL FJ(HJI, X ,XIJMI,XIJPI,XIJIP,XIJIM,FF,100)
   FN=(FF+B(JJ,II))*2
   IF(K=2)30,40,40
30 FA=FN
   K=K+2
   GO TO 100
40 IF(KEY)50,50,60
50 FB=FN
   GO TO 70
60 FA=FN
70 J=J+1
202 FORMAT(1X,E15.8,1X,E15.8,2X,E15.8,1X,E15.8,2X,E15.8,1X,E15.8,
12X,E15.8,1X,E15.8/)
   IF(J=ITER)75,120,120
75 IF(FA-FB)80,80,90
80 X2=XB
   F2=FB
   KEY=1
   XB=XA
   FB=FA
   XA=X1+X2-XB
   X=XA
   GO TO 20
90 X1=XA
   F1=FA
   XA=XB
   FA=FB
   KEY=-1
100 XB=X2-XA+X1
   X=XB
   GO TO 20
120 IF(KEY)130,130,140
130 X=XA
   FN=FA
   GO TO 150
140 X=XB
   FN=FB
203 FORMAT(' OPTIMAL SOLUTION X=',E15.8,' OPTIMAL VALUE FN=',E15.8,
$ 15, 15)
150 WRITE(6,203)X,FN,II,JJ
C 150 RETURN
   RETURN
   END

```

4	32	21	1	-8.0	2.0	.005	1.0	.90	.0001
4									
1.5	8	2.0	14	2.0	20	2.0	25		
1.665		.007		.0000003		.90	.95		
1	1	0							
15	0								
0.9		-.1		0.0		-.1000	0.0	0.25	.168
.500		0.0		0.0		1.10	-.40	0.0	
4	32	25	3	-20.5	2.0	.001	1.0	.0	.0001
4									
1.5	18	2.0	25	2.0	35	2.0	60		
13									
	.01	.002	0		.04	.005	0	.08	.004
	.25	.005	0		.50	.006	0	.35	.007
	.40	.008	0		.45	.009	0	.50	.010
	.55	.011	0		.60	.012	0	.65	.013
	.70	.014	0						
1.665		.007		.0000003		.90	.95		
1	1	0							
15	0								
0.9		-.1		0.0		-.1000	0.0	0.25	.168
.500		0.0		0.0		1.10	-.40	0.0	

N2X= 4 NX= 32 NY= 21 NT= 3 HJ= -8.000 HIT= -8.000 DEPTH= 2.00 HEIGHT= 2.000 DELT= 0.0050 S(1)= 0.9000 SL= 1.000

NRIT1= 1 NRIT2= 1 NSSR= 1 MAX=15

EPR .300E+06

RADIUS OVER WHICH INFILTRATION OCCURS 0.30000 INFILTRATION FLUX= 0.00000 DELS= 0.100 AREA= 0.283

REF. LAMBDA=	0.7000	-3.1000	4.1000																	
0.30000	0.34000	0.38000	0.42000	0.46000	0.50000	0.54000	0.58000	0.62000	0.66000	0.70000	0.74000	0.78000	0.82000	0.86000	0.90000	0.94000	0.98000	1.02000	1.06000	1.10000
0.82000	0.86000	0.90000	0.94000	0.98000	1.02000	1.06000	1.10000	1.14000	1.18000	1.22000	1.26000	1.30000	1.34000	1.38000	1.42000	1.46000	1.50000	1.54000	1.58000	1.62000
0.70000	0.71000	0.72000	0.73000	0.74000	0.75000	0.76000	0.77000	0.78000	0.79000	0.80000	0.81000	0.82000	0.83000	0.84000	0.85000	0.86000	0.87000	0.88000	0.89000	0.90000
0.83000	0.84000	0.85000	0.86000	0.87000	0.88000	0.89000	0.90000	0.91000	0.92000	0.93000	0.94000	0.95000	0.96000	0.97000	0.98000	0.99000	1.00000	1.01000	1.02000	1.03000
3.40000	3.42000	3.44000	3.46000	3.48000	3.50000	3.52000	3.54000	3.56000	3.58000	3.60000	3.62000	3.64000	3.66000	3.68000	3.70000	3.72000	3.74000	3.76000	3.78000	3.80000
3.66000	3.68000	3.70000	3.72000	3.74000	3.76000	3.78000	3.80000	3.82000	3.84000	3.86000	3.88000	3.90000	3.92000	3.94000	3.96000	3.98000	4.00000	4.02000	4.04000	4.06000
-4.10000	-4.15000	-4.20000	-4.25000	-4.30000	-4.35000	-4.40000	-4.45000	-4.50000	-4.55000	-4.60000	-4.65000	-4.70000	-4.75000	-4.80000	-4.85000	-4.90000	-4.95000	-5.00000	-5.05000	-5.10000
-4.47000	-4.52000	-4.57000	-4.62000	-4.67000	-4.72000	-4.77000	-4.82000	-4.87000	-4.92000	-4.97000	-5.02000	-5.07000	-5.12000	-5.17000	-5.22000	-5.27000	-5.32000	-5.37000	-5.42000	-5.47000
0.50000	0.50000	0.50000	0.50000	0.50000	0.50000	0.50000	0.50000	0.50000	0.50000	0.50000	0.50000	0.50000	0.50000	0.50000	0.50000	0.50000	0.50000	0.50000	0.50000	0.50000
0.50000	0.50000	0.50000	0.50000	0.50000	0.50000	0.50000	0.50000	0.50000	0.50000	0.50000	0.50000	0.50000	0.50000	0.50000	0.50000	0.50000	0.50000	0.50000	0.50000	0.50000
1.00000	1.01000	1.02000	1.03000	1.04000	1.05000	1.06000	1.07000	1.08000	1.09000	1.10000	1.11000	1.12000	1.13000	1.14000	1.15000	1.16000	1.17000	1.18000	1.19000	1.20000
1.13000	1.14000	1.15000	1.16000	1.17000	1.18000	1.19000	1.20000	1.21000	1.22000	1.23000	1.24000	1.25000	1.26000	1.27000	1.28000	1.29000	1.30000	1.31000	1.32000	1.33000
0.07000	0.10351	0.13702	0.17053	0.20404	0.23755	0.27106	0.30457	0.33808	0.37159	0.40510	0.43861	0.47212	0.50563	0.53914	0.57265	0.60616	0.63967	0.67318	0.70669	0.74020
0.30434	0.30436	0.30175	0.29656	0.28879	0.27844	0.26551	0.25000	0.23236	0.21175	0.18856	0.16279	0.13444	0.10351	0.07000	0.03499	0.00000	0.00000	0.00000	0.00000	0.00000
0.93000	0.89649	0.85555	0.80721	0.75144	0.68825	0.61764	0.54000	0.45639	0.36278	0.26017	0.14856	0.02795	0.00000	0.00000	0.00000	0.00000	0.00000	0.00000	0.00000	0.00000
0.59561	0.67564	0.73825	0.78344	0.81121	0.72156	0.73449	0.75000	0.76764	0.78625	0.80486	0.82347	0.84208	0.86069	0.87930	0.89791	0.91652	0.93513	0.95374	0.97235	0.99096
78.05464	50.95372	34.76395	24.58922	17.91104	13.37705	10.20881	7.34001	4.74001	2.38001	1.17882	0.54894	0.23981	0.09981	0.03210	0.00000	0.00000	0.00000	0.00000	0.00000	0.00000
2.36735	2.03562	1.75292	1.52307	1.33463	1.17882	1.04894	0.93981	0.84001	0.75000	0.66825	0.59486	0.52847	0.46808	0.41269	0.36130	0.31291	0.26652	0.22213	0.17974	0.13935
-0.03000	-0.03030	-0.03060	-0.03090	-0.03120	-0.03150	-0.03180	-0.03210	-0.03240	-0.03270	-0.03300	-0.03330	-0.03360	-0.03390	-0.03420	-0.03450	-0.03480	-0.03510	-0.03540	-0.03570	-0.03600
-0.03390	-0.03420	-0.03450	-0.03480	-0.03510	-0.03540	-0.03570	-0.03600	-0.03630	-0.03660	-0.03690	-0.03720	-0.03750	-0.03780	-0.03810	-0.03840	-0.03870	-0.03900	-0.03930	-0.03960	-0.03990
-4.10000	-4.17130	-4.24320	-4.31570	-4.38880	-4.46250	-4.53680	-4.61170	-4.68720	-4.76330	-4.84000	-4.91730	-4.99520	-5.07370	-5.15280	-5.23250	-5.31280	-5.39370	-5.47520	-5.55730	-5.64000
-5.07370	-5.15280	-5.23250	-5.31280	-5.39370	-5.47520	-5.55730	-5.64000	-5.72330	-5.80720	-5.89170	-5.97680	-6.06250	-6.14880	-6.23570	-6.32320	-6.41130	-6.50000	-6.58930	-6.67920	-6.76970
-0.03000	-0.03000	-0.03000	-0.03000	-0.03000	-0.03000	-0.03000	-0.03000	-0.03000	-0.03000	-0.03000	-0.03000	-0.03000	-0.03000	-0.03000	-0.03000	-0.03000	-0.03000	-0.03000	-0.03000	-0.03000
-0.03000	-0.03000	-0.03000	-0.03000	-0.03000	-0.03000	-0.03000	-0.03000	-0.03000	-0.03000	-0.03000	-0.03000	-0.03000	-0.03000	-0.03000	-0.03000	-0.03000	-0.03000	-0.03000	-0.03000	-0.03000

INITIAL DISTRIBUTION OF PRESSURE WITH DEPTH
 10.0000000 9.9000000 9.8000000 9.7000000 9.6000000 9.5000000 9.4000000 9.3000000 9.2000000 9.1000000 9.0000000 8.9000000 8.8000000

INITIAL SATURATION THAU PROFILE
 0.1499 0.1854 0.2178 0.2474 0.2742 0.2984 0.3199 0.3389 0.3554 0.3695 0.3812 0.3905 0.3976
 0.4023 0.4064 0.4054 0.4035 0.3996 0.3937 0.3857 0.3758

VALUES OF PRESSURE FOR TIME STEP	1	2	3	4	5	6	7	8	9	10
1	0.3529	0.3529	0.3529	0.3529	0.2279	0.4420	1.0314	8.0517	9.9984	10.0000
2	0.9562	0.9562	0.9562	0.9562	2.5892	4.6874	9.1759	9.8998	9.9000	9.9000
3	8.1409	8.1409	8.1409	8.1412	9.7753	9.7976	9.7999	9.8000	9.8000	9.8000
4	9.6997	9.6997	9.6997	9.6997	9.7000	9.7000	9.7000	9.7000	9.7000	9.7000
5	9.6000	9.6000	9.6000	9.6000	9.6000	9.6000	9.6000	9.6000	9.6000	9.6000
6	9.5000	9.5000	9.5000	9.5000	9.5000	9.5000	9.5000	9.5000	9.5000	9.5000

VALUES OF SATURATION FOR TIME STEP	1	2	3	4	5	6	7	8	9	10
1	0.9000	0.9000	0.9000	0.9000	1.1972	0.7790	0.4618	0.1630	0.1499	0.1499
2	0.5337	0.5337	0.5337	0.5337	0.3156	0.2386	0.1899	0.1854		
3	0.2297	0.2297	0.2297	0.2297	0.2180	0.2178	0.2178			
4	0.2474	0.2474	0.2474	0.2474	0.2474					
5	0.2742	0.2742	0.2742							

VOL. OF WATER ABSORBED = 0.028813 0.028813 RATE= 5.7625 5.7625 INST. RATE= 5.76253 RATEIPUA= 20.3808 20.3808

VALUES FOR HYDRAULIC HEAD FOR TIME STEP	1	2	3	4	5	6	7	8	9	10
1	1.647	1.647	1.647	1.647	1.558	0.969	-6.052	-7.998	-8.000	
2	0.944	0.944	0.944	0.944	-0.689	-2.987	-7.276	-8.000		
3	-6.341	-6.341	-6.341	-6.341	-7.975	-7.998	-8.000			
4	-8.000	-8.000	-8.000	-8.000						
5	-8.000	-8.000	-8.000							

```

HAIRCELL METHOD      0.01000  0.00200  0.00000  0.00300  0  0.08000  0.00400  0  0.25000  0.00500  0
0.30000  0.00000  0.35000  0.00700  0  0.40000  0.00800  0  0.45000  0.00900  0
0.50000  0.01000  0  0.55000  0.01100  0  0.60000  0.01200  0  0.65000  0.01300  0
0.70000  0.01000  0
N2X= 4  N3= 32  N4= 25  N5= 3  H1= -20.500  H1E= -20.500  DEPTH= 2.000  DELT= 0.0010  DE= 0.01000  SL= 1.000
WRITE= 1  WRITE= 1  ASSJ= 0  MAX=15
EPR 3000-05
DEF. L4=24= 0.0000  -3.1000  4.1000  RAUIS= 0.25000= 0.00200DELS= 0.083AREA= 0.190
0.30000  0.33533  0.36667  0.40000  0.43333  0.46667  0.50000  0.53333  0.56667  0.60000  0.63333  0.66667  0.70000
0.73333  0.76667  0.80000  0.83333  0.86667  0.90000  0.93333  0.96667  1.00000  1.03333  1.06667  1.10000
0.70000  0.70433  0.70867  0.71300  0.71733  0.72167  0.72600  0.73033  0.73467  0.73900  0.74333  0.74767  0.75200
0.40000  0.41667  0.43333  0.45000  0.46667  0.48333  0.50000  0.51667  0.53333  0.55000  0.56667  0.58333  0.60000
3.61667  3.63333  3.65000  3.66667  3.68333  3.70000  3.71667  3.73333  3.75000  3.76667  3.78333  3.80000
-4.10000  -4.12500  -4.15000  -4.17500  -4.20000  -4.22500  -4.25000  -4.27500  -4.30000  -4.32500  -4.35000  -4.37500
-4.42500  -4.45000  -4.47500  -4.50000  -4.52500  -4.55000  -4.57500  -4.60000  -4.62500  -4.65000  -4.67500  -4.70000
0.50000  0.50000  0.50000  0.50000  0.50000  0.50000  0.50000  0.50000  0.50000  0.50000  0.50000  0.50000  0.50000
0.50000  0.50000  0.50000  0.50000  0.50000  0.50000  0.50000  0.50000  0.50000  0.50000  0.50000  0.50000  0.50000
1.00000  1.00000  1.00000  1.00000  1.00000  1.00000  1.00000  1.00000  1.00000  1.00000  1.00000  1.00000  1.00000
1.10000  1.10000  1.10000  1.10000  1.10000  1.10000  1.10000  1.10000  1.10000  1.10000  1.10000  1.10000  1.10000
0.97000  0.97000  0.97000  0.97000  0.97000  0.97000  0.97000  0.97000  0.97000  0.97000  0.97000  0.97000  0.97000
0.24500  0.30000  0.35000  0.40000  0.45000  0.50000  0.55000  0.60000  0.65000  0.70000  0.75000  0.80000  0.85000
0.70000  0.70000  0.70000  0.70000  0.70000  0.70000  0.70000  0.70000  0.70000  0.70000  0.70000  0.70000  0.70000
271.02305  180.31472  136.53603  101.11636  76.58801  59.14152  46.44808  37.02950  29.91977  24.47091  20.23613  16.90492  14.26409
12.13701  10.11000  9.01100  7.85200  6.89022  6.08653  5.41052  4.83831  4.35107  3.93378  3.57441  3.26324  2.99167
-0.02771  -0.02792  -0.02813  -0.02835  -0.02857  -0.02879  -0.02901  -0.02923  -0.02945  -0.02967  -0.02989  -0.03011  -0.03033
-4.10000  -4.15000  -4.20000  -4.25000  -4.30000  -4.35000  -4.40000  -4.45000  -4.50000  -4.55000  -4.60000  -4.65000  -4.70000
-0.2500  -0.2500  -0.2500  -0.2500  -0.2500  -0.2500  -0.2500  -0.2500  -0.2500  -0.2500  -0.2500  -0.2500  -0.2500
-0.02500  -0.02500  -0.02500  -0.02500  -0.02500  -0.02500  -0.02500  -0.02500  -0.02500  -0.02500  -0.02500  -0.02500  -0.02500
INITIAL DISTRIBUTION OF PRESSURE WITH DEPTH
22.50000027.41666722.33333322.25000022.166666722.08333322.00000021.916666721.83333321.75000021.666666721.58333321.50000000
21.416666721.33333321.25000021.166666721.08333321.00000020.916666720.83333320.75000020.666666720.58333320.50000000
0.1153  0.1339  0.1705  0.1951  0.2179  0.2388  0.2579  0.2752  0.2906  0.3043  0.3163  0.3265  0.3349
0.3317  0.3367  0.3500  0.3516  0.3515  0.3497  0.3463  0.3412  0.3344  0.3259  0.3157  0.3039
VALUES OF PRESSURE FOR TIME STEP 1 TAU= 0.0010
1 20.5799 20.5799 20.5799 20.5799 20.5799 22.5000 22.5000 22.5000 22.5000 22.5000 22.5000 22.5000 22.5000
2 22.4167 22.4167 22.4167 22.4167 22.4167 22.4167 22.4167 22.4167 22.4167 22.4167 22.4167 22.4167 22.4167
3 22.3333 22.3333 22.3333 22.3333 22.3333 22.3333 22.3333 22.3333 22.3333 22.3333 22.3333 22.3333 22.3333
4 22.2500 22.2500 22.2500 22.2500 22.2500 22.2500 22.2500 22.2500 22.2500 22.2500 22.2500 22.2500 22.2500
5 22.1667 22.1667 22.1667 22.1667 22.1667 22.1667 22.1667 22.1667 22.1667 22.1667 22.1667 22.1667 22.1667
6 22.0833 22.0833 22.0833 22.0833 22.0833 22.0833 22.0833 22.0833 22.0833 22.0833 22.0833 22.0833 22.0833
VALUES OF SATURATION FOR TIME STEP 1 TAU= 0.0010
1 0.1182 0.1182 0.1182 0.1182 0.1182 0.1153
2 0.1439 0.1439 0.1439
VOL. OF WATER ABSORBED = 0.000007 0.000007 0.000007 0.000007 0.000007 0.000007 0.000007 0.000007 0.000007 0.000007 0.000007 0.000007 0.000007
VALUES FOR HYDRAULIC HEAD FOR TIME STEP 1 TAU= 0.0010
1 -14.560 -14.560 -14.560 -14.560 -14.560 -18.560 -20.500
2 -20.500 -20.500 -20.500 -20.500 -20.500 -20.500

```